NOTCH3-FRIZZLED7 signaling regulates luminal cell fate in human breast tissue

by

Vasudeva Bhat

A Thesis submitted to the Faculty of Graduate Studies of

The University of Manitoba

In partial fulfillment of the requirements for the degree of

Doctor of Philosophy

Department of Immunology

Rady Faculty of Health Sciences

University of Manitoba

Winnipeg, Manitoba, Canada

Thesis Summary

Human breast tissue is composed of a network of ducts and alveolar structures that are formed during puberty. During pregnancy, breast tissue expands and subsequently regresses back to its non-pregnant state during involution. This dynamic process of tissue expansion and regression indicates that the mammary gland has a unique regenerative capability that allows it to support multiple pregnancy cycles. This regenerative capacity is due to a small population of self-renewing breast epithelial stem cells (BESCs). BESCs differentiate into bipotential progenitors that give rise to lineage-restricted luminal and myoepithelial progenitors which in turn produce the mature and functionally distinct luminal and myoepithelial cells. Luminal and myoepithelial cells make up the functional cells of the mammary gland. Evolutionarily conserved signaling pathways have been shown to regulate the special functions of these breast stem and progenitor cells. Previous, research from our laboratory demonstrated that signaling through the NOTCH3 receptor (NR3) specifically commits bipotent progenitors to the luminal cell fate. The work presented in this thesis explores the underpinning mechanism by which NR3 regulates luminal cell fate. Through gain and loss of function studies, I found that Frizzled7 (FZD7), a Wnt receptor, is uniquely regulated by NR3 in non-malignant human breast epithelial cells, 184-hTerts. Also, we found that luminal progenitors showed higher expression of FZD7 as compared to bipotent progenitors. This suggests that FZD7 can play an important role in regulating luminal cell differentiation. I, therefore, hypothesized that the commitment of bipotent progenitors to the luminal cell fate is regulated by NR3-specific target genes. Using transcriptome profiling, I found that activation of NR3 signaling in breast epithelial cells is enriched for a Wnt signaling pathway gene signature compared to other Notch receptors. Interestingly, I found that the NR3-FZD7 signaling axis is important for bipotent progenitor commitment to luminal cell fate in *ex vivo* cultures. Next, I observed that a Wnt ligand, Wnt7A,

enhances commitment of the bipotent progenitors to the luminal cell fate in a FZD7-dependent manner. Further characterization of breast epithelial cells revealed for the first time, the presence of a Notch and Wnt signaling-responsive ($NR3^{+}FZD7^{+}CD90^{+}$) basal-like luminal progenitors (BLPs). This is in sharp contrast to the previously identified luminal-restricted progenitors that are non-responsive to Notch and Wnt. My data then suggest that two highly conserved cellular signaling networks, the Notch and Wnt signaling pathways, play essential roles in committing bipotent progenitors to luminal cell lineage. It is inviting to hypothesize that alterations to this signaling axis could lead to an uncontrolled expansion of the luminal progenitor pool, a possible antecedent event to the generation of luminal type tumors. These findings are likely to be important in understanding how alterations in NOTCH3-FZD7 signaling may lead to the development and/or progression of luminal type breast cancers.

Preface

Under the guidance of Dr. Afshin Raouf, I designed and performed most of the experiments conducted in this study. Ms. Yujia Sun and Mr. Steve Weger optimized different notch receptor knockdown and overexpression experiments in HMECs. They also performed Notch signaling qPCR array and interpreted data included in Chapter 3. Victoria Lee-Wing helped in isolation of lentiviral plasmids and reagent preparation.

Mr. Monroe Chan helped me with the isolation of different breast epithelial cell subsets via a flow cytometry. Dr. PingZhao Hu helped me with the analysis of transcriptome data included in Chapter 4. Transcriptome profiling was performed by Robarts Research Institute, Western University, Ontario, Canada. The protocol for obtaining breast reduction samples was approved by the Research Ethics Board of the University of Manitoba (#H2010:292).

This thesis work gave rise to the following publication as included in Chapter 3.

Bhat V, Sun YJ, Weger S, Raouf A. **Notch-Induced Expression of FZD7 Requires Noncanonical NOTCH3 Signaling in Human Breast Epithelial Cells**. *Stem Cells Dev*. 2016 Apr 1;25(7):522-9. doi: 10.1089/scd.2015.0315. Epub 2016 Mar 16. Mary Ann Liebert, Inc., New Rochelle, NY

The data presented in Chapter 4 has been submitted as a research manuscript and is under revision in eLife journal.

Table of Contents

List of Tables

List of Figures

List of abbreviations

ALDH1	Aldehyde dehydrogenase 1
BESCs	Breast epithelial stem cells
BLP	Basal-like luminal progenitor
BSA	Bovine serum albumin
BSC	Biological safety cabinet
CD	Cluster of differentiation
CFC	Colony forming cell
ChIP	Chromatin immunoprecipitation
CK	Cytokeratin
CSL	CBF1-suppressor of hairless-lag-1
DAPI	4′,6-diamidino-2-phenylindole
DAPT	N-[N-(3,5-Difluorophenacetyl)-L-alanyl]-S-phenylglycine t-butyl ester
DCIS	Ductal carcinoma in situ
DH5α	Douglas hanahan 5 alpha
DLL1	Delta-like 1
DMEM	Dulbecco's modified essential medium
DMSO	Dimethyl sulfoxide
DNA	Deoxyribonucleic acid
DNase	Deoxyribose nuclease
EDTA	Ethylenediaminetetraacetic acid
Elf5	E74 like ETS transcription factor 5
EpCAM	Epithelial cell adhesion molecule

ER	Estrogen receptor
ERα	Estrogen receptor alpha
ERβ	Estrogen receptor beta
ERE	Estrogen responsive element
EV	Empty vector
FACS	Fluorescent activated cell sorting
FBS	Fetal bovine serum
FITC	Fluorescein isothiocyanate
FOXA1	Forkhead box A1
FSC	Forward scatter
FZD	Frizzled
GAPDH	Glyceraldehyde-3-phosphate dehydrogenase
GFP	Green fluorescent protein
GSK3-β	Glycogen synthase kinase 3 beta
HBSS	Hanks balanced salt solution
HMECs	Human mammary epithelial cells
IFNγ	Interferon gamma
IgA	Immunoglobulin A
IgG	Immunoglobulin G
INT-3	Insertion-3
IPA	Ingenuity pathway analysis
JAG 1/2	Jagged 1/2
Jak1/2	Janus Kinase 1/2

K5	Keratin 5
LIMMA	Linear model for microarray data
HES1	Hairy and enhancer of split-1
Lrg5	Leucin-rich repeat-containing G-protein coupled receptor 5
LRP	Luminal-restricted progenitor
LRP 5/6	Low-density lipoprotein receptor-related protein 5/6
MAML	Mastermind
MaSCs	Mammary stem cells
MFGE8	Milk fat globule-EGF factor 8 protein
MFI	Median fluorescent intensity
MMTV	Mouse mammary tumor virus
MRU	Mammary repopulating unit
MUC1	Mucin 1
NCBI	National centre for biotechnology information
NCOR2	Nuclear receptor co-repressor 2
Nicd	Mouse notch intracellular domain
NICD	Human notch intracellular domain
Nr	Mouse notch receptor
NR	Human notch receptor
PBS	Phosphate buffered saline
PCP	Planar cell polarity
PCR	Polymerase chain reaction
PE	Phycoerythrin

PI-MECs	Parity-identified mammary epithelial cells
PR	Progesterone receptor
q-RT-PCR	Quantitative real time PCR
RBPJ-κ	Recombinant signal binding protein for immunoglobulin Kappa J region
RMA	Robust multi-array average
RNA	Ribonucleic acid
Ror2	Receptor tyrosine kinase like orphan receptor 2
SF7	Serum free 7
sFRP4	Secreted frizzled receptor protein 4
shRNA	short hair-pin RNA
SIRT1	Sirtulin 1
Stat5	Signal transducer and activator of transcription 5
TCF/LEF	T-cell factor/lymphoid enhancer-binding factor
TDLU	Terminal ductal lobular units
TEB	Terminal end buds
TGF-β	Transforming growth factor beta
THY1	Thymus cell antigen 1
TNBC	Triple negative breast cancer
WAP	Whey acidic protein
WB	Western blot
WNT	Wingless-type MMTV integration site family

Acknowledgements

First and foremost, I would like to thank my thesis supervisor and mentor Dr. Afshin Raouf for giving me this opportunity to work in his lab. He supported and encouraged me throughout my PhD program. He gave me independence to take control of my projects but also provided inputs whenever required. He trained me not just to be a technically skilled person but also to be a critical thinker and a problem solver. He always believed in me and has been very instrumental in helping me build this project and the thesis. He had been a good badminton contender. He was also successful in convincing me that caffeine was vitamin. It has been my privilege and an honor to gain and share his exceptional scientific knowledge during my PhD program.

Besides my supervisor, I would like to express my sincere gratitude to my thesis advisory committee members for their continuous support and also for helping shape up my thesis. Dr. Jude Uzonna has played a very important role in my Ph.D. career. He has been very instrumental in providing valuable inputs and motivation throughout my program. I thank him for believing in me more than I did about my potential. He taught me to be strong and to believe in myself. Dr. Tamra Werbowetski-Ogilvie has seen me progress from the day one and her support and encouragement has been very helpful throughout my study. I thank her for all the valuable advices she gave which has positively influenced my student career. I thank I thank Dr. James Davie for his valuable suggestion which has helped fine tune this project in many ways. His ‘outside the box’ perspective has motivated me to widen my research and knowledge. Words fall short to show how grateful I am to have the most dedicated and amazing committee members who took time to understand my difficulties and guided me towards excellence.

I thank my fellow lab mates, Dr. Sumanta Chatterjee, Dr. Pratima Basak and Alen Paiva for providing constructive suggestions and for all the fun we had in the last 5 and half years. Also,

I thank summer students Victoria Lee-Wing and Alice Su for all help. I am grateful to Mr. Monroe Chan and the Regen Med Flow Cytometry service for helping me with cell sorting. I thank Andrea and the Manitoba Tumor Bank for helping me in the collection of the reduction mammoplasty samples.

I would like to thank all the Regenerative Medicine Program (RMP) faculty members and colleagues for directly and indirectly helping me in my success. Special thanks all the wonderful people Molly, Carl, Ludivine and Jamie for all the help and fun filled conversations. It's been my pleasure knowing you. I cannot proceed without thanking our RMP friends Lisa, Margaret, Brent, Berardino, Leo, Arslan, Scott, Chris, Hardeep, Glen, Nikita, Gazaleh, Narjes, Kong, Kannan, Imam, Sandini, Sari, Dennise, Annan and Marjorie. I had a wonderful time with you all and I cherish the fun events we organized. I was fortunate to have good friends even in the Department of Immunology. It was an honor to be a part of 50 years old department. I specially thank Susan and Karen for helping me with all the official work and for also helping me with the 3MT® talk. It's very important to appreciate your dedication towards the department and also graduate students. Thank you ManLi for helping me with the ultracentrifuge. I also thank all the current members, our Immunology soccer team (Mr. T-cells) for all the fun. I thank our Dungeons and Dragons gamers (Leo, Berardino, Alen, Annan and Dennise) for making Tuesday evenings more memorable. Nonso, Nipun, Grace Choi, Nazanin, Bhavya, Nivedita and Indu, it's been a pleasure knowing you people.

I also thank the HSC badminton group members, Afshin, Anuragh, Vikram, Raju, Manoj, Prajwal, Sajal, Niaz and Manisha.

My sincere thanks to all the members of Manitoba Breast Cancer Research Group especially, Dr. Murphy, Dr. Leygue, Dr. Klonish, Dr. Hombach-Klonish, Dr. Myal, Dr. Hu, Dr.

Kung and Dr. Mowat for their insightful comments and encouragement. I also thank Dr. Pingzhao Hu for helping me with bioinformatics analysis.

No research is possible without the help of the funding agencies. I thank Breast Cancer Society of Canada's HOPE scholarship for supporting my stay in Canada and also for providing an opportunity to visit Dr. Allison Alan Lab in the University of Western Ontario, London, Ontario to learn new techniques in her lab. I also thank NSERC Discovery grant and CancerCare Manitoba (CCMB) foundation for supporting this project. I thank Faculty of Graduate Studies, UofM and University of Manitoba Graduate Student Association and CCMB for providing funds to present my work at national and international conferences.

You always take your best friends for granted. 'Thanks' would appear small in front the things they have done for me. They have stood beside me in both good and worst days. I am extremely lucky to have Anjali and Manoj as a part of my life. They are family to me and have a special place in my heart. You both are such a great blessing and I thank god for that. I am fortunate to have you both by my side. I am deeply thankful for giving me your time and energy which I less deserve.

Last but not the least, I would like to thank my bunnies Juno and Peaches who are my stress busters. Apart from peeing on my bed and shredding research articles, they have changed my life. They made me a better person and have added lot more meaning to my life. I am grateful to them.

Dedication

I dedicate this thesis to

My mom, dad and my little sister for their constant support and unconditional love.

Thank you.

Copyright

The chapter 3 has been published in the journal Stem Cells and Development. It's a part of Mary Ann Liebert, Inc., New Rochelle, NY publisher. Permission to use the original work in this thesis has been approved by the journal.

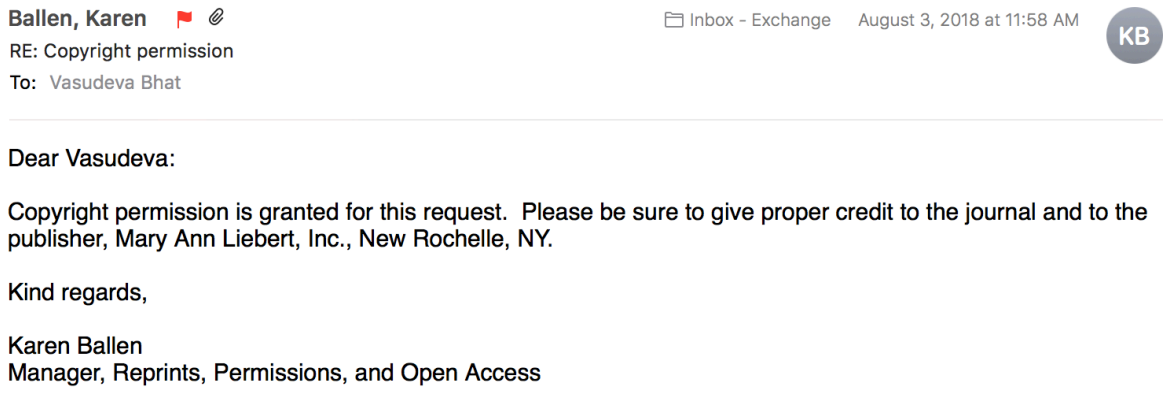

Ballen, Karen Inbox - Exchange August 3, 2018 at 11:58 AM

RE: Copyright permission

To: Vasudeva Bhat

KB

Dear Vasudeva:

Copyright permission is granted for this request. Please be sure to give proper credit to the journal and to the publisher, Mary Ann Liebert, Inc., New Rochelle, NY.

Kind regards,

Karen Ballen
Manager, Reprints, Permissions, and Open Access

1. Introduction

1.1. Mammary gland anatomy and development

1.1.1. Mammary gland anatomy

The anatomy of a female breast was first described by Sir Cooper in 1840 [1]. The adult breast consists of a continuous network of ducts and alveolar structures (Fig. 1.1). The ducts are hollow epithelial tubes which terminate into 15-20 lobes, each of which branches into lobules consisting of 10-100 milk-producing alveoli. The ducts and alveoli collectively are referred to as "terminal ductal lobular units" (TDLUs) [2, 3]. The superficial layer of fascia beneath the skin is responsible for breast development. Breast development can be divided into two phases namely: the developmental phase, starting from nipple epithelium formation and ending with lobule formation and the differentiation phase, which involves the differentiation of mammary epithelium [4]. Development begins between the 4^{th}-6^{th} weeks of fetal stage when the milk lines or mammary (ectoderm) ridges are formed [5]. Similar to skin tissue, breast tissue develops from the ectoderm layer as diverticula of epidermis into the dermis and the mesenchyme in both male and female. Conversely, the ducts and the alveoli arise from ectoderm whereas the connective tissue arises from mesenchyme. A primary mammary bud is formed which grows in length to form a secondary mammary bud. During the 10-12^{th} fetal week, the milk line present in the ventral region of the body extends from the axilla to the inguinal area of the body. The pectoral milk line eventually makes right and left breasts. Adult humans have a single pair of mammary glands whereas rats have six, and mice have five pairs in the majority of strains. During the final trimester or late fetal stage, a shallow depression (mammary pit) is formed below the epidermis, which after birth forms a visible nipple connecting the lactiferous ducts [6, 7]. These ducts terminate into acini during puberty (Fig 1.2).

A

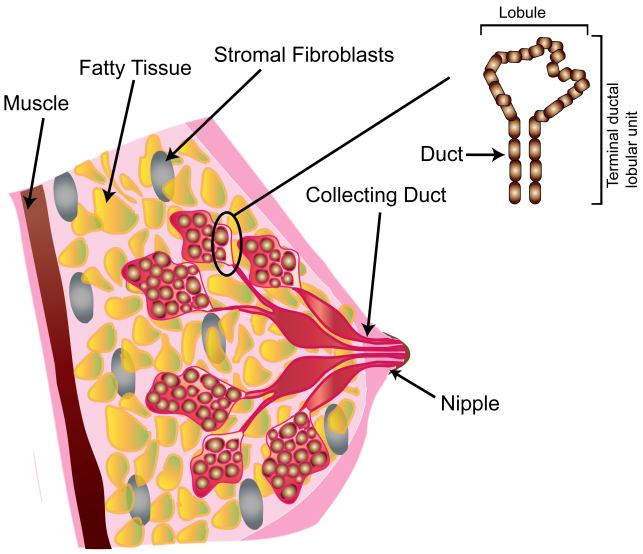

B

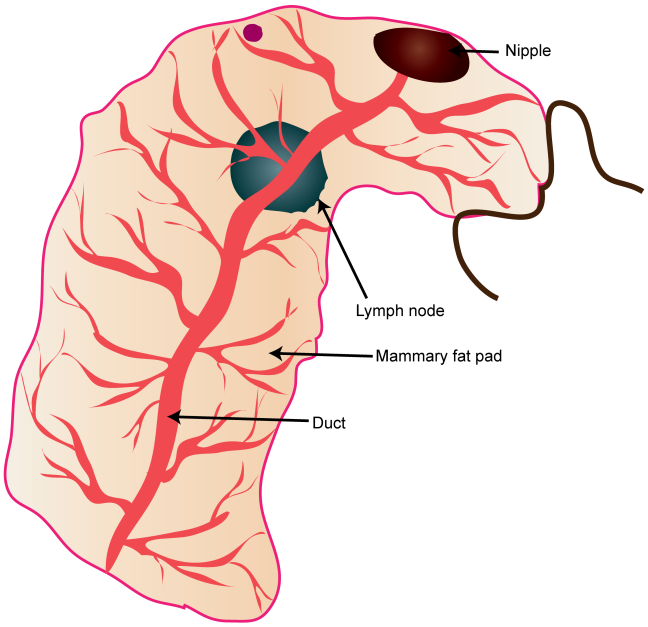

Figure 1.1 Structure of human breast and mouse mammary gland

Schematic showing the sagittal section of female human breast (A) and mouse mammary gland (B). Both human and mouse mammary gland consists of lobules which contain milk producing cells. These cells eject milk into the lactiferous ducts which eventually connect to the nipple.

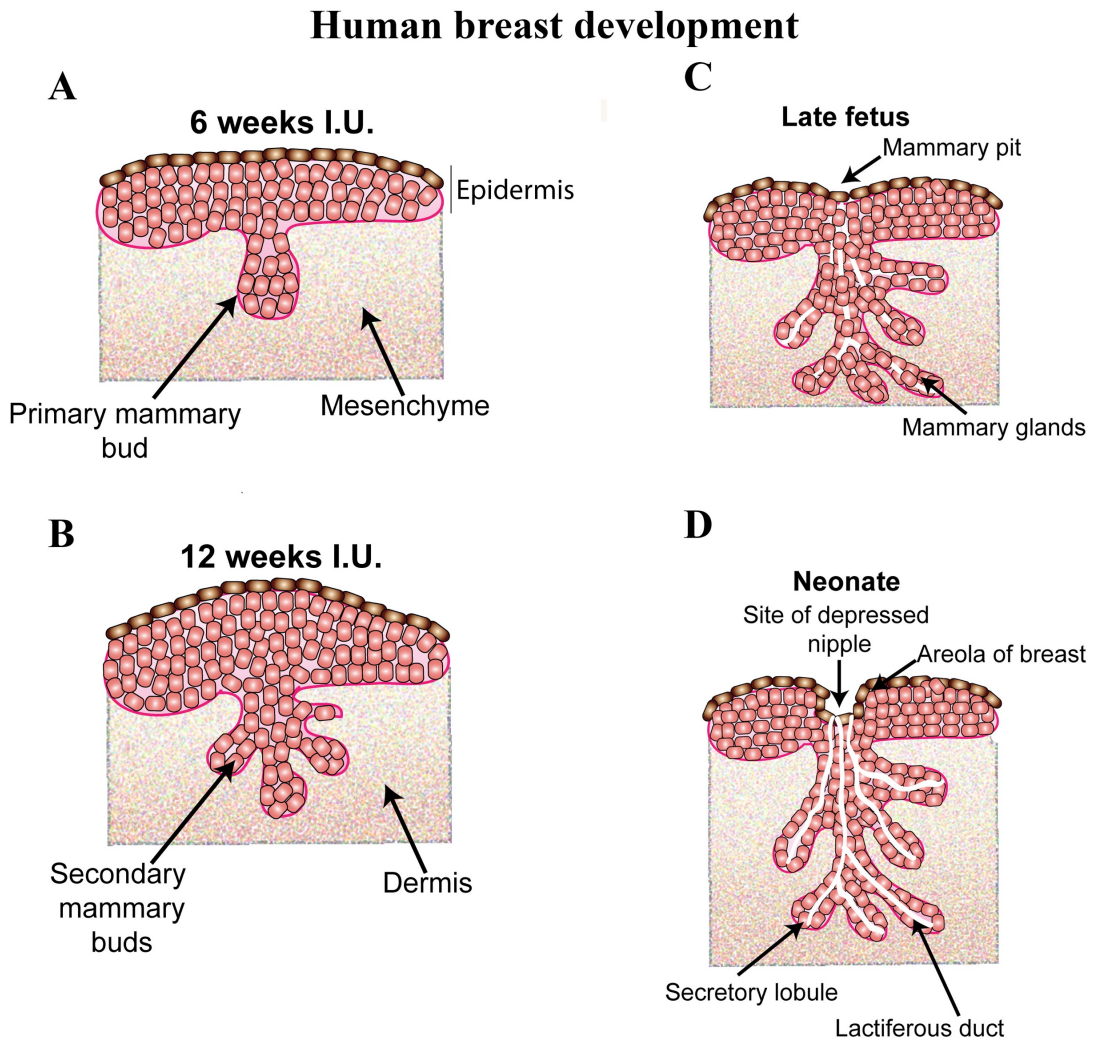

Figure 1.2 Prenatal human breast development

Schematic showing prenatal development of human breast. Development of human breast occurs during 4th- 6th weeks of fetal development and this give rise to the primary mammary bud. Primary bud grows in to a secondary mammary bud and eventually gives rise to lactiferous ducts connected to the nipple.

1.1.2. Postnatal development of the mammary gland

In both mice and humans, the mammary gland remains quiescent after birth and the vast majority of maturation occurs in the presence of female hormones, estrogen and progesterone during puberty. With the surge of female hormones, the epithelial component of ducts and alveoli proliferate along with the increase in size of the breast adipose tissue volume [1, 2, 8]. In the pubertal or nulliparous breast, the most common lobule is a type 1 lobule consisting of alveolar buds [2, 8]. There is a limited increase in the number of alveolar buds resulting in the formation of type 2 and 3 lobules. During the menstrual cycle, the adult breast undergoes cyclic changes. Increased mitotic activity and lobule development happen during the luteal phase. However, during the follicular phase, the lower mitotic activity results in smaller lobules. During pregnancy, there is an increased level of female hormone and growth factors that induce in elongation and branching of ducts and growth of lobules leading to the formation of type 4 lobules [2, 9]. Female hormones such as estrogen, progesterone and prolactin cooperate to induces the production of milk by the alveolus during lactation [10]. Post lactation, the alveoli ceases milk production and due to increased apoptosis, the number of alveoli decreases through a process called involution [11, 12]. In menopausal women, involution is enhanced resulting in regression of type 3 lobules to type 1 or type 2 lobules.

Similar to the adult human breast, the mouse mammary gland is a bilayered structure. In human breasts the ducts terminate into “TDLUs”, whereas ducts in mouse mammary glands give rise to “terminal end buds” (TEBs). Even though TEBs perform a similar function as TDLUs, they differ in structure. TEBs are known to be enriched with stem cells, whereas evidence suggesting that TDLUs are enriched in stem/progenitor cells is lacking [13]. During development, TEBs promote elongation of ducts and branching, whereas in the human breast the ducts undergo

extensive branching to give rise to functional TDLUs [13]. Depending on the stimulus, the TEBs give rise to ducts and promotes branch morphogenesis. Also, the fat pads in mouse mammary glands possess higher adipocyte content compared to the human breast, while the ducts are surrounded by a thin layer of fibrous stroma.

1.1.3. Role of immune cells in postnatal mammary gland development

A recent report suggests that immune cells play an important role at different stages of mammary gland development [14-18]. The role of immune cells in rodent mammary gland development has been well studied. However, the contribution of immune cells to human breast development and maturation is poorly understood due to the lack of appropriate experimental models. Immune cells such as macrophages, eosinophils and mast cells govern mouse mammary gland development in a pubertal gland. They are recruited near the TEBs and mediate ductal outgrowth and branch morphogenesis by remodeling surrounding matrix [15]. Loss of leukocyte function has results in abnormal adult mammary gland development with fewer ducts [15-17]. During pregnancy, colony stimulating factor 1 (Csf1), a regulator of macrophages, is shown to either directly or indirectly regulate branch morphogenesis in mice [18]. Interesting, csf1 has also been shown to maintain the number of tissue resident macrophages and influence stem cell activity in the mammary gland [19, 20]. Macrophages have also been showed to crosstalk with mammary stem cells (MaSCs) by activating Notch and Wnt crosstalk which is discussed in section 1.3.2.2. [20]. During lactation, there is an increased influx of lymphocytes. An increase in plasma B cells has been observed during the early lactation stage. These plasma cells secreted immunoglobulins, especially Immunoglobulin A (IgA) [21, 22] that are transferred to the infant through the mother's milk in order to provide passive immunity against mucosal infections. Histological analysis of

human breast tissue sections obtained from different developmental stages revealed that $CD45^+$ (leukocyte common antigen marker for B-cells, T-cells, neutrophils and macrophages) cells were low in pubertal, pregnant and postpartum specimens. However, there was an increase in $CD45^+$ cells during involution. A similar pattern was observed for expression of a macrophage lysosomal marker, CD68 [23]. During involution, an increase in apoptosis of the epithelial cells can be observed. The clearance of dying mammary epithelial cells was mediated by phagocytic cells, neutrophils and macrophages during the end stage of involution before the gland reverted back to non-pregnant stage [14]. These phagocytotic cells also contribute in clearance of collagen matrix surrounding the involuting lobules [23].

1.2. Cellular composition of the mammary gland

Organ development requires sequentially orchestrated cellular processes, which encompasses lineage fate commitment, proliferation and differentiation of committed progenitor in addition to tissue maintenance. These cellular processes are regulated by paracrine signaling and crosstalk between breast cells, and between breast cells and niche cells. Both human and mouse mammary glands are composed of different cell types including luminal cells and myoepithelial cells (epithelial content arranged as a bilayered structure), fibroblasts, adipocytes, endothelial cells and hematopoietic cells. In ducts, luminal cells are arranged to form a hollow structure that is surrounded by a continuous layer of myoepithelial cells (Fig 1.3), whereas in alveoli, luminal cells are arranged to form a cluster of grape-like cells that is surrounded by basket of myoepithelial cells allowing luminal cells to be in contact with surrounding stroma (Fig. 1.2) [24, 25]. The bilayered arrangement of epithelial cells are surrounded by a basement membrane composed of laminin and collagen. During pregnancy, luminal cells within the alveoli can further differentiate into milk-producing cells. The myoepithelial cells help with ejection of milk into ducts by contracting in the presence of oxytocin [26-28]. These epithelial cells expand during each menstrual cycle by two-fold [29-31]. Interestingly, during pregnancy and lactation, the epithelial content of the breast expands by 9-10 fold [32]. In mice, during pregnancy, a 27-fold increase in epithelial cell number has been observed [32]. Post weaning, there is an increase in apoptosis and the gland reverts back to a non-pregnant state [2, 33]. This dynamic process of expansion and regression makes the gland highly regenerative and allows females to supports multiple pregnancies.

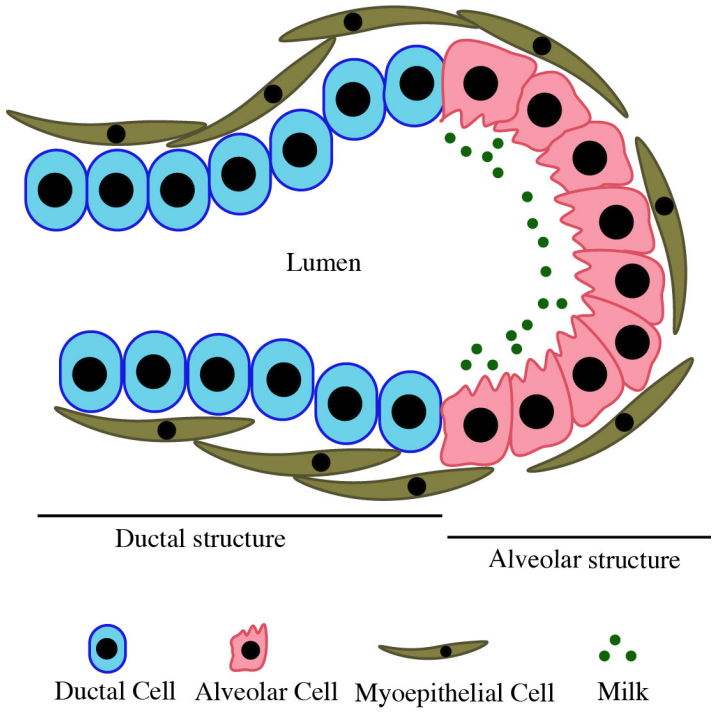

Figure 1.3 Cross section of a human mammary duct and alveolar structure

Pictorial representation of mammary gland cross section showing bilayered arrangement of ducts and alveolar structures containing luminal cells and myoepithelial cells surrounded by a basement membrane. These structures are embedded in a fibrous stroma consisting of immune cells, fibroblasts and adipocytes. In ducts, the apical side of the luminal cell faces a lumen whereas the basal side faces a continuous lining of myoepithelial cells. The myoepithelial cells in alveoli are discontinuous, which allows for luminal cells contact with the surrounding stroma.

1.2.1. Mouse mammary stem cells and progenitors

The regenerative capacity of breast epithelium suggests the presence of stem cells in this environment. It is postulated that these cells differentiated to give rise to bipotent progenitors and lineage-restricted progenitors which eventually generated mature luminal and myoepithelial cells constituting ~90% of epithelial cells in the mammary gland (Figure 1.6). Experimental evidence suggesting that the mammary gland has regenerative potential originates from studies showing that a small fragment from mouse mammary structures can regenerate the entire mammary gland when transplanted into de-epithelized (cleared) mammary fat pads [34]. Following this observation, studies showed that any part of the mammary epithelial tree can produce successful engraftment [35-37], suggesting that cells with a regenerative ability are dispersed throughout the mammary tree. Furthermore, it was hypothesized that the cap cells that line the TEBs may represent the mammary stem cells (MaSCs) as cellular proliferation at the TEBs leads to ductal elongation and without any self-renewing cells the ductal elongation would quickly cease [38-40]. Serial transplantation of retrovirally-marked mammary epithelial fragments into cleared fat pad, showed that a single cell was sufficient to generate the entire mammary epithelium [41]. Subsequent experiments showed that single-cell injections of $CD24^{+}$ $CD49f^{bright}$ (α-6 integrin) or $CD24^{+/mod}$ $CD29^{bright}$ (β1 integrin) into de-epithelized mouse mammary fat pads reconstituted the entire mammary gland [42, 43]. These cells are collectively referred to as the mammary repopulating units (MRUs). Even though MaSCs can be isolated using cell-specific markers ($CD24^{+}CD29^{bright}CD49f^{bright}Sca1^{-}$), this cell fraction offered low enrichment for cells with stem cell activity and therefore researchers examined other parameters such as cell size as a way of improving MaSc enrichment in the fraction. The size of cells was considered and analyzed based on light scatter properties (forward scatter (FSC) using flow cytometry) of the cells. Cells with

smaller size, when transplanted into cleared mammary fat pad, failed to reconstitute the mammary gland while cells with larger size had a regenerative capability and reconstituted entire mammary gland [44]. In another study, the adult intestinal stem cell marker, leucine-rich repeat-containing G-protein coupled receptor 5 (*Lrg5*) gene, was found to be co-expressed with MaSC markers. Interestingly, after birth $Lrg5^{+}$ MaSCs were committed to luminal cell fate. However, 12 days after birth they switched their commitment to the myoepithelial cell lineage [45]. Other studies have shown that both the $Lrg5^{+}$ and $Lrg5^{-}$ subtypes of MaSCs had the ability to reconstitute entire mammary gland upon transplantation [46, 47] challenging the idea that LRG5 is a marker for MaSCs. A more recent study identified a subset of $CD49f^{high}CD24^{+}$ (MRUs) based on high expression of Ox-2 membrane glycoprotein, CD200 and its receptor CD200R1. $CD200^{high}CD200R1^{high}$ MRUs acquired high repopulation ability when injected into cleared mammary fat pads as compared to $CD200^{-}CD200R1^{-}$ MRUs. However, both $CD200^{high}CD200R1^{high}$ MRUs and $CD200^{-}CD200R1^{-}$ subset of MRUs shared some common stem cell markers. This suggested that $CD200^{high}CD200R1^{high}$ MRUs represented stem cells, while $CD200^{-}CD200R1^{-}$ MRUs represented common/bipotential progenitors [48]. Some $CD200^{high}CD200R1^{high}$ cells did not show mammary regenerative activities and were though to represent more differentiated myoepithelial cells. This suggested that CD200 and CD200R1 expression could be potentially used to segregate MaSCs (MRUs) and its progeny, the common/bipotent progenitors from mature luminal and the myoepithelial cells.

In spite of identification of unique stem cell markers, it is still challenging to separate stem cells from other cell types (mature myoepithelial cells and progenitors) in the basal cell compartment. However, identification of multiple surface markers has uncovered distinct subsets of luminal cells. This has allowed researchers to distinguish luminal progenitors from mature

luminal cells as well as the myoepithelial cells. CD24 is one such marker that allows for separation of luminal ($CD24^{high}$) and myoepithelial ($CD24^{low}$) cells [49]. The mouse mammary luminal cell compartment is heterogeneous and contains three major subpopulations of luminal cells; estrogen receptor positive (ER^+) nonclonogenic luminal cells, ER^+ luminal progenitors and ER^- luminal progenitors. It is hypothesized that ER^+ luminal progenitors represent ductal-restricted progenitors as they express FOXA1 a transcription factor, required for ductal morphogenesis [50]. Similarly, ER^- luminal progenitors express high levels of ELF5 and LMO4, which are transcription factors necessary for alveolar fate commitment suggesting its role as an alveolar-restricted progenitor [51]. Additional markers such as CD49b (integrin $\alpha 2$) and CD14 are expressed by all luminal progenitors with restricted expression of CD61 (integrin $\beta 3$) and c-kit [52-55]. The majority of ER^- luminal cells express CD61 with less expression in ER^+ cells. However, these luminal progenitor markers are strain specific. CD61 and a tyrosine-protein kinase kit, c-kit (CD117) can be used only in FVB/N mice but not in C57B16/J mice. Identification of Sca1 and prominin1 as markers of luminal progenitors has been very useful since its expression overlaps with the subset of luminal progenitors expressing, ER and cytokeratin (CK) 8/18. Both Sca1 and prominin1, however, show 100% overlap in expression and therefore appear to be redundant as progenitor cell markers. $CD24^{high}Sca1^+$ or $CD24^{high}prominin1^+$ (luminal progenitors) showed higher expression of CK 8/18 as compared to $CD24^{high}Sca1^-$ or $CD24^{high}prominin1^-$ (mature luminal cells) [53, 56]. In addition, another study suggested that prominin1 expressing cells give rise to ER^+ luminal cells, whereas cells expressing Sox9 give rise to ER^- luminal cells and to some degree basal cells [57]. Another study done on mammary gland from C57BL6/J mice showed that Epithelial Cell Adhesion Molecule (EpCAM) gave better separation of luminal and myoepithelial cell population as compared to CD24 [53]. A combination of different and unique surface marker has been helpful

for isolation of different subsets of mouse mammary epithelial cell populations. To summarize, epithelial cells expressing $CD49f^{high}CD29^{high}CD24^{high}EpCAM^{low}Sca1^{-}CD200^{high}CD200R1^{high}$ are enriched for stem cell activity. The myoepithelial cell population was $CD49f^{high}CD29^{high}CD24^{+}EpCAM^{low}$. Due to expression of common markers and lack of identification of unique markers, it has been a challenge to separate MaSCs from mature and the undifferentiated myoepithelial cell populations. However, a range of unique markers and their expression has helped researchers to isolate luminal subsets. Subset of cells expressing $CD49f^{+}CD29^{low}CD24^{high}EpCAM^{high}CD61^{+}c\text{-}kit^{+}Sca1^{+}CD49b^{+}CD14^{+}$ represented ER^{+} subset of luminal progenitors (ductal progenitors), which gave rise to $CD49^{-}CD29^{-}CD24^{+}EpCAM^{high}CD61^{-}c\text{-}kit^{-}Sca1^{+}CD49b^{-}CD14^{-}$ mature ductal cells. In contrast, $CD49f^{+}CD29^{low}CD24^{high}EpCAM^{high}CD61^{+}c\text{-}kit^{+}Sca1^{-}CD49b^{+}CD14^{+}$ cells represented ER^{-} luminal progenitors (alveolar progenitors), which gave rise to $CD49f^{-}CD29^{-}CD24^{+}EpCAM^{high}CD61^{-}Sca1^{-}CD14^{-}$ mature alveolar cells (Fig 1.6).

1.2.2. Identification of mammary epithelial subtypes via lineage tracing

The transplantation studies have shown that the mammary epithelium consists of a self-renewing population of MaSCs that mediated tissue turnover and homeostasis. These MaSCs had the ability to generate luminal and myoepithelial cells. This suggested that mouse mammary epithelium was organized in a lineage hierarchy. Evidence that defined this hierarchy came from lineage tracing studies.

To track MaSCs and their progeny *in vivo,* researchers have used a tamoxifen-inducible Cre system and a tetracycline-inducible reverse transactivator (rtTA) system. In the tamoxifen-inducible system, the Cre (fused to mutated ligand binding domain of ER) site was engineered downstream of a promoter of interest (Figure 1.4) while in the latter system, rtTA was downstream of a cell-specific promoter which in the presence of doxycycline-induced Cre expression driven by TetO promoter (Figure 1.5) [58]. These transgenic mouse models were used to provide experimental evidence that mouse mammary epithelial cells were organized in a lineage hierarchy, which is discussed in the following sections.

1.2.2.1. Lineage tracking of the bipotent stem/progenitor cells in mouse mammary gland

Evidence for the presence of mammary stem cells and progenitors came from transplantation studies and *in vitro* colony forming assays. However, the nature of the relationship between these undifferentiated cells and their contribution to mammary gland development and tissue maintenance in the adult gland was unknown. Initial lineage tracing experiments were carried out using CK14-Cre/Rosa-YFP reporter mice. During embryonic development, CK14 expression was observed in all mammary epithelial cells, and their progeny (both luminal and myoepithelial cells) were YFP^{+}. However, after birth, during puberty and thereafter, CK14-YFP expression was restricted to myoepithelial cells. This suggested that the bipotent stem/progenitor

cells gave rise to both luminal and myoepithelial lineages during early development. Interestingly, in the postnatal mammary gland, unipotent luminal and myoepithelial progenitors control tissue homeostasis [59]. Another study suggested that AXIN5^{+} cells, which are Wnt signaling-responsive, retained their plasticity in the postnatal mammary gland and can give rise to both luminal and myoepithelial cells depending on specific signals they receive from their niche, suggesting the presence of bipotential stem/progenitor cells. Further proof for the existence of bipotent stem cells was provided using a 3D imaging technique. Chimeric mice expressing a fluorescent protein under control of Elf5 whose expression is restricted to luminal cells [60] and the *Ck5* promoter was used to track luminal and myoepithelial cells accordingly. Three-dimensional confocal imaging at high cellular resolution revealed that CK5^{+} myoepithelial cells generated patches of epithelial cells, comprised of both luminal (ELF5^{+} luminal progenitors) and myoepithelial cells. The ELF5^{+} cells produced patches of luminal only cells [47]. These observations strongly suggested the presence of CK5^{+} bipotent stem/progenitor cells *in vivo*, which gave rise to lineage-restricted progenitor and contributed towards ductal and alveolar morphogenesis. However, lineage tracking study using a $R26^{CreERT2}$; $R26^{Confetti}$ system suggested that MaSCs exhibited lineage bias during the embryonic and postnatal mammary gland development. Tamoxifen induction in these mice resulted in mammary branches containing single as well as multicolor labeled cells. This was due to proliferation of single color labeled cells within TEBs that mediated branch morphogenesis [61].

1.2.2.2. Lineage tracking of the luminal progenitor cells in the mouse mammary gland

Using inducible doxycycline *Elf5* gene promoter in transgenic mice, the luminal progenitor cells were tracked in the developing and postnatal mouse mammary gland. Confocal imaging of

whole mount glands from *Elf5*-rTA-IRES-GFP mice revealed that *Elf5*-GFP expression was restricted to inner luminal layer, suggesting *Elf5* as a unique marker for luminal cells. Interesting, only *Elf5*-GFP positive cells isolated had clonogenic ability, which suggested that all *Elf5*+ cells represented luminal progenitors. Tracking of *Elf5*$^{+}$ cells showed that the pool of *Elf5*$^{+}$ labelled luminal progenitors were observed during puberty and pregnancy, but were gradually depleted during involution as well as in the aging gland, suggesting that they are different from bipotent stem/progenitor cells [47]. Another study showed that a subset of mammary epithelial cells, the Parity-identified mammary epithelial cells (PI-MECs) that are responsive to pregnancy hormones (discussed in a later section), give rise to only ER^{-} luminal cells. PI-MECs survive involution and reside in the luminal layer of ducts. These cells are known to be the major source of milk-producing cells in alveoli in subsequent pregnancies [62]. The PI-MECs were tracked using Whey acidic protein (WAP) promoter, which shows higher expression during pregnancy and the entire lactation phase. 'WAP-Cre;Rosa26-YFP' reporter system revealed that during pregnancy and lactation, the majority of alveoli consisted of YFP^{+} cells. During involution, there was a drastic reduction in YFP^{+} cells, and only the regressed ducts retained them. These cells represented PI-MECs. Interesting, during a second pregnancy, newly formed alveoli contained YFP^{+} cells suggesting that they were derived from involution survived PI-MECs (YFP^{+} cells). This study suggested the presence of unipotent lineage biased cells in the luminal layer of ducts which contributed towards development of alveoli during pregnancy and lactation [63]. A similar observation was made using a chimeric mouse where the origin and fate of CK8+ luminal cells were tracked (CK8-creER/Rosa-YFP reporter system), suggesting the presence of unipotent luminal stem/progenitor cells. Tamoxifen induction at a different time point in postnatal development revealed the presence and clonal expansion of CK8-YFP^{+} cells suggesting that they were derived from a single cell [59].

Interestingly, lineage tracing of NR3 expressing cells revealed that $NR3^+$ cells are transiently quiescent luminal progenitors with the potential to generate both ER^+ and ER^- ductal cells [64].

Unfortunately, lineage tracking of human breast cells *in vivo* has not been very successful as the native niche for human breast epithelial stem and progenitor cells cannot be adequately created in immunodeficient mice. Because of this issue, there is very little experimental evidence to support the presumed lineage hierarchical structure of human breast epithelial cells.

On the other hand, chimeric mouse technology has offered a powerful research tool to follow and study the different mammary epithelial cell lineages. These studies have provided strong proof that the mouse mammary epithelial cells are organized in a lineage hierarchy, where mammary stem cells differentiate to generate bipotent progenitors. These bipotent progenitors further differentiate into unipotent progenitors that ultimately produce mature luminal and the myoepithelial cells required to support multiple regenerative properties of the mammary gland (Figure 1.6).

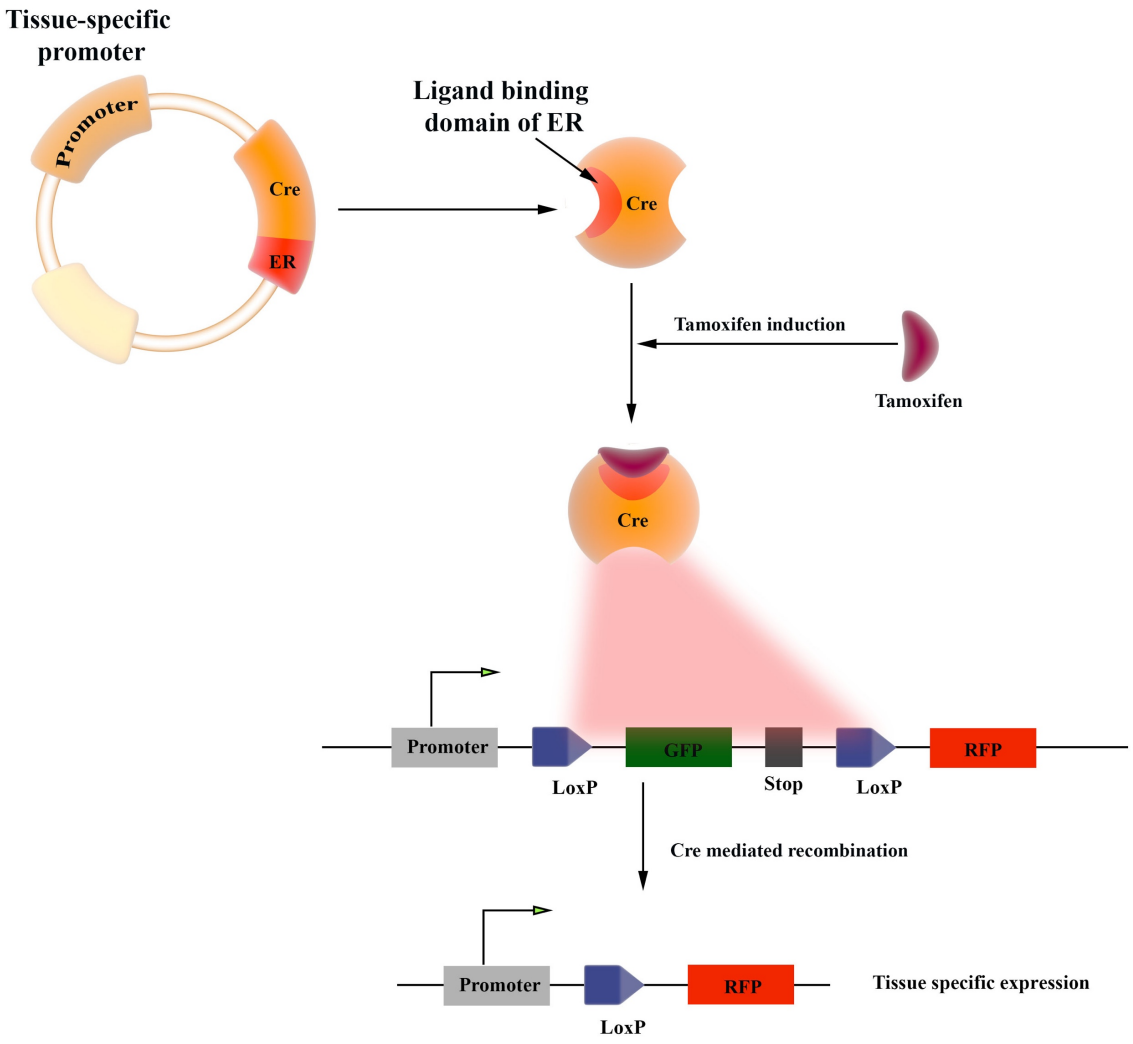

Figure 1.4 Tamoxifen inducible Cre system

Schematic showing the mechanism of tamoxifen inducible Cre system used to regulate specific gene expression for lineage tracking experiments.

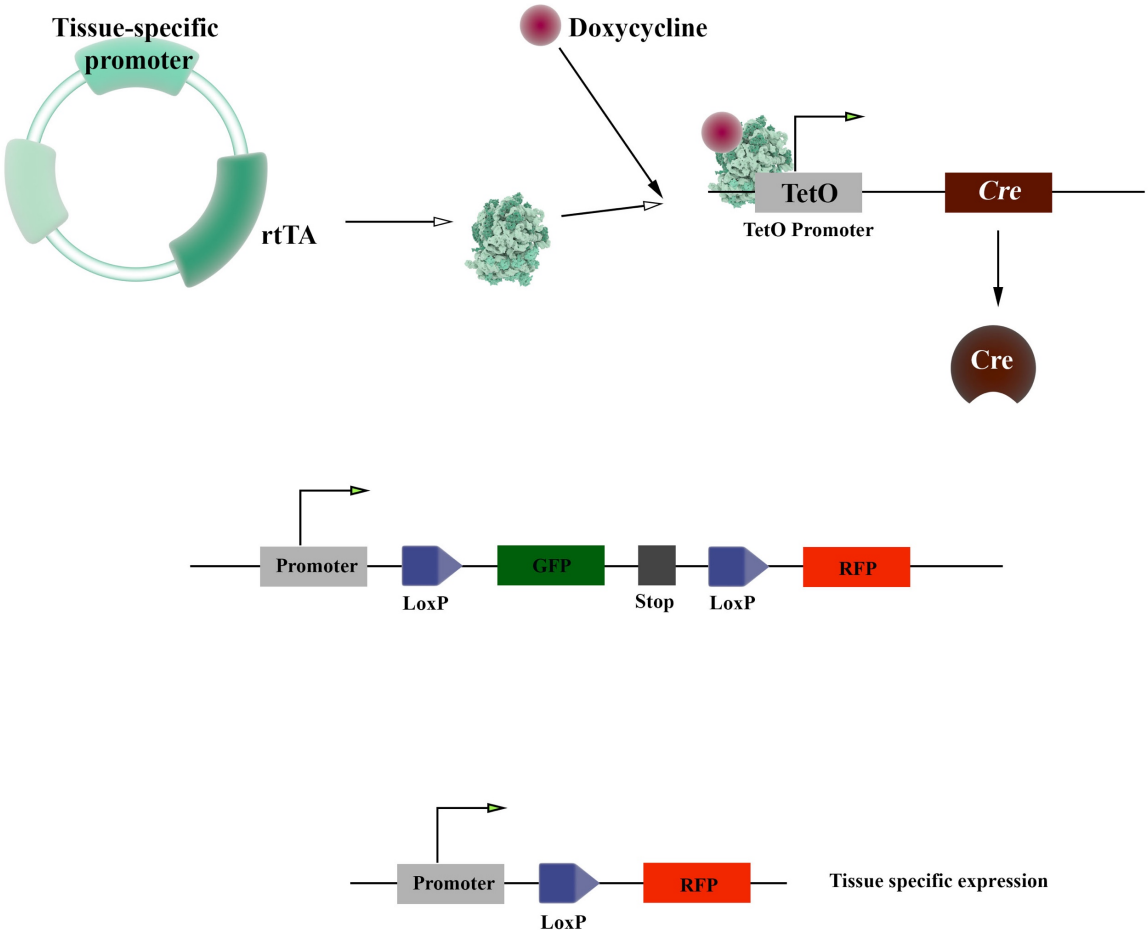

Figure 1.5 Tetracycline inducible reverse transactivator system

Schematic showing the mechanism of tetracycline inducible Cre system used to regulates gene expression for lineage tracking experiments.

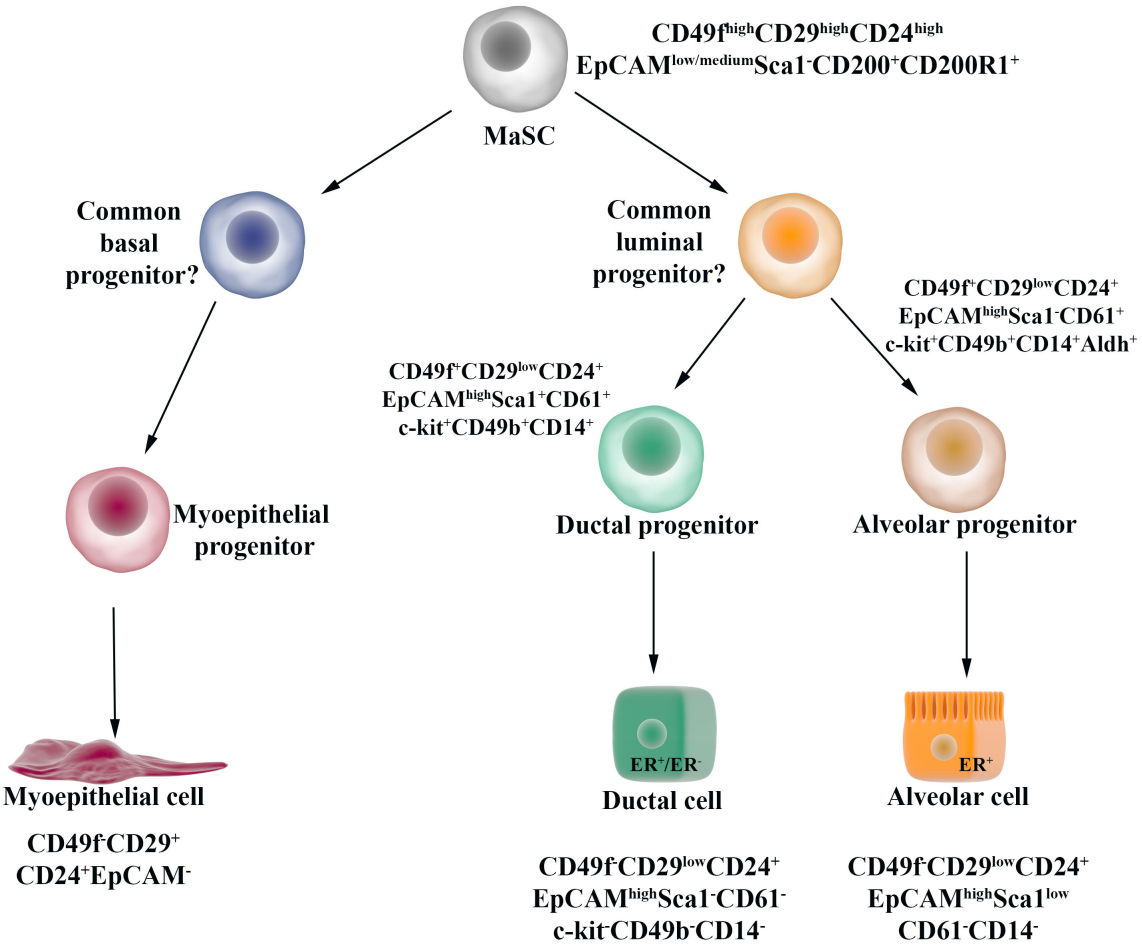

Figure 1.6 Hierarchical arrangement of mouse mammary epithelial cells

Schematic showing the hierarchical arrangement of mammary epithelial cells and the cell surface marker expression profile. The most primitive mammary stem cells occupy the top of the hierarchy as they possess self-renewal and differentiation ability. Stem cells give rise to progeny with limited or no self-renewal capacity such as the luminal-restricted progenitors and myoepithelial-restricted progenitors. These restricted progenitors eventually differentiate to give mature luminal or basal cells of mammary gland.

1.2.3. Human breast epithelial stem cells and progenitors

Insight about stem cells in the human breast came from both *in vivo* and *in vitro* studies. The presence of stem cells in human breast epithelium was confirmed from studies that analyzed the methylation status of X-linked genes resulting in X-chromosome inactivation at the preimplantation stage of development. These studies showed that regions of ducts and lobules of the breast had the same X-chromosome inactivation, suggesting they originated from a single (stem) cell. Cells with similar X-inactivation trait were observed throughout the reproductive life of an individual and multiple breast regeneration cycles [65]. Fat pad injections of fragments of primary human breast organoids proved to be challenging. This was due to an unfavorable microenvironment of the mouse mammary fat pad is adipocyte rich. This problem was overcome when $EpCAM^{-/low}$ and $CD49f^{bright}$ cells along with irradiated human fibroblasts were placed in a collagen gel and xenografted under the kidney capsule of hormone supplemented immunodeficient mice. Estrogen and Progesterone supplementation was necessary to mimic human serum levels of these hormones. Xenografted cells gave rise to bi-layered ductal and alveolar structures [66, 67]. Furthermore, the use of humanized mice, where the mouse mammary fat pads were populated by human fibroblasts proved to be useful to study regenerative ability of human breast stem cells. Serial transplantation experiments showed that $EpCAM^{-ve/low}CD49f^{bright}$ cells have self-renewal capacity and generated mature luminal and myoepithelial cells that make up breast structures and therefore possess similar properties as the breast epithelial stem cells (BESCs) [66, 67]. All these experiments suggested that $EpCAM)^{-/low}CD49f^{bright}$ cells are a heterogeneous population of cells with bi-lineage differentiation capacity. Similar to the mouse mammary gland, the luminal cell population in human breast tissue can be separated from myoepithelial cells based on their expression of EpCAM and CD49f. $EpCAM^{bright}CD49f^{+}$ breast epithelial cells scored as luminal

cells when grown *in vitro*, whereas EpCAM^{bright}CD49f^{-} lacked this colony forming ability and represented terminally differentiated luminal cells [68]. The EpCAM$^{-/low}$CD49f^{bright} cells generated cells with a myoepithelial-like phenotype [67, 69, 70]. An additional marker, C-kit offered further separation of luminal progenitors (CD49f^{+}c-KIT^{+}) from differentiated luminal cells [69, 70]. The luminal progenitors showed increased aldehyde dehydrogenase 1 (ALDH1) activity as compared to bipotent stem/progenitor cells [53] and ALDH1 activity could be used to separate subtypes of luminal progenitors [71]. The ALDH1^{+} subset of EpCAM$^{-/low}$CD49f^{bright} human luminal progenitors showed similarity to ER^{-} mouse luminal progenitors. Interestingly, ALDH1^{-} luminal progenitors showed higher expression of a ductal cell marker FOXA1, and ALDH1^{+} luminal progenitors expressed high levels of ELF5 as well as milk proteins, milk fat globule-EGF factor 8 protein (MFGE8) and lactoferrin (LFT). Thus ALDH1^{+} luminal cells are primed to generate alveolar luminal cells, and ALDH1^{-} luminal cells to ductal luminal cells. However, unlike the mouse, both ALDH1^{+} and ALDH1^{-} cells shared few common molecular profiles. Even though luminal progenitors (EpCAM^{+}CD49f^{+}) can only generate luminal colonies *in vitro* [67, 70], a subset of luminal progenitors (EpCAM^{+}CD49f^{+}ALDH1^{+}) possess bi-lineage potential [72, 73]. Such observations, however, remain controversial as other studies have challenged the luminal-restricted potential of ALDH1^{+} cells. Such studies showed that cells expressing ALDH1 could reconstitute mammary structures in the humanized mouse [73, 74] similar to BESCs [67]. The difference in these reported observations could partially related to different assay condition. Isolating epithelial cells, removed from their niche, could cause reversal of progenitor phenotype (a process referred to as dedifferentiation); however, experimental evidence for this is lacking.

The *in vitro* culture system was developed to study the differentiation ability of breast epithelial progenitor cells. For the purpose of such assays, the leftover tissue from cosmetic breast

reduction surgeries (mammoplasty) are used as the source of primary non-malignant (normal) human breast cells. When epithelial cells dissociated from breast reduction mammoplasty samples were cultured at a clonal density along with irradiated mouse fibroblasts, over a period of 7-10 days, they generated morphologically distinct colonies. These colonies were of three types; pure myoepithelial colonies consisting of dispersed, tear drop shaped cells which stain positively for myoepithelial cell markers (CK14, CD90, p63), pure luminal colonies consisting of tightly organized cuboidal cells with smooth boundary expressing luminal cell markers (Mucin 1 (MUC1), CK8-18 and CK19) and colonies with a tightly organized luminal centre surrounded by dispersed myoepithelial cells (Fig 1.7). This assay then allows for prospective identification of three distinct colony forming cells (CFCs), namely; myoepithelial- restricted colony forming cells (CFC), luminal-restricted CFCs and a more primitive bipotential CFCs that can differentiate to generate colonies consisting of both luminal and the myoepithelial cells. With the exception of myoepithelial-restricted CFCs, it was shown that both bipotential CFC and luminal-restricted CFCs can be isolated as a separate cell population. From freshly isolated human breast epithelial cells, the $EpCAM^{-/low}CD49f^{bright}$ subset generated mostly bipotential CFCs, whereas $EpCAM^{bright}CD49f^{bright}$ cells generated luminal-restricted CFCs in colony assays. It is noteworthy that re-plating experiments showed that these colonies contain cells with significantly diminished colony-forming ability suggesting they contain more mature and differentiated epithelial cells. Based on these observations, CFCs are thought to represent distinct progenitor subsets of breast epithelial cells [75]. However, the purity at which these CFC can be obtained from freshly isolated breast cells was 1-5%, making further characterization difficult. Interestingly, the bipotent and luminal-restricted progenitors can be obtained at higher purities (20-25%) when the breast epithelial cells from reduction mammoplasty samples were pre-cultured for 3-4 days. Among the

pre-cultured human breast epithelial cells, the $EpCAM^{+}CD49f^{+}$ represented cells with clonogenic potential whereas, the $CD49f^{-}$ population lacked the colony forming ability. Within the $EpCAM^{+}CD49f^{+}$ population, the $MUC1^{-}AC133^{-}CD90^{+}$(THY1) subset was enriched for the bipotent progenitors and the $MUC1^{+}AC133^{+}CD90^{-}$ cells represented luminal-restricted progenitors with approximately 45% and 33% purity respectively [76]. Thereby, preculturing the primary human breast cells and the use of 5 different cell surface markers, different progenitor subsets can be obtained at high enough purity allowing their further characterization [69, 76-78]. These advances allowed the bipotent and luminal-restricted progenitors to be obtained at sufficiently high purities to enable their further characterization at the molecular level [46]. Interestingly, while the $MUC1^{-}CD133^{-}CD90^{+}$ subset of $EpCAM^{+}CD49f^{+}$ cells enriched for bipotent progenitors, yet this subfraction of cells also contained luminal CFCs though at low frequencies (3-5%). In contrast, the luminal-restricted progenitor subset of $EpCAM^{+}CD49f^{+}$ cells were 100% pure luminal CFCs and contained no other CFC subtypes.

1.2.3.1. Hierarchical arrangement of human mammary stem cells

Human breast tissue undergoes continuous tissue remodeling during pubertal, pregnant and postpartum stages. This process of remodeling requires constant replacement of cells within the breast that is only possible in the presence of BESCs which possess the ability to self-renew and differentiate to generate luminal and the myoepithelial cells. The evidence that BESCs give rise to epithelial cells (luminal and myoepithelial cells) that are different from its precursor cells suggests that the breast epithelial cells could be organized in a lineage hierarchy [66, 67, 76] (Fig 1.8). Using cell surface markers, it was possible to isolate different subtypes of breast epithelial cells at the highest purity. $EpCAM^{+}CD49f^{+}CD10^{+}CD90^{+}MUC1^{-}CD133^{-}$ (bipotent CFCs) epithelial cells

generated both luminal and the myoepithelial cells in the CFC assay. Whereas the $EpCAM^{+}CD49f^{+}CD10^{-}CD90^{-}MUC1^{+}CD133^{+}$ (luminal-restricted CFCs) epithelial cells generated limited number of luminal colonies only. The $EpCAM^{+}CD49f^{-}MUC1^{+}CD133^{+}CD90^{-}CD10^{-}$ (mature luminal cells) did not have the ability to form colonies *in vitro* [68, 79]. Similarly, myoepithelial-restricted progenitors generated only myoepithelial colonies [79, 80]. These results suggested that bipotent CFCs can be placed on top of luminal-restricted CFCs and the myoepithelial-restricted progenitors in the hierarchy and mature luminal and the myoepithelial cells are progenies of luminal-restricted and myoepithelial-restricted progenitors, respectively.

While much is known about the stem and progenitor cells in mouse mammary gland, much less is known about the exact relationship between human breast epithelial stem and progenitor cells. Due to the overlapping expression of EpCAM and CD49f, the bipotent progenitors cannot be distinguished from stem cells. Moreover, due to lack of lineage tracking experiments, the experimental evidence that the bipotent progenitors give rise to lineage-restricted progenitors remains a conjecture at this point.

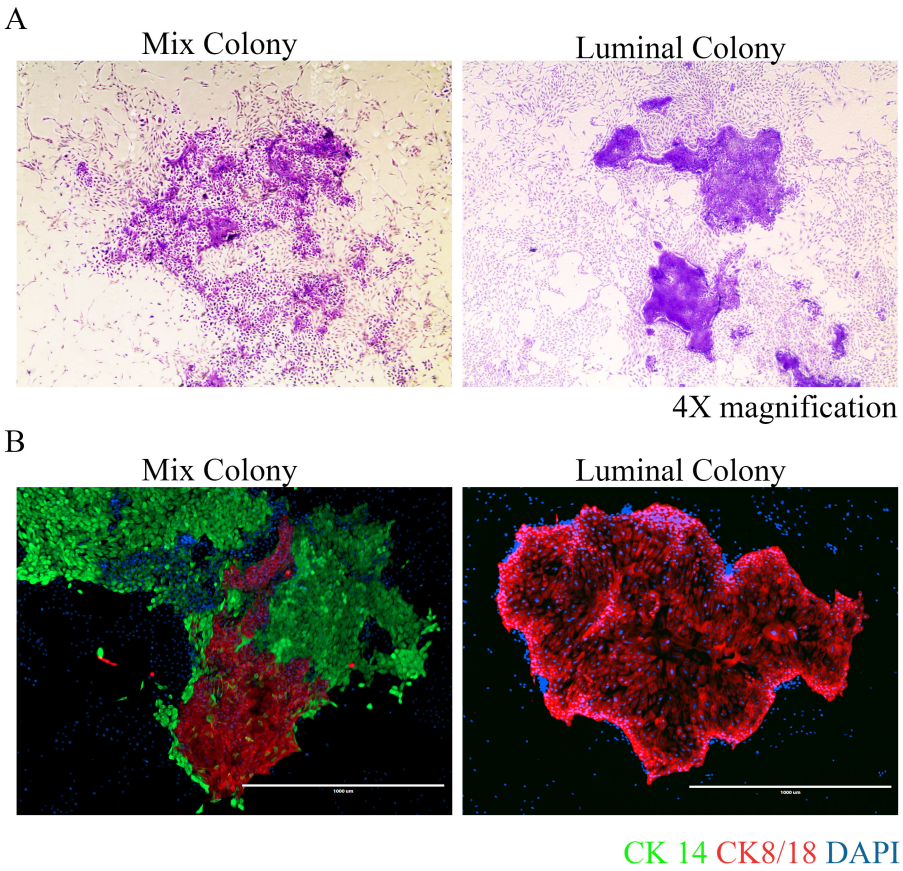

Figure 1.7 Types of human mammary epithelial colonies generated in vitro

(A) Crystal violet staining of breast epithelial colonies generated from human bipotent progenitors and the luminal progenitors placed in colony forming cell (CFC) assay after 7-10 days. The bipotent progenitors generated both types of colonies; pure luminal colony (right) with defined boundary and contains cuboidal luminal cells only and the mix colony (left) containing both luminal and tear drop shaped myoepithelial cells. (B) Cytokeratin 8/18 and 14 staining of luminal and mix colonies. CK8/18 is a luminal cell specific marker and CK14 is a myoepithelial cell specific marker. Scale =1000µm.

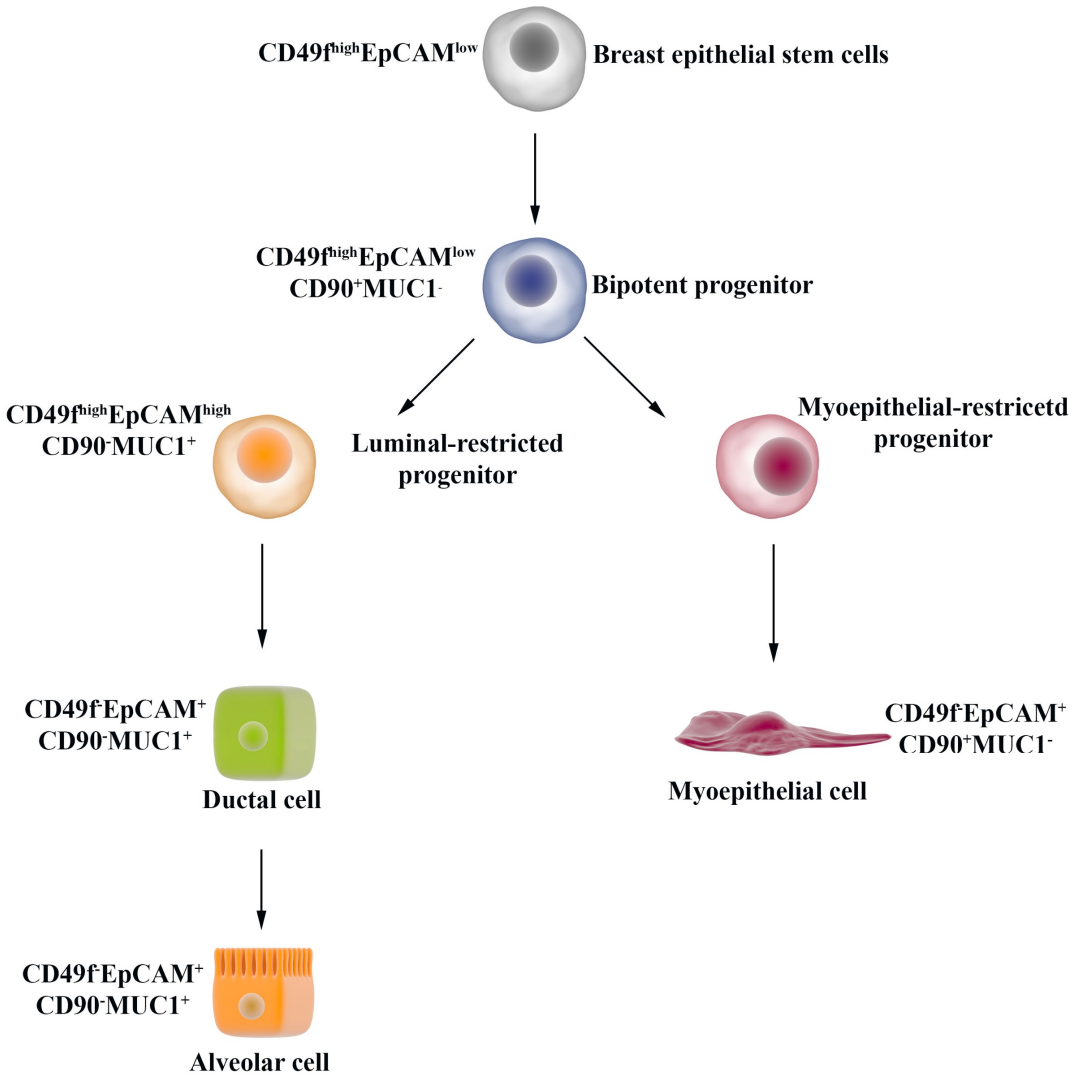

Figure 1.8 Hierarchical arrangement of human mammary epithelial cells

Schematic showing the hierarchical arrangement of human mammary epithelial cells. The human mammary stem cells with unlimited self-renewal ability differentiate to generate bipotent progenitors. The bipotent progenitors have the ability to either differentiate into luminal-restricted progenitor and the myoepithelial progenitors. From these progenitors, mature mammary epithelial cells are generated which form ducts or the alveolar structures of the breast tissue.

1.2.4. Growth factors and molecular regulation of mammary gland development

The proper functioning and homeostasis of mammary epithelium rely on intrinsic and extrinsic signals. In this regard, the breast tissue environment of the niche plays a critical role in regulating stem cell and progenitor cell functions. Mammary stem cell niche is enriched for growth hormones such as the estrogen and progesterone and during pregnancy the prolactin hormone. Other secreted factors that have been shown to play essential roles in mammary gland development include insulin-like growth factors (IGFs) and their binding proteins (IGFBPs) such as IGFBP3 and IGFBP7 [81].

Transcription factors as effectors of the highly conserved Notch and Wnt signaling networks [82-85] have been shown to play essential roles in mammary gland development by regulating lineage commitment (differentiation), proliferation and the self-renewal potential of the breast epithelial stem and progenitor cells [76, 85-88]. Similarly, the presence of other cell types in the niche (e.g. immune cells) could impact stem and progenitor cell function. In this regard, mammary tissue-resident macrophages were shown to help in regulation of mammary stem cell function via activation of Notch and Wnt signaling crosstalk [20].

These secreted factors and hormones along with activation of signaling pathways and their crosstalk work in concert to carefully regulate breast epithelial stem and progenitor cell function to enable the multiple regenerative cycles of breast tissue.

1.3. Signaling pathways regulating mammary gland development and function

The knowledge about the role of genes and signaling pathways involved in mammary gland development and maturation is very limited. However, the availability of techniques to isolate different mammary epithelial populations has allowed the study of gene expression pattern and the signaling pathways in the subtypes of mammary epithelial cells. Some of the pathways include estrogen signaling, the Notch, the Wnt and the NF-κB signaling.

1.3.1. Role of hormone signaling

The majority of epithelial cells in the postnatal mammary gland express receptors for female hormones. The function of the mammary gland is regulated directly or indirectly by steroid (estrogen and progesterone) and simple peptide hormones (prolactin). Female hormones, estrogen and progesterone produced in the ovaries play a crucial role in normal mammary gland development and function [2, 89].

1.3.1.1. Steroid hormones (Estrogen and Progesterone)

Estrogen is a steroid hormone that is required for the female reproductive system, however, it has no role in embryonic mammary gland development. Estrogen signaling is essential to the postnatal mammary gland development and its further maturation during puberty. Estrogens are typically found in 4 forms where 17-β-estradiol (estradiol) is the most prevalent form during reproductive age. In humans, until puberty, both male and female mammary gland development pattern is the same. However, once puberty is attained, ovaries produce estrogen and progesterone in females which promotes mammary gland development into an intricate network of ducts and alveolar structures. On the other hand, the male mammary gland doesn't undergo any change

during puberty and has only rudimentary mammary structures. In some conditions, males with increased estrogen and decreased androgen (Gynecomastia) results in an enlarged breast.

Similar to most hormones, estrogen is hydrophobic and crosses the cell membrane with ease to exert its biological effects. Estrogen signals through two receptors, estrogen receptor alpha (ERα) and estrogen receptor beta (ERβ) (Fig 1.9). The active form of estrogen, 17-β-estradiol (estradiol) activates both. ERβ is ubiquitously expressed within the mammary gland, whereas ERα expression is restricted to luminal epithelial cells. Gene knockout studies in mice have demonstrated that loss of ERα but not ERβ resulted in development of rudimentary ducts only, indicating that ERα was necessary for ductal elongation and invasion of ducts into the mammary fat pad during puberty [89-92]. ERα expression analysis in purified progenitors from human breast reduction mammoplasty samples revealed that a very weak ERα expression was seen in bipotent progenitors, whereas luminal-restricted progenitors had higher expression of ERα.

Along with estrogen, progesterone is involved in pregnancy-induced changes to the mammary gland and during lactation. Progesterone is required for regulating ductal branching and lobuloalveolar development [93]. Using the mouse estrous cycle as a model, the influence of progesterone on MaSCs was investigated. Serum progesterone levels peak during dioestrus phase and analysis of inguinal gland showed enhanced branching and development of lobuloalveolar structures. The presence of progesterone induces a ~10-fold increase in PR^- MaSCs in a paracrine fashion [94].

The progesterone effect is mediated through activation of the progesterone receptor (PR) isoforms PR-A (N-terminus truncated version of full-length PR-B) and PR-B (Fig 1.10). Progesterone has been shown to play an important role in mammary gland development especially during early pregnancy and its loss has resulted in defective alveolar development [95]. PR-A

isoform-specific mutational studies in mice which have normal PR-B isoform levels showed normal ductal branching and alveolar development suggesting PR-B isoform was sufficient in this context [96]. The abnormal branching phenotype of PRB-deficient mammary glands shows the importance of progesterone signaling in branching morphogenesis. In the human mammary gland, PR-B expression is mainly observed in ERα$^-$ luminal epithelial cells that are surrounded by ERα$^+$ cells. However, in mouse mammary tissue, expression of ER and PR are quite different. The majority of the mammary epithelial cells express both receptors. This suggests the existence of different estrogen and progesterone signaling process and regulation of mammary gland development and function in humans compared to the mouse. Since breast stem cells and progenitors are responsible for generating the millions of mature cells that are required during pregnancy and the menstrual cycles, it is not surprising that estrogen and progesterone signaling regulates the proliferation and differentiation of these primitive undifferentiated cells. Detailed study of undifferentiated breast epithelial progenitors reveals that while ERα expression is very low/undetectable in bipotential progenitors, PR transcription is high [76]. On the other hand, luminal-restricted progenitors showed significant ERα transcript expression and very low PR transcript levels. A recent study demonstrated a direct link between estrogen signaling and the luminal progenitor expansion as well as differentiation at the molecular level. Luminal progenitors generated more colonies in the presence of estradiol, whereas treatment with fulvestrant (selective estrogen receptor degrader) abrogated colony forming ability. Estradiol stimulated the proliferation of luminal progenitors but not the bipotent progenitors. They further showed that the pro-proliferative effect of estrogen on the luminal progenitors required expression of a non-protein coding RNA, H19 [97].

1.3.1.2. Role of peptide hormone (Prolactin)

Prolactin is a peptide hormone secreted from the anterior pituitary gland that in combination with estrogen and progesterone are referred to as pregnancy hormones. They work together to facilitate pregnancy-related changes in the mammary gland. Prolactin influences enhanced proliferation of lobuloalveolar epithelium during pregnancy and lactation. Indeed, these hormones induce lobule generation during mammary gland development and maintenance of milk secretion during lactation. Prolactin-deficient mice showed a normal ductal tree; however, the ducts failed to generate lobular structures due to a lack of luminal cell proliferation, suggesting its role in lobuloalveolar development [98, 99]. Mice with a germ-line mutation in the prolactin receptor showed reduced mammary gland development and impaired milk production [100]. Injection of prolactin into prolactin deficient mice resulted in the generation of rudimentary lobules. These data suggested that progenitor cells in ductal epithelium respond to exogenous prolactin by activating lobuloalveolar development [101-103]. Interestingly, prolactin can also induce expression of the progesterone receptor in mammary epithelium, and it can promote secretion of progesterone by inhibiting 20α hydroxysteroid dehydrogenase [104]. Thus, loss of prolactin can indirectly affect progesterone secretion. Prolactin signaling is initiated upon binding to the prolactin receptor that regulates the gene expression of milk protein genes such as those encoding β-casein, β-lactalbumin, β-lactoglobulin and Whey acidic protein (WAP). Binding of prolactin to its receptor results in homodimerization of the receptors and activation of tyrosine kinase Jak2. This, in turn, promotes autophosphorylation of Jak2 and phosphorylation of both Stat5 (pStat5) and the prolactin receptor itself. pStat5 then translocate into the nucleus and regulates expression of milk protein genes by binding to “Stat5 binding elements” present in 5’ regulatory

regions of these genes. These data suggested that prolactin plays an important role during mammary gland development especially during pregnancy and lactation.

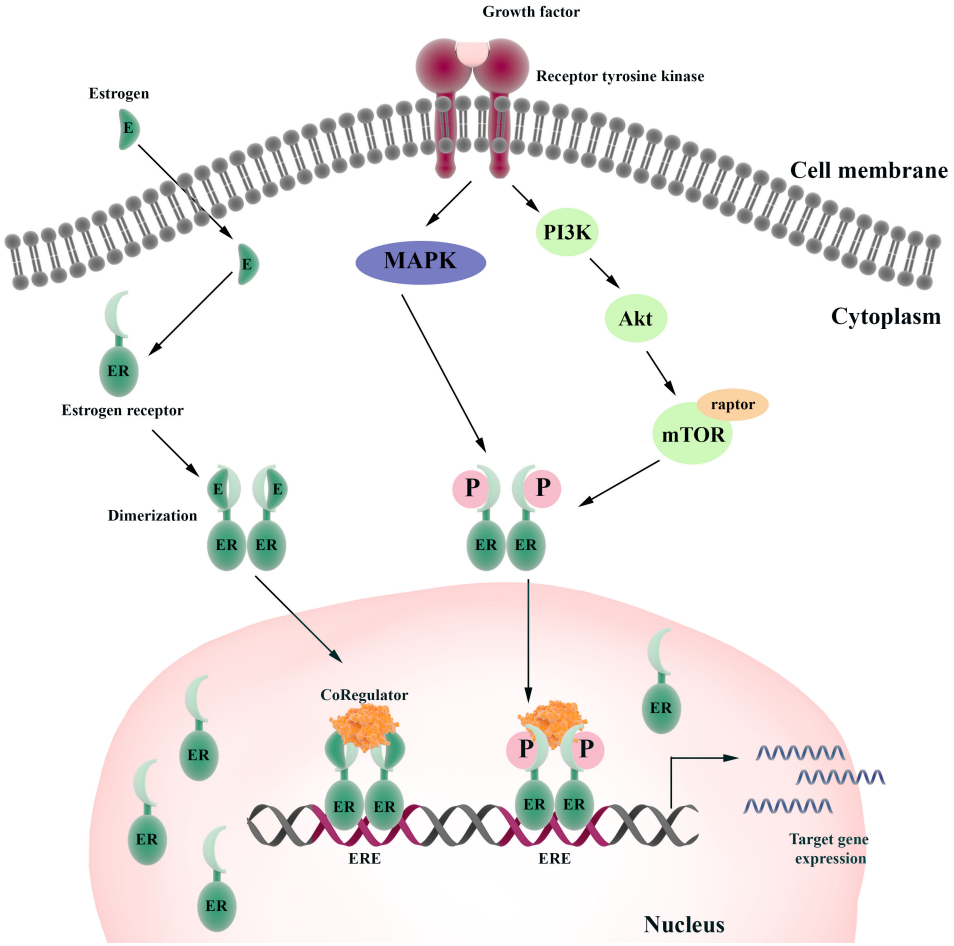

Figure 1.9 Estrogen receptor signaling

Schematic showing estrogen receptor (ER) signaling. Under ligand-dependent signaling conditions, in the presence of estrogen, the ER dimerizes and translocates into the nucleus and binds to estrogen responsive element (ERE) on the promoter and enhancer region of target genes. Under ligand independent signaling condition, ER dimerization can be stimulated by growth factor signaling. The ERE bound estrogen receptor in presence of other cofactor regulates expression of estrogen responsive genes.

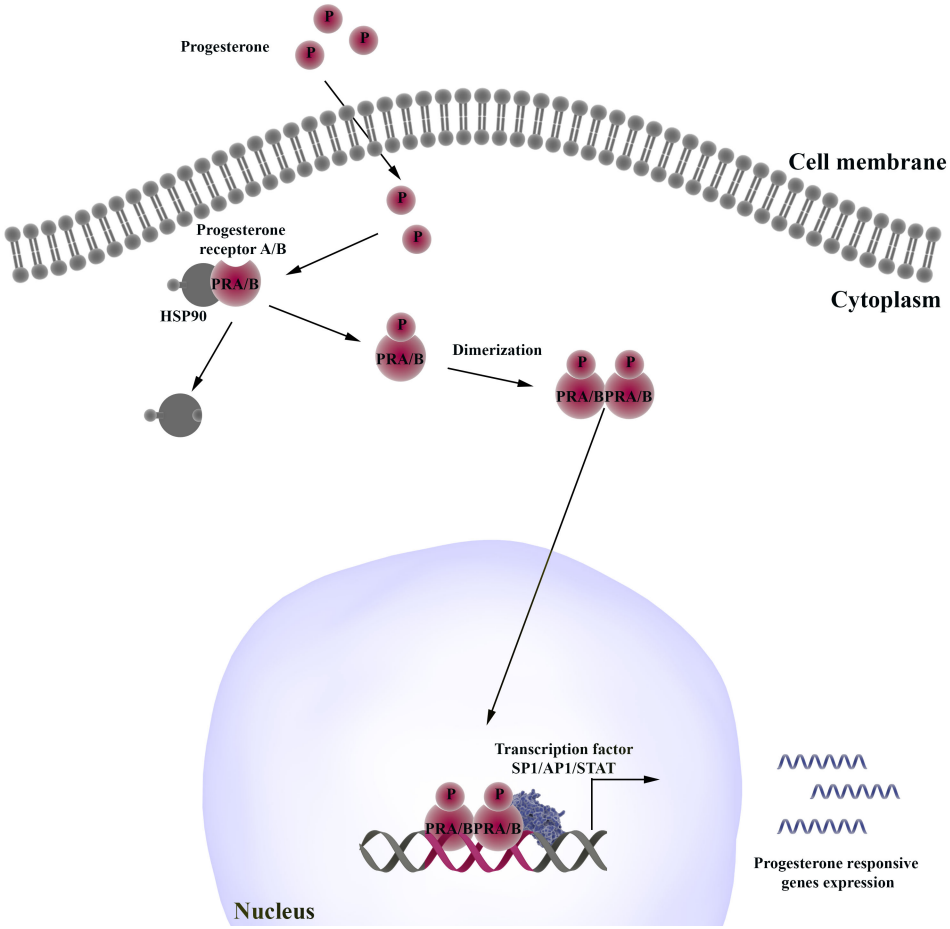

Figure 1.10 Progesterone receptor signaling

Schematic showing the progesterone signaling mechanism. Progesterone binds to progesterone receptors A and B (PR-A and PR-B) which translocate into the nucleus and activate progesterone responsive genes. Female hormone progesterone binds to progesterone receptor which translocate into the nucleus and activates progesterone responsive genes.

1.3.2. Role of Notch receptor signaling

The evolutionarily conserved Notch signaling pathway plays a major role in embryonic development and the maintenance of the adult tissue [105]. This pleiotropic pathway is also associated with cell fate decisions, especially the stem cells and progenitors [106, 107].

1.3.2.1. Notch signaling network

Notch signaling occurs between neighboring cells. The Notch gene encodes a transmembrane receptor (4 different NOTCH receptor (NRs) 1-4) expressed on the surface of "signal-receiving" cells. These receptors interact with 5 different Notch ligands (Delta-like 1, 3 and 4, Jagged1 and 2) expressed on the surface of a "signal-sending" cell that are neighboring the "signal-receiving" cells and thus requires cell-cell contact [108]. Structurally, all four Notch receptors share a similar basic backbone. However, NOTCH1 (NR1) and NOTCH2 (NR2) are most similar, whereas NOTCH3 (NR3) and NOTCH4 (NR4) show a significant divergent from NR1 and NR2 [109]. In humans, NR1 is widely expressed whereas NR2-4 expression is limited to a few cell types. However, cells can express both Notch receptors and ligands simultaneously [110, 111] but when a strong signal is sent to a signal-receiving cell, ligand expression is usually downregulated while Notch receptor expression is increased at the same time. In this way, Notch signaling is unique from other signaling pathways in that its activation can induce different signaling and thus different fates in signal-receiving and signal-sending cells, a mechanism also referred to as lateral inhibition [112]. This cellular communication via receptor-ligand interaction triggers two successive rounds of proteolytic cleavage of Notch receptors. The first is mediated by metalloprotease ADAM17 at the S2 extracellular domain of the receptors resulting in the release of the Notch extracellular domain. This is followed by γ-secretase mediated proteolysis of

the Notch Intracellular domain (NICD), releasing this portion of receptor into the cytoplasm. The NICD is also referred to as the active form of a Notch receptor since this fragment transduces the Notch signal [113-116]. Cleaved NICD does not bind to DNA directly but binds to Recombination signal Binding Protein for immunoglobulin Kappa J region (RBPJ-κ), also known as CBF1-Suppressor of Hairless-Lag-1 (CSL). CSL is typically bound to its consensus DNA binding sites (TGGGAA) in the promoter and enhancer regions of the Notch target genes, and functions as a transcriptional repressor in the absence of NICD. However, upon binding of NICD, it displaces corepressors including Nuclear receptor co-repressor 2 (NCOR2) and nucleates a transcriptional activating complex by recruiting Mastermind-like 1 (MAML1) and other transcription factors and coactivators such as p300 and CREB binding protein (CBP) and p300/CBP- associated factor (PCAF), [117-123] (Fig 1.11). This newly formed CSL transcriptional activator then initiates transcription of Notch target genes (Table 1.1) [124-126]. In this way, it is generally believed that Notch receptors have overlapping functions as they act through a CSL complex to activate transcription of common target genes. Recent data are emerging to suggest that NICD can activate target gene expression independent of CSL complex [87], which challenges the notion of Notch receptor function redundancy.

Thus Notch signaling is highly conserved and plays an important role in regulating complex cellular processes such as lateral inhibition, lineage determination, tissue boundary formation, cellular differentiation, proliferation, self-renewal and apoptosis in organisms from *Drosophila* to man [76, 127-147].

Table 1.1 List of some common Notch target genes

Notch target genes	**Reference**
HES1, Hairy and enhancer of split 1	[124, 148, 149]
HES5, Hairy and enhancer of split 5	[148, 149]
HES7, Hairy and enhancer of split 7	[148]
HEY1, Hairy enhancer of split related with YRPW motif protein 1	[148, 150]
HEY2, Hairy enhancer of split related with YRPW motif protein 2	[148, 150]
HEYL, Hairy enhancer of split related with YRPW motif protein	[148, 150]
EPBR2, Ephrin B2	[151]
DTX1, Deltex1	[152]
c-Myc	[153, 154]
CCND1, Cyclin D1	[155]
GATA3, GATA binding protein 3	[156, 157]
NRARP, Notch regulated ankyrin repeat-containing protein	[158]

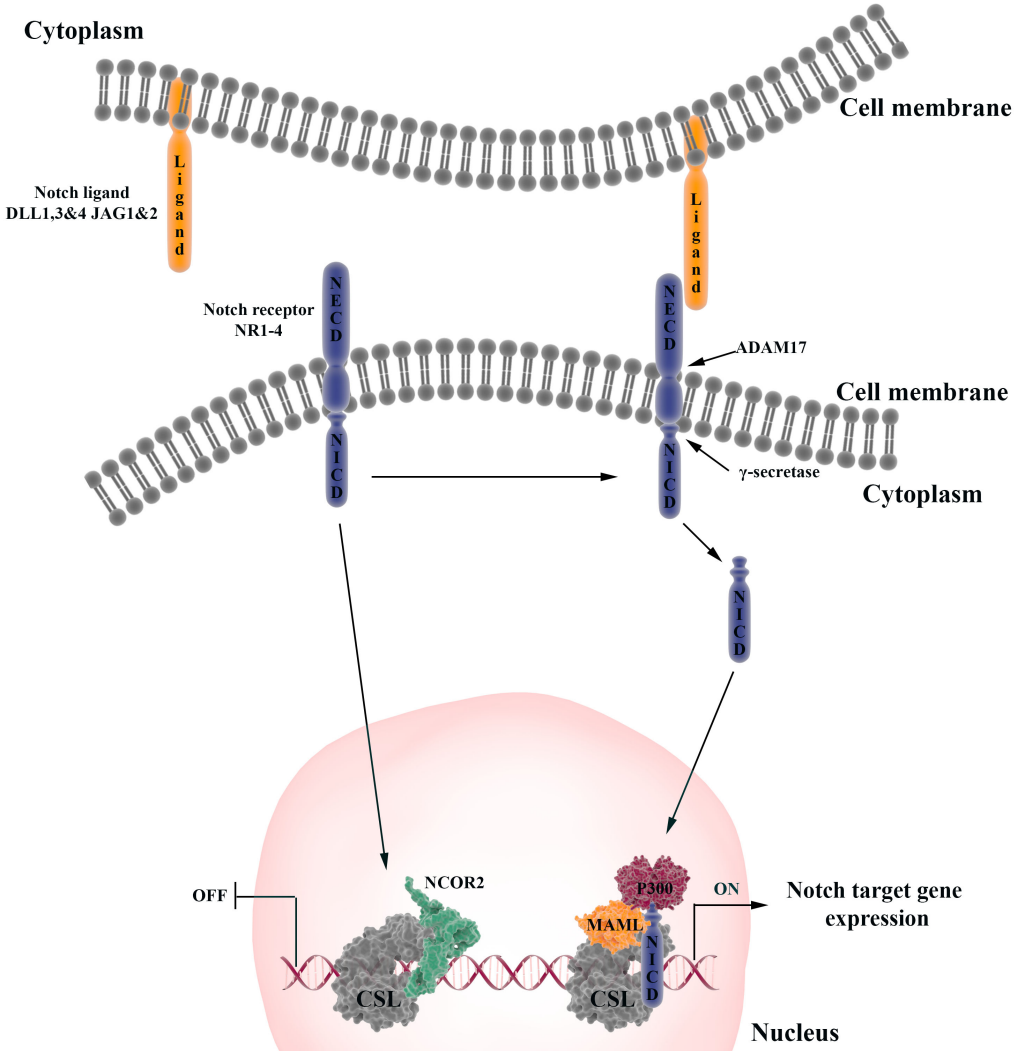

Figure 1.11 Notch signal transduction

Notch signaling occurs by interaction between two adjacent cells, one expressing notch ligand (DLL1, DLL3, DLL4, JAG1 & JAG2), which are referred as signal-sending cells and the adjacent cell expressing the notch receptor (NR1-4), which are referred to as signal-receiving cells. Binding of notch ligands to the receptors initiates enzymatic cleavage of notch receptor releasing the Notch intracellular domain (NICD). NICD then translocates into to the nuclease and binds to the CSL complex which is in a suppressed state (CSL bound to NCOR2). Binding of NICD to CSL complex results in release of suppressor molecule NCOR2 and the recruitment of activators such as MAML and p300 to initiate transactivation of notch target genes (Table 1.1).

1.3.2.2. Role of Notch Signaling in mammary gland development

Notch signaling plays an important role during mammary gland development and tumorigenesis. Most of the data supporting the essential role of Notch signaling in mammary gland development has been generated in chimeric mice. However, some very interesting data have also been generated using human breast epithelial progenitors which are discussed in this section.

During murine mammary gland development, *Nr3* transcripts are the most dominant among the Notch receptors and *Nr4* was reported to be the lowest [83, 159]. Notch signaling has been shown to regulate self-renewal and lineage-specific differentiation in normal human breast stem cells and progenitor cells. Mouse mammary epithelial cells lacking Notch effector CBF-1 (CSL/RBPJ-κ) demonstrated abnormal luminal cell differentiation in transplantation studies which suggested the importance of Notch signaling in the regulation of luminal-fate [96]. Nr1 expression was high in luminal subsets and constitutive expression of N1icd in stem cells ($CD29^{high}CD24^{+}$) lead to the formation of hyperplastic nodules containing luminal cells in transplanted fat pads suggesting the role of notch signaling in luminal cell commitment [84]. Overexpression of N1icd or N3icd in transgenic mice resulted in defective ductal and lobuloalveolar development and also decrease in β-casein was observed [160]. In mammary ducts, a strong Nr3 expression has been observed in cap cells of actively proliferating end buds. This study showed that Nr3 expression was mostly found in the luminal compartment, especially the alveolar region, while Nr4 expression was restricted to basal cells [161]. Using a 3D culture system, it was demonstrated that ligand-induced activation of Nr4 signaling enhanced MaSC self-renewal and branching morphogenesis [85]. Another study, however reported that overexpression of the active form of Nr4, Notch4 intracellular domain (N4-icd) inhibited branching morphogenesis providing further support for the role of Nr4 in branching of mammary structures [162].

Notch signaling's regulation of MaSCs has been extensively studied. Nr1-3 expression was found to be restricted to the luminal cell compartment as compared to MaSC which expressed high levels of Nr4 [163]. Using *in vitro* 3D culture system, it was demonstrated that ligand-induced activation of Nr4 signaling enhanced branch morphogenesis and the Nr4 induced branch morphogenesis was ablated in the presence Nr4 neutralizing antibody [85]. Previous studies have shown that Notch signaling maintains luminal cell fate during pregnancy in mouse mammary gland. The mammary gland of mice lacking the notch effector Csl show expansion of basal cells and transdifferentiation of the luminal cells (i.e. they express basal cell markers) [84]. Notch signaling has been shown to regulate MaSC function and luminal cell fate commitment. Loss of notch signaling resulted in aberrant end bud formation due to enhanced stem cell activity *in vivo*. On the contrary, constitutive activation of notch signaling led to ductal hyperplasia [83]. This study also demonstrated that the occupancy of N1icd on *Gata3* promoter region and the expression of *Gata3* was higher in luminal cells. Gata3 is a transcription factor which is upregulated in the luminal subtype of breast cancer [164-167] which demonstrated the role of Notch-Gata3 signaling in luminal cell fate commitment. Analysis of mammary gland development in mice lacking *Gata3* (MMTV-cre;$Gata3^{+/f}$) revealed that Gata3 was necessary for nipple formation during development. Loss of *Gata3* in virgin mice showed defective ductal development and during pregnancy, it resulted in impaired lactogenesis due to reduced lobuloalveolar development [52]. Loss of *Gata3* also leads to the expansion of luminal progenitor population suggesting that Gata3 plays an important role in differentiation of luminal progenitors to mature luminal cells [52, 168].

Transcriptome profiling of purified breast epithelial progenitors obtained from human breast tissue showed differential expression of Notch receptors. NR4 expression was found to be highly expressed in the undifferentiated bipotential progenitors, whereas NR3 expression was

strongly detected in the luminal-restricted progenitors. NR1 and NR2 expressions were found to be high but not restricted to different cell type. These data suggested that NR3 signaling could be important to the luminal cell lineage in breast tissue. To this end, the lentivirally transduced bipotent progenitors with decreased NR3 expression showed significantly diminished commitment to the luminal cell fate using *in vitro* progenitor differentiation assay, the CFC assay. However, the luminal-restricted progenitors' potential to generate mature luminal cells was found to be independent of NR3 signaling [76]. Prior to this study, it was believed that Notch receptors carried out overlapping redundant functions to regulate proliferation and differentiation potentials of primitive cells. However, the above study showed that each Notch receptors could have non-redundant functions and perhaps are capable of regulating the expression of unique target genes. Using inducible Nr3 transgenic mouse model it has been shown that Nr3 is expressed in luminal cell subsets and the activity of Nr3 maintains the luminal progenitors in a non-proliferative state in the normal mammary gland [64]. On the contrary, Numb, a suppressor of Notch signaling, has been shown to play an important role in determining myoepithelial cell fate [169]. During mammary gland development, V-ATPase a2 isoform has been shown to regulate ductal morphogenesis and lactation through Notch signaling [170]. Nr1 expressing luminal progenitors represents alveolar progenitors and its expression helps in expansion during pregnancy [171]. These above evidences suggest that signaling through different notch receptor elicits different cellular response during mammary gland development.

Activation and transduction of Notch signaling require initial ligand-receptor interaction. Differential expression of notch ligands elicits a different response in cells that express notch receptor (signal-receiving cells). Higher expression of notch ligands such as, *Jag1* and *Dll3* was observed in nulliparous and pregnant mice which decreased during lactation. A low expression of

Dll1, *Dll4* and *Jag2* transcript was observed throughout mammary gland development [159]. Another study reported that expression of notch ligand *Jag1* was found in luminal cell compartment while *Dll1* expression was restricted to MaSC [83]. Conditional knockout of *Dll1* impaired ductal elongation and branching and a severe defect in lobuloalveolar development was observed during pregnancy. Dll1 expressed on MaSCs could interact with Nr3 expressed on adjacent macrophages and result in activation of notch signaling in them. This interaction was necessary for the maintenance of macrophage numbers as well as secretion of Wnt ligands such as Wnt3a, Wnt10 and Wnt16. These secreted Wnt ligands from macrophages, through positive feedback mechanism, regulated MaSC activity [20]. Transcriptome profiling of purified breast epithelial progenitors revealed that *DLL1*, *JAG1* and *JAG2* expression was highest in bipotent progenitors as compared to luminal progenitors which had higher expression of notch receptor NR3 [76]. This observation suggests that cell-cell communication is possible between the bipotent and luminal progenitors during breast tissue development. Another study reported that JAG1-NR3 signaling enhanced mammosphere formation of both normal breast epithelial cells as well as cancer stem cells *in vitro* [86], suggesting a role for JAG1-NR3 in self-renewal.

1.3.2.3. Role of non-canonical Notch signaling in mammary gland development

During activation of canonical notch signaling, the ligand-receptor interaction facilitates translocation of the active form of notch receptor, NICDs into the nucleus where it binds to sequence-specific DNA binding protein complex, RBPJ-κ (or CSL) and activates canonical target genes [121, 122, 125, 126, 128]. However, accumulating evidence suggests the existence of a non-canonical notch signaling, a ligand- and CSL independent pathway. Published reports so far indicate that CSL independent signaling is mostly observed in the most primitive stem

cell/progenitor cell populations in various tissues [172]. *In vitro* studies suggested that CSL independent signaling inhibits their differentiation potential of myoblasts cells. Indeed, these cells did not show upregulation of a well characterized notch target gene *Hes1,* suggesting a role for non-canonical Notch signaling in the myoblasts [173-175]. In *Drosophila*, notch signaling was active in muscle precursor cells even in the absence of ligand and its downstream target gene expression [176], suggesting that notch can activate expression of genes by either binding to a different DNA binding protein or by interacting with other protein complexes with transcription activation function. These observations suggest that non-canonical notch signaling occurs in cells with self-renewal and proliferation potential. NR1 has been shown to antagonize canonical Wnt signaling through post-translation regulation of β-catenin in cardiac progenitor cells as well as in embryonic stem cells [177, 178]. In this study, the authors demonstrated a physical interaction between N1icd and β-catenin which resulted in lysosomal degradation of β-catenin. A similar observation was made during early development of *Xenopus* [179]. Notch-induced degradation of β-catenin was independent of Gsk3-β [179]. In peripheral T cells, Nr1 directly regulated interferon γ (Ifnγ) expression by binding to NF-κB binding region present in the Ifnγ promoter [180]. An active form of Nr1 and Nr2 inhibited a transcription factor E47 independent of CSL in mouse embryonic fibroblast NIH3T3s [181]. Nr1 could also activate expression of a known mammary stem cell marker, β1 integrin (CD29), in a CSL-independent fashion in Chinese hamster ovary (CHO) cells [182]. Also, NR1 has been shown to form an activating complex with the *YY1* transcription factor and enhances c-Myc expression in a CSL-independent manner suggesting non-canonical regulation of notch target genes [183]. Notch signaling has also been shown to negatively regulate Wnt signaling through a CSL-independent as well as the ligand-independent mechanism [184]. A ligand-dependent but γ-secretase-independent activation of notch signaling

was essential for expression of synaptic proteins in post-mitotic neurons [185] which added an additional level of complexity in Notch signal transduction mechanism. These observations indicate a deviation from the conserved Notch signaling pathway (canonical) and provide strong evidence for the existence of an alternate Notch signaling (non-canonical) pathway across species.

Notch signaling transduction can also be regulated by posttranslational modification of NICDs. N1ICD and N4ICD have been shown to interact with NAD-dependent protein deacetylase sirtulin 1 (SIRT1). This interaction results in destabilization and degradation of the NICDs, thus regulating its turnover [186]. On the contrary, N3ICD acetylation resulted in its proteasomal-mediated degradation [187]. GSK3-β which is a key component of canonical Wnt signaling was shown to phosphorylate N3ICD which leads to its degradation and therefore decreased NR3-mediated signaling. Interestingly, serine-threonine kinase receptor-associated protein (STRAP) reduced N3ICD ubiquitination and stabilized the protein [188]. All these observations suggest a complex and multifaceted signaling network that coordinate to regulate Notch signal transduction that plays an integral role in fundamental cellular processes such as proliferation and differentiation.

Unfortunately, very little is known about non-canonical notch signaling during mammary gland development and maturation. In breast cancer cells, notch signaling activated *IL6* expression independent of CSL. This non-canonical notch signaling was regulated by inhibitor of nuclear factor kappa-B kinase subunit alpha (IKKα) and inhibitor of nuclear factor kappa-B kinase subunit beta (IKKβ) gene activity [189]. *In vivo*, overexpression of N4icd in CSL deficient mice resulted in mammary tumors, suggesting a non-canonical role of notch signaling in mammary tumorigenesis [190].

1.3.2.4. Notch signaling in breast carcinogenesis

Breast cancer development involves the altered function of many genes that are essential to normal breast development and its maturation at puberty. It is therefore not surprising that apart from its role in mammary gland development, Notch signaling has been associated with breast tumorigenesis [191, 192]. High levels of notch receptors and their ligands are associated with breast cancer pathogenesis [193]. Characterization of Czech II mice revealed insertion of the mouse mammary tumor virus (MMTV) provirus within the *Notch4* gene (also referred to as *Int-3* locus) caused mammary adenocarcinomas [194, 195], leading to the discovery of this gene in mammals and also its role breast tumorigenesis. This insertion of provirus leads to aberrant expression of a truncated form of the Notch4 receptor which contained the transmembrane and the intracellular domain of Nr4. Similar insertions were later found within the *Notch1* gene as well [196] which generated lactation-dependent mammary tumor via direct activation of *Myc* gene [197]. These observations gave the first indication that altered notch signaling could play an important role in mammary tumorigenesis. Transgenic mice expressing N4icd driven by MMTV or WAP promoter (restricted to secretory epithelial cells) showed poor mammary gland development with adenocarcinomas containing poorly differentiated cells [198-200]. Ectopic expression of MMTV/N1icd and MMTV/N3icd resulted in impaired ductal and lobuloalveolar development and eventually mammary tumors. This phenotype was also observed in transgenic mice overexpressing activated Notch1 and Notch3 [160, 201].

The role of aberrant activation of Notch signaling in human breast cancers was examined in a study by Weijzen S et al which showed overexpression of N1ICD in four different patient tumor samples with H-Ras overexpression [202]. *In silico* analysis of transcriptome data from 3554 breast cancer patients revealed that elevated *NR1* transcript levels are associated with the

worst overall survival in progesterone receptor negative breast cancer patients, while *NR2* expression was found to have better overall survival in patients with lymph node negative breast cancer [203, 204]. Elevated levels of NR1 and NR4 were reported in the early breast cancer lesions, ductal carcinoma in situ (DCIS), and the triple negative breast cancer tumors [205, 206]. Elevated levels of NR1 and JAG1 were correlated with poor patient prognosis, and shorter disease-free survival [207-212]. Although *NR3* gene amplification was observed in breast cancer specimens at a low frequency [213], higher expression of NR3 was associated with improved recurrence-free survival in luminal A, luminal B and basal-like subtypes of breast cancers except for the HER2 overexpressing subtype [88]. And finally, the high expression of Notch ligands like JAG1 and DLL4 was associated with poor prognosis in breast cancer patients [193, 207].

Immunohistochemical analysis of DCIS tissue sections revealed the presence of active (intracellular domain) form of notch receptors, suggesting increased notch signaling. In addition, combined inhibition of ERBB2 and Notch signaling blocked the activity of DCIS with stem cell and progenitor activity [214]. Activation of NR1 signaling in ER-negative breast cancer cells resulted in upregulation of anti-apoptotic factors and cell cycle regulator, Survivin [215, 216]. Notch signaling is critical for survival of breast cancer stem cells where blocking Notch signaling via numb-1 peptide eliminated cancer stem cells [217, 218]. In addition to this, Notch signaling has also been shown to play an important role in the maintenance of the BCSC population [219, 220]. These data provide compelling evidences that blocking Notch signaling could be a promising therapeutic target to treat different cancers.

The regulation of proliferation and differentiation is a complex process that requires the coordinated action of several different signaling pathways. As part of this complex signaling network, Notch signaling coordinates (crosstalk) with other signaling pathways to exert its

important biological functions. Notch and the Wnt signaling have been shown to cooperate and coordinate to carry out important cellular processes that are discussed in the next section.

1.3.3. Role of Wnt signaling

Similar to Notch, Wnt is another evolutionarily conserved signaling pathway that plays an important role during development, maturation and the normal function of different tissue types. Insertional activation of *Insertion1* (*Int1*) gene (now referred to as *Wnt1*) by MMTV resulted in mouse mammary tumors. This gene was later found to be the homologue of the *Drosophila* developmental gene *Wingless* (*Wg*) and hence the name Wingless-Insertion (Wnt). Different Wnt genes that work together to make up the Wnt signaling pathway have been shown to play an essential role in the mammary gland development during embryogenesis as well as in regulating mammary stem cell function. In vertebrates, there are 19 Wnt ligands, each of which are secreted and 10 Wnt FRIZZLED (FZD) receptors. Binding of different Wnt ligands to the FZD receptors results in activation of two different signaling cascades; Canonical or β-catenin dependent Wnt signaling and Non-canonical Wnt signaling. The role of Wnt signaling in mammary gland development was first observed during the commitment of embryonic ectoderm to mammary fate and later in the maintenance of adult stem cells [221].

1.3.3.1. Canonical or β-catenin dependent Wnt signaling

Among the 19 secreted Wnt ligands, Wnt-1A, -2, -3A, -8A, -8B, -10A and -10B have been shown to activate the canonical Wnt signaling pathway [222]. Canonical Wnt signaling plays an important role in mammary gland development as well as breast carcinogenesis. In the absence of ligand, β-catenin protein present in the cytoplasm is prone to proteasomal degradation. GSK3-β

and the destruction complex (GSK3-β, adenomatous polyposis coli (APC) and AXIN) [223] phosphorylate β-catenin resulting in degradation and reduction in its cytosolic levels. However, binding of a canonical Wnt ligand to FZD receptor results in dimerization of FZD with the co-receptor LRP protein on the cell membrane. Such interaction results in phosphorylation of GSK3-β and the destruction complex, preventing degradation of β-catenin. As a result, β-catenin is stabilized, and its cytosolic levels are increased allowing it to translocate into the nucleus. The nucleated form of β-catenin binds to TCF-LEF protein complex that is bound to their cognate binding site on the promoter (proximal and/or distal) of Wnt target genes (Fig 1.12). Evidence suggests that Wnt ligands promote mouse mammary stem cell self-renewal and long-term expansion. Loss of function and gain of function approaches have been taken due to the non-redundant expression of some of the Wnt ligands, FZD receptors and its coreceptors. Loss of Wnt signaling during embryogenesis has resulted in improper mammary gland formation. The Wnt co-receptor Lrp is important for transducing canonical Wnt signaling. Expression of Lrp receptors, Lrp5 and 6 is limited to the myoepithelial cells of the mammary gland [224]. Lrp6 deficient mice were embryonic lethal and therefore its role in the mammary gland is not well studied. However, heterozygous deletion of Lrp6 showed defects in branching morphogenesis of the mammary gland [225]. On the other hand, loss of Lrp5 reduced ductal mammary stem cell activity [224, 226]. Studies in mice have shown that overexpression of Wnt1 (using MMTV-Wnt1, expressing Wnt1 in mammary cells) induced ductal hyperplasia and basal-like tumors [227-229]. These studies together suggested that Wnt1-activated canonical Wnt signaling was oncogenic in nature. Expression of a allele of β-catenin, Δ*N-β-catenin* (using MMTV-LTR) induced hyperplasia of luminal origin and luminal-type tumors [230]. Interestingly, transgenic mice expressing a stable form of β-catenin driven by Ck5 promoter (expressed in basal cells) reported ductal hyperplasia

and formation of invasive and non-invasive basal type tumors. Activation of β-catenin signaling in the mammary epithelium led to the defective differentiation of myoepithelial cells which resulted in basal-type tumor development. In addition to this, the proliferation and differentiation of luminal cells were also affected [231]. Axin is a part of the β-catenin destruction complex, which results in inhibition of Canonical Wnt-β-catenin signaling. Transgenic mice (MMTV-rtTA;TRE2-*Axin*-GFP) expressing Axin in mammary gland exhibit defective lobular-alveolar development during pregnancy. In the postnatal mammary gland, ectopic activation of Axin inhibited alveolar development, demonstrating the importance of Wnt-β-catenin signaling during mammary gland development [232, 233]. Expression of Wnt ligand Wnt10b was observed during differentiation of mammary placode [234]. These data showed that early activation of Wnt components and Wnt signaling is necessary for the initiation of mammary-specific development from the ectoderm. Wnt signaling has been shown to play an important role in regulating mammary stem cell functions. Mammary epithelial cells overexpressing Wnt1 showed higher expression of ΔN*p63 (*a p53 family of transcription factor lacking transactivation domain) [224]. Its expression is restricted to the basal compartment and promotes myoepithelial lineage specification [231, 235, 236]. A study has shown that ΔN*p63-Fzd7* regulates MaSC function via activation of Wnt signaling pathway. Loss of ΔN*p63* resulted in defective ductal elongation with reduced MaSC number and function [237]. Gu et al has demonstrated a link between Notch and Wnt signaling crosstalk which regulates luminal/alveolar differentiation. They have demonstrated that Pygopus2 (Pygo2)-β catenin complex occupies *Notch3* promoter region and suppresses its activation in the MaSC-enriched subset of mouse mammary cells thereby diminishing luminal/alveolar differentiation in these cells [238]. Interesting, in human bipotent progenitors, *PYGO2* expression was found to be higher as compared to luminal-restricted progenitors [76].

Studies in mouse mammary cell lines have shown that exogenous introduction of Wnt3a inhibited differentiation in presence of prolactin or insulin and this inhibition was reversed in presence of secreted frizzled receptor protein 4 (sFRP4) that acts as a competitive blocker of signaling activation. Addition of high concentration of Wnt3a to cultures of primary mammary epithelial cells resulted in extended mammary stem cell activity [239]. Interestingly, Wnt3a is not secreted in mammary gland despite its *in vitro* function [240]. Effort has been made to identify Wnt ligand which binds to Fzd/Lrp receptors and transduce Wnt signaling. Currently studied Wnt ligands are lipidated which allows them to have only short-range effects [241, 242]. This suggests that the ligands are expressed locally either by surrounding epithelial cells or stroma.

1.3.3.2. Non-canonical Wnt signaling

Very little is known about the role of non-canonical Wnt signaling during mammary gland development. Activation of non-canonical (β catenin independent) Wnt signaling can have two different outcomes; activation of the Wnt-Planar Cell Polarity (PCP) pathway or Wnt/Ca^{++} pathway (Fig 1.13). The Wnt-PCP pathway is activated when a non-canonical Wnt ligand binds to FZD receptor and its co-receptors such as RAR-related orphan receptors 2 (ROR2), Receptor-like tyrosine kinase (RYK), Protein tyrosine kinase 7 (PTK7) or Vangl. This interaction results in activation of the small G-protein RhoA, which in turn activates Rho-associated kinase (ROCK) which regulates cytoskeletal rearrangements. RhoA can also activate JNK which in turn activates expression of non-canonical Wnt target genes in a JNK-dependent manner [243, 244]. The Wnt-Ca^{++} pathway is activated upon binding of the ligand to FZD receptors and their direct interaction with trimeric G-proteins and Dishevelled protein (Dsh) [243]. This interaction activates phospholipase C (PLC) and subsequently breaks down phosphatidylinositol bisphosphate (PIP2) to diglyceride (DAG) and inositol triphosphate (IP3). IP3 increases the cytoplasmic calcium

concentration and thereby activating protein kinase C (PKC), calcineurin and Calmodulin-dependent protein kinase II (CaMKII). CaMKII further activates transcription factor NFAT, which translocate into the nucleus to activate gene transcription of Wnt signaling effectors [243]. In a given cell, the canonical and non-canonical Wnt signaling can be activated at the same time. Considering the number of Wnt ligands (19) and receptors (10), 190 different combinations of ligand-receptor interaction could be possible in a cell. Wnt5a and Wnt5b which represent two non-canonical Wnt ligand are expressed in mammary gland and known to transduce signals through Ror1 and Ror2 [60, 163, 245-248]. Activation of Wnt signaling in these complex scenarios completely depends on the concentration of ligands and level of receptors and co-receptors as well as the degree of affinity between ligand and receptor. Interestingly, the ligand-receptor interaction can either result in synergistic activation of other Wnt signaling parhways or inhibition. In the case of melanoma, non-canonical Wnt signaling induced by Wnt5a/Ror2 promotes tumor growth in presence of high levels of canonical Wnt signaling. TGF-β, a known inhibitor of mammary gland development, induces Wnt5a activity which in turn inhibits Wnt3a/Wnt1 induced canonical signaling that supports mammary gland development. In Wnt5a deficient mice, mammary gland shows a hyperproliferative phenotype [248] and exogenous Wnt5a inhibits ductal extension. Interestingly, this phenotype is not observed in mice overexpressing Wnt5a (driven by MMTV promoter). These observations suggest that non-canonical ligands can inhibit canonical Wnt signaling. Wnt5a and Wnt5b differentially regulate mammary gland development as well as progenitor cell function. While the exogenous presence of Wnt5a increased the size and number of mammosphere, the Wnt5b inhibited mammosphere formation *in vitro*. Wnt5b treated mammary epithelial cells showed a decrease in gene expression related to luminal cell differentiation. This effect was dependent on differential expression of non-canonical Wnt coreceptors such as Ror2

and Ryk. Wnt5a interaction with Ror2 resulted in inhibition of mammary epithelial branching, while its interaction with Ryk promoted mammosphere formation [249]. Thus, in addition to the presence of Wnt ligand, the expression of Wnt coreceptors contribute to differential function during mammary gland development.

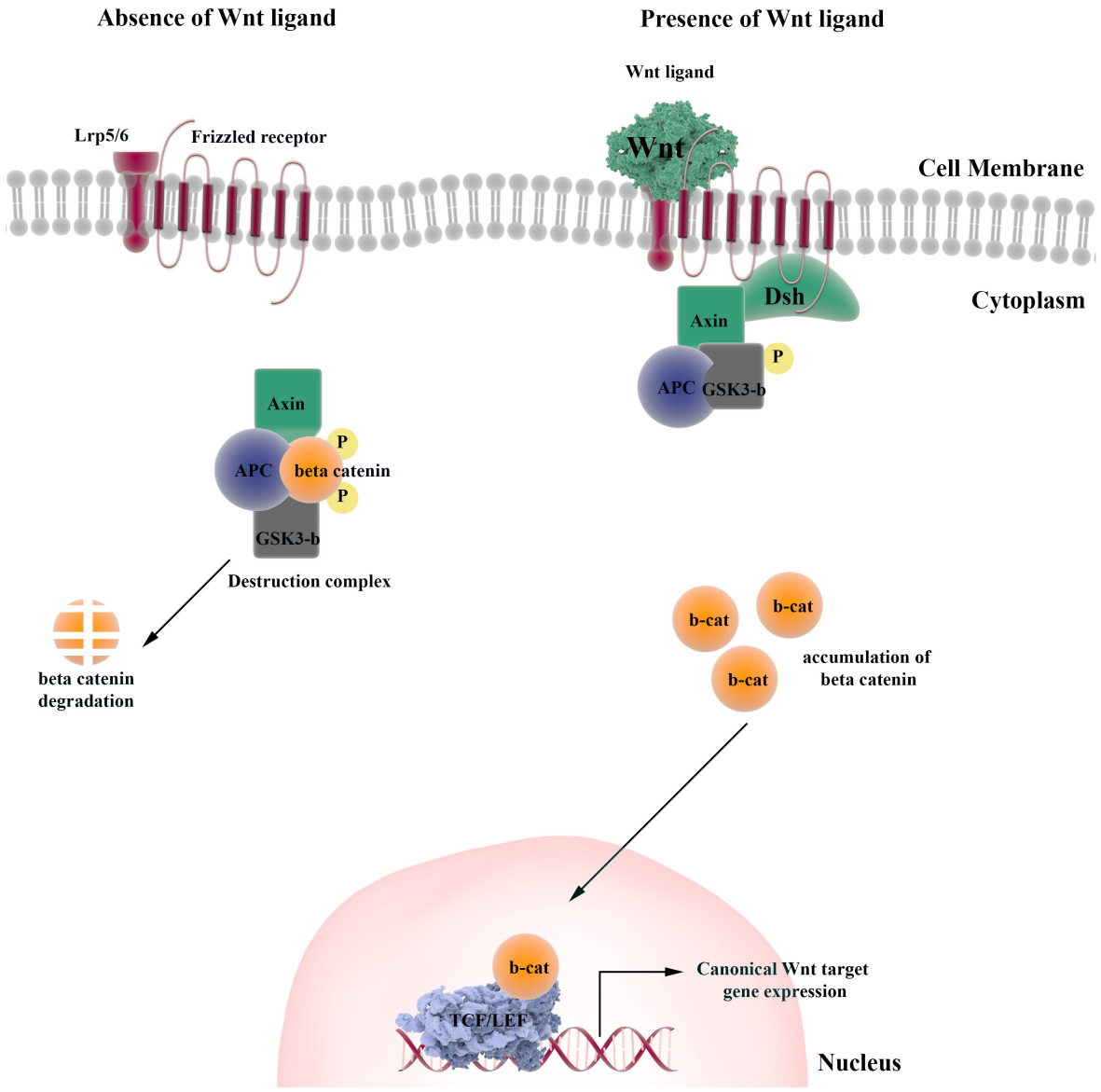

Figure 1.12 Schematic showing canonical Wnt signal transduction

Wnt signaling occurs by binding of secreted Wnt ligands to the Wnt receptors (FZD1-10). Binding of a canonical Wnt ligand (e.g., Wnt3A) to frizzled receptor results in accumulation of β-catenin in the cytoplasm. This induces translocation of β-catenin into the nucleus where it binds to TCF/LEF complex on the promoter region of canonical Wnt target genes and initiates gene transcription. This pathway is also referred to as β-catenin dependent Wnt signaling pathway.

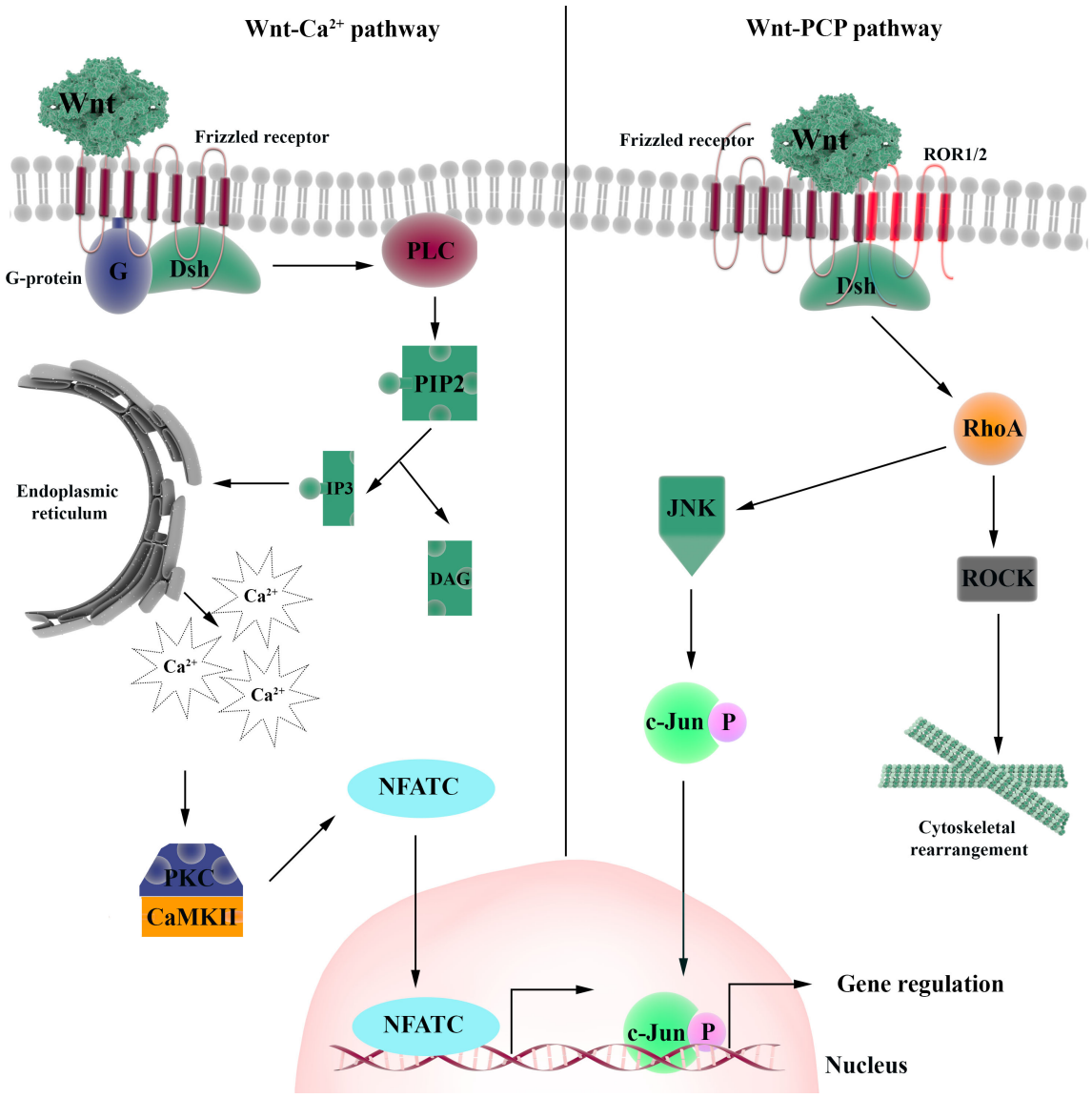

Figure 1.13 Schematic showing non-canonical Wnt signal transduction

Non-canonical Wnt signaling is also referred to as β-catenin independent signaling. Binding of non-canonical Wnts (e.g., Wnt5A, 7A) to frizzled receptors, activates one of two pathways namely, Wnt-Ca^{2+} and Wnt/planar cell polarity pathways. In Wnt-Ca^{2+} pathway, intracellular accumulation of Ca^{2+} triggers translocation of transcription factor NFAT and activates gene transcription. In Wnt-PCP pathway, RhoA activates ROCK and c-Jun which results in cytoskeletal rearrangement and gene transcription respectively.

1.4. Study rationale

Despite recent advances in early diagnosis, breast cancer remains the most frequent cause of cancer-related death among women. The majority of breast tumors consists of estrogen-responsive, luminal type cells [250]. The human mammary gland is a highly regenerative organ in that it supports multiple pregnancy cycles [29-32]. This regenerative ability is generally by proliferation, differentiation and self-renewal of a small population of cells called breast epithelial stem cells (BESCs). These BESCs proliferate and differentiate to produce specialized progenitors (the early bipotent progenitors and restricted luminal and myoepithelial progenitors). These specialized progenitors ultimately produce the mature luminal and the myoepithelial cells that are required during breast tissue regeneration cycles (e.g. pregnancy). Often, the regenerative property of breast tissues can be hijacked by oncogenic processes to produce malignant tumors. Evidence now suggests that inappropriate functioning of genes that regulate breast cell proliferation in health are responsible for breast cancer initiation, progression, and recurrence. Therefore, the development of more effective and possibly, curative therapies against breast cancer depends on furthering our understanding of the genes and molecular events that regulate human breast cell function in health, in particular, the process of generation of luminal cells.

Transcriptome profiling of purified bipotent and luminal progenitors has revealed a number of differentially expressed genes both common and unique to each progenitor subtypes. *In silico* analysis of the perturbed gene list showed enrichment for elements of conserved signaling pathways such as the Notch, NF-κB and Wnt signaling psthways. Interestingly, a known mammary oncogene, NR4, was observed to be highly expressed in bipotent progenitors, while high expression of another oncogene, NR3, was found in luminal-restricted progenitors. This observation suggested that NR3 might be involved in luminal cell fate commitment in the breast.

Previously, from loss of functional studies, it was demonstrated that *NR3* plays a key role in commitment of undifferentiated bipotential progenitors to the luminal cell lineage [76]. This finding was as functional redundancy between members of the Notch receptor family was assumed. This 2008 study then indicated that only signaling through NR3 was required for luminal cell commitment of bipotent progenitors and that it might do so through regulation of unique target genes. In addition, using a Notch signaling specific qPCR array on non-malignant human mammary epithelial cell, we identified genes like DLL3, LRP5 and FZD7 which were regulated by NR3. Interestingly, LRP5 and FZD7 are components of the Wnt signaling pathway.

1.5. Central hypothesis

Based on these preliminary observations, the hypothesis of my study was that NOTCH3 receptor signaling, through regulation of its unique target genes, plays a critical role in the differentiation of bipotent progenitors to the luminal cell lineage.

1.6. Aims and Objectives

The overall objective of this study was to use human models to understand the NOTCH3 regulation of FZD7 signaling and how NOTCH3-FZD7 signaling regulates luminal fate commitment in breast tissue

Aim 1: To study the mechanism by which NOTCH3 regulates FZD7 expression in breast epithelial cells

Aim2: To study the role of NOTCH3-FZD7 signaling in luminal cell fate commitment in breast tissue

2. Materials and Methods

2.1. Non-malignant human breast epithelial cell lines

The Human Mammary Epithelial Cell strain (HMEC) was obtained from Lonza (www.Lonza.com) and cultured according to the manufacturer's protocol using the MEGM growth media. These cells were subcultured every 3-4 days using standard trypsin method as described below.

The 184-hTert cells were a kind donation from Dr. Sam Apparicio (B.C. Cancer Agency, Vancouver B.C. Canada [251]) and were maintained in growth media containing; 10ng/mL EGF, 25µg/mL insulin, 500µg/mL hydrocortisone, 2.5ng/mL sodium selenate, 400µg/mL G418, 0.15U/mL prolactin, 1.6µg/mL transferin and 10nM/mL isoproterenol. These cells were subcultured every 2-3 days or according to the confluency. Both the cell types were kept in a humidified chamber at 37°C and 5% CO2.

2.2. Preparation and isolation of primary breast epithelial cell subsets from freshly digested organoids

The breast reduction samples were obtained through informed written consent (University of Manitoba, Research Ethics Board #H2010:292). The tissue samples obtained were cut into 0.5-1.0cm^2 pieces and transferred into a flask containing disassociation media (300U/mL collagenase + 100U/mL hyaluronidase, 25µg/mL insulin, 500µg/mL hydrocortisone, 1x PenStrep, 2% BSA) and incubated at 37°C in a shaker incubator (105-110rpm) for 14-16 hours. The undigested chunks of tissue were discarded, and the organoid-enriched fractions were isolated by differential centrifugation method and preserved in liquid nitrogen. Subsequently, the organoids were turned into single-cell suspension as described below [252]. Single cells were stained with antibodies

raised against EpCAM, conjugated to fluorescein isothiocyanate (FITC) and α6 integrin (CD49f), conjugated to Alexafluor 647. Propidium iodide exclusion was used to identify live cells. Lineage positive cells ($CD31^+$ and $CD45^+$) were removed by using biotinylated specific antibodies and streptavidin-PE Texas-Red secondary antibody. The luminal progenitors ($EpCAM^{bright}CD49f^{low}$) or the bipotent progenitors ($EpCAM^{low}CD49f^{bright}$) were isolated via fluorescent activated cell sorting (FACS) as described before [76].

2.4. Preparation of single cell suspension

The cryopreserved organoids isolated from the reduction mammoplasty samples were thawed in the water bath which is maintained at 37°C and resuspended in 10mL of cold HFN (1X hanks+2% FBS) and centrifuged at 1200rpm for 5 minutes (Sorvall ST16R, Rotor#75003629). The pelleted organoids were dissociated with 1mL of pre-warmed trypsin and incubated at 37°C for 5 minutes in a water bath. Subsequently, trypsin was deactivated with cold HFN and the dissociated organoids were pelleted via centrifugation at (1200rpm for 5 minutes). The organoid pellets are further dissociated with 1mL of dispase added with 100µL of DNase. The pellet was mechanically disassociated by pipetting up and down (15-20 times) and incubated in the water bath (37°C) for 3-5 minutes. Dispase is deactivated with cold HFN and the cells are passed through a 40µm cell strainer to remove any residual clumps. Cells were then pelleted by centrifugation (1200 rpm for 5 minutes) and the pellet is resuspended in 1mL of cold HFN and used for CFC assay. The cell suspension was observed under the microscope and if more than 10% of cells are in doublets or triplets, the dispase dissociation was repeated.

2.5. Isolation of primary mammary epithelial subsets from pre-cultured epithelial cells

Single cells generated from the organoids were immunomagnetically depleted of lineage cells ($CD45^+$ and $CD31^+$) and lineage negative cells (~$3x10^6$ cells) were co-cultured with mouse embryonic fibroblasts, NIH3T3 (45,000 cells/mL) in SF7 (10ng/mL of EGF, 1µg/mL of insulin, 500ng/mL of hydrocortisone, 10ng/mL of cholera toxin, 0.1% BSA and 2% FBS) media in a 60mm dish pre-coated with 1:30 dilution type 1 bovine collagen (3mg/mL, StemCell Technologies Inc. or Neuromics, USA) in PBS. On day 4, the cells were trypsinized, made into single cells and were resuspended in 10% human serum (to block non-specific antibody binding). Cells were stained with anti-EpCAM antibody, conjugated to Fluorescein Isothiocyanate (FITC) and α6 integrin (CD49f) antibody conjugated to Alexa fluor 647, anti-THY1 (CD90) antibody conjugated to phycoerythrin (PE) and anti-MUC1 antibody. Goat anti-mouse Alexa fluor 405 was used to detect MUC1. Propidium iodide exclusion was used to identify live cells. The antibody stained cells were visualized and sorted via MoFlo (Beckman Coulter, Inc) fluorescent activated cell sorter (FACS). Gates were drawn to select viable cells (PI^-) and dual labeled $EpCAM^+CD49f^+$ cells were further gated to exclude stromal ($EpCAM^-CD49f^-$) and differentiated epithelial cell fraction ($EpCAM^+CD49f^-$). Further, CD90 and MUC1 expression was used to isolate bipotent progenitors ($EpCAM^+CD49f^+CD90^+MUC1^-$) and luminal progenitors ($EpCAM^+CD49f^+CD90^-MUC1^+$).

2.6. *In vitro* colony forming cell (CFC) assay

Bipotent progenitors and luminal progenitors were placed in co-cultures with mouse fibroblasts, NIH3T3 (45000 cells/mL of media) in SF7 media supplemented with 2% FBS on a collagen coated plate for 7-10 days. From non-cultured breast epithelial cells, a minimum of 5000

bipotent or luminal progenitors were plated in a 60mm dish for the assay. From pre-cultured breast epithelial cells, a minimum of 50 progenitor cells (maximum 200 cells) were plated per 60mm dish in this assay. After 7-10 days (7 days for precultured and 8-10 days for uncultured) resulting colonies formed were fixed, permeabilized (Methanol: Acetone, 1:1), stained with crystal violet and colonies numbers recorded. Some colonies were co-stained with CK8/18 and CK14 antibodies to distinguish between pure luminal (CK8/18 expressing) and the mix/basal colonies (expressing both CK14 and CK8/18).

2.7. Immunocytochemistry

Colonies from CFC assays were fixed and permeabilized with chilled Methanol: Acetone (1:1 vol/vol) for 30 seconds. To prevent nonspecific binding of antibodies, colonies were blocked with 5% BSA in PBS for 30 minutes and incubated with specific primary antibodies (CK 8-18, CK 14, CD90, ERα) in PBST (PBS+0.1% Tween 20) with 1% BSA for 1 hour. Thereafter, colonies were incubated with fluorescent conjugated secondary antibody (in PBS) for 1 hour. A concentration of 1μg/mL DAPI was used to stain the nucleus. The stained colonies were visualized and imaged in EVOS®-FL (Thermo Fisher Scientific) cell imaging system. Antibody dilutions are indicated in Table 2.2.

For ERα staining, breast epithelial progenitor subsets were sorted from precultured breast epithelial cells, air-dried on clean glass slides and fixed with 100% Methanol at -20°C for 20 minutes. The slides were washed with PBS and blocked with 10% goat serum in PBST (PBS+0.3% Tween 20) for one hour. ERα antibody was resuspended in PBST containing 1% goat serum (1:50 dilution) and cells incubated for 1 hour at room temperature. PE-conjugated secondary antibody was used to detect ERα expression in breast epithelial cells. DAPI (1μg/mL) was used to stain the

nucleus. ERα expression was visualized and imaged in EVOS®-FL (Thermo Fisher Scientific) cell imaging system.

2.8. Protein expression analysis

Flow cytometry was used to examine FZD7 protein expression and the different Notch Receptors. For this purpose, specific antibodies raised against FZD7, NR1, NR2 NR3 where utilized. For flow cytometry, single-cell suspensions were prepared from breast reduction samples,184-hTert cells or from HMECs essentially as described [252]. Protein expression was detected using a goat anti-mouse antibody conjugated to PE and quantified using FlowJo Software (TreeStar Inc.). Expression of NR4 and the CSL protein levels were examined using a polyclonal anti NR4 antibody and polyclonal anti-CSL antibody respectively, using a conventional Western blot assay normalized to β-actin protein expression. Specific antibody clones and their dilutions are listed in Table 2.2.

2.9. Generation of lentiviral particles

Human embryonic kidney (HEK) 293T cells were plated at a density of $4x10^6$ cells per 10cm cell culture plate in 7mL of DMEM supplemented with 10% FBS. Next day, the growth media was changed 3 hours prior to transfection. A cocktail of lentiviral vector of interest, packaging vector and envelope vector was prepared (for one 10cm dish, 10µg of lentiviral vector, 6.5µg of deltaR, 2.5µg of REV and 3.5µg of V-SVG was used). To this cocktail, $CaCl_2$ (250µM) was added dropwise and the $CaCl_2$-DNA complex formed was mix with equal volume of 2X HBSS buffer. The transfection mix was then added to 10cm dish dropwise. After 16 hours (or overnight), media was changed to DMEM supplemented with 5% FBS. The following day, the growth

medium containing viral particles was collected and passed through 0.4μ low-protein binding filter to remove cell debris and the supernatant was centrifuged at 25,000rpm (Beckman Coulter, Optima XE-90, rotor# SW32Ti) for 90 minutes. The pelleted lentivirus was then resuspended in 100μL of DMEM and the concentration of active lentiviral particles was determined by transducing them in HeLa cells in serial dilution. The viral titer (live viral particles/mL) was calculated as follows.

Titer = No. of cells plated x **% GFP$^+$ cells** x **dilution factor/100**

2.10. Lentiviral transduction

HMECs or the 184-hTERT cells was transduced with lentivirus expressing a short hair-pin RNA (shRNA) to knockdown expression of each Notch receptor separately. The lenti-shRNA constructs (pool of 3 separate lenti-shRNA for each Notch receptor), as well as a lenti construct carrying a scrambled shRNA sequence, were obtained from OpenBio Systems (Thermo Fisher Scientific). Each lentivirus was separately tested for its ability to produce knockdown of its target transcript. The lenti-shRNA transduced cells were selected using puromycin (2μg/mL, Sigma Aldrich). The forced expression of human Notch Receptors was achieved using lentivirus expressing the constitutively active (intracellular domain, ICD) form of each Notch receptor. Plasmid constructs carrying human NOTCH-ICD cDNA were obtained as follows; the pcDNA3-Notch1-ICD vector was a kind gift from Dr. Andrew Weng (Terry Fox Laboratory, Vancouver, B.C. Canada), NOTCH2-ICD and NOTCH3-ICD cDNA fragments were PCR cloned (Table 1) using RNA isolated from the 184-hTERT cell and the MIY-NOTCH4-ICD which was a kind gift from Dr. Aly Karsan (Genome Sciences Centre, B.C. Cancer Agency, Vancouver, Canada). All cDNA fragments were sequence-verified and cloned into the lentiviral vector KA391. The lentiviral supernatant was generated and used to infect live cells as described [253]. The Lenti-

NOTCH-ICD transduced cells were isolated via FACS based on Green Fluorescent Protein (GFP) expression and cultured as described.

Empty vector control and NOTCH3-expressing 184-hTERT cells were re-infected with 3 separate lentiviruses expressing 3 different short hair-pin RNA (shRNA) to knockdown CSL expression or lentivirus construct carrying a scrambled shRNA sequence. The scrambled shRNA and lenti-shCSL transduced cells were selected using puromycin (2μg/mL, Sigma Aldrich) for 48 hr.

Breast reduction samples where dissociated into single cells and cultured overnight as described and subsequently infected either with lenti virus expressing empty vector (EV) or NOTCH3-ICD expressing lenti virus for 4 hrs. After 72 hrs, cells expressing the green fluorescent protein (GFP^+) cells (i.e. NOTCH3 overexpressing cells) were examined for their expression of FZD7 via flow cytometry.

2.11. Transcript expression analysis

RNA was isolated from the lenti-shNOTCH or lenti-NOTCHICD or Lenti-shScrambled or lenti-empty vector control-transduced cells (3 separate infections using pool of 3 different lenti-shRNA virus) using the Trizol reagent (Invitrogen) according to the manufacturer's protocol and treated with RNase-free DNase (Promega). The differential transcript expression of specific genes in these RNA samples was obtained using quantitative real time PCR (qPCR). The qPCR data were analyzed using the comparative threshold cycle method (ΔCT) and normalized against the β-actin and GAPDH transcript expression.

2.12. Chromatin immunoprecipitation

184-hTERT cells were infected with lentivirus expressing a FLAG-tagged version of NOTCH1 or NOTCH3 (Addgene, USA) or a construct expressing FLAG-GFP alone. The FLAG alone construct used is a non-lentiviral vector (pTAG-1) that contained a mammalian promoter to express FLAG in the transfected cells. The transduced cells expressing GFP were isolated via FACS. Sorted cells were dual cross-linked as described previously [254]. The dual cross-linked chromatin was sonicated (optimized to 30 cycles of 15 seconds ON/15 seconds OFF) to obtain 250 to 500bp DNA fragments and chromatin immunoprecipitation (ChIP) was performed using anti-FLAG antibody. The immunoprecipitation was confirmed through western blots using anti-NOTCH1 and anti-NOTCH3 antibodies. The ChIP DNA was used as a template for qPCR. Upstream promoter sequence of FZD7 was retrieved from The Eukaryotic Promoter Database (www.epd.vital-it.ch) and screened for putative CSL binding sites [255, 256]. Promoter-specific primers (Table 2.1) were designed flanking the CSL binding sites for qPCR analysis and the fold enrichment was calculated compared to isotype control.

2.13. Molecular cloning of full length *FZD7* gene

cDNA of full length FZD7 gene sequence was retrieved from National Centre for Biotechnology Information (NCBI) and were PCR cloned with PCR primers flanking AscI and PacI restriction endonuclease cut sites (Table 1). The amplified PCR fragment was size confirmed and digested with restriction enzymes. The digested cDNA fragment was purified and ligated into lenti viral backbone, KA391 in 1:6 vector:insert ratio. The ligation mix was then transformed into DH5α competent bacterial cells as per the manufacturer's instructions (Thermo Fisher Scientific). The transformed cells were plated on a LB agar plate supplemented with 100μg/mL ampicillin.

The plates are placed in 37°C incubator for 12-16 hours. Positive bacterial colonies (carrying plasmid of interest) generated on the agar plate was confirmed by PCR followed by restriction digestion with AscI and PacI.

2.14. Notch signaling qPCR Array

RNA was isolated from the Lenti-sh*NOTCH4* or Lenti-sh*NOTCH3* or Lenti-shScrambled control-infected HMEC cells (3 separate infections using pool of 3 different lenti-shRNA virus) using the Trizol reagent (Invitrogen) according to the manufacturer's protocol and treated with RNase-free DNase (Promega). The differential expression of 84 Notch-associated and/or target genes in these RNA samples was investigated using the Notch signaling Pathway quantitative real-time PCR (q-RT-PCR) Array kit (SABiosciences, PAHS-059Z) based on the manufacturer's protocols. The PCR array data were analyzed using the comparative threshold cycle method (ΔCT), and normalized against the β-actin and GAPDH transcript expression using the SABiosciences online program. Potential *NR3* and *NR4* target genes were validated using q-RT-PCR assay and primer set independently of the qPCR Array kit reagents and the relative mRNA expression levels were normalizing to the *GAPDH* transcript levels.

2.15. Transcriptome profiling of N1ICD and N3ICD overexpressing 184-hTert cells

184-hTert cells were plated in 6 well plate at a density of $2x10^5$ cells per plate. The next day, the cells were lentivirally transduced with either empty vector (EV) control or N1ICD or N3ICD expressing lentivirus. Forty-eight hours post infection, the transduced (GFP positive) cells were sorted via FACS and total RNA was extracted using Trizol® from three independent EV, N1ICD and N3ICD-expressing samples. The RNA samples were then reverse transcribed, labeled

and hybridized onto Affymetrix Human 2.0 ST array GeneChip™. The probe intensities obtained were imported to Partek® Genomic Suite® software (version 6.6) and the data were normalized using Robust Multi-array Average (RMA) algorithm [257]. We first selected the top most variable probeset across the 9 samples using a coefficient of variation (standard deviation divided by mean) for each probeset. A hierarchical clustering was performed using Partek® Genomic Suite®. The differential analysis was performed for three comparisons (N1ICD vs Control, N3ICD vs Control, N3ICD vs N1ICD) using LIMMA package (version 3.36.3) [258]. The adjusted p-value or false discovery rate was performed after multiple testing correction. A gene with adjusted p-value ≤0.05 was considered significant. The differentially regulated N1ICD and N3ICD gene list was compared to identify genes uniquely regulated by NR3 and NR1 signaling. Furthermore, using the Ingenuity Pathway Analysis (IPA) algorithm, the canonical pathways enriched in N3ICD and N1ICD datasets were determined.

2.16. Statistical Analysis

The statistical analysis and graphs generation in this study were performed using GraphPad Prism software (GraphPad Software Inc, version 6). Depending on the nature of the experiment and data obtained, an unpaired Two-tailed t-test or one-way or 2way ANOVA was performed. An asterisk symbol was used to represent the level of significance, *p≤0.05, ** p≤0.01, ***p≤0.005, ****p≤0.001.

Table 2.1 List of primers sequences used in this study

	Gene		Primer Sequence
qPCR primers			
	GAPDH	F	GCCTCCGCTTCGCTCTC
		R	CCGTTGATCCGACCTTCACC
	NOTCH1	F	GCGGGGCTAACAAAGATATGC
		R	GCACCTTGGCGGTCTCGTA
	NOTCH2	F	GATGCCCAGGACAACATGG
		R	GACTCGGTTGCGAATCAGAA
	NOTCH3	F	CGTGGTGTCTGCCAGAGTT
		R	CTGGCAGGGAGCAGTCAG
	NOTCH4	F	TCCCCAGGAATCTGAGATGGA
		R	GGACTGTACTTCCCCACAGCAAAC
	FZD7	F	TCTCCCATTTGGATCCTTTG
		R	GGACAAAATGGCTCTTTGCT
	HES1	F	GGAAGCACCTCCGGAACCT
		R	GGTCACCTCGTTCATGCACTC
	CSL	F	ATTCCAGTTCTCCGGGTTTT
		R	GAGGGACGTACGTGGAGACT
	ROR1	F	GACCGTCAGTGTGACCAAATCAG
		R	GAAACGAAGGGCGGTGAAAGT
	SECTM1	F	TCTTGGTCGCTCTGGTCATGT
		R	TCATCTGGGGTTCTAGGAGGAAG
	GABRE	F	GACACTGGCATTATCCCTTTAGG
		R	GGAGAGGGAGATGTCACAGCAG
	RGS2	F	AGAAAAGGAAGCTCCAAAAGAGA
		R	GCAGTTGTAAAGCAGCCACTTGT
	SCNN1B	F	TGAAGAATCAGCAGCCAATAAC
		R	ATGATCTCCCCAAACTCGATG
	ANPEP	F	GATTCTCCACCGAGTATGAGCTG
		R	TTGATGTTGGCTTTCGTCTTCTC
	CD24	F	TCCAGTGAAACAACAACTGGAAC
		R	GTGGTGGCATTAGTTGGATTTGG
	B4GALNT3	F	CGCCAGATGAAGACGCTGTAG
		R	CACTCCCCATCCCTGAACAGTAG
	CCL28	F	GTGTTGCTGTCAGTGCCAGTAGG
		R	AGGCAATGGGAAGTATGGCTTCTG
	PROM2	F	GACTCCTGGACTCCCTCTATGGCA
		R	GTAGGGCCTTTACCAACTCTGAAGG
	TRPM4	F	CGATGCACACACCACGGAGAAG
		R	GGTCAGAGAGCCGGAGGAAATTG
	EPHB3	F	CAGAAAGTGGGTGGGAAGAGGTG
		R	AGCCAGTTGTTCTGGCTTGACTC
	GGT6	F	GAGGACAGTGGAAAGAGTGCAGA

		R	AAGGACAGAGATGCCAACAGTACC
	GALNT6	F	CCTCTGGAACTTGGAGGGTTGTTC
		R	ACGTCTGGGTCTGCGATGATTG
	NEBL	F	CAACTGCCTGGATAAGTATTGGCA
		R	GGGTAGTGTGCATTACAATAGGGCT
	KRT15	F	GCATCAGGGAAGCCTCTTCAGG
		R	TTGTGGGAAGAAACCACCTGTCC
	HTATIP2	F	GGATGACTACGCCTCTGCCTTTC
		R	CAACACGAACAAATCCCTCCGCC
	PRICKLE1	F	GCGCGAGCAGCCATTGTTTGA
		R	CTCTGACAGCCAAAGGCCAGTTT
Cloning Primers	*NOTCH2*	F	aataggcgcgccgAAACGAAAGCGTAAGCATGGCTCTCTC
		R	aaattaattaaCGCATAAACCTGCATGTTGTTGTGTG
	NOTCH3	F	aataggcgcgccgTCATTCTCGTCCTGGGTGTCAT
		R	aaattaattaaGAGTGTTAACTATTCCTTTATTAGGTGGTGAGG
	FZD7	F	TTggcgcgccATGCGGGACCCCGGCGCGGCC
		R	CCttaattaaTCATACCGCAGTCTCCCCCTTGC
Promoter Primers	*FZD7-1*	F	TCCCTATGATCCCCCAATGG
		R	CAGGAAAAAATGACGATCAAG
	FZD7-2	F	TTGGCCAGAGTTAGGGTTCTG
		R	CACCCTTCAAAGTTTGCCCAAG
	HES1	F	CGTGTCTCCTCCTCCCATT
		R	GGCCTCTATATATATCTGGGACTGC

Table 2.2 List of antibodies used in this study

Antibody	**Clone ID**	**Dilution**	**Company**
EpCAM	VU-1D9	1:100	StemCell Technologies
EpCAM-FITC	VU-1D9	1:10	StemCell Technologies
CD49f-647	G0H3	1:100	Biolegend
MUC1	214D4	1:100	Millipore
CD90-PE	5E10	1:100	Biolegend
CD45-biotin	HI30	1:100	Biolegend
CD31-biotin	WM-59	1:100	eBiosciences
NOTCH1 (intracellular)	polyclonal	5μg/mL	Bethyl Labs
NOTCH2 (intracellular)	polyclonal	5μg/mL	Bethyl Labs
NOTCH3 (intracellular)	polyclonal	5μg/mL	Cell Signaling Technologies
NOTCH4 (intracellular)	polyclonal	1:500	Aviva Systems Biology
CSL/RBPJ-κ	H-50	1:500	Santa Cruz Biotechnology
FZD7 (extracellular)	151143	1:50	R&D Systems
FZD7 (intracellular)	polyclonal	1:200	Abcam
Beta-catenin	14	1:200	BD Biosciences
NOTCH3 (extracellular)	603532	1:50	R&D Systems
ER-alpha	6F11	1:200	Abcam
ER-alpha	HC-20	1:50	Santa Cruz Biotechnology
Beta actin	polyclonal	1:1000	Cell Signaling Technologies
FLAG	M2	1:100	Sigma
Cytokeratin 14	EPR17350	1:400	Abcam
Cytokeratin 8 &18	5D3	1:400	Abcam
α-Smooth muscle actin	polyclonal	1:200	Abcam
Anti-mouse PE		1:100	Biolegend
Anti-mouse Alexa Fluor 488		1:500	Invitrogen
Anti-mouse Alexa Fluor 405		1:500	Invitrogen
Anti-Rabbit Alexa Fluor 488		1:500	Invitrogen
Anti-Rabbit PE		1:500	Invitrogen
Anti-mouse PE		1:500	Jackson ImmunoResearch Lab

Chapter 3

Notch-Induced Expression of FZD7 Requires Noncanonical NOTCH3 Signaling in Human Breast Epithelial Cells

Bhat V, Sun YJ, Weger S, Raouf A.

Stem Cells Dev. 2016 Apr 1;25(7):522-9. doi: 10.1089/scd.2015.0315. Epub 2016 Mar 16.

Mary Ann Liebert, Inc., New Rochelle, NY

3. Notch-induced expression of FZD7 requires non-canonical NOTCH3 signaling in human breast epithelial cells

3.1. Abstract

The evolutionarily conserved Notch and Wnt signaling pathways have demonstrated roles in normal mammary gland development and in breast carcinogenesis. We previously reported that in human mammary gland, signaling through NOTCH3 alone regulates the commitment of the undifferentiated bipotential progenitors to the luminal cell fate, indicating that NOTCH3 may regulate the expression of unique genes apart from the other Notch receptors. In this study, we used gain of function and loss of function experiments and found that a Wnt signaling receptor, Frizzled7 (*FZD7*), is a unique and non-redundant target of *NOTCH3* in human breast epithelial cells. Interestingly, neither the constitutively active forms of *NOTCH1-2*, *4* nor loss of expression of these receptors was able to alter expression of *FZD7* in human breast epithelial cells. We further show that *FZD7*-expressing cells are found more frequently in the luminal progenitor-enriched subpopulation of cells obtained from breast reduction samples compared to the undifferentiated bipotent progenitors. As well, we show that *NOTCH3*-induced expression of *FZD7* occurs in absence of CSL (CBF1-Suppressor of Hairless-Lag-1). Our data suggest that non-canonical Notch signaling through *NOTCH3* could modulate Wnt signaling via *FZD7* and in this way, might be involved in luminal cell differentiation.

3.2. Introduction

The highly conserved Notch signaling pathway is a major mediator of proliferation, differentiation and cell survival during embryonic development, in regenerating adult tissue, and during breast cancer development [255, 256, 259]. Notch signaling is unique from the other signaling pathways in that it relies on the ability of a ligand on the neighboring cells to bring about proteolysis of the Notch receptors (NR1, 2, 3, and 4) resulting in release of the Notch intracellular domain (NICD) of these receptors [159, 260]. In the case of canonical signaling, the NICD will interact with DNA-binding protein CSL [159, 260] and form complexes with transcriptional activators such as MAMML1 and P300, leading to initiation of transcription at the promoter of the Notch target genes such as the HES family of transcription factors [118]. In addition to the canonical signaling, the CSL-independent (non-canonical) signaling by Notch receptors has also been reported [261]. While the mammalian Notch receptors display both overlapping and distinct tissue expression patterns during development and in adult tissues [262], the current model of canonical Notch signaling suggests that these receptors play redundant functions in terms of their transactivation functions and their biological roles [118].

Notch signaling plays important roles in luminal cell fate determination in the mammary gland [76, 84]. Luminal cells in the mouse and human mammary glands are continuously produced due to the proliferation and differentiation of luminal progenitors that are themselves generated from uncommitted bipotential progenitors [68, 75, 78]. The bipotent progenitors are ultimately produced from a self-renewing population of breast stem cells [42, 78]. We previously reported that NOTCH3 transcripts were highly expressed in the human luminal progenitors compared to the bipotent progenitors and the opposite expression pattern was observed for the NR4 transcript levels [76]. However, NR1 and NR2 receptors were ubiquitously expressed in both progenitor subtypes

as well as in their differentiated progeny. Furthermore, we showed that loss signaling through NR3 alone led to decreased production of luminal cells from bipotent progenitors [76]. These findings suggest that NR3 could exhibit non-redundant functions during the process of bipotent cell commitment to the luminal differentiation pathway and that NR3 may regulate expression of specific genes, apart from the other Notch receptors.

In this study we provide evidence that the Notch-induced expression of a Wnt signaling receptor, *FZD7*, is exclusively regulated by non-canonical signaling through NR3 receptor in the human mammary epithelial cells, suggesting that the Notch-mediated modulation of the Wnt signaling pathway could be regulated through the NR3-FZD7 signaling network.

3.3. Results

3.3.1. PCR array identifies FZD7 as a potential NOTCH3-specific target gene

To identify the unique gene targets of *NOTCH3* signaling, the lentviral transduction was employed to knock down *NOTCH3* and *NOTCH4* expression or to express a short hairpin scrambled control sequence in HMEC cells, and the differential expression of 84 Notch signaling targets and associated genes were examined using the SABiosciences, Notch signaling qPCR array. The qPCR array analysis revealed that a Wnt signaling receptor, *FZD7*, Low-density lipoprotein receptor-related protein 5 (*LRP5*) and Delta-like 3 (*DLL3*) transcript levels were decreased in Lenti-shNOTCH3-transduced cells and not in the Lenti-shNOTCH4-transduced cells (Fig 3.1). The preliminary data obtained through the qPCR array were validated using independent primer sets and HMECs transduced with lenti-shNOTCH1-4. The knockdown level of each Notch receptor in the transduced cells was determined through quantitative qPCR and intracellular fluorescent activated cell sorting (FACS) (Fig 3.2A-C). Whereas *LRP5* transcript levels remained unchanged in the transduced cells, the *DLL3* transcript levels were decreased in lenti-shNOTCH3 and lenti-shNOTCH4 HMECs, which is contrary to the qPCR array data. This discrepancy could be due to different primers used in the qPCR array plates to detect *DLL3* and *LRP5* transcripts. *FZD7* transcripts however, were decreased only in the lenti-shNOTCH3 HMEC cells as compared to scrambled control transduced HMECs (Fig 3.3A). To further validate this observation, another source of non-malignant human breast epithelial cells (184 hTert cell line), were infected with different lenti-shNOTCH virus (Fig 3.4A, B) and *FZD7* transcript expression was examined using qPCR. Similar to the HMEC cells, we found that *FZD7* transcript levels were only decreased in the lenti-shNOTCH3-infected 184-hTert cells (Fig 3.3B). Therefore, this preliminary qPCR array analysis suggests that *FZD7* may be a unique target of NR3 signaling.

3.3.2. Notch-induced FZD7 expression is regulated by NOTCH3 only

Essential to the initiation of Notch signaling is the release of the active NICD, which upon nucleation governs transcriptional regulation of Notch-target genes. Therefore, we forced the expression of a constitutively activated form of each Notch Receptor (*NR1-4*) in the 184-hTERT cells (Fig 3.5A, B) and examined changes in the *FZD7* transcript. Interestingly, only increased signaling through *NR3* significantly increased the expression of *FZD7* transcripts (2.98 ± 0.198 folds) (Fig 3.6A). Using flow cytometry, we observed that *FZD7* protein expression level also changes only when signaling through *NR3* is activated (Fig 3.6B-D). Previous studies have shown that *NR1* could affect the expression of *NR3* and *NR4* [263, 264]. Therefore, it is likewise possible that changes in *NR3* expression could alter the expression of other Notch Receptors. Using qPCR, we found that loss of *NR3* in 184-hTert cells led to small (< 2-fold) decrease in the transcript expression of *NR1* and *NR2* while the transcript expression of *NR4* remained unperturbed (Fig 3.7 and Fig 3.8A). Also, overexpression of active form of *NR3* led to a 2-fold increase in *NR1* and *NR2* expression without altering the expression of *NR4* (Fig 3.8B). However, we found that activation of signaling though *NR1*, *2* or *4* had no effect on *FZD7* expression (Fig 3.6A-D**).** Since only activated *NR3* signaling enhances *FZD7* expression. This suggests that preferential activation of *NR3* may not be required for specific transcriptional activation of *FZD7*.

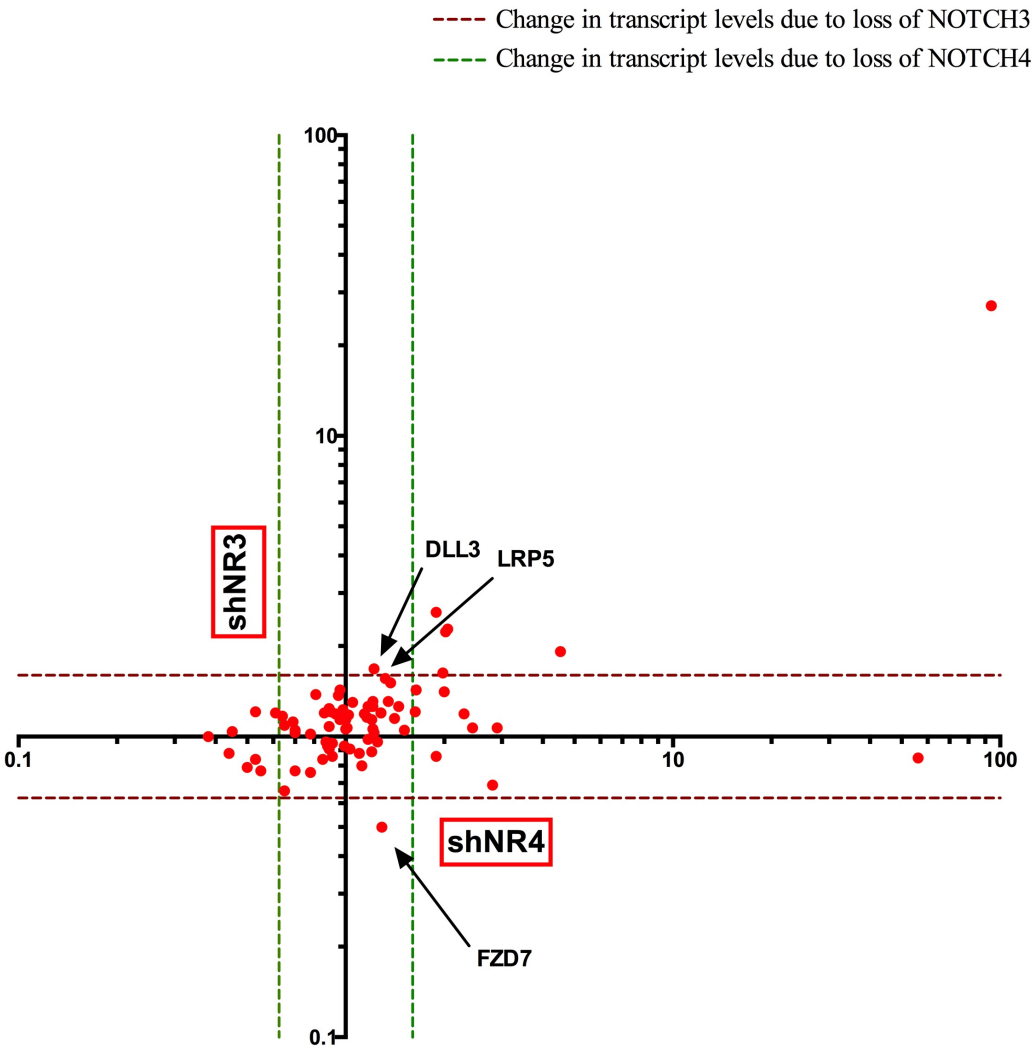

Figure 3.1 Notch signaling pathway PCR Array identified potential NOTCH3 target gene

Human mammary epithelial cell strain, HMECs, were infected with the Lenti virus expressing short hairpin RNA to knockdown *NR3* (shNOTCH3) *or NR4* (shNOTCH4) or Lenti-shScramble control virus and were used to examine changes in the transcript expression of different Notch signaling-related genes using the SABiosciences Notch pathway-specific qPCR array (N=3). The dotted lines represent the arbitrary cutoff of 1.6-fold change in the transcript levels of different genes. This preliminary screen identified 3 potential NR3 target genes namely; *DLL3*, *LRP5*, and *FZD7*. *Figure generated by Dr. Raouf.*

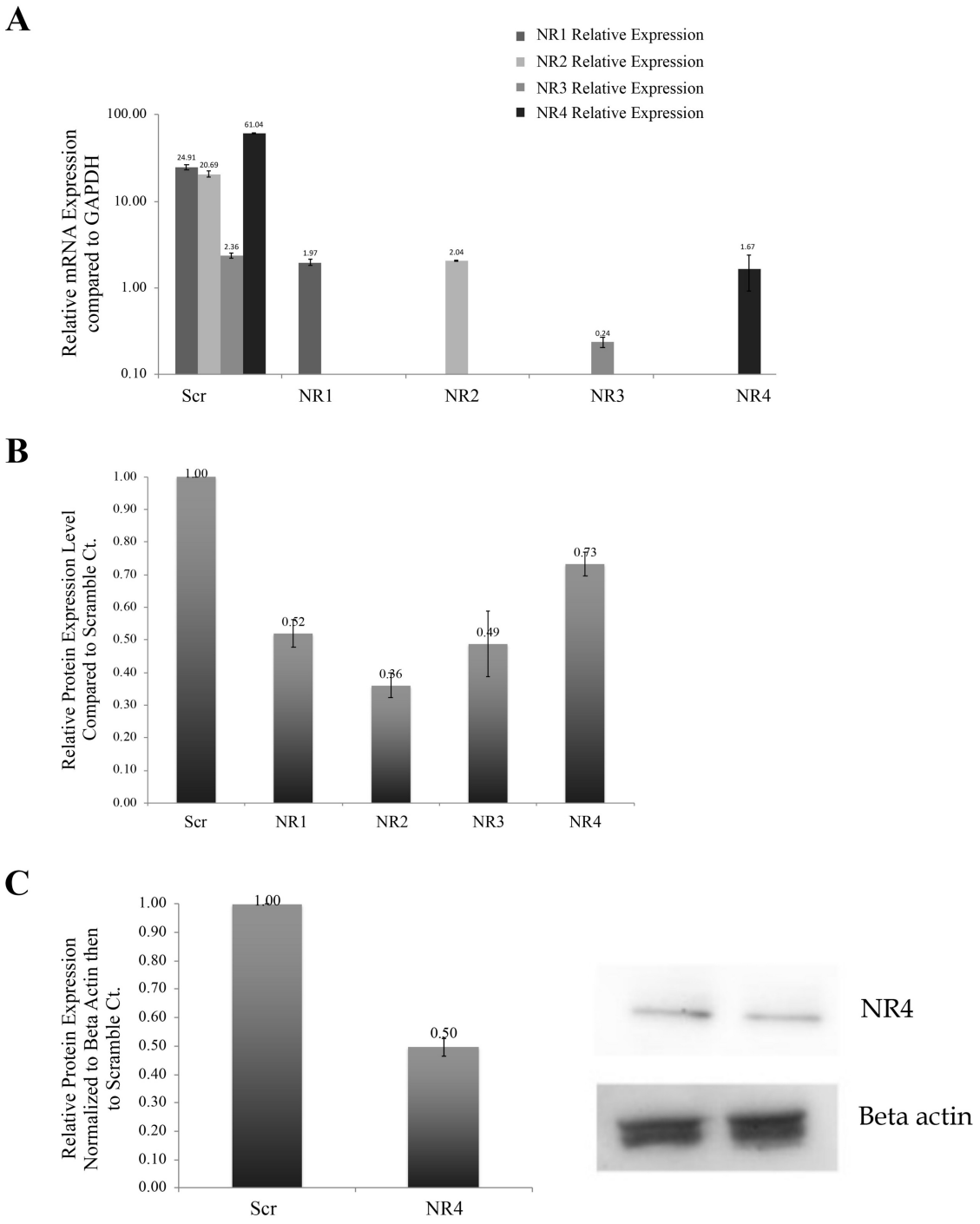

Figure 3.2 Knockdown of NOTCH receptors in HMECs using lentiviral transduction method

Cells from human mammary epithelial cell strain (HMECs) were infected with lentivirus expressing short hairpin (sh) RNA to knockdown expression of each Notch receptor (shNOTCH1

- 4). Also, HMECs where infected with lentivirus expressing a scrambled sequence as a control. The transcript levels for each Notch receptor was quantified using qPCR and normalized with respect to the *GAPDH* transcript levels. Average of 3 independent infections is depicted in a bar graph (A). (B, C) The protein expression of each Notch receptor in transduced cells as in (A) was measured using intracellular fluorescent activated cell sorting or FACS (B). The lenti shNR-infected cells show 50%-70% knock down on each receptor. Since *NR4* knockdown was measured to be only 30% using FACS, we utilized the Western Blot analysis (C) to detect its knockdown and found that lenti sh*NOTCH4* infected cells show a 50% reduction in the *NR4* expression. The error bars show standard deviation, n=3

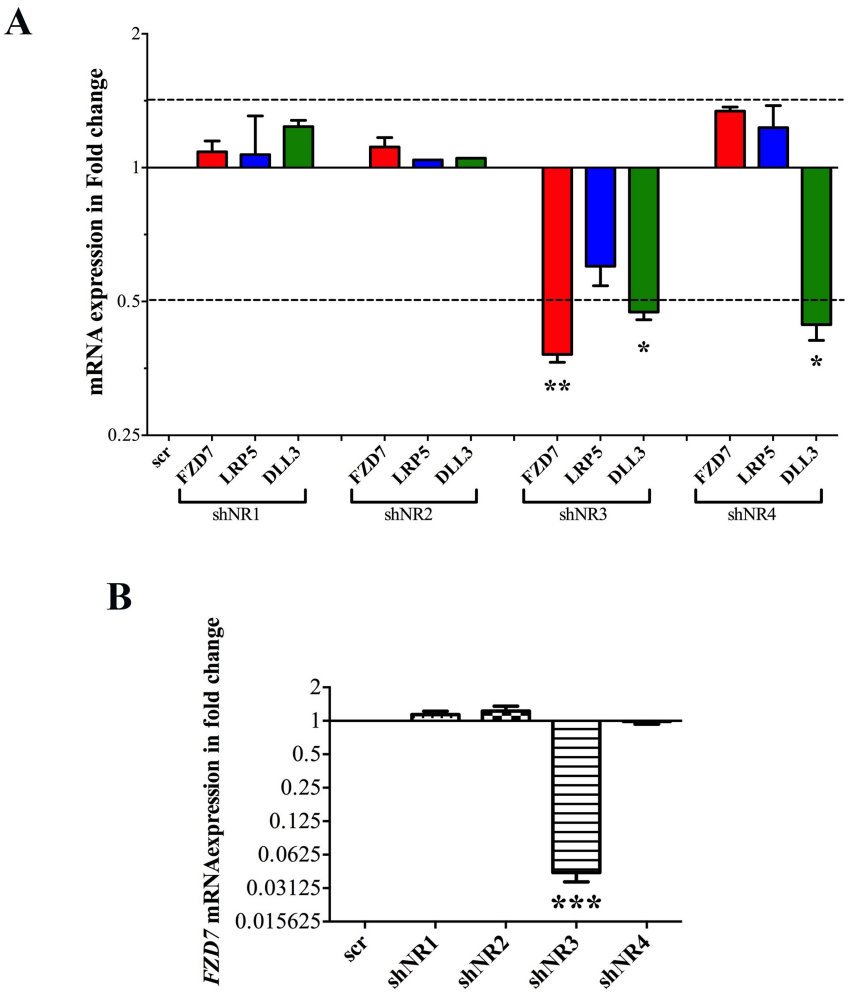

Figure 3.3 NOTCH3 regulates expression of FZD7

(A) The human breast epithelial cell strain, HMECs, were transduced with different lenti-sh*NOTCH1-4* virus, and transcript expression of *FZD7, LRP5* and *DLL3* was examined using qPCR and normalized with respect to *GAPDH* and then to the scrambled control-infected cells.

(B) 184-hTert cells were infected separately with different Lenti-Sh*NOTCH1-4* or a Scrambled control expressing virus and FZD7 transcript expression was determined as in (A). As shown, the transcript expression of *FZD7* is only decreased when *NR3* expression is decreased. (the error bars show standard deviation, n=3, *** p-Value ≤ 0.0005).

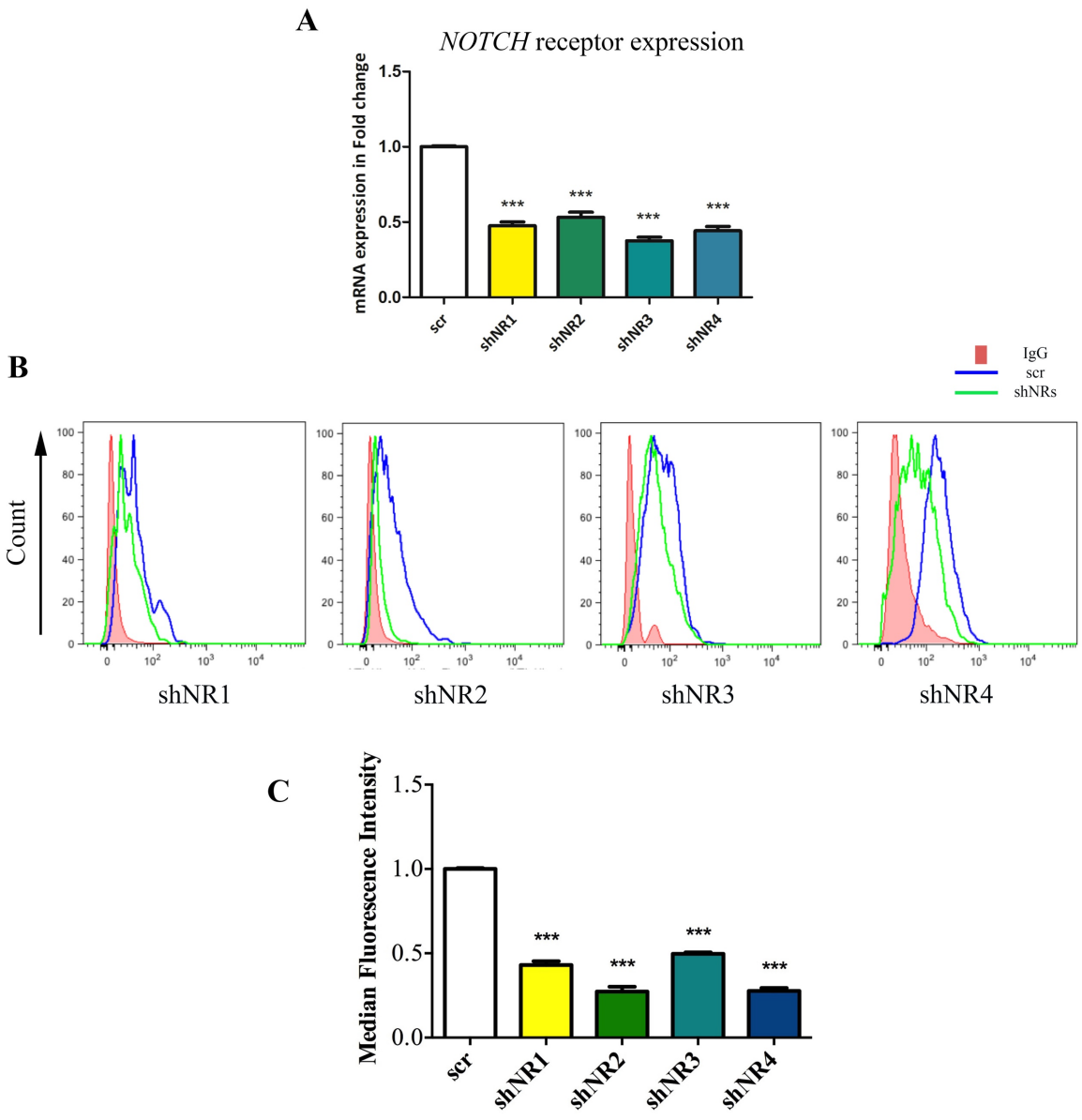

Figure 3.4 Knockdown of NOTCH receptors in 184-hTert cells

Same strategy as in Supplementary Figure 3.2A was employed to knockdown the expression of individual Notch receptors (shNOTCHR1-4) in the 184-hTert cells. qPCR was used to quantify the transcript levels of each receptor (A) and intracellular FACS (fluorescent activated cell sorting) was used to examine the protein level of each receptor in the lenti shNR infected cells. (A) Average

transcript levels (N=3) of each receptor is normalized with respect to the *GAPDH* levels and then compared to scramble control infected cells (set to 1). (B&C) The average median fluorescent intensities were obtained from 3 separately infected cells and depicted in the bar graph. Representative histograms are also shown. Overall the data shows that in 184-hTert cells, a robust knockdown of the Notch receptor levels at the RNA and protein levels can be achieved. The error bars show the standard deviation *** p-Value ≤ 0.0005.

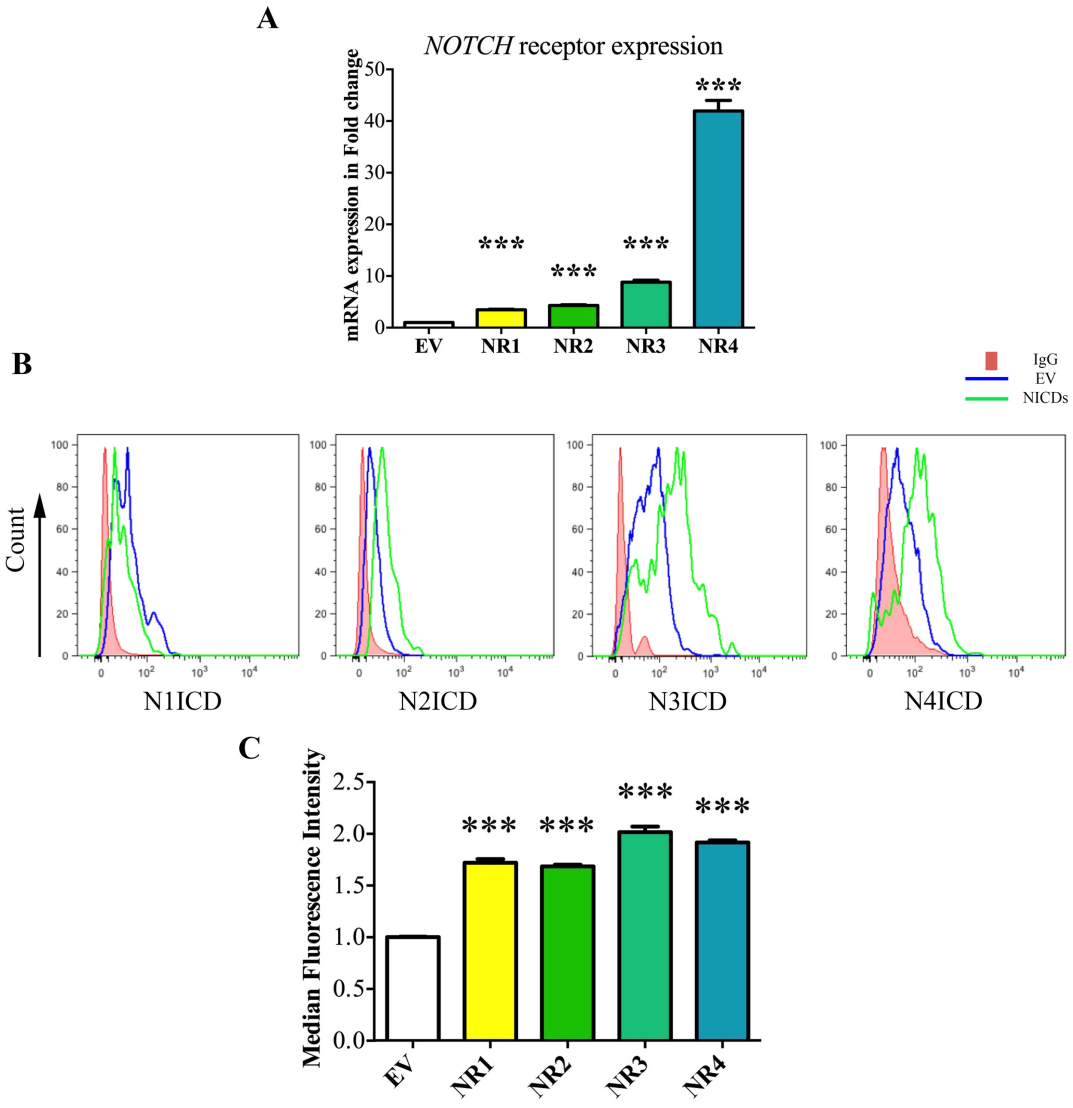

Figure 3.5 Overexpression of active form of different NOTCH receptors in 184-hTert cells

Lentivirus expressing the intracellular domain (constitutively active form) of different Notch Receptors (NOTCH1 - 4) or an empty virus (EV) was used to infect the 184-hTert cells. (A) The transcript expression of each NR was determined using qPCR and normalized to the *GAPDH* expression. The expression of each NR in the EV-infected cells was used as reference (Set = 1). (B) The NR protein expression in the transduced 184-hTert cells was ascertained using

intracellular FACS. IgG antibody staining was used as background control. Representative histograms are shown and the average median fluorescent intensities (MFI) from 3 independent infections are shown in a bar graph. The MFI of different NR expression in the EV infected cells were used as reference (set to 1). The error bars show the standard deviation *** p-Value ≤ 0.0005.

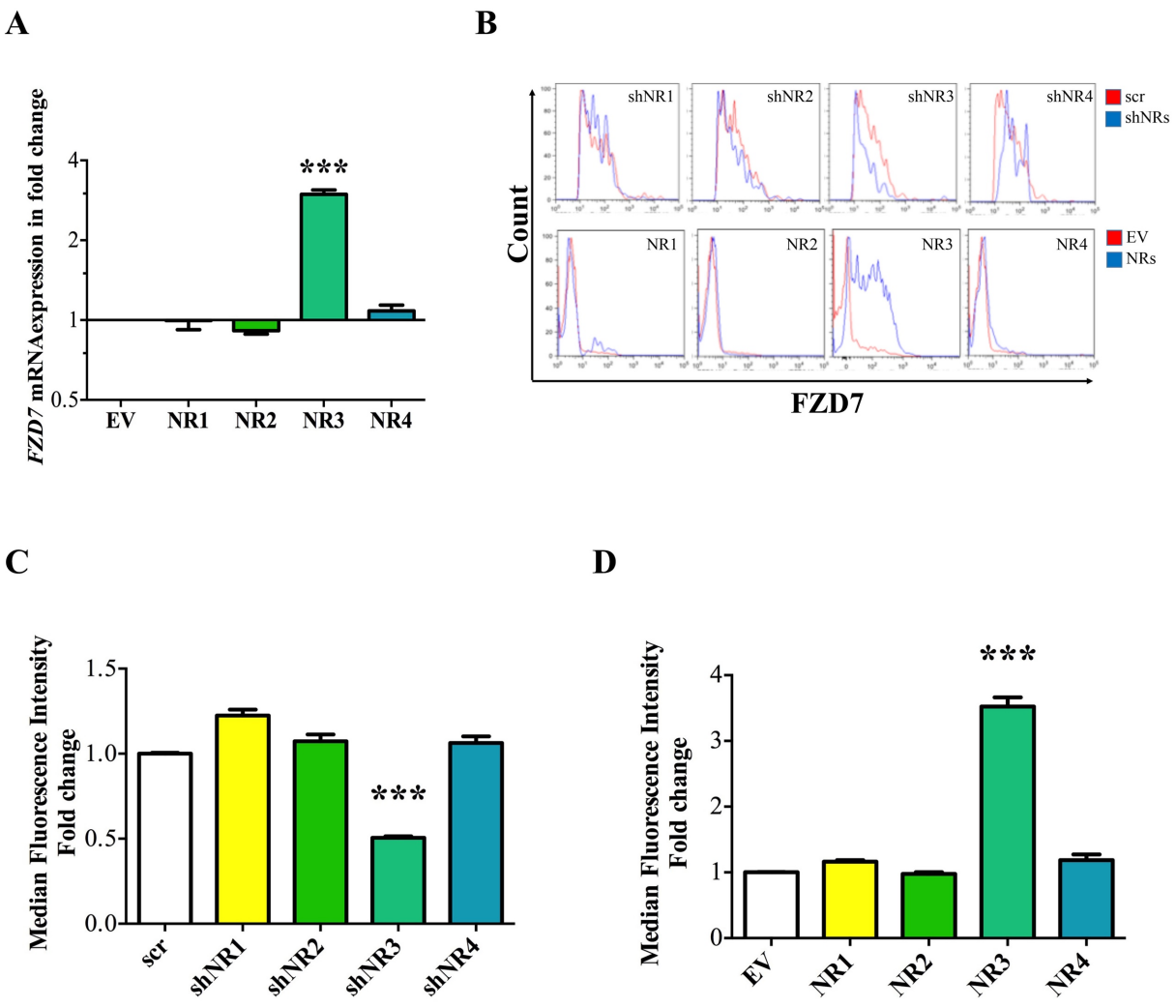

Figure 3.6 FZD7 is a unique target of NOTCH3

184-hTert cells were infected with lenti virus expressing the constitutively active form of each Notch receptor (NR1-4) or empty vector (EV) control and the transcript expression of *FZD7* was examined via qPCR (A). The data is quantified relative to the *GAPDH* expression and is presented relative to the EV control transcript expression. As shown, only increased signaling through *NR3* increased *FZD7* expression. (B) Flow cytometer was used to examine *FZD7* protein expression levels in 184-hTert cells separately transduced to express different Notch receptors (NR1-4) or transduced with different lenti-sh*NOTCH* (shNR1-4) to knockdown expression of each receptor

separately. Some cells were transduced with a lenti shScrambled-expressing virus (scr) as controls. Representative histograms are shown and average (N=3) median fluorescent intensities are depicted as bar graphs (shNOTCH-infected cells in C and lenti NR-infected cells in D). As shown, *FZD7* protein expression is only altered when signaling through *NR3* is modulated. The error bars show the standard deviation *** p-Value ≤ 0.0005.

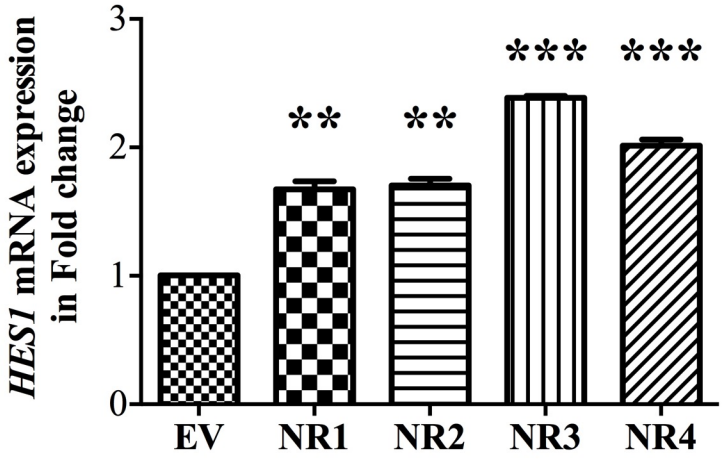

Figure 3.7 HES1 expression in 184-hTert cells

To ensure that overexpression of different Notch Receptors results in activation of Notch signaling, the expression of a well-established NOTCH target, *HES1*, was examined in the Lenti-NOTCH1-4 (NR1-4) infected 184-hTert cells. The relative *HES1* transcript level was examined using qPCR where the *GAPDH* transcript levels were used as internal control and then normalized to the EV-infected cells (set to 1). Average *HES1* transcript levels from 3 independently transduced cells are depicted in a bar graph. The error bars show standard deviation, n=3, ** p-Value ≤ 0.005 *** p-Value ≤ 0.0005

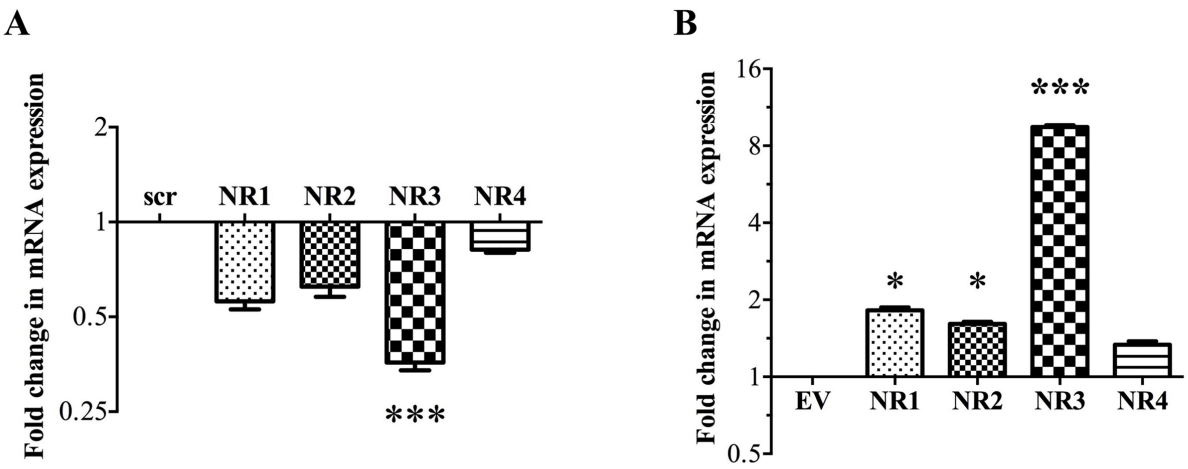

Figure 3.8 NOTCH receptor expression in NOTCH3 knockdown and overexpressing 184-hTert cells

(A) The average expression of different Notch Receptors (NR) in the lenti-shNR3-transduced 184-hTert cells was determined using qPCR. Average transcript levels were first normalized to the *GAPDH* transcript levels and then to the scrambled control levels (set to 1). Average of 3 independently transduced 184-hTert cells are shown. (B) Likewise, expression of different NR in the NR3-overexpressing 184-hTert cells was examine via qPCR. The statistical significance was determined using the student t-test (The error bars show standard deviation, n=3, * p-Value ≤ 0.05, ** p-Value ≤ 0.005, *** p-Value ≤0.0005).

3.3.3. Luminal progenitors exhibit high expression of NOTCH3 and FZD7

FZD7 is a Wnt signaling receptor that is involved in the proliferation and differentiation of progenitors and stem cells [265-268]. We therefore examined if *FZD7* is differentially expressed among the undifferentiated human breast epithelial cells (i.e. stem and progenitor cells). Previously, we showed that the stem cells/bipotential progenitors and the luminal progenitors could be obtained from the breast reduction samples based on their expression of EpCAM and CD49f [67]. We observed that overall, only 1-1.5% of the uncultured normal human breast cells express *FZD7* and that the bipotent and the luminal progenitors express the *FZD7* protein. Interestingly however, luminal progenitors contained more *FZD7*$^{+}$ cells and expressed *FZD7* transcripts and protein at a higher level compared to the bipotent progenitors (Fig 3.9A-D). In addition, increased signaling through *NR3* significantly increased *FZD7* expression in the primary human breast epithelia cells obtained from breast reduction samples. These observations are significant because we had previously shown that the luminal progenitors express *NR3* at a much higher level compared to the stem/bipotent progenitors (Fig 3.9D and [76]). Moreover, it was recently shown that Wnt signaling could restrict luminal/alveolar differentiation and decrease *NR3* expression by modulating the Pygo2 expression [238], suggesting that a strong crosstalk between *NR3*-Wnt exists. In addition, *FZD7* has also been reported to regulate progenitor cell functions in endoderm cells [268]. Therefore, it is inviting to hypothesize that *NR3* could regulate luminal cell differentiation through *NR3-FZD7* signaling axis.

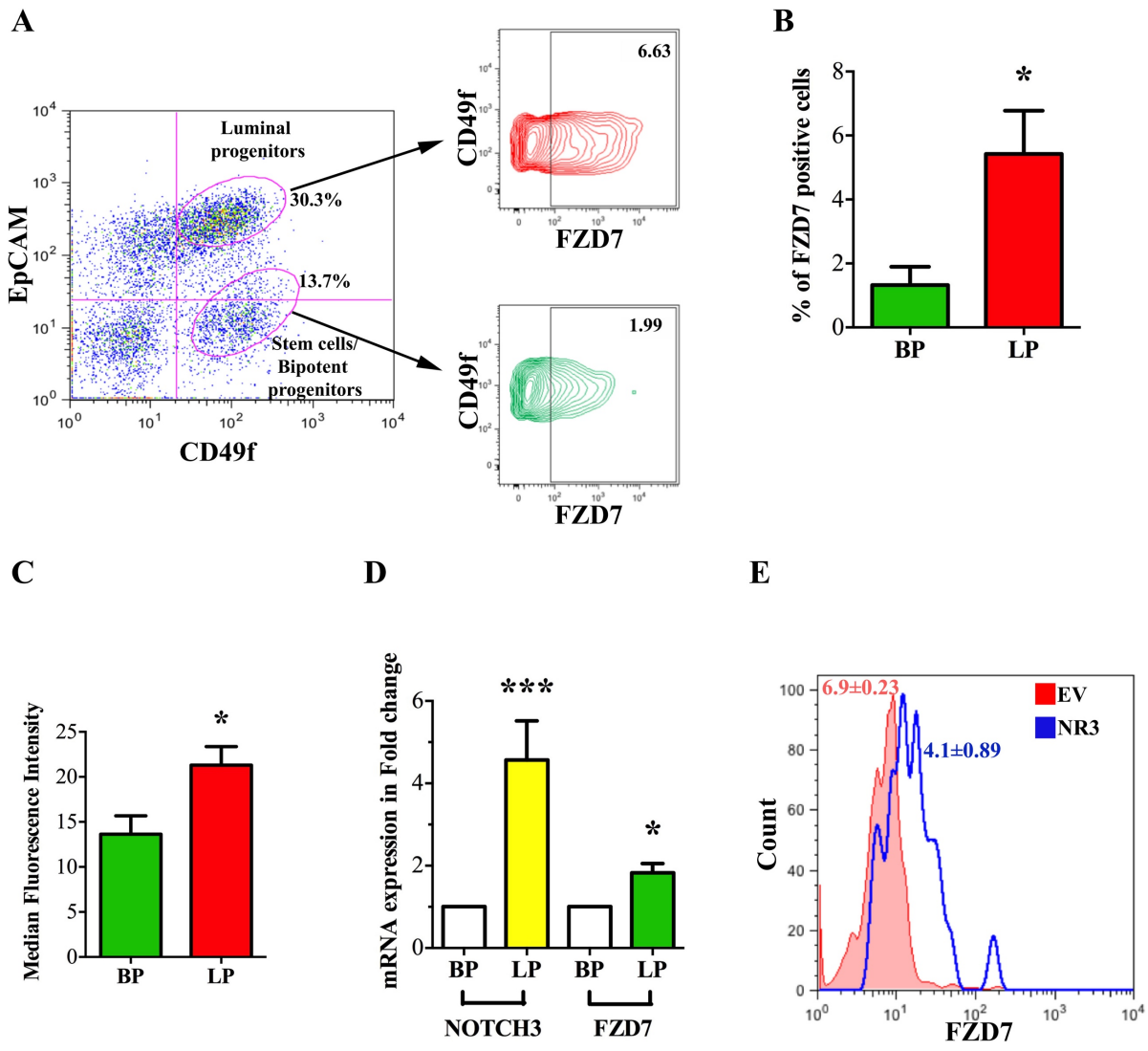

Figure 3.9 Luminal progenitors show higher expression of FZD7 and NOTCH3

(A) To examine the expression level of *FZD7* in the undifferentiated subpopulations of human breast epithelial cells, luminal and the stem/bipotential progenitor-enrich cell populations were obtained from breast reduction samples based on their expression of Epithelial Cell Adhesion (EpCAM) molecule and α-6 Integrin (CD49f). (B-C) Flow cytometry was used to examine *FZD7* protein expression in the luminal progenitor (LP)-enriched population ($EpCAM^{bright}CD49f^{low}$) and the stem/bipotential progenitor (BP)-enriched subpopulation ($EpCAM^{low}CD49f^{bright}$). As shown,

the LP subpopulation was more enriched for *FZD7*-expressing cells and that they also expressed *FZD7* at a higher level compared to BP (20.56 ±3.3, 12.23 ±1.3 respectively). (D) RNA was extracted from LP and the BP subpopulations isolated from 3 different breast reduction samples and the *FZD7* and *NR3* transcript levels were examined suing qPCR. As shown, LP cells express *FZD7* and *NR3* transcripts at a higher level compared to the BP cells. The transcript levels are normalized to GAPDH transcript levels and then normalized to BP transcript expression levels (* p-Value ≤ 0.05, *** p-Value ≤ 0.0005). (E) Breast reduction samples (N=3) where dissociated into single cells and infected either with lenti virus expressing empty vector (EV) or NR3 expressing vector. After 72 hours, cells expressing the green fluorescent protein (GFP^+) were examined for their expression of *FZD7* via flow cytometry. One representative histogram is shown depicting FZD7 expression in the lenti-EV or -NR3 transduced cells and the average median fluorescence intensity of 3 samples is shown with standard deviations. The error bars show standard deviation, n=3, * p-Value ≤ 0.05, ** p-Value ≤ 0.005, *** p-Value ≤ 0.0005.

3.3.4. NOTCH3-regulated expression of FZD7 is CLS-independent

To study if *NR3* regulates *FZD7* expression through canonical signaling we used chromatin immunoprecipitation (ChIP) to quantify *NR3* enrichment on the *FZD7* promoter. 184-hTERT cells were transduced with FLAG, N1ICD-FLAG, and N3ICD-FLAG expressing constructs and ChIP was performed using anti-FLAG antibody. Compared to IgG isotype control, no significant enrichment for *NR1* or *NR3* could be observed on the 2 putative CSL binding sites in the *FZD7* enhancer/promoter region. *HES1* promoter showed significant enrichment for both *NR1* and *NR3* (Fig 3.10A-B and Fig 3.11A). These observations suggest *NR3* could regulate *FZD7* expression in a non-canonical manner. To investigate this possibility, *NR3*-expressing 184-hTERT cells were transduced with lenti-scrambled or lenti-shCSL and expression of *FZD7* was determined via qPCR and FACS (Fig 3.11C-D). Interestingly, in absence of CSL, *FZD7* expression showed significant increase in *NR3*-expressing cells, suggesting that the *NR3*-induced *FZD7* expression does not require CSL (Fig 3.11C). As expected, *NR3* regulation of *HES1* transcript expression however, required CSL expression (Fig 3.11B).

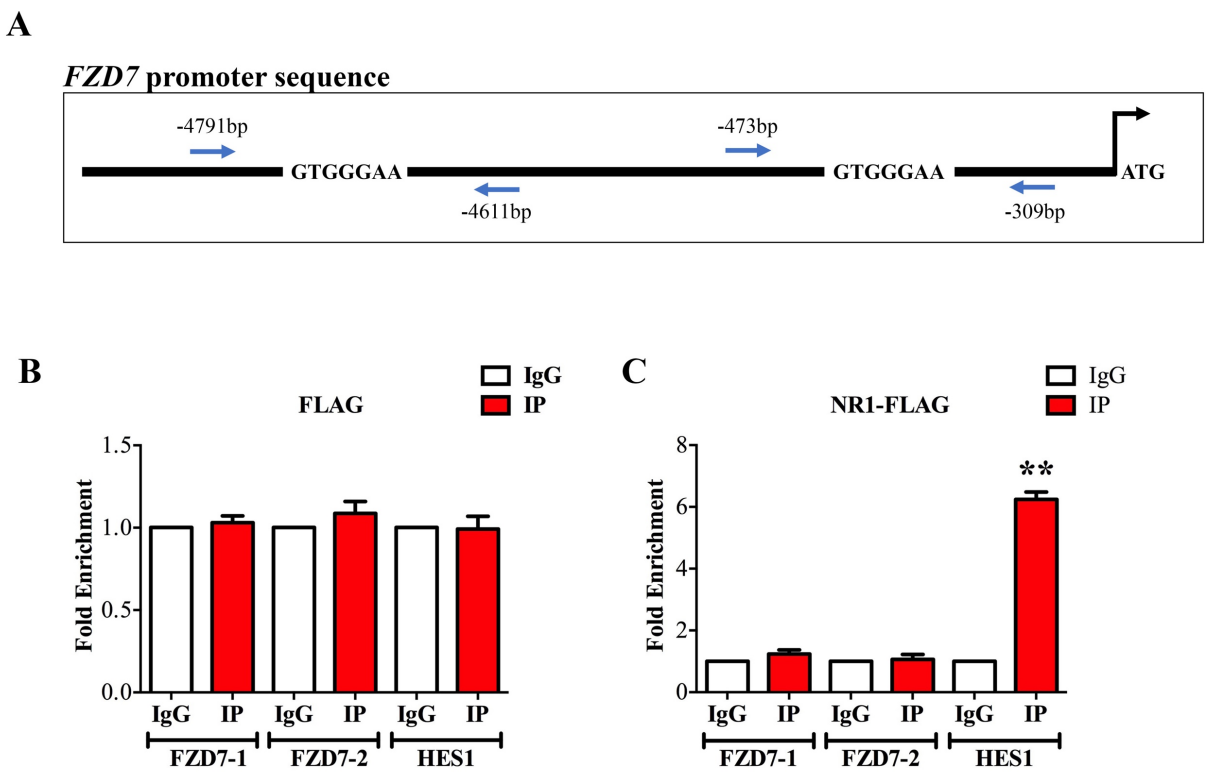

Figure 3.10 Chromatin immunoprecipitation reveals no enrichment for NR1 on FZD7 promoter

184-hTERT cells were transduced with vectors expressing a constitutively active form of N1ICD-FLAG or FLAG alone and Chromatin Immunoprecipitation was performed using anti-FLAG antibody. The ChIP DNA was used to examine the occupancy of NR1 or NR3 on putative CSL binding sites (GTGGGAA) on the *FZD7* promoter using qPCR. The blue arrow shows the primer binding sites (A). IgG isotype was used as negative control. The occupancy enrichment was compared to the IgG control ChIP DNA. ChIP DNA did not show any significant enrichment for FLAG or NR1 proteins (B&C). As expected however, NR1 binding was significantly enriched on the *HES1* Promoter. The error bars show standard deviation, n=3, p-Value ≤ 0.005 ***.

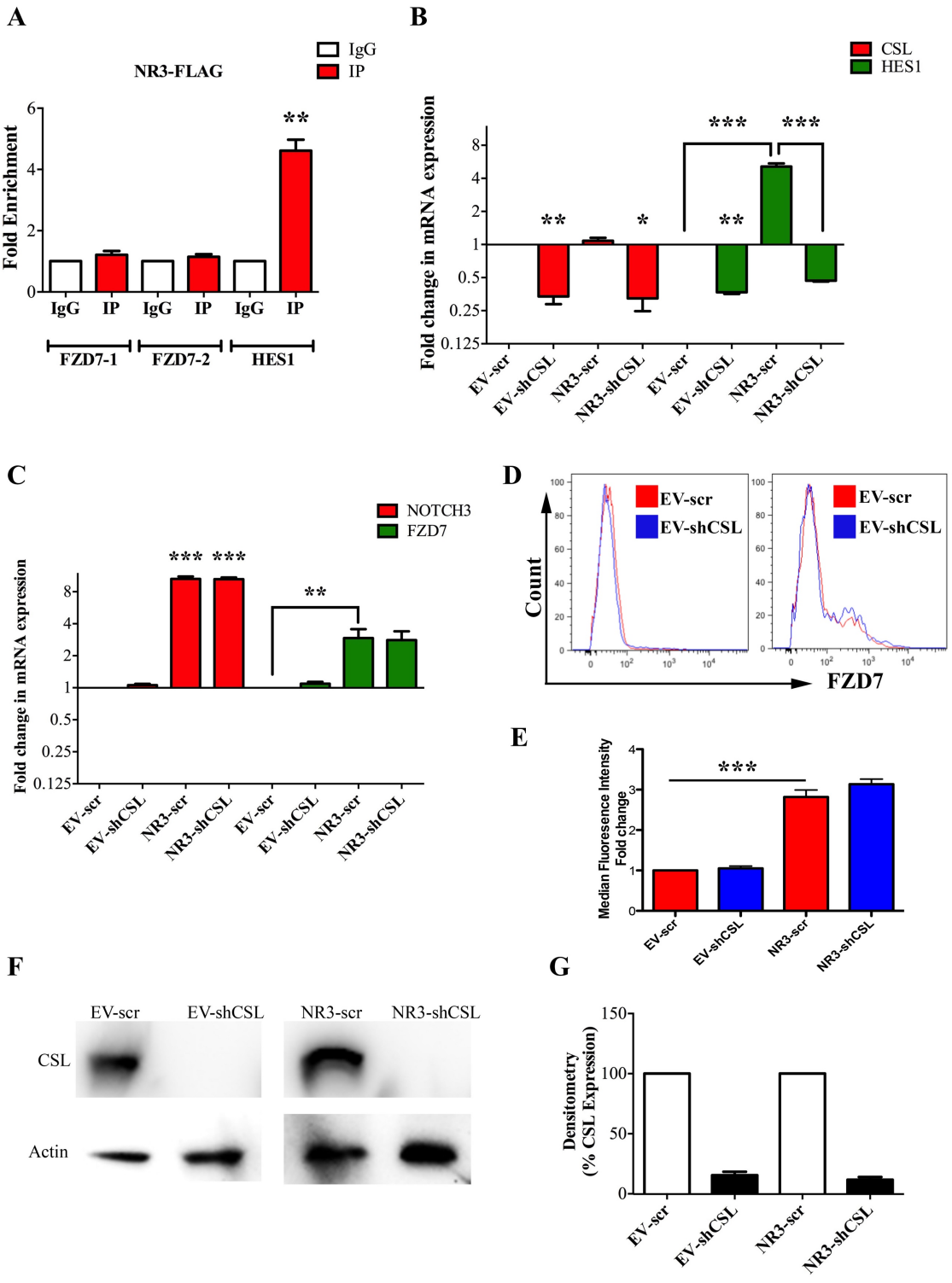

Figure 3.11 NOTCH3 regulates FZD7 expression in a CSL-independent manner

(A) 184-hTERT cells were transduced with a N3ICD-FLAG expressing constructs and chromatin immunoprecipitation (ChIP) was performed using anti-FLAG antibody. FLAG only expressing cells were used as controls and the data obtained from these cells are depicted in the Fig 3.9A**.** The NR3 binding and enrichment on *FZD7* promoter on 2 putative CSL binding sites was assessed via qPCR compared IgG isotype control (set to1). Using primers flanking the CSL binding sites, no significant enrichment of NR3 on *FZD7* promoter could be detected. As a positive control, the enrichment for binding of NR1 and NR3 on the HES1 promoter was also examined. (B-C) 184-hTERT cells overexpressing NR3 or empty vector (EV) control were additionally transduced with lenti-sh*CSL* or lenti-*Scrambled* control (scr) and transcript expression of *CSL and HES1* (B) *NR3* and *FZD7* (C) was examined via qPCR. The data were quantified relative to the *GAPDH* expressions and then to the EV-Scr (set to 1). The lenti-shCSL transduced 184-hTert cells showed >90% reduction in CSL transcript expression. (D&E) Flow cytometry was used to examine FZD7 protein expression in the EV-CSL-knockdown (EV-shCSL), EV-Scr control (EV-Scr), NR3-overexpressing-CSL-knockdown (NR3-shCSL), and the NR3-overexpressing-Scr control (NR3-Scr) cells. A representative histogram is shown (D), and average median fluorescence intensities are shown in the bar graph (E). Western blots were used to quantify CSL expression in the EV-Scr, EV-shCLS, NR3-Scr, and the NR3-shCSL cells. (F) CSL expression was quantified relative to the actin protein expression (one representative WB is shown) and average CSL expression from 3 separate experiments is shown in the bar graph (G). As shown, NR3 increases *FZD7* transcript and protein expression in absence of *CSL* expression. The error bars show standard deviation, n=3, * p-Value$\leq$ 0.05, ** p-Value $\leq$ 0.005, *** p-Value $\leq$ 0.0005.

3.4. Conclusion

Notch is an evolutionarily conserved signaling pathway which plays a critical role in a plethora of cellular processes. In vertebrates, there are 4 notch receptors and 5 notch ligands. Interaction between a ligand and the receptor activates notch signaling and regulation of notch target genes. Notch-activated genes play an important role in different cellular processes such as proliferation, differentiation, self-renewal and apoptosis. The ubiquitous expression of some of the notch receptors (NR1, NR2) as well as the common canonical signaling mechanisms utilized the NRs in many different cell types has led to the conclusion that all receptors regulate a common set of gene and regulate overlapping cellular functions. However, emerging evidence has challenged this notion. Previous data indicated that NR3 signaling alone was required for commitment of the bipotent progenitors to luminal cell fate [76]. This suggested NR3 signaling activated unique genes required for lineage commitment. In this study we showed that NR3 uniquely regulated the expression of a Wnt receptor, FZD7 in human mammary epithelial cells. This finding then suggests that each receptor could regulate unique set of gene and therefore regulate unique cellular function. Further we showed that the NR3-induced expression of FZD7 was CSL independent, which is a deviation from the conserved canonical Notch signaling mechanism. Taken together, the findings from this study suggest that NR3-Wnt signaling crosstalk could regulate the luminal cell fate commitment in human mammary epithelial cells.

4. Characterization of NOTCH3 signaling responsive basal-like luminal progenitors in human breast

4.1. Abstract

Role of NOTCH3 receptor (NR3) in luminal fate specification of human breast cells was discovered based on its high expression in luminal-restricted progenitors (LRPs). Interestingly, however, although NR3 signaling enhanced commitment of bipotent progenitors to the luminal cell fate, it had no effect on proliferation and differentiation of the LRPs. I, therefore, examined if FZD7, a specific target of NR3, is involved in luminal cell fate specification. Indeed, activation of FZD7 receptor through its ligand, Wnt7A, enhanced commitment of bipotent progenitors to a luminal cell fate while it had no effects on LRPs. Using gain and loss of function studies, I found that FZD7 signaling was required for efficient luminal fate specification of bipotent progenitors. However, NR3 had a more dominant role in this process. Both NR3-FZD7 signaling had no effects of LRP differentiation. Based on these data, I found that a $NR3^{+}FZD7^{+}$ basal-like luminal progenitors ($CD49^{+}EpCAM^{+}CD90^{+}$) differentiated to form luminal cells only. On the other hand, the $NR3^{-}FZD7^{+/-}$ subset only formed mix colonies of luminal and myoepithelial cells. For the first time, I identified and characterized the "basal-like luminal progenitors" (BLPs) which are different from LRPs with respect to their response to NR3 and Wnt7A signaling. To gain a broader view on the NR3-regulated signaling network, I employed an unbiased transcriptome profiling approach and identified 816 unique targets of NR3 which highlighted retinoate biosynthesis I, Ephrin B signaling, Cell Cycle regulation, Endothelin signaling, phospholipase signaling, p38 MAPK signaling, Vitamin C signaling and Wnt signaling pathways. These observations suggested that NR3 and Wnt signaling cooperated to promote the commitment of bipotent progenitors to luminal cell lineage.

4.2. Introduction

The human breast undergoes dynamic changes of expansion and regression throughout the reproduction phase of a female. The adult breast tissue is maintained through continuous turnover of luminal and myoepithelial cells. These mature breast epithelial cells, produced from bipotent progenitors [68, 75, 76, 78], are ultimately derived from the primitive breast epithelial stem cells [42, 78]. However, unlike in the mouse system, the distinction between breast epithelial stem cells and the bipotent progenitor cells is not clearly understood. This is mainly due to the lack of unique markers that can segregate stem cells from bipotent progenitors. Moreover, evidence that bipotent progenitors give rise to luminal-restricted progenitors (LRPs) and myoepithelial-restricted progenitors is still lacking. Recent single-cell RNA sequencing analysis of human breast epithelial cells offered some new insights into the hierarchical structure of human breast epithelium. A psuedotemporal reconstruction of differentiation trajectories algorithm was used to organize cells based on the transcriptome profile of individual cells. This analysis performed on breast epithelial cells suggested that the bipotent progenitors could be placed above LRPs in the hierarchy. This analysis also suggested that LRPs could give rise to both estrogen hormone responsive and secretory luminal epithelial cells [269, 270]. However, experimental evidence in support of lineage hierarchy in the human breast does not exist. Moreover, the molecular mechanism that regulates lineage cell commitment is poorly understood. Understanding such molecular mechanisms could provide new insight into breast cancer initiation and progression as cancer is often referred to an inappropriate execution of developmental program [70, 271].

Our previous study reported that NR3 expression in bipotent progenitors specifies luminal lineage and it also uniquely regulated Wnt receptor FZD7 [76, 87]. This suggested that NR3 regulated expression of unique target genes that could potentially play an important role in luminal

lineage commitment. The purpose of this study is to examine if the NR3-FZD7 signaling is important for luminal cell lineage specification in human breast epithelial cells. We show that breast bipotent progenitors that express NR3 and FZD7 are Wnt7A responsive and give rise to only luminal colonies only. LRPs are unresponsive to Notch and Wnt signaling. To the best of our knowledge, this is the first identification and characterization of a Wnt and Notch-responsive basal-like luminal progenitors.

4.3. Results

4.3.1. NOTCH-FZD7 signaling commits bipotent progenitors to the luminal cell fate

To investigate the role of NR3-FZD7 signaling in luminal cell lineage commitment, I employed gain and loss of function approaches using primary human breast epithelial cells, obtained from breast reduction samples. Lineage depleted ($CD45^{+}CD31^{+}$ removed, Lin^{-}) breast epithelial cells were co-cultured with NIH3T3, mouse embryonic fibroblasts overnight to increase progenitor frequencies [76]. Subsequently, cells were transduced with lentivirus expressing either short hairpin RNA (shRNA) to target NR3 or FZD7 transcripts. Alternatively, lentivirus to overexpress NR3 intracellular domain (N3ICD) or full-length FZD7 were also used. Lentivirus expressing on sh-scrambled sequence or green fluorescent protein (GFP)-only were used as controls.

Transduced GFP positive bipotent progenitor ($EpCAM^{+}CD49f^{+}CD90^{+}$) and luminal-restricted progenitor ($EpCAM^{+}CD49f^{+}CD90^{-}$) enriched populations were sorted via fluorescent activated cell sorting (FACS) and colony forming cell (CFC) assays were performed to assess their differentiation potential (Fig 4.1A). *NR3* and *FZD7* knockdown and transgene expression efficiencies in primary human breast epithelial cells were assessed by flow cytometry (Fig 4.1B-E). shRNA-transduced cells showed 82.33±1.76% decrease in *NR3* and 75.0±2.88% decrease in FZD7 protein levels, respectively. Cells transduced with have activated NR3 virus showed 6.93±0.95 fold increase in NR3 and 4.45±0.71% fold increase in FZD7 levels. Furthermore, NR3-regulated FZD7 expression was confirmed in shNR3 and N3ICD-transduced primary cells (Fig 4.1F&G).

Knock down of *NR3* in the bipotent progenitor-enriched population significantly diminished (2.50±1.32 fold decrease) their luminal colony forming potential (Fig 4.2A) while at

the same time enhanced their mix colony-forming potential, although by a small but statically significant margin (Fig 4.2B). Very interestingly, decreased FZD7 expression in bipotent progenitor-enriched population also resulted in decreased luminal colonies (Fig 4.2C, 1.51±1.15 fold decrease). However, this decrease in the luminal colony numbers was not as striking as occurred in response to the loss of NR3 in the same population (Fig.4.2C). The mix colony-forming potential of the shFZD7-Bipotent progenitor-enriched population was unaffected (Fig 4.2D). Interestingly, the loss of *NR3* or *FZD7* and also ectopic expression of active form of NR3 or FZD7 had no effect on luminal-restricted progenitor-enriched population suggesting that they were independent of NR3 or FZD7 signaling (Fig 4.2E&F).

Bipotent progenitor-enriched population overexpressing N3ICD or FZD7 (Fig 4.3A&B) gave rise to more luminal colonies as compared to empty vector control. The mix/basal colony numbers were unchanged under both conditions (Fig 4.3C&D). As seen with the loss of function approach, overexpression of N3ICD or FZD7 did not have any influence on luminal-restricted progenitors (Fig 4.3E&F). Thus, NR3 and its downstream gene target FZD7 play a critical role in restricting bipotent progenitor-enriched population to luminal cell fate. However, the dominant role of NR3 in this process suggests that in addition to FZD7 other NR3 gene targets might be involved.

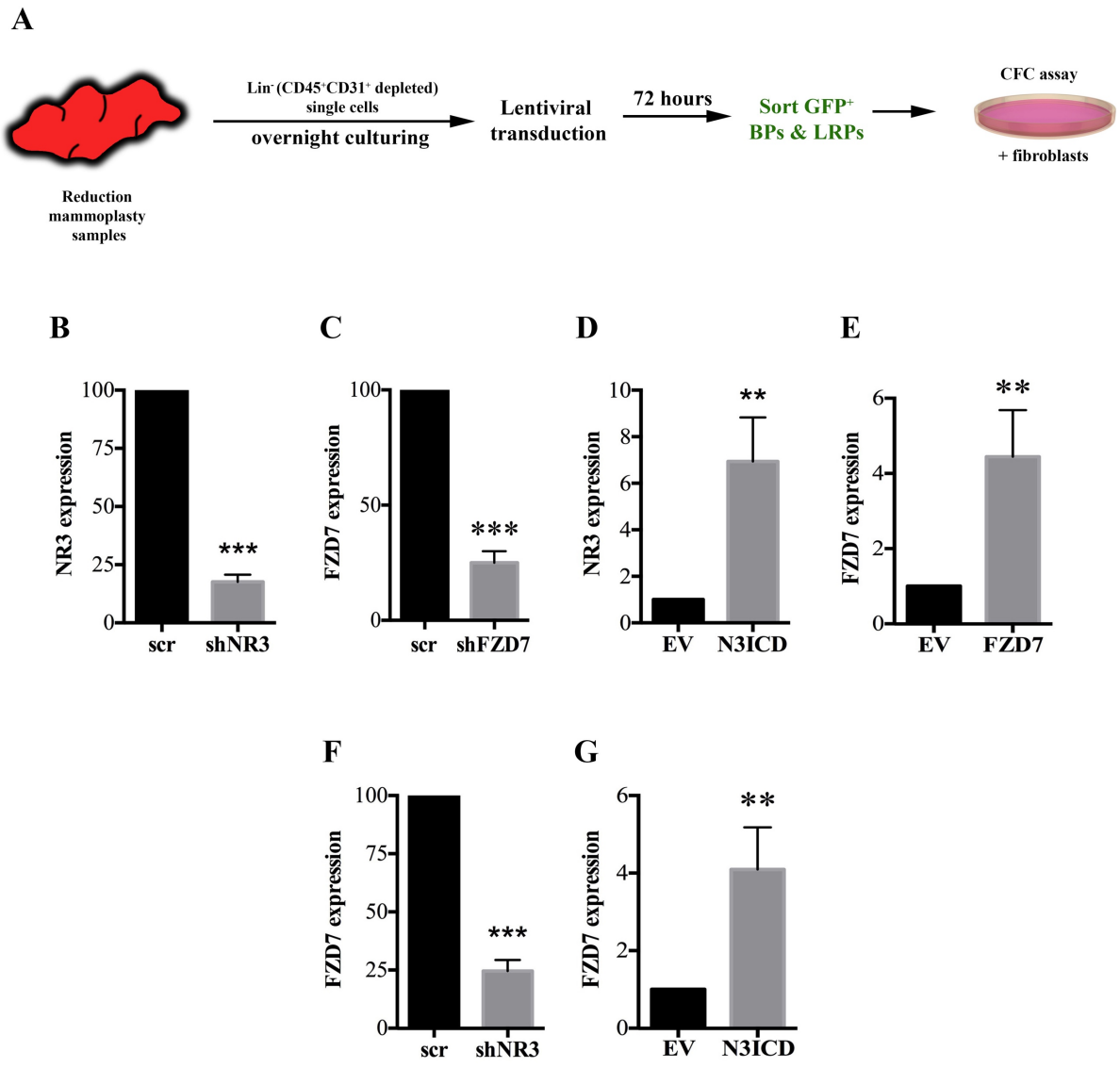

Figure 4.1 Successful knockdown and overexpression of NOTCH3 and FZD7 in primary human breast epithelial cells

(A) Breast reduction samples where dissociated into single cell suspension, lineage depleted and co-cultured with NIH3T3, mouse embryonic fibroblasts overnight. Cells were lentivirally transduced with scrambled control (scr) vs NR3 or FZD7 targeting short hairpin RNA (shRNA) or empty vector (EV) control vs N3ICD or FZD7 overexpressing lentivirus. After 72 hours, the transduced green fluorescent protein (GFP^+) expressing cells within the bipotent

(EpCAM^{+}CD49f^{+}CD90^{+}) and luminal (EpCAM^{+}CD49f^{+}CD9^{-}) progenitor-enriched population were obtained via FACS. Progenitors were cultured in the colony forming cell assays for 7 days and colony type and numbers were recorder. (B-G) Bar graphs show the average knockdown and overexpression of NR3 and FZD7 in human breast epithelial cells was quantified using flow cytometry. NR3 and FZD7 expression in scr cells was set to 100 whereas EV control cells were set to 1. (B & C) Data shows the knockdown levels of *NR3* and *FZD7* in epithelial cells transduced with lentivirus expressing shRNA targeting *NR3* (shNR3) and *FZD7* (shFZD7). (D & E) Bar graphs show the overexpression levels of NR3 and FZD7 in N3ICD and full length FZD7 overexpressing epithelial cells respectively. (F&G) shows protein expression level of FZD7 in breast epithelial cells transduced with shNR3 and N3ICD lentivirus respectively. (The error bars show standard deviation, n=3, **p≤0.01, *** p≤0.0005).

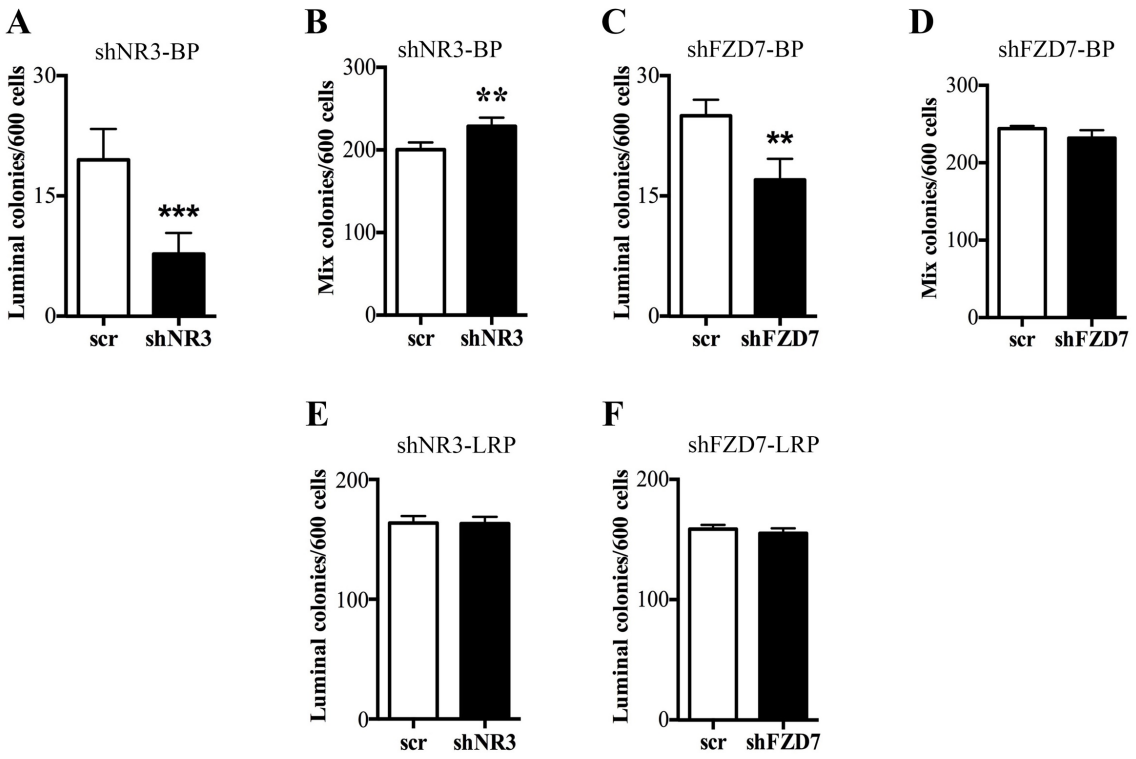

Figure 4.2 Loss of NOTCH3-FZD7 signaling inhibits luminal cell fate commitment of cells within bipotent progenitor-enriched population

(A&B) Shows the total number of luminal and mix colonies generated from bipotent progenitor-enriched population lacking NR3 expression (shNR3-BP) as compared to controls. (C&D) Total number of luminal and mix colonies formed in CFC assay from bipotent progenitor-enriched population lacking FZD7 expression (shFZD7-BP) as compared to controls. (E&F) Total number of luminal colonies observed in colony forming cell assay (CFC) assay from luminal-restricted progenitors lacking either NR3 (shNR3-LRP) or FZD7 (shFZD7-LRP) expression. (The error bars show standard deviation, n=3, **p≤0.01, *** p≤0.005).

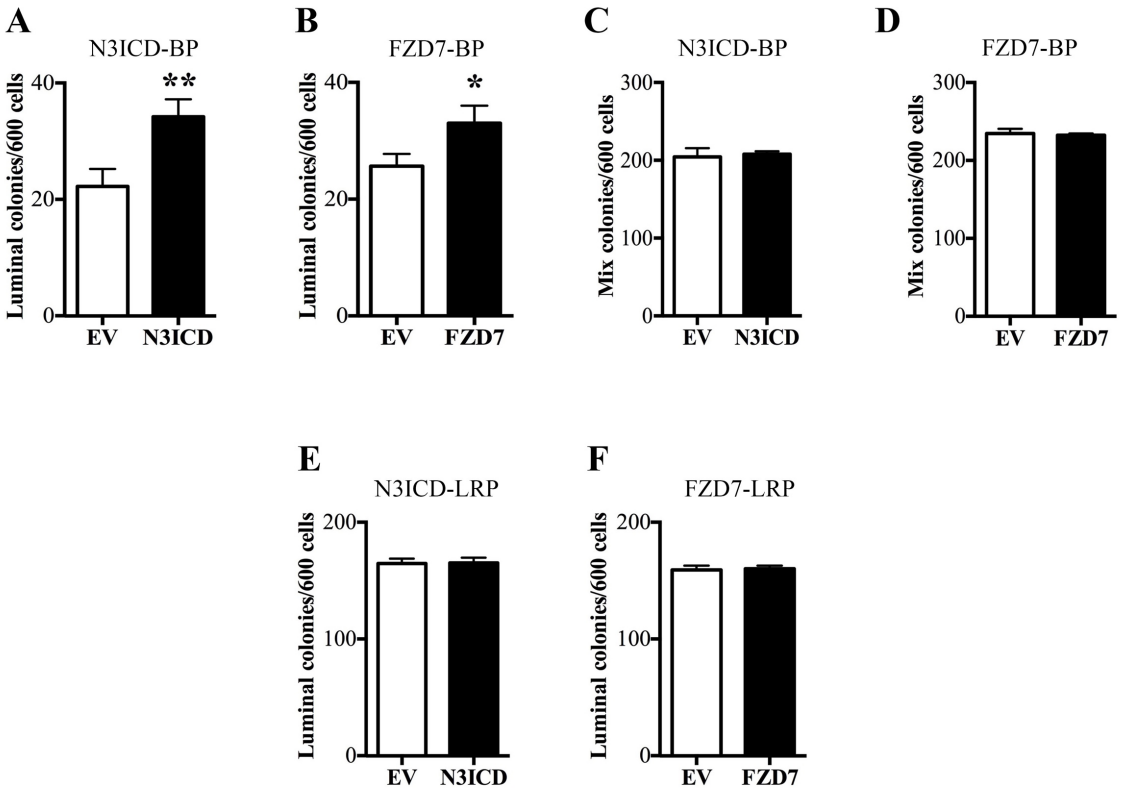

Figure 4.3 NOTCH3-FZD7 signaling regulates luminal fate commitment of cells within a bipotent progenitor-enriched population

(A&B) Total number of luminal formed in CFC assay from bipotent progenitor-enriched population overexpressing either N3ICD (NICD-BP) or FZD7 (FZD7-BP). (C&D) Total number of mix colonies formed in CFC assay from bipotent progenitor-enriched population overexpressing either N3ICD (NICD-BP) or FZD7 (FZD7-BP). (E&F) Total number of luminal colonies formed in CFC assay from luminal-restricted progenitor-enriched population overexpressing N3ICD (N3ICD-LRP) or FZD7 (FZD7-LRP). (The error bars show standard deviation, n=3, *$p \leq 0.05$, ** $p \leq 0.01$).

4.3.2. Wnt7A-induced increase in luminal colony number requires FZD7 receptor

FZD7 is a Wnt receptor shown to transduce both canonical and non-canonical Wnt signaling [265, 272-278]. To investigate the effect of Wnt signaling on luminal cell fate, the bipotent and luminal-restricted progenitor-enriched population were treated with a known canonical ligand Wnt3A or a non-canonical Wnt ligand Wnt7A [20, 276]. The use of Wnt7A is particularly interesting since previous reports indicated that Wnt7A is a ligand and activator of FZD7 signaling [276, 279]. Breast epithelial cells were isolated from reduction mammoplasty samples and cultured for 4 days as before and the bipotent and luminal-restricted progenitor-enriched population were generated by FACS sorting and CFC assays were performed with vehicle control vs recombinant human Wnt3A (rhWnt3A) or Wnt7A (rhWnt7A) (Fig 4.4A). Using dose-response experiments, the optimum dose of rhWnt7A or rhWnt3A was determined (Fig 4.4B-D). To avoid any potential effects of rhWnt3A and rhWnt7A on initial attachment of progenitors to culture plates, the recombinant proteins were added 16 hours after start of the CFC assays. We found that addition of rhWnt3A did not have any effect on colony forming ability for bipotent or the luminal restricted progenitors. However, the addition of 50ng/mL and 100ng/mL rhWnt7a to bipotent progenitor-enriched population increased the luminal colony number by 2.4±0.25 and 2.3±0.34 folds respectively, as compared to vehicle control (Fig 4.4B). The mix colony forming potential of bipotent progenitor-enriched population were not affected by rhWnt7A (Fig. 4.4C). Interestingly, rhWnt7A had no measurable effects on the colony forming potential of the luminal-restricted progenitor-enriched population (Fig 4.4D). Previously it was shown that Wnt7A secreted by breast tumor cells causes fibroblasts to assume an activated fibroblast phenotype that expresses alpha smooth muscle actin (αSMA) [280]. To test whether addition of rhWnt7A to the CFC cultures could transform fibroblasts into an activated state, fibroblasts-only cultures were treated

with either vehicle control or 50ng/mL of rhWnt7A. The cells were fixed after 7 days and stained with αSMA antibody to detected activated fibroblasts. I found that exogenous addition of rhWnt7A did not transform the fibroblasts into an activated state (Fig 4.5A&B). Tumor-associated fibroblasts were isolated from ER^+ tumor patient samples as described previously [281] and were used as positive control for immunofluorescent staining of αSMA (Fig 4.5A, TAF).

Next, I assessed whether Wnt7A-induced increase in luminal colony forming potential of the bipotent progenitor-enriched population requires FZD7. For this purpose, the bipotent or luminal-restricted progenitor-enriched population transduced with lentivirus to knockdown FZD7 expression or overexpress full-length FZD7 receptor were obtained by FACS and placed in CFC assays treated with either vehicle control or rhWnt7A 16 hours after the initial plating. As expected, in presence of rhWnt7A, the luminal colony forming potential of the bipotent progenitor-enriched population was significantly increased (sh-scrambled control-bipotent progenitors). However, in bipotent progenitors that show significantly reduced FZD7 expression (shFZD7 or shNR3-bipotent progenitors), rhWnt7A was unable to increase the luminal colony forming ability of these cells (Fig 4.6C). Interestingly, the addition of rhWnt7A to bipotent progenitor-enriched population overexpressing FZD7 or N3ICD further increased their luminal colony forming ability (Fig 4.6D) but it had no effects on the mix colony numbers (Fig 4.6E&F). Luminal-restricted progenitor-enriched population with gain and loss of NR3 or FZD7 functions were not affected with rhWnt7A treatment (Fig 4.6G&H).

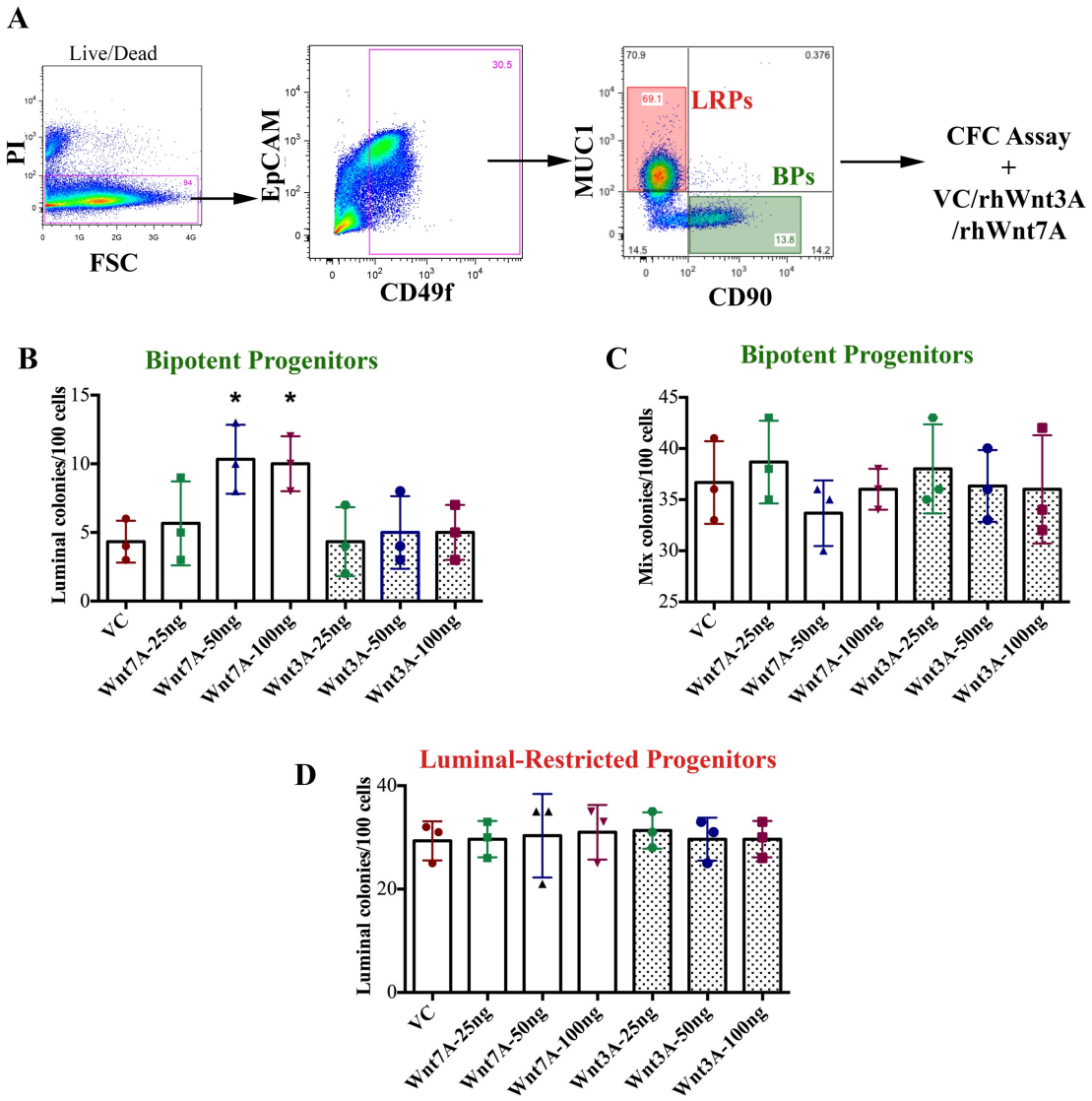

Figure 4.4 Dose dependent effect of Wnt ligands on Bipotent progenitors and luminal-restricted progenitor-enriched populations

(A) The bipotent progenitors (BPs) and luminal-restricted progenitor-enriched population (LRPs) were isolated from pre-cultured human mammary epithelial cells. The progenitor-enriched population were cultured and the next day they were treated with vehicle control or different doses of either Wnt7A or Wnt3A. (B & C) Show the dose dependent effect of Wnt7A and Wnt3A on mix/basal and luminal colonies generated from bipotent progenitor-enriched population respectively. (D) shows the dose dependent effect of Wnt7A and Wnt3A on luminal colonies

generated from luminal-restricted progenitor-enriched population. (The error bars show standard deviation, n=3, *$p \leq 0.05$).

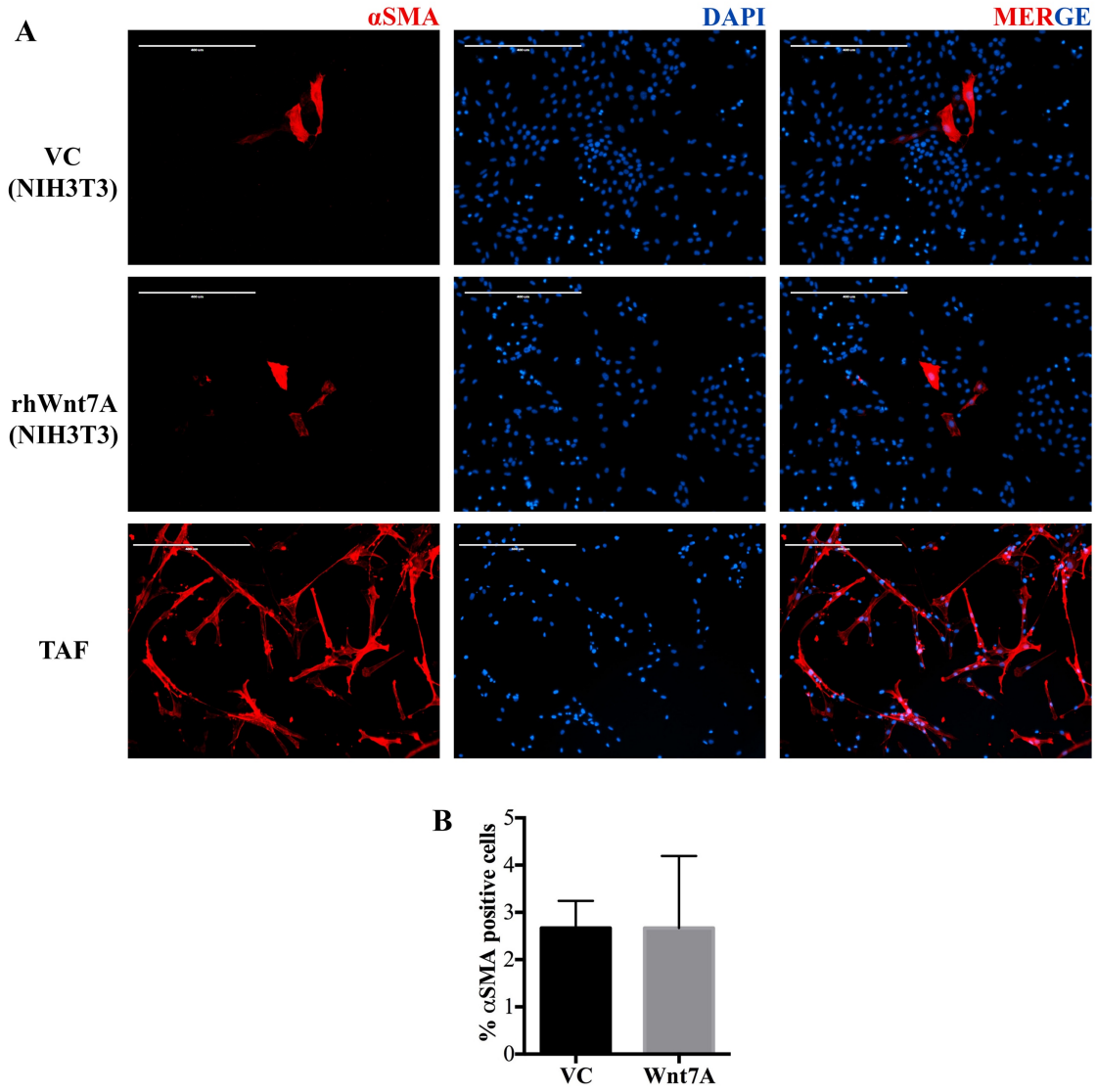

Figure 4.5 Wnt7A does not activate NIH3T3 fibroblasts

NIH3T3 fibroblasts were cultured in CFC assay condition without breast epithelial cells and treated with either vehicle control (VC) or 50ng/mL recombinant human Wnt7A (rhWnt7A) for 7 days. Cells were fixed and stained with a fluorescent antibody to detect alpha smooth muscle actin (αSMA) expression in the treated cells (red). DAPI (blue) was used to identify the nucleus. Tumor associated fibroblasts (TAF) was used as a positive control for αSMA expression. Representative images are shown (A). (B) Average±SD frequency of SMA^{+} fibroblasts in the treated with either

VC or rhWnt7A is shown in bar graphs (n=3). (scale 1000μm, the error bars show standard deviation).

Figure 3

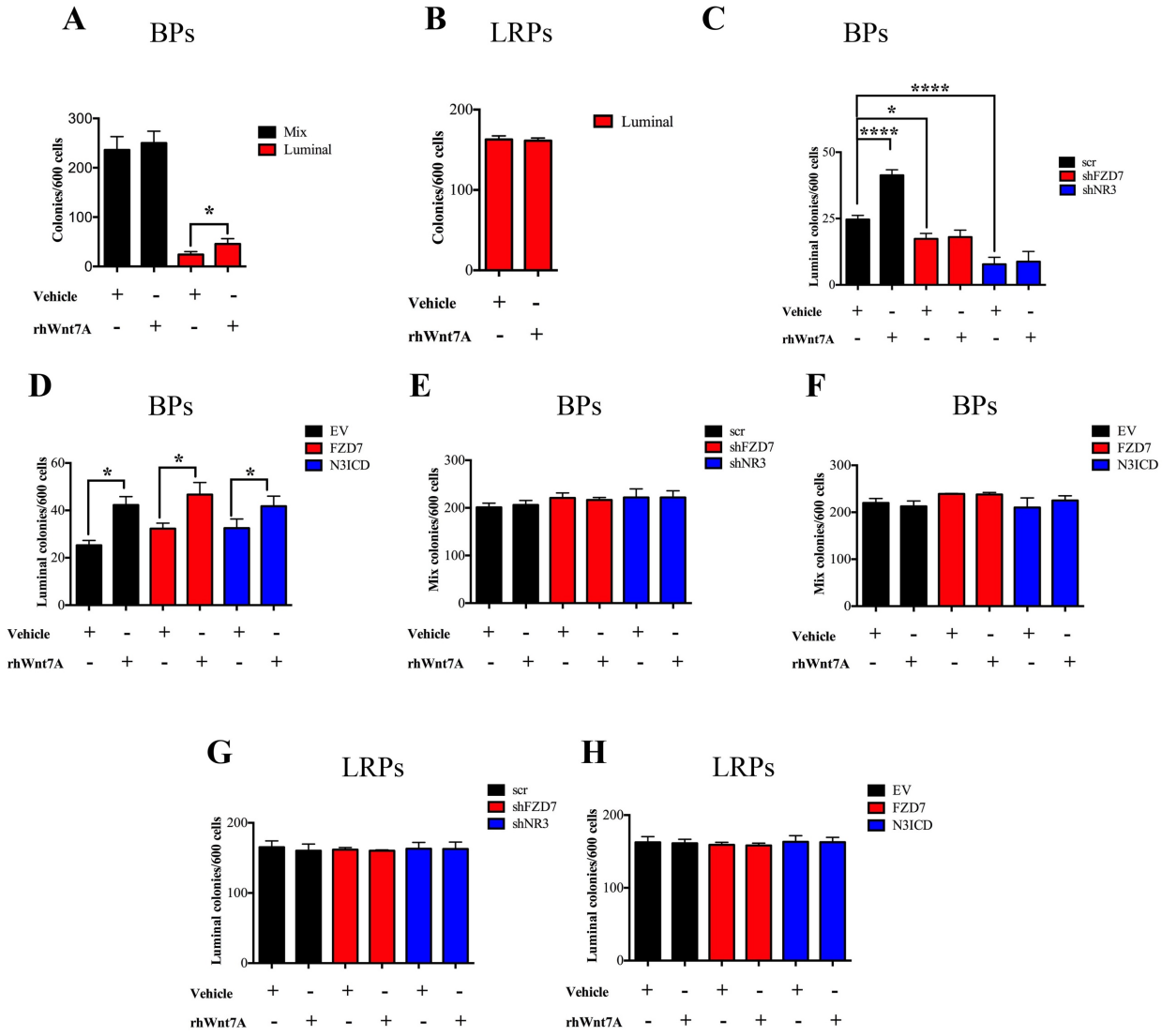

Figure 4.6 Wnt7A increases basal-like luminal progenitor-enriched population in a NOTCH3-FZD7 dependent manner

Primary breast epithelial cells obtained from precultured breast reduction samples and bipotential and luminal-restricted progenitor-enriched population were obtained based on their expression of Epithelial Cell Adhesion Molecule (EpCAM), CD49f and CD90 by fluorescent activated cell sorting (FACS). The progenitor-enriched populations were placed in colony forming cell (CFC) assays and treated with either vehicle control or 50ng/mL of recombinant human Wnt7A (rhWnt7A). After 7 days colonies were fixed and counted. Average ±SD CFC frequency in the

bipotent progenitor-enriched population (BPs) (A) and luminal-restricted progenitor-enriched population (LRPs) (B) cultures treated with rhWnt7A and controls are shown in the bar graphs. Some precultured primary cells were transduced with lentivirus expressing either short hairpin RNA to target *NR3* (shNR3) or *FZD7* (shFZD7) transcripts, or with lentivirus expressing the constitutively active form of NR3 (N3ICD) or full-length FZD7 (FZD7), vs a shScrambled sequence or empty virus as controls. The transduced- BPs and transduced-LRPs were isolated by FACS based on their expression of GFP and placed in CFC assays with rhWnt7A as described. The average frequency ±SD of luminal (C) and mix colonies (E) in shNR3 and shFZD7-transduced BPs is shown as bar graphs. The average ±SD frequency of luminal (D) and mix colonies (F) from N3ICD- and FZD7-transduced BPs is shown as bar graphs. (G &H) Shows the average frequency ±SD of luminal colonies in in shNR3 and shFZD7-transduced LRPs and N3ICD- and FZD7-transduced LRPs respectively. (The error bars show standard deviation, n=3, *$p \leq 0.05$, **** $p \leq 0.001$).

4.3.3. NOTCH3^{+}FZD7^{+} cells represent a basal-like luminal progenitor in human breast tissue

So far, my data demonstrated that NR3-FZD7 signaling plays an essential role in the luminal lineage commitment of the bipotent progenitors. I, therefore hypothesized that the NOTCH3^{+} FZD7^{+} BLPs represent luminal colony forming cells which are committed to luminal cell fate. Toward this hypothesis, I used breast epithelial cells that were pre-cultured for 4 days as before. To accommodate the additional fluorescent colors needed to detect NR3 and FZD7, the EpCAM^{+} cells were immunomagnetically isolated first (>90% purity, Fig 4.7). The EpCAM^{+} cells were then stained with fluorescently-tagged antibodies against CD49f, CD90, NR3 and FZD7 and the CD49f^{+} CD90^{+} (bulk bipotent progenitors), CD49f^{+} CD90^{+} NR3^{high} FZD7^{+} (subset a), CD49f^{+} CD90^{+} NR3$^{low/-}$ FZD7^{+} (subset b), CD49f^{+} CD90^{+} NR3^{medium} FZD7^{+} (subset ab), and the CD49f^{+} CD90^{+} NR3^{-} FZD7^{-} (double negative, dn) cells were obtained via FACS from the same breast reduction sample (Fig 4.8A). The bulk bipotent progenitors (EpCAM^{+} CD49f^{+} CD90^{+}) gave rise to 39.5±5.4% mix and 5.2±2.2% luminal colonies (Fig 4.8B). Interestingly, I found that every NR3^{high} bipotent progenitors (subset a) cells were FZD7 positive, corroborating our earlier finding that NR3 uniquely regulating FZD7 expression [87]. I found that "subset a" cells gave rise to only luminal colonies at a frequency of 33.3±13.67% (Fig 4.8C). All colonies developed from the "subset a" were CK8/18 positive with no detectable CK14 expression (Fig 4.9A). This suggested that "subset a" represented the "basal-like luminal progenitors" (BLPs). On the other hand, the NR3^{low} bipotent progenitors (subset b) only generated mix colonies (Fig 4.8D) with cytokeratin14 and cytokeratin 8/18 positive colonies (Fig 4.9B). Interestingly, the NR3^{medium} bipotent progenitors (subset ab) give rise to both luminal-only and mix colony types (Fig 4.8E), while the NR3^{-} bipotent progenitors produced only mix colonies (Fig 4.8F). Very interestingly, luminal colony forming

cells in the bulk bipotent progenitor-enriched population were selectively and specifically enriched in the BLP subpopulation (99.66±39.60) (Fig 4.8G) while the mix colony forming cells were enriched in the $NR3^-$ non-BLP cells (53.67±5.42) (Fig 4.8H).

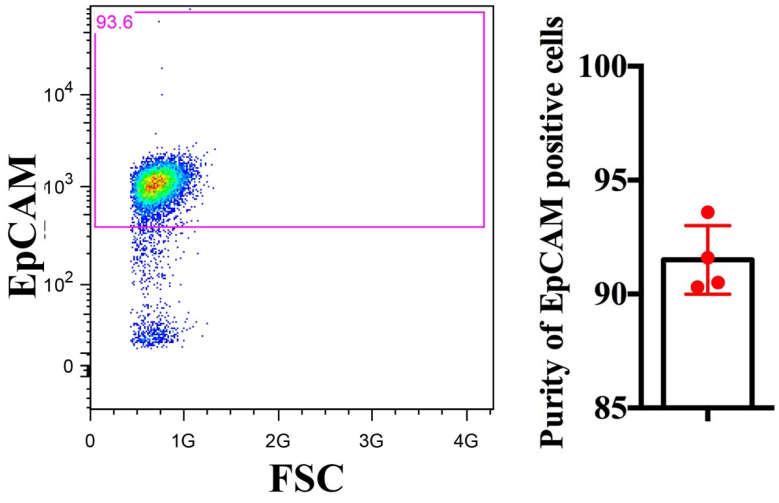

Figure 4.7 Immunomagnetic separation provided high enrichment of EpCAM$^+$ cells

Immunomagnetic cell separation was applied to single-cell suspensions from breast reduction samples to obtain EpCAM$^+$ cells. Cells were allowed to recover their EpCAM expression (1hour incubation on ice) and EpCAM expression was assessed using a fluorescently-tagged anti EpCAM antibody, and protein expression was analyzed using a flow cytometer. Left panel is a representative FACS plot showing the purity of EpCAM positive cells after immunomagnetic separation. Right, shows the average of EpCAM positive cell purity (n=4). The error bars show standard deviation.

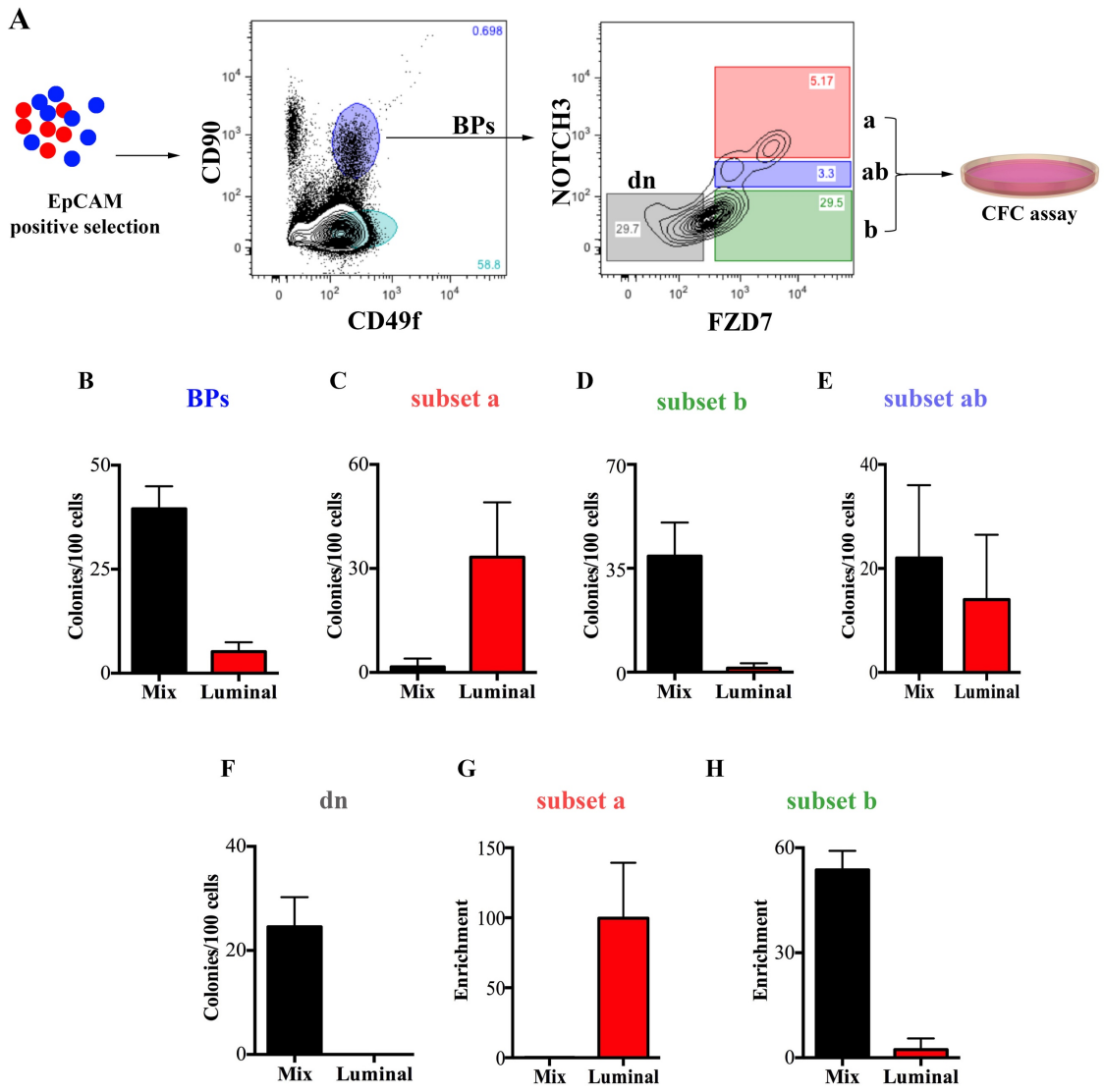

Figure 4.8 NOTCH3 and FZD7 expression identify a basal-like luminal progenitor-enriched fraction

(A) Bipotent progenitors (BPs) were isolated from reduction mammoplasty samples and further separated based on their expression of NR3 and FZD7 receptors. Based on NR3 expression, 4 distinct subsets of BPs were identified; $NR3^{high}$ (region a), $NR3^{low}$ (region b), $NR3^{med}$ (region ab) and $NR3^{-}$ (region dn, double negative). Cells isolated from regions a, b, ab and dn were placed in colony forming cell (CFC) assays and progenitor frequency in each subset was determined based on colony numbers and colony types observed (C-F). The bulk BPs (regions a, b, ab and dn) were

placed in CFC assay as well, to provide the initial progenitor subtype frequency and yield (B). Total progenitor subtype yields in the bulk bipotent progenitors is used to calculate the enrichment of each progenitor subtype in cells obtained from regions a and b (G&H). (n=4, the error bars show standard deviation)

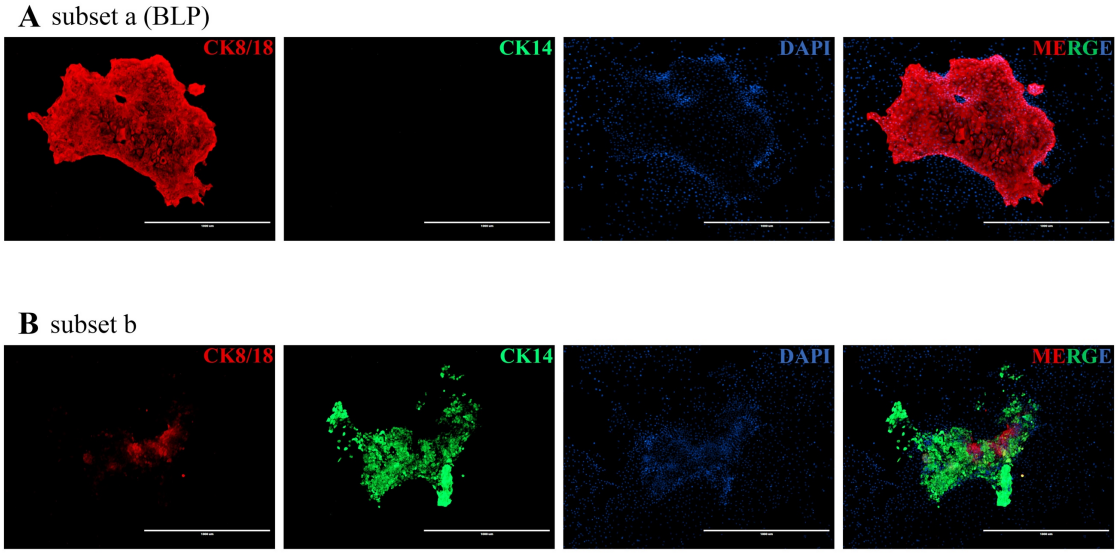

Figure 4.9 Subset 'a' of the bipotent progenitor-enriched population generate luminal-only colonies whereas subset 'b' forms mix colonies

Representative immunofluorescent staining of colonies generated from cells obtained from the "a" and "b" subsets of bipotent progenitors. (A) Colony from subset 'a' express cytokeratin (CK)8/18 and not CK14 which the typical characteristic luminal-only colonies. (B) Colonies from subset 'b' show positive staining for both CK 14 and CK 8/18, indicating their mix colony characteristics. (scale=1000μm)

4.3.4. $CD90^+$ BLPs differentiate to form $CD90^-$ luminal colonies

Previous studies demonstrated that culturing primary human breast epithelial cells *in vitro*, significantly enhanced progenitor yields in each sample. This overnight preculturing, allowed bipotent progenitors to be obtained at an unprecedented high frequency of >40%. These reports also suggested that bipotent progenitors thusly obtained, contained 5% of contaminating luminal-restricted progenitors (LRP) that give rise to luminal-only colonies [76, 282]. Although the new breast epithelial progenitor that I have identified as a basal-like luminal progenitor (BLPs) form luminal-only colonies similarly to LRPs, yet they exhibit many different characteristics. Unlike LRPs, the BLPs cells are $CD90^+MUC1^-$ and they are NR3 and FZD7 signaling-dependent while LRPs are not [76]. Therefore, I further characterized the luminal-only colonies that are generated from BLPs and LRPs. To this end, the bipotent progenitors (BPs), BLPs ($EpCAM^+CD49f^+CD90^+NR3^{hi}FZD7^+$), bulk LRPs ($EpCAM^+CD49f^+CD90^-$), and two subsets of LRPs ($NR3^{hi}FZD7^+$ and $NR3^{lo}FZD7^+$) were sorted from precultured breast epithelial cells and placed in CFC assays (Fig 4.10A). Interestingly, NR3 and FZD7 expression was higher in BLPs as compared to LRP-enriched population (Fig 4.10B&C). The colonies generated from each progenitor subtype were immunofluorescently stained for CD90 expression. As expected, mix colonies generated from BP-subset b progenitors stained positive for CD90 (Fig 4.10D, used as a positive control). $CD90^-$ LRPs gave rise to $CD90^-$ colonies (Fig 4.10E, LRP-subset a) and the colony forming cell frequency in $NR3^+FZD7^+$ LRP-enriched population as well as $NR3^-FZD7^+$ LRP-enriched populations were similar, suggesting that NR3 and FZD7 expression does not enrich for LRPs (Fig 4.11). Very interestingly, however the $CD90^+$BLPs gave rise to $CD90^-$ colonies (Fig. 4.10B). The BLPs were further characterized with respect to the estrogen receptor alpha (ERα) expression. The BLP cells were on average 2.9±1.69% ERα positive, whereas 79.77±4.63%

of LRPs and only 0.83±0.38% of bipotent progenitors were positive for ERα expression (Fig 4.12A&B). Interestingly, luminal colonies generated from BLPs were ERα positive (Fig 4.12C). The bipotent progenitors do not express surface marker MUC1, while the LRPs and the luminal colonies generated from them are MUC1 positive [76] (Fig 4.4A). Interestingly, the luminal colonies generated from $MUC1^-$ BLPs contained $MUC1^+$ cells which immunophenotypically resembled luminal colonies generated from LRPs (Fig 4.13). These observations suggest that BLPs could be an earlier pre-progenitor of LRPs.

The previous study demonstrated that LRPs lose their colony forming ability upon re-plating under CFC assay conditions which is in keeping with their phenotype as a more differentiated, restricted progenitors [68]. Since BLPs exhibit different characteristics that LRPs and yet differentiated to generate $CD90^-$ luminal colonies, I tested whether if BLPs retained their colony-forming potential or, similarly to LRPs, generated to non-clonogenic mature luminal cells. For this purpose, BLPs were cultured in CFC assays. One set of cultures was used to establish the initial colony forming cell frequency of BLPs. Another set of culture was grown for 4 days when the initial luminal colonies are visible. Cells were trypsinized, made into single-cells and re-plated into CFC assays and allowed to grow for 7 days. As before, initially, BLPs generated pure luminal colonies at a frequency of 47.33±13.61 (Fig 4.14). Interestingly, the BLP-generated colonies on day 4 contained 6.61±0.07 fold more luminal colony forming cells compared to the starting BLP cells, suggesting that, unlike LRPs, the BLPs retain their colony-forming potential (Fig 4.14).

My previous data demonstrated that Wnt7A, a FZD7 ligand, significantly increase the number of luminal colonies when bipotent progenitors were placed in CFC assays. I, therefore, investigated if this increase in luminal colonies is due to BLPs' response to Wnt7A. For this purpose, BLPs ($NR3^+FZD7^+$), subset "ab" and the subset "b" of bipotent progenitors (subsets are

distinguished based on NR3 & FZD7 expression as described in Fig. 4.8) were obtained from precultured breast reduction samples and placed in CFC assays treated with either a vehicle control (VC) or rhWnt7A. Very interestingly, rhWnt7A significantly increased the luminal colony numbers generated from the BLPs (Fig 4.15A). Even though the "ab" subsets of the bipotent progenitor-enriched populations generated more luminal colonies, this effect was not statistically significant (Fig 4.15B). rhWnt7A had no effect on the "b" subsets (Fig 4.15C).

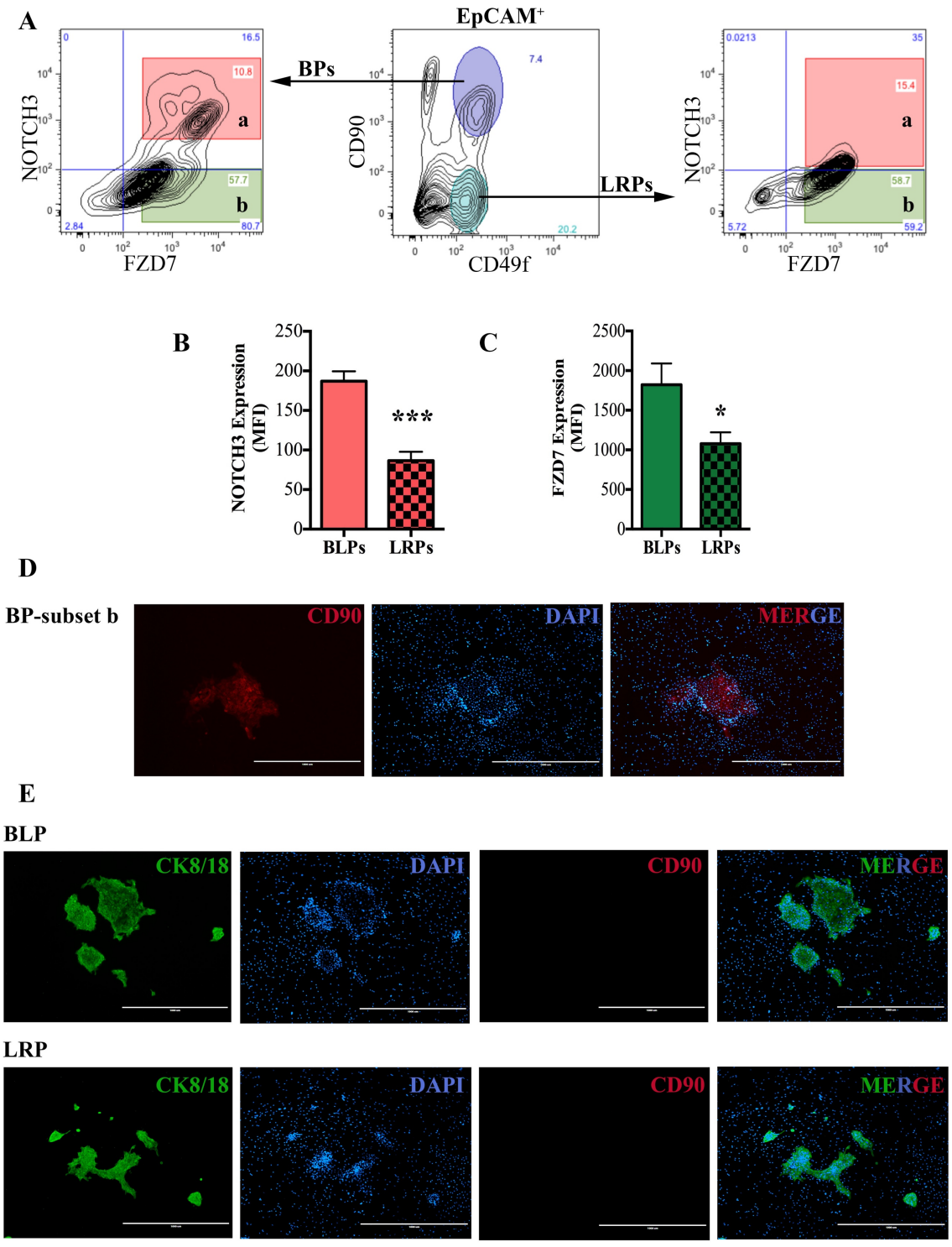

Figure 4.10 BLPs lose CD90 expression during in vitro differentiation

(A) NOTCH3^{+}FZD7^{+} bipotent and luminal-restricted progenitor-enriched population were isolated from breast reduction samples and placed in colony forming cell (CFC) assays. (B) Bar graph shows the average of Mean fluorescence intensity of NOTCH3 receptor expression in BLPs and LRPs analyzed by flowcytometry. (C) Bar graph shows the average of Mean fluorescence intensity of FZD7 receptor expression in BLPs and LRPs analyzed by flowcytometry. (D) Immunofluorescence staining of mix colony generated from BP-subset b progenitors, which serves as a positive control. (E) Immunofluorescent staining of luminal colonies (generated from BP-subset a and LRP-subset a) with cytokeratin 8/18 (green), DAPI (blue) and CD90 (red). All data obtained from 3 independent breast reduction samples (*** $p \leq 0.005$). (scale 1000μm, n=3, the error bars show standard deviation)

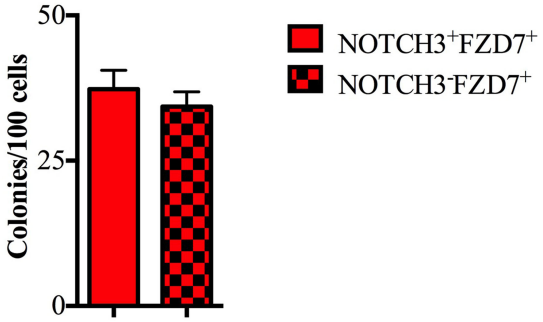

Figure 4.11 Luminal-restricted progenitors are independent of NR3 signaling

The $NR3^{high}FZD7^{+}$ and $NR3^{low}FZD7^{+}$ subset of LRPs were obtained by fluorescent activated cell sorting and placed in CFC assays. Bar graph shows the average colony forming cell frequencies ±SEM from each LRP subset. All data obtained from 3 independent breast reduction samples. The error bars show standard deviation.

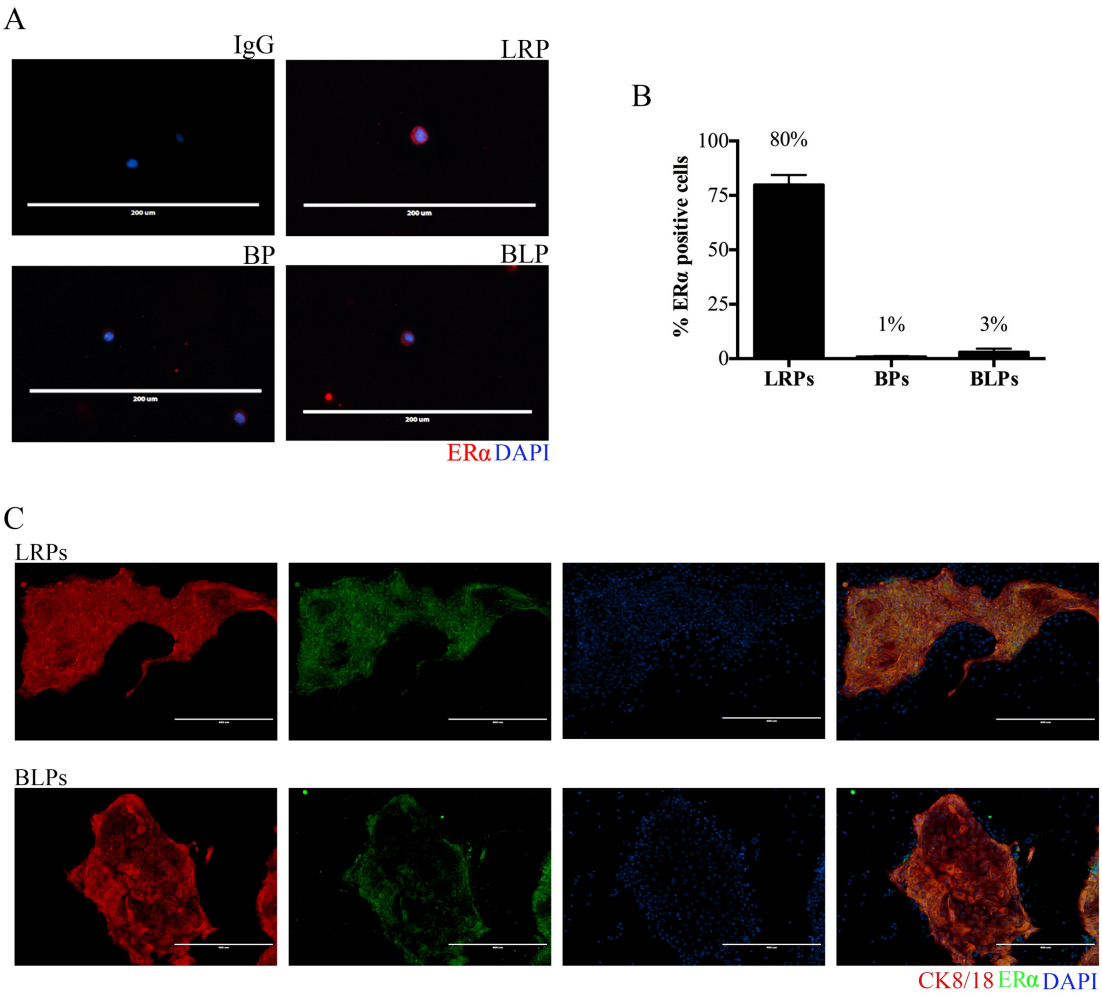

Figure 4.12 Unlike LRPs, BLPs show weak ERα expression

The bipotent progenitors (BPs), basal-like luminal progenitors (BLPs) and the luminal-restricted progenitors (LRPs) were obtained from precultured breast reduction samples, fixed, and stained with fluorescent antibodies to detect estrogen receptor alpha (ERα) expression. (A) Representative images of ERα expression in different subsets of breast epithelial cells are shown. (B) The mean frequency and ±SEM of $ERα^+$ cells in LRPs, BPs and the BLPs obtained from 4 independent breast reduction samples are shown in bar graphs. (C) LRPs and BLPs were cultured in colony forming cell (CFC) assay and the colonies were stained with CK8/18 (red), ERα (green) and DAPI (blue). Scale=200μm (A) and 1000μm (C). The error bars show standard deviation.

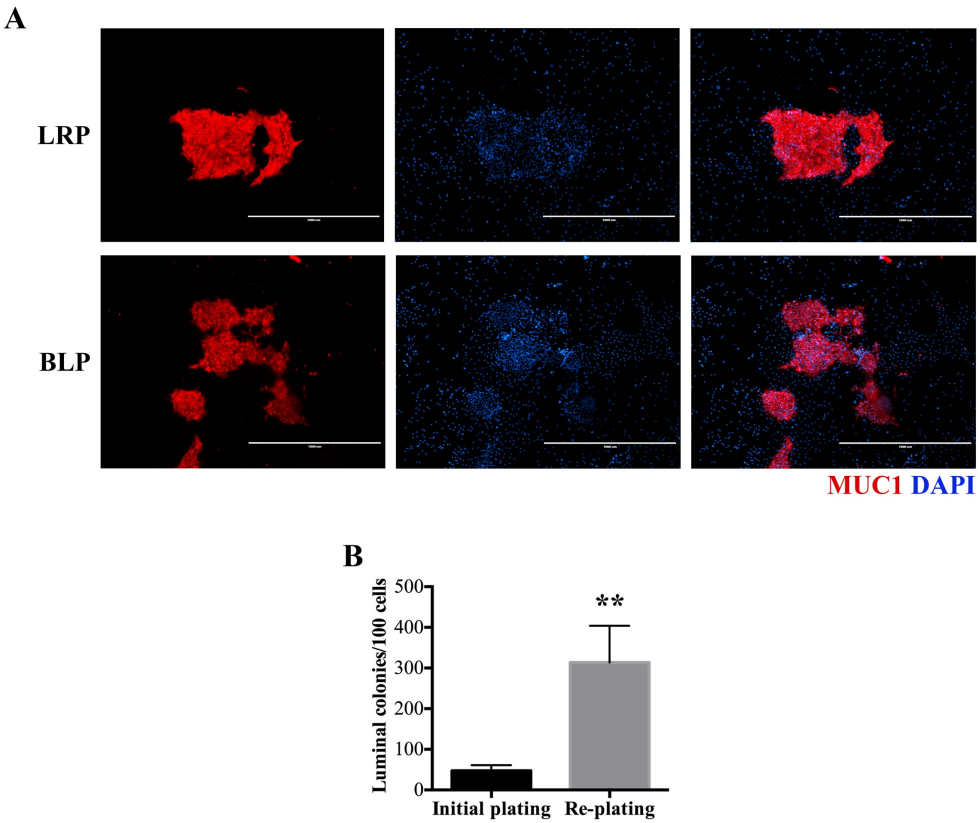

Figure 4.13 MUC1^{-} BLPs generate MUC1^{+} luminal colonies

Basal-like luminal progenitors (BLPs) and the luminal-restricted progenitors (LRPs) were obtained from precultured breast reduction samples and cultured in colony forming cell (CFC) assay, fixed and stained with fluorescent labelled MUC1 antibody [MUC1 (red) and DAPI (blue)]. The error bars show standard deviation, n=3.

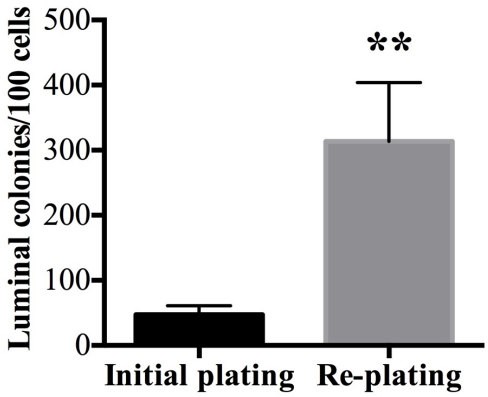

Figure 4.14 BLPs retain colony forming ability in vitro

The basal-like luminal progenitors (BLPs) were obtained from 3 separate precultured breast reduction samples and placed in colony forming cell (CFC) assays. On day 4, some cells CFC plates were trypsinized and made into single-cell suspensions and placed in secondary CFC assays. After 7 days, colonies were fixed, and colony numbers were obtained. The mean and ±SEM CFC frequencies are shown in bar graphs (n=3, **p≤0.01). The error bars show standard deviation.

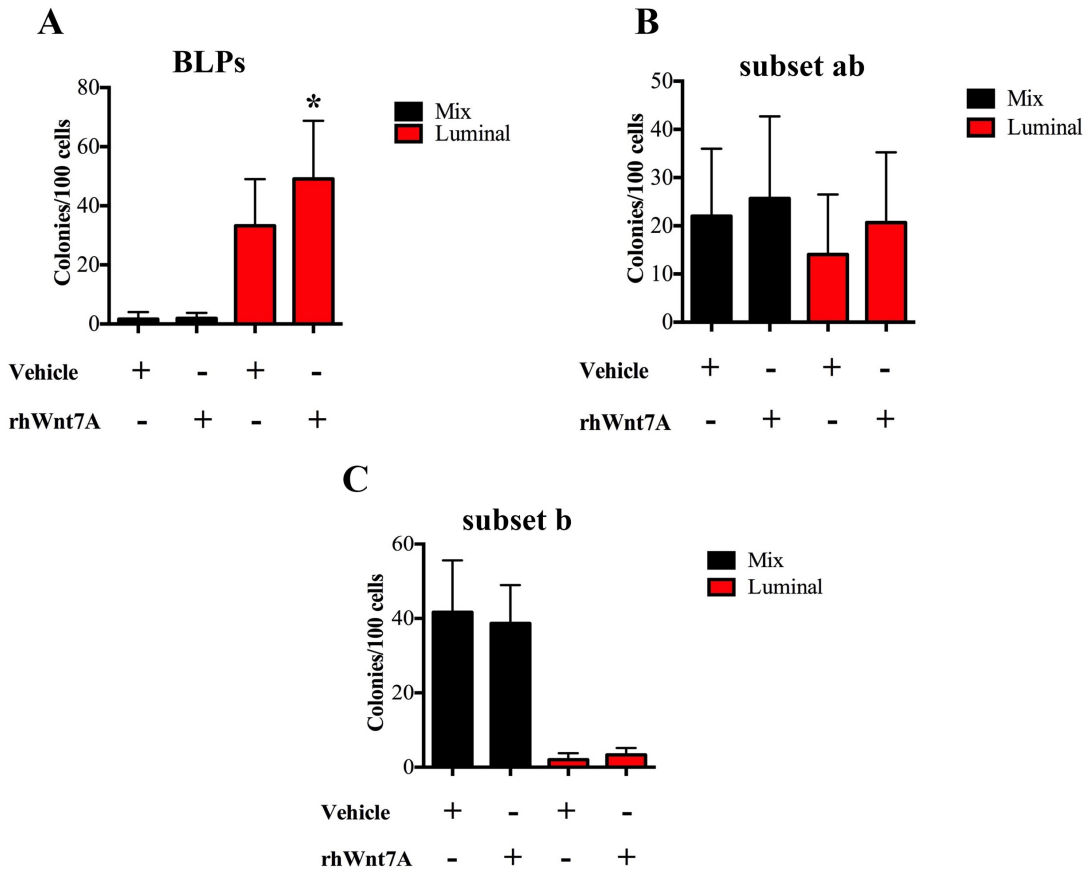

Figure 4.15 BLPs respond to Wnt7A exposure

(A-C) The basal-like luminal progenitors (BLPs or subset "a", subset "ab" and subset "b" were isolates as shown in Fig. 3A and placed in CFC assays treated with rhWnt7A or vehicle control. After 7 days, the colonies generated were fixed, stained with crystal violet and counted (n=3, *p≤0.05). The error bars show standard deviation.

4.3.5. BLPs can be isolated from non-cultured primary breast epithelial cells

Pre-culturing mammary epithelial cells could introduce culturing artifacts. In order to rule out this possibility, I set up experiments to detect the presence of BLPs in freshly dissociated breast reduction samples. It was previously reported that bipotent progenitors are enriched in $EpCAM^{low/-}CD49f^{bright}$ non-cultured human breast epithelial cells [66, 67]. Therefore, the expression of BLP markers, NR3, CD90, and FZD7, were examined in the non-cultured bipotent progenitors (ncBPs). Similar to pre-cultured cells, a majority of $NR3^+$ cells also expressed FZD7 and therefore, FZD7 was not pursued further as a potential BLP marker in non-cultured cells (Fig 4.16). CD90 was strongly expressed in ncBPs (78.90±4.61%) but it was ubiquitously expressed in $EpCAM^{low}$ and $EpCAM^-$ ncBPs (Fig 4.17A). On the other hand, only 1.21±0.25% of ncBPs express NR3 (Fig 4.17B) however, NR3 was strongly expressed in the $EpCAM^{low}$ ncBPs as compared to the $EpCAM^-$ ncBPs (Fig 4.17B). Next, bulk ncBPs and their $CD90^+NR3^+$ (subset a), and $CD90^+NR3^-$ (subset b) subsets were obtained and in CFC assays to assess the frequency of mix and luminal colony forming cells in each population (Fig 4.17C). As expected, ncBPs gave rise to mix colonies at a higher frequency (1.21±0.15) than the luminal colonies (0.03±0.01). Interestingly, the mix colony forming cells were more enriched in $CD90^+NR3^-$ subset of ncBPs compared (Fig 4.17E) to the $CD90^+NR3^+$ subset. However, luminal colony forming cells were more frequent in $CD90^+NR3^+$ population (Fig 4.17F).

These observations indicate that BLPs can be separately obtained from non-cultured bipotent progenitors. However, due to the low frequency at which they can be obtained, their further characterization via functional assays is very challenging.

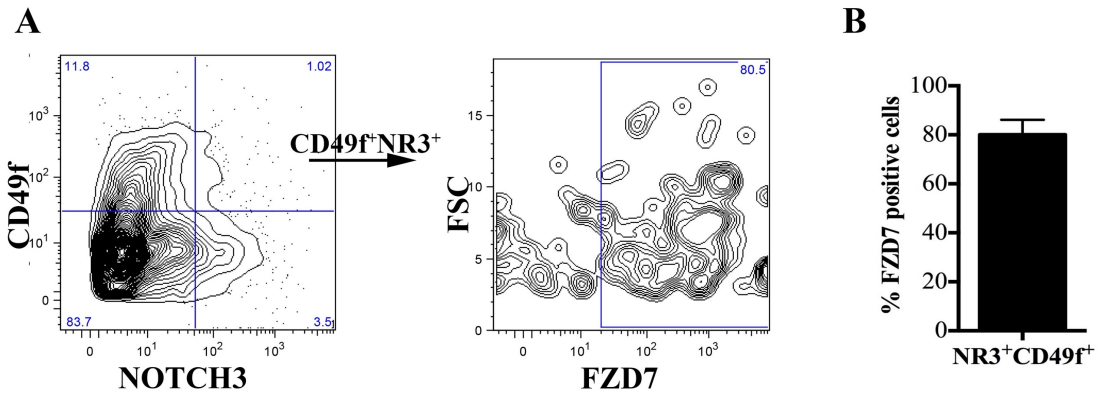

Figure 4.16 NOTCH3 signaling regulates FZD7 expression in non-cultured breast epithelial cells

(A) Non-cultured breast epithelial cells were stained fluorescently-tagged CD49f, NOTCH3 and FZD7 antibodies. The percentage of $FZD7^{+}$ cells in $CD49f^{+}NOTCH3^{+}$ fraction was analyzed via flowcytometry. (B) Bar graphs show the average ±SD of FZD7 expression in $CD49f^{+}NOTCH3^{+}$ cells (n=3). The error bars show standard deviation.

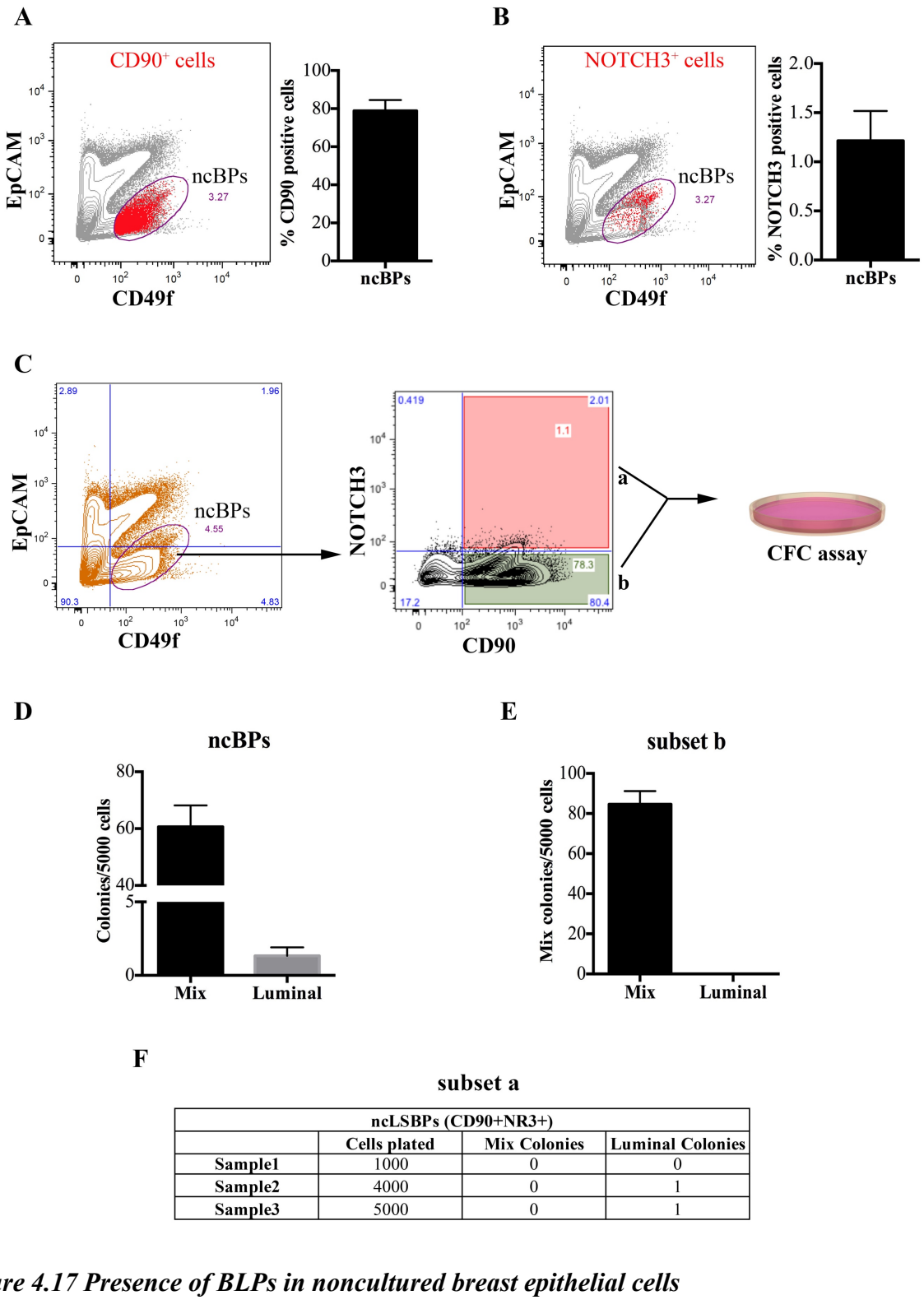

F

subset a

ncLSBPs (CD90+NR3+)			
	Cells plated	Mix Colonies	Luminal Colonies
Sample1	1000	0	0
Sample2	4000	0	1
Sample3	5000	0	1

Figure 4.17 Presence of BLPs in noncultured breast epithelial cells

(A) Shows the expression profile (left) and percentage positivity (right) of CD90 in noncultured bipotent progenitors (ncBPs). (B) shows the expression profile (left) and percentage positivity (right) of NR3 expression and the percent positivity in ncBPs. (C) ncBPs were isolated from reduction mammoplasty samples based on surface marker expression ($EpCAM^{-/lo}CD49f^{bright}$). Different subset of bipotent progenitors were isolated based on NR3 and CD90 expression and functional assay was performed. (D) Bar graph shows the total number of mix and luminal colonies generated form bulk ncBPs (E) Bar graph shows the total number of mix-only colonies generated form $CD90^{+}NR3^{-}$ (subset b) subset of ncBPs. (F) Table shows the number of colonies generated from BLPs (subset a) (n=3). The error bars show standard deviation.

4.3.6. NOTCH3-specific signaling network in breast epithelial cells

My data so far indicate that although FZD7 is a specific gene target of NR3, it does not completely recapitulate the role of NR3 in differentiation of bipotent progenitors to BLPs. Therefore, I hypothesized that other NR3-specific gene targets might also play important roles in this process. Apart from FZD7, there are 9 other FZD receptors capable of transducing Wnt signaling. I, therefore examined the transcript expression of all 10 FZD receptors in the bipotent and luminal-restricted progenitor-enriched population. I chose to quantify transcript expression for different FZD receptors since homology between these receptors has hampered availability of specific antibodies to detect each protein. Interestingly, I observed that in addition to FZD7, FZD9 was also expressed at a higher level in luminal-restricted progenitor-enriched population (Fig 4.18A). However, FZD6, 8 and 10 receptors were expressed more significantly in the bipotent progenitors (Fig 4.18A). Subsequently, I tested whether FZD6, 8-10 receptors were uniquely regulated by NR3. For this purpose, non-malignant human breast epithelial 184-hTERT cells were infected with lentivirus expressing constitutively active NOTCH Receptors (described earlier in Fig 3.5) and the transcript expression of FZD6, 8-10 mRNA was examined by qPCR. FZD6 expression was increased when NR3 signaling was active, however, NR4 signaling had the opposite effect on FZD6 expression (Fig. 4.18B). FZD8-10 transcript expression was not altered by any of the NOTCH ICD proteins (Fig. 4.18B).

To further identify more unique gene targets and signaling pathways regulated by NR3, I employed an unbiased transcriptome profiling approach. RNA samples were obtained from 184-hTert cells transduced to express the activated form of NR3 (N3ICD) or NR1 (N1ICD) or GFP and was used to generate cDNA. Using specific primers, increased transcript levels of *NR1*, *NR3* and *HES1* in transduced cells was confirmed by real-time qPCR (Fig 4.19). Also, increased FZD7

expression was seen in N3ICD-184-hTERT cells but not in the N1ICD-184-hTERT cells as previously seen (Fig 4.20A). Transcript expression of different genes in 3 separately transduced 184-hTERT cells was analyzed using the Affymetrix Human 2.0 ST array GeneChip™. The signals detected from the array were quantified to generate a normalized log2 value for each gene expression. Hierarchical clustering analysis was performed to assess the reproducibility of the data obtained from biological replicates (Fig 4.20B), and I observed that all biological replicates were grouped together. Compared to controls and using 2-fold change in transcript expression with p-value <0.05 as cutoff, the differentially up and down regulated gene lists were generated (Table 7.1&7.2). By cross-comparing NR1 and NR3-regulated gene lists, I generated a sub-list of NR3 and NR1 unique gene targets (Fig 4.20C). This analysis yielded 816 NR3 targets, 216 NR1 targets and 932 genes whose expression was regulated by both NR1 and NR3. Using the Ingenuity Pathway Analysis (IPA) software, I determined the canonical signaling pathways enriched in the NR1- and NR3-unique targets (Fig 4.21A&B). Interestingly, NR3-unique gene targets were enriched for Retinoate biosynthesis I, Ephrin B Signaling, Cell cycle regulation, Endothelin signaling, phospholipase signaling, p38 MAPK signaling, Vitamin C signaling and Wnt signaling pathways. On the other hand, NR1-unique gene targets showed enrichment for acute phase response signaling, and Neuregulin signaling pathways (Fig 4.21B). To further validate NR3-unique targets, the differential expression of 19 genes was examined in N1ICD-, N2ICD-, N3ICD-, N4ICD-184-hTERT cells by qPCR. Very interestingly, *Ephrin type-B receptor 3* (*EPHB3*), *GABA receptor ε (GABRE) and Regulator of G-protein signaling 2 (RGS2)* genes were found to be specific and unique targets of NR3. The preferential induction of *GABRE* by NR3 was further validated at the protein level using flow cytometry (Fig 4.22). These very interesting and unique datasets for the first time identified NR3-unique target genes in human breast epithelial cells.

Interestingly, Wnt signaling pathway genes were significantly enriched in NR3-unique gene targets. Some of these newly identified NR3-unique gene targets could be important for differentiation of bipotent progenitors to BLPs.

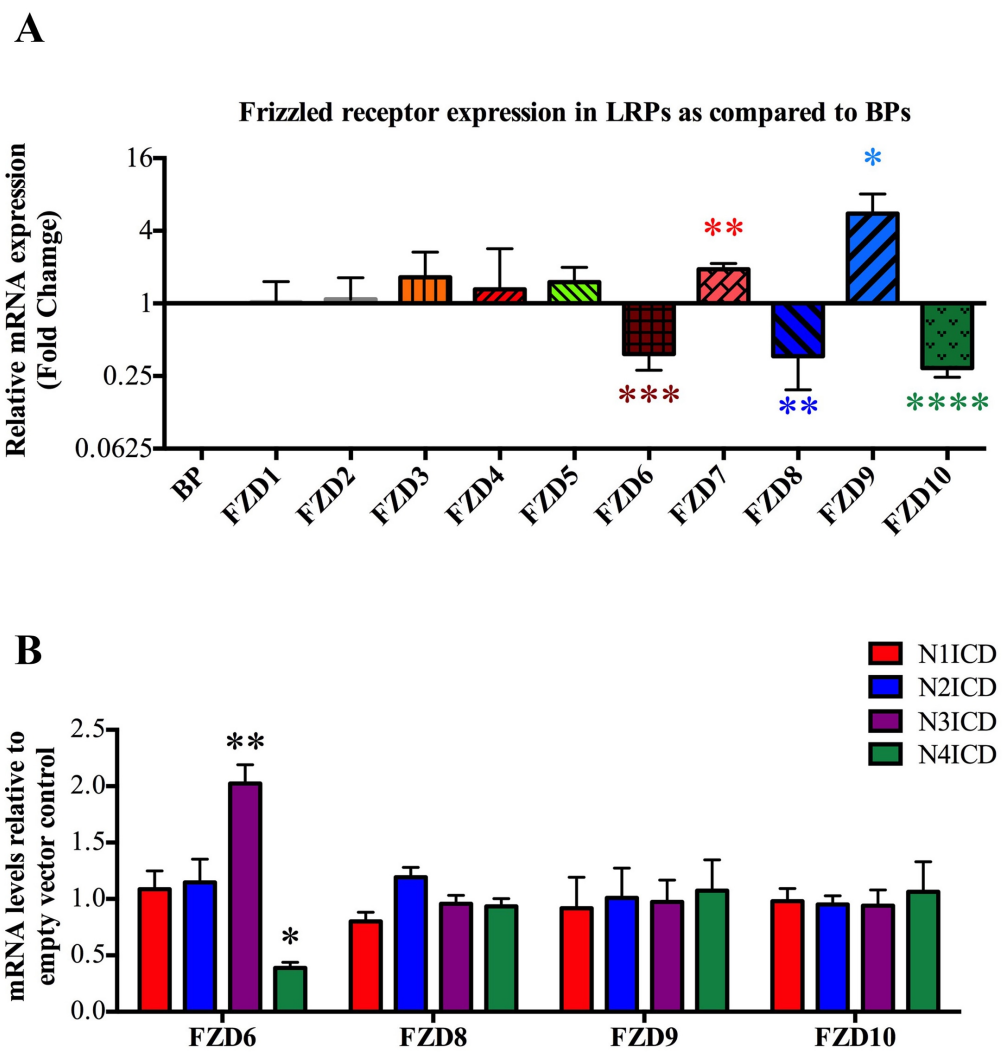

Figure 4.18 FRIZZLED receptor expression in Luminal-restricted progenitors as compared to bipotent progenitors

(A) Transcript levels of all frizzled receptor were quantified in both the bipotent progenitors and luminal-restricted progenitors. Fold change in mRNA expression in the luminal-restricted progenitors were measured and plotted as compared to the bipotent progenitors. (B) Bar graph shows the mRNA expression of FZD6 and FZD8 in 184-hTert cells overexpressing active form of notch receptors (n=3, *p≤0.05, **p≤0.01, ***p≤0.005, ****p≤0.001). The error bars show standard deviation.

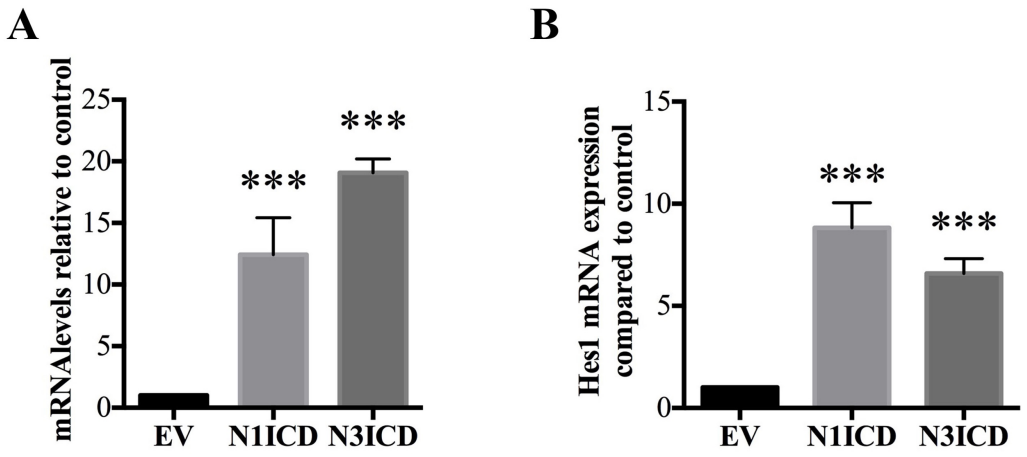

Figure 4.19 mRNA levels of Notch receptors and its target gene HES1

Quantification of transcript levels in 184-hTert cells. (A) Transcript levels of NOTCH1 and NOTCH3 in 184-hTert cells overexpressing active form of NOTCH1 and NOTCH3 respectively. (B) Transcript levels of known common target gene HES1 in 184-hTert cells overexpressing active form of NOTCH1 and NOTCH3 respectively (n=3, ***p≤0.005). The error bars show standard deviation.

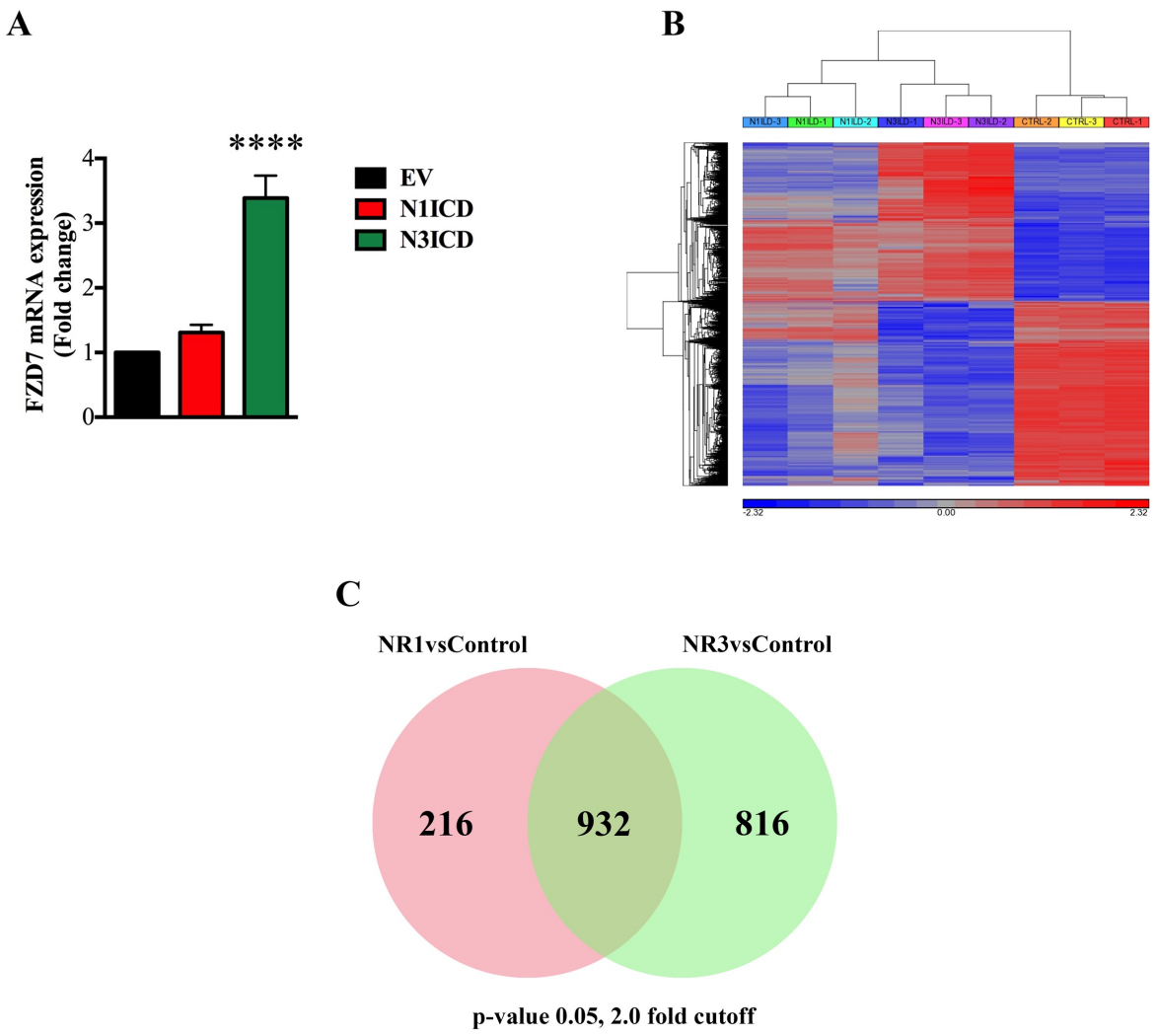

Figure 4.20 Transcriptome profiling of NOTCH3 regulated genes

The transcriptome profiles of NOTCH3 (NR3) and NOTCH1 (NR1) overexpressing non-malignant human breast epithelial cells (184-hTERT) was compared using the affymetrix platform. (A) Validation of FZD7 mRNA in 184-hTert cells overexpressing active form of NR1 & NR3. (B) Hierarchical cluster analysis of microarray data set. (C) Venn diagram showing the number of commonly and uniquely regulated genes by NR1 & NR3. (n=3, ****p≤0.001). The error bars show standard deviation.

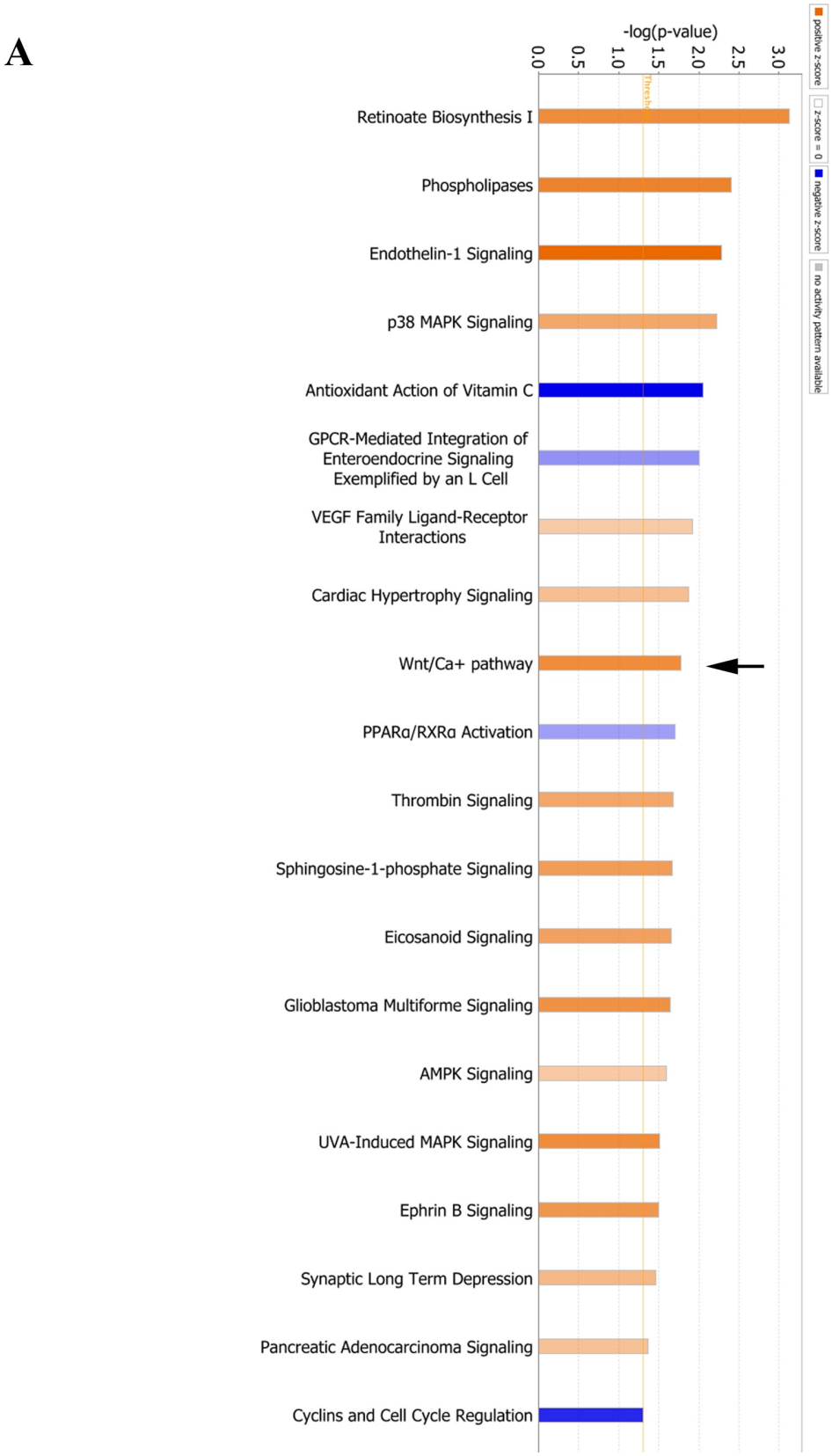

Figure 4.21 Ingenuity Pathway Analysis (IPA) of NOTCH3 unique gene list

B

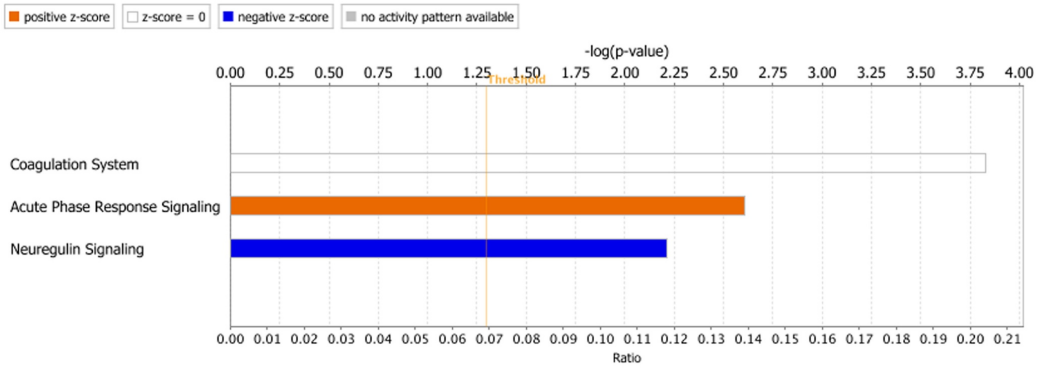

C

	N1ICD	N2ICD	N3ICD	N4ICD
CCL28	0.79±0.10	0.99±0.30	1.97±0.12	0.74±0.01
B4GALNT3	1.95±0.09	1.45±0.12	22.87±0.90	4.84±0.20
PROM2	2.12±0.31	0.87±0.06	3.35±0.25	2.73±0.19
TRPM4	1.84±0.06	1.32±0.50	3.46±0.70	2.66±0.08
ROR1	1.9±0.80	0.9±0.02	20.98±1.01	4.47±0.85
SECTM1	1.92±0.61	1.75±0.45	22.38±1.10	42.74±1.54
ANPEP	110.98±2.06	190.36±1.89	268.86±1.12	208.00±1.28
EPHB3	1.68±0.10	0.15±0.01	4.68±0.36	1.34±0.41
GGT6	24.51±1.30	1.8±0.87	20.2±0.99	4.18±0.53
GALNT6	2.34±0.06	2.3±0.91	6.39±1.03	2.49±0.67
GABRE	1.08±0.65	1.86±0.05	19.89±1.11	1.59±0.56
CD24	2.34±0.77	3.15±0.36	2.66±0.09	4.29±1.00
NEBL	1.96±0.32	7.63±1.08	41.97±1.55	21.46±1.41
KRT15	1.91±0.01	50.39±1.64	38.88±1.87	675.78±2.09
HTATIP2	0.29±0.03	68.9±1.12	89.37±1.45	216.65±1.73
PRICKLE1	1.89±0.66	1.38±0.31	4.99±0.91	42.69±2.02
RGS2	1.84±0.44	1.90±0.19	7.11±0.75	1.19±0.08
SCNN1B	36.03±0.99	88.29±1.38	65.48±1.76	53.28±2.02
FZD7	1.48±0.12	0.98±0.06	3.89±0.86	1.06±0.04

(A) IPA shows the enrichment of canonical pathways in NR3 unique data set. (B) IPA shows the enrichment of canonical pathways in NR1 unique data set. (C) qPCR validation of NOTCH3 regulated gene in 184-hTert cells. The bright red color indicates genes uniquely regulated by NOTCH3 receptor (n=3, standard deviation).

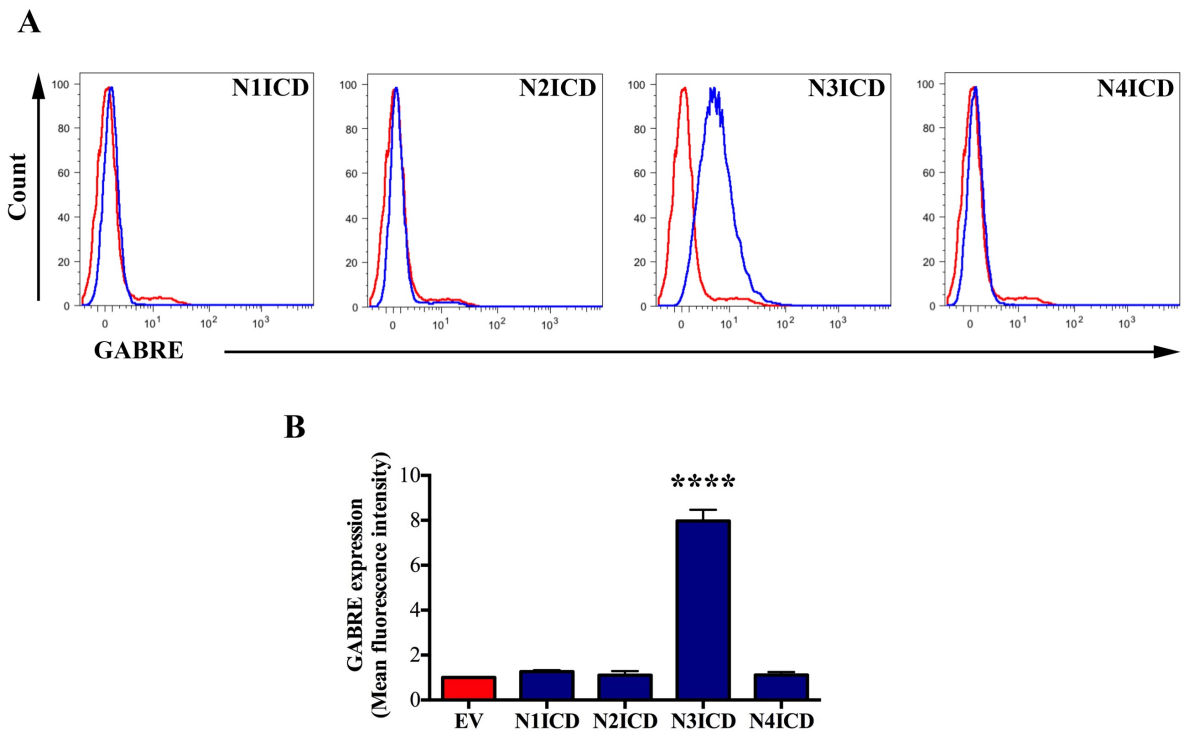

Figure 4.22 NOTCH3 uniquely regulates GABRE expression in 184-hTert cells

The GABRE protein expression in the 184-hTert cells overexpressing active form of Notch receptors was examined by flow cytometry. (A) Representative histograms are shown and (B) the average mean fluorescent intensities (MFI) from 3 independent infections are shown in a bar graph. The MFI of GABRE expression in the empty vector (EV) control infected cells were used as reference (set to 1) (n=3, ****p≤0.001). The error bars show standard deviation.

4.4. Conclusion and Discussion

In this study, I have explored signaling mechanism that regulates lineage commitment of bipotent progenitors to luminal cell fate. It was previously demonstrated that NR3 signaling was necessary to commit bipotent progenitors to a luminal cell fate [76]. However, molecular mechanisms underpinning NR3 signaling as well as the different subset of bipotent progenitors that are regulated by NR3 signaling were not explored. In the work presented here, I have identified *FZD7* as NR3-specific target genes [87]. Very interestingly, I identified a basal-like luminal progenitors (BLPs, $NR3^{+}FZD^{+}CD90^{+}$) that generated luminal only colonies based on NR3 and Wnt7 signaling which makes them distinct from $CD90^{-}$ luminal-restricted progenitors (LRPs) that were identified before. Furthermore, I also found that while BLPs are mostly ER^{-} but 100% $NR3^{+}$, only ~45% of LRPs are $NR3^{+}$ but >75% of them express ERα [283, 284] (Fig 4.12B).

My data thus indicate that bipotent progenitors represent a heterogeneous population of cells and that NR3-FZD7 signaling was required to promote their differentiation to LRPs. Interestingly, by knocking down of *NR3* in in this population, their ability to generate mix colonies increased, suggesting that bipotent progenitors by default generated mix colonies and the decision to differentiate into LRPs requires *NR3* signaling. A previous study suggested that *NR3* expression could be controlled by a Pygo2-β-catenin complex in MaSCs in that loss of Pygo2 in MaSCs resulted in increased Nr3 signaling and luminal fate specification [238]. To this end, transcriptome profiling of different human breast epithelial progenitor subsets by Raouf et al, suggested that *PYGO2* expression was higher in bipotent progenitor-enriched population as compared to LRPs [76] indicating that perhaps loss of *PYGO2* was required for activation of *NR3* expression in bipotent progenitors and their differentiation into the LRPs. However, the gain and loss of NR3 did not affect LRP functions, suggesting they were independent of NR3 signaling.

Although the loss of *FZD7* in the bipotent progenitor-enriched population resulted in a decrease in luminal colony number, this decrease was not as drastic as seen with loss of *NR3,* suggesting that in addition to FZD7, other NR3-specific targets play important roles in the commitment of bipotent progenitors to LRPs. Transcriptome profiling of 184-hTert cells overexpressing active form of NR3 revealed a number of NR3 unique target genes some of which could be involved in lineage restriction of bipotent progenitors to the luminal compartment. This analysis also revealed enrichment for Wnt pathway genes in the NR3-specific target gene list, suggesting crosstalk between NR3 and Wnt signaling pathways. Among these genes, *GABRE* was validated as an NR3-specific target and it will be interesting to examine if GABRE plays a role in commitment of bipotent progenitors to LRPs.

The BLPs ($NR3^{+}FZD7^{+}$) generated luminal only colonies in our CFC assays whereas, $NR3^{lo/-}FZD7^{+}$ cells exclusively generated mix colonies. Interestingly, the $NR3^{med}FZD7^{+}$ BLPs gave rise to both luminal as well as mix colonies. This observation suggested that $NR3^{med}FZD7^{+}$ cells could represent a transient progenitor cell state where increase in NR3 expression results in differentiation into BLPs.

Ligand binding to FZD receptors activates Wnt signaling. Different Wnt ligands have been shown to play an important role in mouse mammary gland development [285]. It was previously reported that a non-canonical Wnt ligand, Wnt7A induces symmetric expansion of muscle stem cells by binding to FZD7 receptor and activating the non-canonical Wnt signaling pathway [276, 279]. In this study, I demonstrated that Wnt7A enhanced the bipotent progenitor commitment to LRPs in a FZD7-dependent manner. This conclusion is based on the observation that the BLPs generated more luminal colonies when exposed to Wnt7A, whereas non-BLPs ($NR3^{lo/-}FZD7^{+}$) did not. Interestingly, Wnt7A had no effect on LRPs.

Bipotent progenitors were distinguished from LRPs based on CD90 and MUC1 expression. The bipotent progenitors are $CD90^{+}MUC1^{-}$ while LRPs are $CD90^{-}MUC1^{+}$ [68, 76] (Fig 4.4A). In this study, I observed that the $CD90^{+}MUC1^{-}$ ER^{-} BLPs generate luminal colonies containing $CD90^{-}MUC1^{+}ER^{+}$cells in the CFC assays, which are cells generated by LRPs in similar assays. Therefore, my data indicate that BLPs represent pre-LRP population. Taken together, this study demonstrates that cooperation between two evolutionarily conserved signaling pathways, the Notch and Wnt, plays a critical role in differentiation of bipotent progenitors to luminal-restricted progenitors.

5. General Discussion

Throughout the reproductive life of an adult female, the breast tissue undergoes dynamic changes in its epithelial cell compartment (both luminal and myoepithelial cells). The most primitive BESCs and their progeny (bipotent progenitors and lineage-restricted progenitors) play a vital role in tissue maintenance and regeneration during puberty, pregnancy and lactation through the process of lineage specification. This process allows females to have multiple pregnancies. Interestingly, the function of stem/progenitor cells are tightly regulated by different evolutionarily conserved signaling pathways and often dysregulation within these pathways can lead to cancer. Unfortunately, 60-70% of breast cancers are luminal type (hormone responsive). Therefore, understanding molecular pathways that regulate the function of stem/progenitors becomes crucial in defining alterations and further designing therapeutic strategies against them especially towards luminal type of breast cancers.

This study was based on the hypothesis that NOTCH3 receptor signaling through regulation of its unique target genes, plays a critical role in the differentiation of bipotent progenitors to the luminal cell lineage. In this regard, I was able to demonstrate that NOTCH3 receptor signaling uniquely regulated the expression of a Wnt receptor, *FRIZZLED7* in human breast epithelial cells. And that the NOTCH3-FRIZZLED7 signaling was required for commitment of bipotent progenitors to luminal cell lineage.

5.1. Non-redundant function of NR3 in breast epithelial cells

In this study, I showed that the Notch-induced FZD7 expression is regulated by NR3 in a CSL-independent manner in human breast epithelial cells. Non-canonical regulation of Notch target genes has been previously demonstrated where it was shown that NR1 forms an activating complex

with the *YY1* transcription factor and enhances c-Myc expression in a CSL-independent manner [183]. It is, therefore, possible that through this or similar mechanisms, *NR3* specifically regulates expression of its unique target genes including *FZD7*. The role of *FZD7* in regulating mouse mammary gland development was recently described by Chakrabarti et al [237] where the authors showed that cooperation between ΔN*p63* and *fzd7* could regulate mouse MaSC functions providing further support for the role of *FZD7* in regulating human stem/bipotent progenitor cell functions. The link between Notch-Wnt signaling crosstalk and luminal/alveolar differentiation was recently demonstrated by Gu et al [238]. Using the Pygopus 2 (Pygo2)-null mouse mammary cells, these authors demonstrated that canonical Wnt signaling antagonizes *Nr3* expression in a Pygo2-dependent manner and diminishes luminal/alveolar differentiation potential of breast cells. In this study, we found that *FZD7* expression was higher in committed luminal-restricted progenitor-enriched population that also express high levels of *NR3* compared to the uncommitted bipotent progenitor-enriched population that express very little *NR3*. The potential crosstalk between the *Nr1* and *Fzd6 & 10* was observed during dendritic cell differentiation in mice, indicating that the Notch-Wnt crosstalk could regulate important cellular processes [286].

Notch and Wnt represent two highly conserved signaling pathways that regulate many fundamental aspects of embryonic development as well as cell turnover and tissue regeneration in adult tissues. Therefore, understanding how these two signaling pathways interact would expand our understanding of their contributions to tissue development and regeneration, but also, would provide a framework to examine how altered Notch-Wnt crosstalk may contribute to disease processes. To this end, the potential role of *FZD7* in breast cancer development, particularly in the context of triple-negative breast tumors, has been described previously [287-289].

5.2. Notch and Wnt signaling crosstalk in luminal cell fate commitment

A recent study by Chakrabarti et al. has demonstrated crosstalk between Notch and Wnt in regulates MaSC activity. In this study, the authors showed that cell-cell communication between the MaSCs expressing notch ligand Dll1 and macrophages expressing Notch3 receptor activated Nr3 signaling in macrophages and resulted in secretion of Wnt ligands which in turn through a feedback loop regulated MaSC function [20]. Similarly, in this study I found that the Wnt ligand, Wnt7A enhanced the commitment of the bipotent progenitors to LRPs through FZD7 receptor. FZD7 has been shown to play an important role in transducing both canonical and non-canonical Wnt signaling [265, 272-278] depending on the availability of the canonical and non-canonical Wnt ligands. For example, binding of Wnt7A to FZD7 receptor was shown to activate noncanonical Wnt signaling [276, 279]. To this end, my transcriptome profiling of N3ICD overexpressing breast epithelial cells identified NR3 unique target genes that were enriched in noncanonical Wnt signaling providing strong evidence for a crosstalk between NR3 and Wnt signaling in human breast epithelial cells.

5.3. NR3 expression redefines breast epithelial cell hierarchy

Recently a single-cell transcriptome analysis of human breast epithelial cells suggested that LRPs could be derived from bipotent progenitors [269]. However, the experimental evidence to support this notion is still lacking. In this study, I have used functional studies to demonstrate that the bipotent progenitor-enriched population in the human breast epithelial cells represent a heterogeneous pool of undifferentiated cells. Using NR3 and FZD7, I was able to isolate and characterize a new basal-like luminal progenitor that are committed to the luminal cell lineage (i.e. the BLPs). Accordingly, the bipotent progenitor-enriched population ($EpCAM^{+}CD49f^{+}CD90^{+}$)

could be divided into four different subpopulations, (i) BLPs ($MUC1^{-}NR3^{high}FZD7^{+}$), (ii) undifferentiated bipotent progenitor-enriched population ($MUC1^{-}NR3^{low/-}FZD7^{+}$), (iii) the transient luminal/bipotent ($MUC1^{-}NR3^{med}FZD7^{+}$) progenitor-enriched population and (iv), the double negative subset ($MUC1^{-}NR3^{-}FZD7^{-}$). Furthermore, knocking down NR3 in the bipotent progenitors significantly decreases BLP population. When BLPs are placed in a differentiation assay, they produce luminal cell only colonies that with significantly decreased NR3 expression. Furthermore, the medium expression of NR3 identified transient luminal/bipotent cells. Moreover, the BLPs ($CD90^{+}MUC1^{-}NR3^{high}FZD7^{+}ER^{-}$) generated luminal cells that were ($CD90^{-}MUC1^{+}NR3^{med}FZD7^{+}ER^{+}$) which is a distinct feature of LRPs (Fig 5.1, Model 1). Taken together, these observations suggest that $NR3^{high}$ BLPs are progenies of the $NR3^{-}$ bipotent progenitors that differentiate to generate $NR3^{mid}$ LRPs. In this way, my thesis work has further extended the hierarchical organization of the human breast epithelial cells.

A recent study by Lafkas et al. demonstrated that Nr3 expressing luminal progenitors represented a quiescent subpopulation of breast epithelial cells that could become highly clonogenic in presence of appropriate cellular signals [64]. Here I found that the BLPs are present in the non-cultured bipotent progenitors at a frequency of 1 in 4000 (0.025%). But upon a short period of preculturing their frequency increases to ~35%, suggested that BLPs could represent a transient quiescent state *in vivo* and upon *in vitro* culturing they receive appropriate signals from fibroblasts and/or growth medium factors that result in their expansion.

Interestingly, the $NR3^{-}$ bipotent progenitors generated only mix colonies consisting of both luminal and myoepithelial cells while $NR3^{+}$ bipotent progenitors (BLPs) generated luminal cell only colonies. Thus, it is possible that these BLPs represent a separate lineage than the bipotent progenitors and directly differentiate into the mature luminal cells found in the alveolar structures

whereas the bipotent progenitors produce both the luminal and the myoepithelial cells need to generate the ductal structures (Fig 5.1, Model 2).

The CD90 and MUC1 expression in human breast epithelial cells have been useful in separating the bipotent progenitors ($CD90^{+}MUC1^{-}$) from LRPs ($CD90^{-}MUC1^{+}$) [68, 69, 76]. Here I found that the upon differentiation, the BLPs generated cells that lacked CD90 expression but now show strong MUC1 expression. Interestingly, colonies generated from LRPs which are $CD90^{-}MUC1^{+}$ were also $CD90^{-}MUC1^{+}$ providing further support for the notion that LRPs are the progenies of the BLPs. Previously, it was shown that CD90 marker expression could be used to distinguish hematopoietic stem cells from the multipotent progenitors where the $CD90^{+}$ stem cells differentiated to give rise to $CD90^{-}$ multipotent progenitors *in vitro* [290, 291].

Previously it was reported that the LRPs could only give rise to a limited number of pure luminal colonies upon re-plating [68] serial CFC assay experiments. Interestingly, however I observed that re-plating of BLPs generated 6-fold more luminal colonies. These data suggested that BLPs still retained their progenitor function during the differentiation assay which again gives credence to the notion that BLPs should be placed above LRPs in the lineage hierarchy of the human breast epithelial cells.

Dou et al. demonstrated that NR3 activates ERα expression in breast cancer cells thereby maintaining luminal phenotype and suppressing tumorigenesis [88]. This observation is interesting because I have found that ERα is not expressed in the non-BLPs, expressed in ~3% of the BLPs but expressed in more than 75% of the LRPs. It is, therefore, inviting to hypothesize that NR3 expression also regulates ERα expression in the BLPs and subsequently in the LRPs and eventually generating mature luminal cells.

5.4. BLPs represent a unique subset of breast epithelial progenitors

Previous studies suggested that the luminal colonies generated from the bipotent progenitors were contaminating luminal-restricted progenitors (LRPs) [76, 282]. However, our data suggest that the BLP population represents a unique subset of the breast progenitors which are different from the previously identified LRPs. Our data suggested that BLPs are NR3 signaling dependent and Wnt7A responsive as compared to LRPs which are NR3 signaling independent, Wnt7A non-responsive. Moreover, the BLPs differed from LRPs based on CD90 and MUC1 surface markers expression. The BLP were $CD90^{+}MUC1^{-}$ whereas LRPs were $CD90^{-}MUC1^{+}$ and both generated luminal cell-only colonies containing $CD90^{-}MUC1^{+}$ cells. Interestingly, the BLPs expressed very low levels of ERα as compared to LRPs (>75% of cells express ERα) but generated luminal cells that are $ER\alpha^{+}$. Interestingly, 100% of BLPs were $NR3^{+}$ while only 45% of LRPs were $NR3^{+}$. Table 6.1 describes the differences between the bipotent progenitors, BLPs and LRPs. These distinct characteristics provide compiling evidence suggesting that BLPs are different form LRPs and represented the primitive cell type committed to luminal cell fate. Therefore, I have identified a subset of the breast epithelial progenitors, BLPs which was not known earlier.

Further characterization of LSPBs in the luminal type of breast cancer tumors would reveal if BLPs could be the cell of origin for the luminal type breast cancer tumors which make up the most frequently diagnosed form of breast cancer in women. Such knowledge then may help in developing therapeutic strategies to treat this type of tumors.

Table 5.1 Differences between bipotent progenitors, BLPs and LRPs

	Bipotent progenitors	**BLPs**	**LRPs**
NR3 expression	Low/Negative	100% of BLPs are $NR3^+$	45% of LRPs are $NR3^+$
CD90 expression	Positive	Positive	Negative
MUC1 expression	Negative	Negative	Positive
ERα expression	~1%	~3%	>75%
Wnt7A responsive	Non-responsive	Responsive	Non-responsive
NR3-FZD7 signaling status	Independent	Dependent	Independent

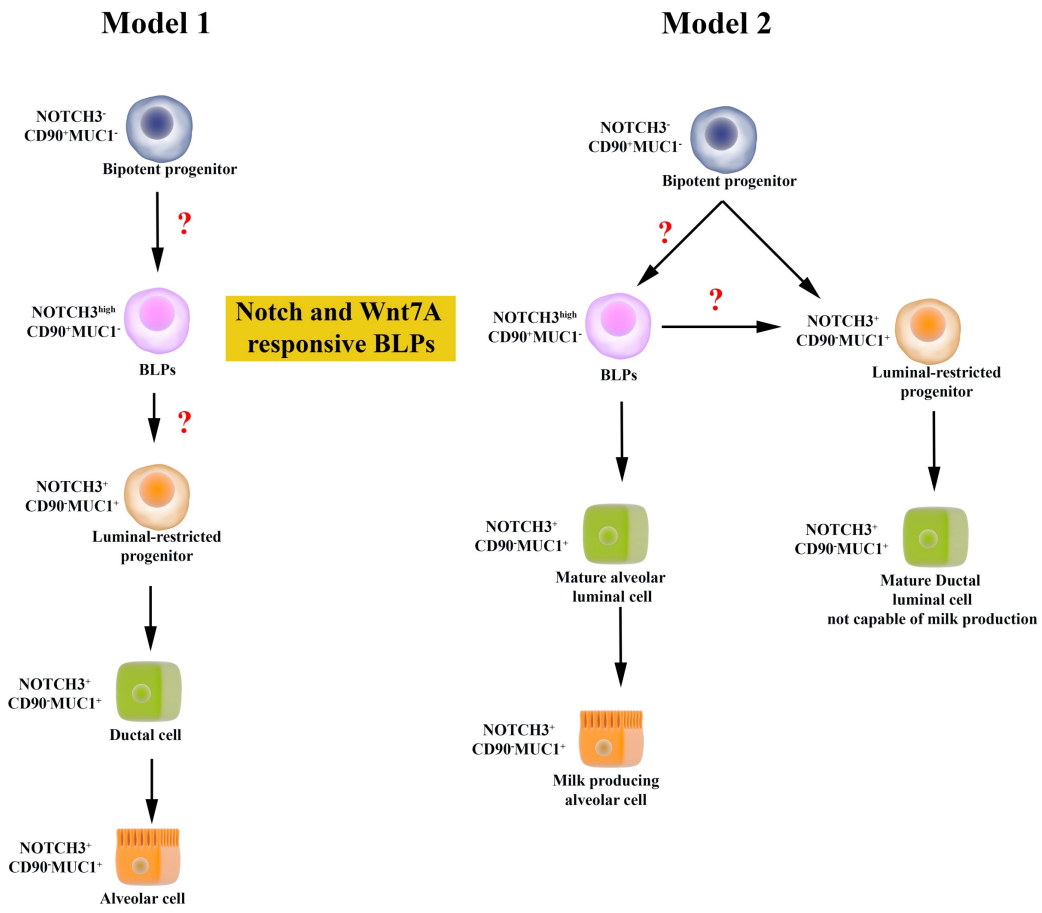

Figure 5.1 Proposed models for luminal cell origin in breast tissue

Schematics showing the different models proposed for luminal cell origin in breast tissue based on the observations made in this study. The first model proposes that the NR3^{-}CD90+ bipotent progenitors (BPs) could give rise to the BLPs (NR3^{+}CD90^{+}) which under the influence of NR3 and Wnt7A-FZD7 signaling differentiate to give rise to luminal-restricted progenitors (LRPs) which are CD90^{-}, NR3 and Wnt7A nonresponsive. These LRPs then generate the mature luminal cells of the ducts and the alveolar structures (Model 1). The second model proposes that the NR3^{-} CD90^{+} BPs can differentiate to give rise to either LRPs or the BLPs. The LRPs differentiate produce mature ductal-luminal cells that are not capable of milk production. While the BLPs could either differentiate to produce more LRPs or differentiate into alveolar luminal cells which under

the influence of pregnancy hormone further differentiate into milk producing cells (Model 2). Further understanding of this intricate differentiation process will help in understanding the issues underpinning lactation insufficiency syndrome in nursing mothers. Also, better understanding of the hierarchical organization of breast epithelial cells will help in defining how alteration in molecular mechanism that regulate cell fate and differentiation could result in luminal type of breast cancers.

6. Future Directions

The findings reported in this current study opens up different avenues for future studies to further our understanding on the role of NR3-Wnt signaling in breast tissue maintenance and regeneration and also to understand how alteration in this signaling mechanism causes luminal type breast cancers.

In this study, we showed a non-redundant function of NR3 signaling in human breast epithelial cells. We demonstrated that NR3 signaling uniquely regulates *FZD7* expression in a CSL-independent fashion. This suggested that N3ICD interacted with a different transcriptional machinery occupied on the proximal or distal promoter regions of *FZD7* gene. Since NR3 does not bind to DNA on its own, ChIP-Sequencing analysis would reveal novel binding sites for NR3-activating protein complexes to the *FZD7* promoter/regulatory region. Such studies will also help in the identification of additional unique targets of NR3 signaling in human breast epithelial cells. It is also possible that NR3 regulates FZD7 without binding to DNA as part of an activation protein complex. In that case, employing the kinome profiling technique would be beneficial to examine the active kinases under the regulation of NR3 signaling.

Outstanding important questions that remain are whether $NR3^-$ bipotent progenitors differentiate to generate BLPs and how *NR3* gene expression is regulated in the bipotent progenitors. Lineage tracing experiments are needed to determine if BLPs are generated from the bipotent progenitors or represent a distinct subset of epithelial progenitors. Such studies require the use of a promoter-reporter construct that includes NR3 promoter region that is specifically active in the bipotent progenitors. Unfortunately, such NR3 regulatory region has not been identified at the time of preparing this thesis. Therefore, initial experiments must focus on identifying the distal promoter elements that are specifically active in the bipotent progenitors. Gu

at al has demonstrated that Pygo2 and β catenin forms a complex and maintain the Nr3 promoter region in a suppressed state [238]. Interestingly, higher expression of PYGO2 has been observed in the purified bipotent progenitors as compared to LRPs [76]. Using of gain and loss of function of PYGO2 in breast epithelial cells could provide insight into how the $NR3^-$ bipotent progenitors differentiate into $NR3^+$ BLPs. Further, understanding the molecular mechanism that regulates *NR3* gene regulation in breast epithelial cells will provide evidence about the sequential event in the lineage commitment process in breast tissue. Lineage tracking experiments have demonstrated that the mouse mammary epithelial cells are organized in a lineage hierarchy [38, 46, 47, 53, 61, 282]. A similar lineage tracking approach in human breast epithelial cells will provide a better understanding of their hierarchical organization and the relationship between the different progenitor subtypes.

My data also demonstrate that compared to the LRPs, the BLPs have very low ERα levels but give rise to luminal colonies containing >75% $ER\alpha^+$ luminal cells. Therefore, tracking ERα expression and activity in human breast epithelial cell will help in understanding the generation of luminal cells from the primitive undifferentiated BLPs.

A study by Eirew et al. has demonstrated that increased ALDH (Aldehyde dehydrogenase) activity was found in the LRPs as compared to bipotent progenitors from freshly disassociated reduction mammoplasty samples. Transcript levels of *ALDH1A3* was specifically found to be higher in LRPs as compared to bipotent progenitors [71, 76]. The low ALDH activity in bipotent progenitors could suggest that an increase in this enzyme's activity results in differentiation of bipotent progenitors into BLPs and potentially into LRPs. It will be interesting therefore to examine ALDH activity in the BLPs and determine if gain of ALDH activity is required for differentiation of bipotent progenitors into BLPs.

In this study, I observed that loss of FZD7 function did not completely recapitulate the loss of *NR3*. This observation suggests that other genes regulated specifically by NR3 also play a role in regulating BLP functions. Very interestingly, I found that expression of GABA receptor ε, GABRE, was found to be uniquely regulated by NR3. It was previously reported that *GABRE* expression increases in response to estrogen (17β-estradiol) alone or in combination with progesterone in rhesus macaque brain. However, the role of GABRE in breast epithelial cells has not yet been explored. It is, therefore, an inviting hypothesis that NR3 unique targets of NR3 could form a signaling network that regulates luminal cell lineage commitment from bipotent progenitors. It would be interesting to functionally characterize $NR3^{+}FZD7^{+}GABRE^{+}$ BLPs and LRPs to better understand the role of NR3 targets in luminal lineage commitment.

A study by Lafkas et al. suggested that luminal progenitors in mouse mammary gland with higher expression of NR3 tend to remain quiescent while cell expressing lower NR3 levels actively proliferate [64]. In this study, I observed that BLPs had higher expression of NR3 as compared to LRPs and that BLPs are present at very low frequencies in the pre-cultured or freshly dissociated human breast tissue. This observation could suggest that BLPs *in vivo* are quiescent or less proliferative and that the LRPs represent the actively proliferative (transient amplifying progenitor) population that generate many mature luminal cells.

One of the major differences that distinguish BLPs from LRPs is the expression of ERα. Whereas >75% of LRPs are $ER\alpha^{+}$, only 3% of BLPs express ERα. Estrogen signaling was recently shown to enhance LRP expand in 3D Matrigel cultures [97]. It will be interesting to investigate if estrogen signaling results in expansion of the few $ER\alpha^{+}$ BLPs under similar culturing conditions. Identifying the population of cells analogous to BLPs in mice will be even more interesting since it will offer a powerful tool to further characterize these BLPs.

Furthermore, single-cell transcriptome analysis of the $NR3^-$ bipotent progenitors, BLPs and LRPs will allow us to understand in more detail the clonal heterogeneity that exists within the different progenitor subsets of the human breast epithelial cells. For example, on average ~3% of the BLPs express ERα. Single-cell transcriptomic of BLPs will reveal if the $ER\alpha^+$ BLPs are more closely related to the LRPs as compared to the $ER\alpha^-$BLPs. Such studies will allow revealing new insights into the function of these cells based on their unique expression of growth factors and signaling molecules.

The majority of breast cancer tumors consist of luminal cells. It has been suggested that alteration to luminal cell differentiation process could result in these types to breast cancer tumors. Since BLPs represent an early luminal progenitor subset, it is inviting to hypothesize that these cells could represent cancer initiating cells in luminal type breast cancers. Therefore, characterization of the $CD90^+NR3^+FZD7^+$ BLP cells in luminal type of breast cancer tumours will be very interesting. Identification of tumour initiating cell subset of luminal type breast cancer tumors will help in the development of more effective therapies with decreased risk of therapy resistance and metastatic recurrences.

7. Supplementary Information

Table 7.1 List of genes specifically regulated by NOTCH3 (2 fold cutoff)

Gene Name	Fold-Change	Gene Name	Fold-Change
PALMD	22.7881	CLIP1	2.08004
KRT6C	21.8868	DLEU2L	2.07961
SGPP2	21.1493	LOC100506748	2.07905
LPAR3	20.0631	SNORD92	2.07756
AKR1B10	20.0127	CYP4F22	2.07739
A2ML1	18.644	ENTPD2	2.07557
SPRR1B	17.5493	CPE	2.07447
GPNMB	16.2677	TOM1	2.07233
MUC15	15.3983	NRARP	2.07143
POF1B	15.1099	TTC39B	2.07056
CERS3	14.5717	ZNF766	2.07033
TSHZ2	14.0645	DTX4	2.07026
PIK3C2G	14.0311	DDR1	2.06936
GJB2	13.6802	SLC10A6	2.06834
DSC1	13.4235	OTTHUMG00000164075	2.06631
SULT1E1	13.361	ZNF770	2.06302
ALOX12B	11.8323	SLC22A15	2.06248
LOC100505633	11.1657	TP53I13	2.0619
FLG-AS1	9.94158	LINC00689	2.05882
TMEM45A	9.74614	OTTHUMG00000073721	2.0571
CA2	8.80896	TMEM168	2.05666
SCEL	8.70537	RAB11FIP4	2.05627
KRTDAP	8.06332	CBR3-AS1	2.0558
CDHR1	7.61129	LGALS7	2.05176
LIPK	7.53653	OARD1	2.05124
LURAP1L	7.47511	MKNK2	2.05031
PRMT8	7.46962	TIPARP	2.04839
PLA2G4F	7.27203	RSPH3	2.04838
KRT14	7.24304	GTF2IRD1	2.04617
GPR1	7.18814	MACF1	2.04382
BBOX1	7.04864	OTTHUMG00000161717	2.04347
CAPNS2	6.83009	NEBL	2.03958
PAMR1	6.71882	LRP11	2.03946
ROR1	6.67758	SQSTM1	2.03909
KRT6B	6.5226	PSAP	2.03801
MMP28	6.51078	PXDC1	2.03793
DAPK1	6.31671	TSHZ3	2.03748
LPHN2	6.23103	SNORA75	2.03712
TMEM79	6.16605	FRRS1	2.03684
DLX3	6.16263	TENM4	2.03265

HTATIP2	6.03785	FGD6	2.03071
SESN3	5.89997	TNFAIP8	2.03042
CWH43	5.87285	WEE1	2.03034
CYP4F3	5.64945	FNIP2	2.03011
SDR16C5	5.60433	OTTHUMG00000159435	2.02996
KRT16P2	5.5235	CKMT1A	2.02641
SECTM1	5.50935	BCL2L10	2.02469
LEPREL1	5.47273	GCSHP3	2.02466
CLCA2	5.45594	RDH16	2.02392
HENMT1	5.44832	HIST1H2AC	2.02138
CSTA	5.40957	MIR550A1	2.01596
NCF2	5.40649	SPRR2A	2.01584
KRT15	5.40254	FYB	2.01518
PRICKLE1	5.37131	GDF15	2.0126
CLEC7A	5.3348	ABCG1	2.01173
AQP3	5.29323	OTTHUMG00000154962	2.00918
FOXN1	5.22415	TGFB2	2.00889
SLC28A3	5.15993	LY6G6C	2.00854
XG	5.15895	SNORA9	2.00852
SULT2B1	4.9395	RDH10	2.00687
GSDMC	4.91094	TRIM16L	2.00662
CPEB2	4.85877	OAS1	2.00655
SPINK5	4.7864	NPAS2	2.00624
TFCP2L1	4.75787	SNORA84	2.00578
GPR115	4.73246	TAS2R5	2.00437
SERPINB2	4.68954	RGL2	2.00189
PRDM1	4.64519	IFI16	2.00086
SPTSSB	4.63103	FAP	-26.5271
SPSB1	4.57961	ADAM23	-9.56411
TIMP3	4.56588	FARP1	-9.24751
ARHGEF37	4.51363	SLC7A2	-8.24102
SPRR1A	4.37204	ENPP1	-7.33169
KRT16P3	4.31647	SCCPDH	-7.25027
SBSN	4.29378	AADAT	-7.07146
GABRE	4.28107	RPL23AP32	-6.62159
FAM83F	4.24334	EPB41L2	-6.32917
KLF4	4.24049	PCDHB13	-6.28278
IFFO2	4.21954	FAXC	-5.93558
SPTLC3	4.20697	TRAF5	-5.83015
PDZD2	4.19652	SAMHD1	-5.6812
SEMA3F	4.10587	VCAN	-5.37909
BMP2	4.0674	Mar-02	-5.03563
STEAP4	4.05361	MATN3	-5.0111
FABP5	4.03933	PYGO1	-4.97139
SLC2A1	3.97999	LHFP	-4.95195

GRHL1	3.96939	GLT8D2	-4.9471
EPGN	3.95274	PCDHB2	-4.65418
LIPN	3.94007	AASS	-4.62092
HBEGF	3.93633	PRTG	-4.58734
FAM213A	3.91855	LRRC34	-4.56888
NCCRP1	3.89151	CYP2J2	-4.54114
RAB27B	3.88223	BLMH	-4.51716
PITPNM3	3.87241	TTLL7	-4.49524
BPIFC	3.85742	PDE5A	-4.42722
S100A7A	3.83039	WDR17	-4.36403
ITPRIP	3.81422	ALDH1B1	-4.23185
ATP10B	3.81364	ZDHHC2	-4.17977
CYB5R1	3.79877	KRT7	-4.15396
IVL	3.7847	CADPS2	-4.14134
FOXQ1	3.76051	IFI6	-4.10042
GJA1	3.73543	HSD17B11	-4.0873
PLA2G4E	3.71842	FSTL1	-4.06028
DUOXA1	3.69915	CEP112	-4.04015
ANKRD22	3.66971	AKT3	-4.02126
NCKAP5	3.598	ABCC4	-3.97272
RASEF	3.5939	ICAM1	-3.96999
AKR1C2	3.58485	PRKACB	-3.89642
AHR	3.53199	DAB2	-3.88671
BCL11B	3.47287	EPHX4	-3.87555
GPCPD1	3.47123	NDUFC2-KCTD14	-3.86162
VAV3	3.4643	GOLM1	-3.76616
SRD5A1	3.45045	SH3BGRL2	-3.75143
LGALSL	3.4197	LIFR	-3.72382
TMEM63C	3.41801	PLAGL1	-3.68884
SCNN1G	3.40488	FAM171A1	-3.68127
KCNMA1	3.38821	SCN2A	-3.63609
FLJ10489	3.38514	MYL9	-3.63367
IGSF9	3.35365	MT2A	-3.60368
EPHA4	3.34354	ANKRD6	-3.47589
SYT14	3.30809	SCRN1	-3.44975
MIR33B	3.29269	TBC1D1	-3.42086
NCKAP5-IT1	3.24686	DZIP1	-3.40846
MIR1537	3.24289	KLF12	-3.39457
CA12	3.22645	TLR6	-3.36245
THEM5	3.20994	ZNF618	-3.33804
COL1A1	3.20239	CD83	-3.33515
SH3PXD2B	3.20176	FAT4	-3.33168
PORCN	3.20175	SFXN2	-3.29597
FAM84A	3.19192	FKBP11	-3.28904
FAM110C	3.15984	FBN2	-3.28411

MFGE8	3.15378	FAM105A	-3.26844
OTTHUMG00000167286	3.142	CCDC144CP	-3.26508
TRPV3	3.12336	PSIP1	-3.21392
CCDC8	3.1109	CTSZ	-3.18317
DAPK1-IT1	3.08936	CCL20	-3.16952
CEBPA	3.06625	SLC47A1	-3.16697
CPA4	3.05178	CDCA7L	-3.16672
KLF3	3.04584	LOC646329	-3.15798
SNN	3.04042	CFL2	-3.08671
BICD2	3.03769	MAP9	-3.0737
SLC22A3	3.03724	PGM2L1	-3.05937
EPHB6	3.03538	MCOLN2	-3.01334
SLC15A2	3.01908	SMARCA1	-3.01082
ACSL1	3.01472	CAPRIN2	-3.00881
GRIP1	3.00683	ZNF43	-3.00706
MIR22HG	3.00289	OTTHUMG00000168357	-2.99381
TINCR	2.98601	SLC39A8	-2.96861
RNLS	2.98019	RAI14	-2.94059
DENND2C	2.9699	SLC41A2	-2.94058
TNNI2	2.95883	SLC46A3	-2.9369
UNC5C	2.95802	MFI2	-2.8867
PGLYRP4	2.95585	OTTHUMG00000168366	-2.88517
CYYR1	2.95554	MCOLN3	-2.88297
PGLYRP3	2.94561	PLEKHH2	-2.87951
IRX4	2.92663	AKT3-IT1	-2.86141
SLC6A11	2.91734	LOC400043	-2.84798
RHOB	2.91272	ZYG11A	-2.83743
HSPG2	2.90101	OTTHUMG00000171577	-2.83656
RAB24	2.89612	SKP2	-2.83524
FOLR3	2.89604	TRNAI2	-2.83216
KLF8	2.88803	LOC375295	-2.832
PDCD4	2.8863	TBC1D30	-2.82789
OTTHUMG00000169048	2.88301	KIAA1549	-2.81425
ROS1	2.88238	TSPAN13	-2.81253
ADRB2	2.88028	PDK3	-2.79163
MIR383	2.85442	KCNQ5-IT1	-2.78062
EPHB3	2.83104	GCNT1	-2.74467
RGS2	2.8217	CTSS	-2.74087
FAM102A	2.78797	PIFO	-2.72586
STON2	2.77863	OTTHUMG00000019252	-2.71669
LDLRAD3	2.77376	PHLPP2	-2.70127
COL17A1	2.77231	PAPSS2	-2.68358
KRT6A	2.77115	FADS2	-2.68281
FAT2	2.76595	PRKD1	-2.68257
SNORA14A	2.76342	LOC286467	-2.66666

LOC146880	2.76281	NHLRC1	-2.65822
KLF9	2.75629	RBMS2	-2.65658
CUTC	2.75481	TSPAN1	-2.65424
VIPR1	2.75326	TBX18	-2.64994
C21orf91	2.72713	GRB14	-2.64276
GLTP	2.72695	ERO1LB	-2.63533
ZMIZ1	2.71851	MANEAL	-2.6341
NID1	2.71581	GSPT2	-2.62781
KITLG	2.7146	TRPC1	-2.62579
ZBTB7C	2.71449	PLS1	-2.61836
BNIPL	2.71295	ZDHHC23	-2.60153
SERPINB7	2.70349	ZNF681	-2.60143
SLC6A9	2.70273	EXTL2	-2.58947
LOC100506374	2.69472	STX2	-2.57148
CNKSR3	2.69218	SPATA5	-2.57065
NOD2	2.68735	DHTKD1	-2.56926
LINC00294	2.68521	LMO7	-2.55634
FAM89A	2.68129	MT1CP	-2.54959
DDIT3	2.66198	ADCY3	-2.54948
HR	2.65652	RNU7-47P	-2.54923
C6orf132	2.64858	TMEM106A	-2.54606
PRICKLE2	2.63597	Sep-06	-2.54338
TCF4	2.63457	EDARADD	-2.54303
SFRP1	2.62737	AGMAT	-2.53561
VLDLR	2.62648	LMNB2	-2.52848
FBXW7	2.62537	SAMD5	-2.52719
RAET1G	2.62115	SYK	-2.52574
GATA3	2.61052	COL5A2	-2.52402
GALNT6	2.60597	ZBTB38	-2.52393
ZNF551	2.59633	CMTM7	-2.52214
RDH12	2.59394	SIX4	-2.51828
SEMA5A	2.59343	ITGA1	-2.4943
HEG1	2.59091	CHD1L	-2.4912
TMPRSS4	2.58838	FXYD5	-2.48813
ZNF302	2.58725	NXPE3	-2.46281
JUP	2.57759	C7orf31	-2.46172
INHBB	2.57058	EHD3	-2.4602
METRNL	2.57028	ZNF385B	-2.45901
LINC00893	2.56915	TRIM2	-2.45511
RASSF5	2.56639	GCH1	-2.44985
SLITRK6	2.56412	FANCL	-2.44214
IRF2BP2	2.56167	LINC00960	-2.44141
ABLIM1	2.55801	C17orf53	-2.44099
TTC22	2.55056	EXOC6	-2.43483
FLRT2	2.54724	AKAP7	-2.4348

PRSS8	2.54683	NRG4	-2.43406
FZD6	2.54386	HFE	-2.42907
TSC22D3	2.53732	AFAP1L2	-2.42314
ARL4C	2.52248	LINC00240	-2.41675
PLB1	2.51885	MEST	-2.41491
CCL28	2.51724	L3MBTL3	-2.41206
ZBTB7B	2.51043	PARP1	-2.39467
LOC100506714	2.49931	MYADM	-2.39056
STL	2.49177	CHPT1	-2.38856
CNTN3	2.48819	QRFPR	-2.38393
CELSR2	2.48701	GALNT12	-2.38329
GLRX	2.48631	CES4A	-2.38218
TEX9	2.48571	OTTHUMG00000018330	-2.38187
FGFR2	2.48325	PM20D2	-2.38034
LTB4R2	2.47955	TPM2	-2.37951
SCPEP1	2.47671	NCAPD2	-2.3776
OTTHUMG00000166314	2.46586	PVRL3	-2.37748
PTGS1	2.46573	RIBC2	-2.36767
RNF144B	2.46554	NEDD1	-2.36718
C1orf116	2.46255	RACGAP1	-2.36213
GPX2	2.44684	E2F3	-2.35703
ZNF826P	2.44536	CEP57L1	-2.35689
PCDH1	2.43473	CLN6	-2.34629
RASA4	2.43391	LY6E	-2.33735
CEBPG	2.42736	E2F5	-2.32975
CSNK1A1	2.42633	FOXD2-AS1	-2.32819
POU2F3	2.41361	MSN	-2.32669
C6orf141	2.40736	SLC35B4	-2.32567
TMPRSS13	2.39987	MCIDAS	-2.32233
GPR56	2.39936	STARD3NL	-2.31792
CELSR1	2.39887	FAM64A	-2.31782
TACC2	2.397	MIS18BP1	-2.31567
EP300	2.39584	LOC81691	-2.31358
ABHD6	2.39325	TIFA	-2.30855
KCTD1	2.39269	CCSAP	-2.30658
OVOL1	2.38751	HOXA2	-2.30658
CD55	2.38372	ATIC	-2.30197
SNORA11	2.38264	BID	-2.29485
ELL3	2.3758	HPRT1	-2.28904
SCNN1B	2.37361	RFX3	-2.28894
LOC440300	2.37051	SYT1	-2.28744
OTTHUMG00000040659	2.3672	Mar-01	-2.28716
GPC6	2.36561	SYTL4	-2.28309
PLEKHM1	2.36182	SOAT1	-2.28024
ZNF506	2.35473	BICC1	-2.2769

ZNF556	2.35457	ZNF695	-2.27652
SNORA31	2.34986	USP32P2	-2.27113
DGAT2	2.34579	CNTNAP1	-2.27047
TREML1	2.34315	PTPLAD1	-2.26865
CD24	2.34245	CEP152	-2.26859
JMJD7-PLA2G4B	2.34104	HLTF	-2.26734
MTUS1	2.33994	DOCK11	-2.26653
TRIM16	2.33721	CHEK2	-2.26304
LOC100129550	2.33439	LOC202181	-2.2573
GGT6	2.33274	AAED1	-2.25244
TCP11L1	2.32757	DKK1	-2.24947
PTCHD4	2.31698	PI3	-2.24498
TRIB2	2.31595	LOC442075	-2.24433
ZNF608	2.31595	ACTN1	-2.23855
CIDEB	2.30785	SHROOM1	-2.23854
PPP2R3A	2.30698	GEN1	-2.23822
EAF2	2.30631	CTGF	-2.23533
LOC101060008	2.30567	GPD2	-2.23244
NFE2L2	2.30282	SMURF2	-2.22961
TMEM163	2.2999	CA13	-2.2266
KLF10	2.29701	OTTHUMG00000165727	-2.22491
HSD11B2	2.29637	HIST2H2AA4	-2.22335
PELI1	2.29582	FAM81A	-2.21749
OTTHUMG00000035468	2.28953	CTPS2	-2.2145
RCBTB2	2.28579	SORT1	-2.21083
ZNF436	2.27962	STEAP2	-2.20536
LOC283588	2.27946	TRAM2	-2.20199
NOTCH2NL	2.27765	RANBP17	-2.20084
PLCD1	2.27519	SIMC1	-2.19592
KIAA1671	2.27144	RAB23	-2.19329
ZNF350	2.26632	OTTHUMG00000175906	-2.19288
ACER1	2.26338	OTTHUMG00000154623	-2.18912
LIMK2	2.26298	IPO9	-2.18623
ANPEP	2.26091	KDELR3	-2.18268
DAAM1	2.25504	PFN1	-2.18094
ID3	2.2536	C10orf25	-2.17864
SPDYA	2.25113	GEMIN4	-2.17817
RPS6KA5	2.2468	PFAS	-2.17242
OTTHUMG00000152676	2.24628	TMEM171	-2.16773
HTRA1	2.24361	FAM72B	-2.16547
KAT2B	2.24194	SNRPA	-2.16321
SYT8	2.24013	C5orf54	-2.16286
TNNT1	2.2381	CEP135	-2.16194
NRP2	2.23572	USP18	-2.15324
UPK1A	2.23565	MRPL16	-2.1521

ELMSAN1	2.23323	NDUFAF3	-2.15085
FOXC2	2.23243	CLDN7	-2.15083
THRB	2.2299	BEND7	-2.14987
ATP1B3	2.22974	ICA1	-2.14927
MPZL2	2.22814	HN1	-2.1467
MIR3973	2.22357	LYN	-2.14484
ABCA10	2.22087	HMGN2P15	-2.14319
MAP1LC3B	2.21744	LOC101060654	-2.14073
PLEKHA1	2.21396	PDXP	-2.13969
KRCC1	2.2098	C17orf51	-2.13738
MAPKBP1	2.20921	TMEM139	-2.13608
ZNF706	2.20897	APOC1	-2.13005
GDPD3	2.20773	TUSC1	-2.12724
CBX4	2.2075	ABHD10	-2.12614
PAIP2B	2.206	CCAT1	-2.12562
LAD1	2.20553	C12orf23	-2.12099
TPD52L1	2.20539	TMEFF1	-2.11974
TNKS1BP1	2.2052	GSTM3	-2.11853
RTN4RL1	2.20373	OTTHUMG00000003643	-2.11597
CHMP1B	2.20283	OTTHUMG00000170886	-2.11361
PROM2	2.19427	HIST2H3D	-2.11356
MIR4668	2.19373	ANKRD44	-2.11146
EXOC6B	2.19228	SNRPB	-2.11137
FAM83B	2.19216	CDC27	-2.11009
B4GALNT3	2.18823	RBBP7	-2.10928
CDH1	2.18666	TMEM173	-2.10713
TERC	2.18428	MAP2K3	-2.1059
RASA4B	2.17994	TRAM1L1	-2.10504
MIR4774	2.17964	BACE2-IT1	-2.10338
SNX18	2.17876	CCNYL1	-2.10229
AJAP1	2.17864	PAQR4	-2.10142
SLC30A1	2.17753	RASSF8	-2.10059
DTX2P1	2.17735	HPSE	-2.09992
SLC39A6	2.17703	NARR	-2.0988
COL16A1	2.17592	SNAR-C1	-2.09673
FAM160A1	2.17442	SNAR-C1	-2.09673
CNFN	2.17371	SNAR-C1	-2.09673
TRPM4	2.17274	CHAMP1	-2.09438
GK	2.17193	KRT222	-2.09242
NBEAP1	2.16937	MYH10	-2.09189
RASA4	2.166	KRT18	-2.091
NPNT	2.16571	COMMD4	-2.09052
PLD3	2.16562	PDLIM4	-2.08879
PRKAB2	2.16246	IL27RA	-2.08836
PIM1	2.16243	SCARA3	-2.08819

ZNF354C	2.1596	STYK1	-2.08623
PLCD3	2.15769	PRR7-AS1	-2.08397
POLR2J2	2.1526	PCDH18	-2.08369
RNF141	2.1519	TWIST2	-2.08253
PLCH2	2.14935	HMGB2	-2.08223
SH3PXD2A	2.14934	RBPMS	-2.07604
RRAD	2.14866	PLOD1	-2.07244
SNORD91B	2.14675	SYBU	-2.07226
ISM1	2.14622	TRIM21	-2.07121
C1orf21	2.14595	SP4	-2.07062
PLEKHF2	2.14473	IFIT3	-2.07028
PTPRU	2.14255	CHST7	-2.06913
PTPN14	2.14151	SAMD4A	-2.06581
OGFRL1	2.14075	SLCO4A1	-2.06577
TP63	2.1406	MEIS3P1	-2.06466
TGM5	2.14038	RMI2	-2.0586
SLC31A2	2.13527	GALNT1	-2.05668
GNAO1	2.133	TMEM237	-2.05558
LOC388152	2.13231	GCA	-2.05106
MIR331	2.13148	MIR181A2HG	-2.05105
CNTNAP3	2.12853	ITGB5	-2.05057
PLXNB2	2.12593	NF2	-2.04911
AKR1C1	2.12399	RNA5SP221	-2.04849
SLC2A1-AS1	2.12019	SLC35G2	-2.04773
PPP1R14C	2.12009	CHST14	-2.04078
TMEM63B	2.11959	CNN2	-2.03988
KLHL21	2.11506	FLOT2	-2.03799
TPRG1L	2.11255	SLC25A40	-2.0379
LRRK2	2.11005	OTTHUMG00000163317	-2.03672
C11orf87	2.10908	ADAM22	-2.03646
DOPEY2	2.10874	COQ2	-2.03499
PLEKHM1	2.10701	ISOC1	-2.03315
BDKRB1	2.1028	FUT8	-2.03248
ENTPD7	2.1015	MIR3143	-2.03173
GTF2IRD2P1	2.10098	SKIL	-2.03094
LOC100129233	2.10035	THRA	-2.03009
PYHIN1	2.10026	CSRNP3	-2.02919
LOC100293044	2.09758	BACE2	-2.02493
GNAL	2.09706	CYP2U1	-2.02438
IFRD1	2.09652	TTL	-2.01772
TENM2	2.09365	PPIL1	-2.0155
JHDM1D	2.09356	PDIA4	-2.01468
TLE4	2.09161	IMPDH1	-2.01455
R3HDM2	2.0904	FASTKD3	-2.01405
EPB41L4A	2.08926	C3orf37	-2.01297

RFX2	2.08678	PRDX3	-2.01155
SERINC5	2.08631	PID1	-2.01042
P4HTM	2.08468	GTF2H2	-2.00797
XKRX	2.08361	SNHG6	-2.0035
ZNRF2	2.08348	HERC6	-2.00334
AHCYL2	2.08299	COL4A1	-2.00216
WWC3	2.08286	PIM2	-2.00102
LGALS7B	2.08198	BCAP29	-2.00033

Table 7.2 List of genes specifically regulated by NOTCH1 (2 fold cutoff)

Gene Name	Fold-Change	Gene Name	Fold-Change
C1S	9.43779	ZBTB10	2.07145
FAXDC2	8.27627	RNU7-45P	2.07113
GHR	6.4279	HNRNPA1P33	2.06617
C1R	6.30337	WDR19	2.05936
MIR3671	5.45569	IFITM3	2.05614
CFB	5.09742	RABL2B	2.0551
CLDN16	4.90101	MIR548I1	2.05474
CYP3A5	4.56852	ADAM20P1	2.05442
ACSS1	4.50421	POLR2J4	2.05346
OR5P2	4.49613	MIR29B2	2.04806
KDR	4.34214	WBP1L	2.04442
VNN3	4.1932	CEBPD	2.04008
LOC283299	4.16106	SPATA7	2.03935
SOD2	4.10391	OTTHUMG00000161604	2.03007
NNMT	3.94861	SIAE	2.02532
OTTHUMG00000175906	3.90802	MIR548I1	2.02282
ERRFI1	3.8075	MYCBP	2.02275
NEIL1	3.71152	YTHDC1	2.01914
OTTHUMG00000058631	3.46119	OCLN	2.01652
TPTE2P1	3.40393	AGO4	2.01582
N4BP2L1	3.15643	OTTHUMG00000019429	2.0137
TRIM35	3.09475	LOC644794	2.00903
CYBRD1	3.08973	TCEA2	2.0086
OR7A5	3.05688	ALYREF	-2.21889
TTC18	3.02103	ANKRD22	-4.45015
GBP2	2.93539	APOO	-2.3749
OTTHUMG00000163338	2.90747	AREG	-2.94203
OTTHUMG00000015939	2.87232	AREGB	-2.9403
BCL11A	2.86633	ARL4C	-3.20651
OVCH2	2.84337	ASNS	-2.22345
OR5P3	2.83543	ATP1B1	-2.39937
NFKBIA	2.83394	C19orf10	-2.06118
GADD45B	2.82086	C19orf40	-2.12054
SYT17	2.8021	CCRN4L	-2.28481
CLYBL	2.79049	CD3EAP	-2.01654
PCDHB9	2.76774	DUSP4	-3.91272
TMEM27	2.73641	EFNB2	-2.78655
OTTHUMG00000162778	2.72747	EIF4EBP1	-2.47051
NDRG1	2.72566	ENC1	-2.14574
NMNAT2	2.70687	EPGN	-2.7183
OTTHUMG00000154108	2.69857	EZH2	-2.20142
CLU	2.6937	FOXA2	-2.0883

ERBB3	2.67572	FSCN1	-2.88647
STOM	2.63855	FUT11	-2.00711
SNORA47	2.61295	GMPPB	-2.21516
GOLGA8B	2.60647	HMGA1	-2.01362
IFITM4P	2.60579	HNRNPAB	-2.18902
C1RL	2.58252	HOMER3	-2.09487
OTTHUMG00000162476	2.56819	ITGB6	-2.08503
GALNT15	2.56312	JPH1	-2.12193
MUC1	2.55528	KRT34	-2.62015
GOLGA8A	2.54475	LCE3D	-2.09166
ACSF2	2.54133	LDLR	-2.01733
ALDH6A1	2.54099	LIPG	-4.2757
PCDHB15	2.53811	LOC100129361	-2.0297
PIGZ	2.52256	LOC100292922	-2.58796
PLAG1	2.51123	MIR1244-1	-2.01145
BHLHE41	2.45917	MIR3198-1	-2.54904
GRAMD1C	2.44078	MIR31HG	-2.87324
MIR3182	2.43827	MPV17L2	-2.02163
GLUD1	2.42857	MTHFD2	-2.14013
KIAA1407	2.4215	MYO19	-2.08129
DKFZP434F142	2.41414	NRG1	-2.3891
CTSB	2.40186	NRP1	-4.37405
LINC00921	2.38263	NUDT15	-2.68361
ANG	2.36994	OTTHUMG00000165711	-2.21602
PCDHB18	2.36756	OTTHUMG00000169784	-3.76781
METTL7A	2.33673	OTTHUMG00000171045	-2.58701
TMC4	2.33661	PEA15	-2.30297
TMEM255A	2.33	PHLDA1	-2.7044
C1orf63	2.32596	PHLDA2	-2.60751
APMAP	2.32233	PIGW	-2.1755
HCAR2	2.31979	PLA2G4A	-2.35396
RAD51-AS1	2.29971	PLAT	-2.19217
SEL1L3	2.29404	PLXNA2	-2.37622
LOC100506934	2.27414	POPDC3	-2.40003
IP6K3	2.25341	PSAT1	-3.14862
TLR3	2.24542	PTMA	-2.01145
FLJ14186	2.2422	PTMA	-2.01145
PCDHB5	2.23633	RBBP8	-2.39791
SLC35E2	2.22404	RNA5-8SP3	-2.16239
MIR34A	2.22108	RNASE7	-2.08982
ISYNA1	2.20777	SERPINE1	-3.75863
C20orf96	2.20701	SFR1	-2.40134
C11orf80	2.20487	SH3PXD2A-AS1	-2.09991
LOC647859	2.19806	SLC25A33	-2.01071
TPTE2P6	2.19581	SLC37A2	-3.20023

LRRC37A	2.19562	SLC7A11	-4.55448
PROS1	2.19453	SLITRK6	-3.13661
FTX	2.19244	SNORA2B	-2.10121
ZFP90	2.18495	SPIN4	-2.70884
LOC100132707	2.18389	SPRED1	-2.12348
EZH1	2.17988	SPRED2	-2.04988
PCED1A	2.17897	SRPX2	-2.53291
ZNF630	2.17281	SSX2IP	-2.17983
PCDHB9	2.16205	STIP1	-2.03425
ZNF655	2.15753	TARS	-2.1205
OPTN	2.14346	TINAGL1	-2.90207
LRLE1	2.13551	TPM4	-2.05027
RGCC	2.13198	TRIB3	-3.09847
MYCL1	2.12956	TUBB2A	-2.0343
F2R	2.12526	TUBB2A	-2.0343
SLC11A2	2.1231	UBE2MP1	-2.33208
STAT2	2.11808	URB2	-2.02013
EIF3J-AS1	2.1135	VDR	-2.03308
NAIP	2.09277	VTRNA1-3	-2.15706
FAM19A2	2.09019	ZNF165	-2.09469
CTGF	2.08448	ZNF714	-2.04933

8. References

1. Geddes, D.T., Inside the lactating breast: the latest anatomy research. J Midwifery Womens Health, 2007. 52(6): p. 556-63.
2. Russo, J. and I.H. Russo, Development of the human breast. Maturitas, 2004. 49(1): p. 2-15.
3. Wuringer, E., et al., Nerve and vessel supplying ligamentous suspension of the mammary gland. Plast Reconstr Surg, 1998. 101(6): p. 1486-93.
4. Hughes, E.S., The Development of the Mammary Gland: Arris and Gale Lecture, delivered at the Royal College of Surgeons of England on 25th October, 1949. Ann R Coll Surg Engl, 1950. 6(2): p. 99-119.
5. Medina, D., The mammary gland: a unique organ for the study of development and tumorigenesis. J Mammary Gland Biol Neoplasia, 1996. 1(1): p. 5-19.
6. Sternlicht, M.D., Key stages in mammary gland development: the cues that regulate ductal branching morphogenesis. Breast Cancer Res, 2006. 8(1): p. 201.
7. Jolicoeur, F., Intrauterine breast development and the mammary myoepithelial lineage. J Mammary Gland Biol Neoplasia, 2005. 10(3): p. 199-210.
8. Sternlicht, M.D., et al., Hormonal and local control of mammary branching morphogenesis. Differentiation, 2006. 74(7): p. 365-81.
9. Cheatle, G.L., The Relation between Ducts and Acini to Cysts and Cancer of the Breast. Proc R Soc Med, 1914. 7(Surg Sect): p. 241-4.
10. Gompel, A., et al., Steroidal hormones and proliferation, differentiation and apoptosis in breast cells. Maturitas, 2004. 49(1): p. 16-24.
11. Sekhri, K.K., D.R. Pitelka, and K.B. DeOme, Studies of mouse mammary glands. I. Cytomorphology of the normal mammary gland. J Natl Cancer Inst, 1967. 39(3): p. 459-90.
12. Richards, R.C. and G.K. Benson, Ultrastructural changes accompanying involution of the mammary gland in the albino rat. J Endocrinol, 1971. 51(1): p. 127-35.
13. Dontu, G. and T.A. Ince, Of mice and women: a comparative tissue biology perspective of breast stem cells and differentiation. J Mammary Gland Biol Neoplasia, 2015. 20(1-2): p. 51-62.
14. Monks, J., et al., Do inflammatory cells participate in mammary gland involution? J Mammary Gland Biol Neoplasia, 2002. 7(2): p. 163-76.
15. Gouon-Evans, V., M.E. Rothenberg, and J.W. Pollard, Postnatal mammary gland development requires macrophages and eosinophils. Development, 2000. 127(11): p. 2269-82.
16. Sferruzzi-Perri, A.N., S.A. Robertson, and L.A. Dent, Interleukin-5 transgene expression and eosinophilia are associated with retarded mammary gland development in mice. Biol Reprod, 2003. 69(1): p. 224-33.
17. Lilla, J.N. and Z. Werb, Mast cells contribute to the stromal microenvironment in mammary gland branching morphogenesis. Dev Biol, 2010. 337(1): p. 124-33.
18. Pollard, J.W. and L. Hennighausen, Colony stimulating factor 1 is required for mammary gland development during pregnancy. Proc Natl Acad Sci U S A, 1994. 91(20): p. 9312-6.
19. Gyorki, D.E., et al., Resident macrophages influence stem cell activity in the mammary gland. Breast Cancer Res, 2009. 11(4): p. R62.

20. Chakrabarti, R., et al., Notch ligand Dll1 mediates cross-talk between mammary stem cells and the macrophageal niche. Science, 2018. 360(6396).
21. Weisz-Carrington, P., M.E. Roux, and M.E. Lamm, Plasma cells and epithelial immunoglobulins in the mouse mammary gland during pregnancy and lactation. J Immunol, 1977. 119(4): p. 1306-7.
22. Bourges, D., et al., New insights into the dual recruitment of IgA+ B cells in the developing mammary gland. Mol Immunol, 2008. 45(12): p. 3354-62.
23. O'Brien, J., et al., Alternatively activated macrophages and collagen remodeling characterize the postpartum involuting mammary gland across species. Am J Pathol, 2010. 176(3): p. 1241-55.
24. Deugnier, M.A., et al., The importance of being a myoepithelial cell. Breast Cancer Res, 2002. 4(6): p. 224-30.
25. Petersen, O.W. and K. Polyak, Stem cells in the human breast. Cold Spring Harb Perspect Biol, 2010. 2(5): p. a003160.
26. Gimpl, G. and F. Fahrenholz, The oxytocin receptor system: structure, function, and regulation. Physiol Rev, 2001. 81(2): p. 629-83.
27. Wagner, K.U., et al., Oxytocin and milk removal are required for post-partum mammary-gland development. Genes Funct, 1997. 1(4): p. 233-44.
28. Haaksma, C.J., R.J. Schwartz, and J.J. Tomasek, Myoepithelial cell contraction and milk ejection are impaired in mammary glands of mice lacking smooth muscle alpha-actin. Biol Reprod, 2011. 85(1): p. 13-21.
29. Potten, C.S., et al., The effect of age and menstrual cycle upon proliferative activity of the normal human breast. Br J Cancer, 1988. 58(2): p. 163-70.
30. Soderqvist, G., et al., Proliferation of breast epithelial cells in healthy women during the menstrual cycle. Am J Obstet Gynecol, 1997. 176(1 Pt 1): p. 123-8.
31. Vogel, P.M., et al., The correlation of histologic changes in the human breast with the menstrual cycle. Am J Pathol, 1981. 104(1): p. 23-34.
32. Suzuki, R., et al., Proliferation and differentiation in the human breast during pregnancy. Differentiation, 2000. 66(2-3): p. 106-15.
33. Russo, J. and I.H. Russo, Development pattern of human breast and susceptibility to carcinogenesis. Eur J Cancer Prev, 1993. 2 Suppl 3: p. 85-100.
34. Deome, K.B., et al., Development of mammary tumors from hyperplastic alveolar nodules transplanted into gland-free mammary fat pads of female C3H mice. Cancer Res, 1959. 19(5): p. 515-20.
35. Hoshino, K., Morphogenesis and growth potentiality of mammary glands in mice. I. Transplantability and growth potentiality of mammary tissue of virgin mice. J Natl Cancer Inst, 1962. 29: p. 835-51.
36. Daniel, C.W., et al., The in vivo life span of normal and preneoplastic mouse mammary glands: a serial transplantation study. Proc Natl Acad Sci U S A, 1968. 61(1): p. 53-60.
37. Smith, G.H. and D. Medina, A morphologically distinct candidate for an epithelial stem cell in mouse mammary gland. J Cell Sci, 1988. 90 (Pt 1): p. 173-83.
38. Visvader, J.E. and J. Stingl, Mammary stem cells and the differentiation hierarchy: current status and perspectives. Genes Dev, 2014. 28(11): p. 1143-58.
39. Inman, J.L., et al., Mammary gland development: cell fate specification, stem cells and the microenvironment. Development, 2015. 142(6): p. 1028-42.

40. Williams, J.M. and C.W. Daniel, Mammary ductal elongation: differentiation of myoepithelium and basal lamina during branching morphogenesis. Dev Biol, 1983. 97(2): p. 274-90.
41. Kordon, E.C. and G.H. Smith, An entire functional mammary gland may comprise the progeny from a single cell. Development, 1998. 125(10): p. 1921-30.
42. Stingl, J., et al., Purification and unique properties of mammary epithelial stem cells. Nature, 2006. 439(7079): p. 993-7.
43. Shackleton, M., et al., Generation of a functional mammary gland from a single stem cell. Nature, 2006. 439(7072): p. 84-8.
44. Machado, H.L., et al., Separation by cell size enriches for mammary stem cell repopulation activity. Stem Cells Transl Med, 2013. 2(3): p. 199-203.
45. Plaks, V., et al., Lgr5-expressing cells are sufficient and necessary for postnatal mammary gland organogenesis. Cell Rep, 2013. 3(1): p. 70-8.
46. de Visser, K.E., et al., Developmental stage-specific contribution of LGR5(+) cells to basal and luminal epithelial lineages in the postnatal mammary gland. J Pathol, 2012. 228(3): p. 300-9.
47. Rios, A.C., et al., In situ identification of bipotent stem cells in the mammary gland. Nature, 2014. 506(7488): p. 322-7.
48. Rauner, G., et al., High Expression of CD200 and CD200R1 Distinguishes Stem and Progenitor Cell Populations within Mammary Repopulating Units. Stem Cell Reports, 2018. 11(1): p. 288-302.
49. Sleeman, K.E., et al., CD24 staining of mouse mammary gland cells defines luminal epithelial, myoepithelial/basal and non-epithelial cells. Breast Cancer Res, 2006. 8(1): p. R7.
50. Bernardo, G.M., et al., FOXA1 is an essential determinant of ERalpha expression and mammary ductal morphogenesis. Development, 2010. 137(12): p. 2045-54.
51. Maningat, P.D., et al., Gene expression in the human mammary epithelium during lactation: the milk fat globule transcriptome. Physiol Genomics, 2009. 37(1): p. 12-22.
52. Asselin-Labat, M.L., et al., Gata-3 is an essential regulator of mammary-gland morphogenesis and luminal-cell differentiation. Nat Cell Biol, 2007. 9(2): p. 201-9.
53. Shehata, M., et al., Phenotypic and functional characterisation of the luminal cell hierarchy of the mammary gland. Breast Cancer Res, 2012. 14(5): p. R134.
54. Asselin-Labat, M.L., et al., Gata-3 negatively regulates the tumor-initiating capacity of mammary luminal progenitor cells and targets the putative tumor suppressor caspase-14. Mol Cell Biol, 2011. 31(22): p. 4609-22.
55. Regan, J.L., et al., c-Kit is required for growth and survival of the cells of origin of Brca1-mutation-associated breast cancer. Oncogene, 2012. 31(7): p. 869-83.
56. Sleeman, K.E., et al., Dissociation of estrogen receptor expression and in vivo stem cell activity in the mammary gland. J Cell Biol, 2007. 176(1): p. 19-26.
57. Wang, C., et al., Lineage-Biased Stem Cells Maintain Estrogen-Receptor-Positive and -Negative Mouse Mammary Luminal Lineages. Cell Rep, 2017. 18(12): p. 2825-2835.
58. Feil, S., N. Valtcheva, and R. Feil, Inducible Cre mice. Methods Mol Biol, 2009. 530: p. 343-63.
59. Van Keymeulen, A., et al., Distinct stem cells contribute to mammary gland development and maintenance. Nature, 2011. 479(7372): p. 189-93.

60. Lim, E., et al., Transcriptome analyses of mouse and human mammary cell subpopulations reveal multiple conserved genes and pathways. Breast Cancer Res, 2010. 12(2): p. R21.
61. Lloyd-Lewis, B., et al., Neutral lineage tracing of proliferative embryonic and adult mammary stem/progenitor cells. Development, 2018. 145(14).
62. Wagner, K.U., et al., An adjunct mammary epithelial cell population in parous females: its role in functional adaptation and tissue renewal. Development, 2002. 129(6): p. 1377-86.
63. Chang, T.H., et al., New insights into lineage restriction of mammary gland epithelium using parity-identified mammary epithelial cells. Breast Cancer Res, 2014. 16(1): p. R1.
64. Lafkas, D., et al., Notch3 marks clonogenic mammary luminal progenitor cells in vivo. J Cell Biol, 2013. 203(1): p. 47-56.
65. Tsai, Y.C., et al., Contiguous patches of normal human mammary epithelium derived from a single stem cell: implications for breast carcinogenesis. Cancer Res, 1996. 56(2): p. 402-4.
66. Eirew, P., J. Stingl, and C.J. Eaves, Quantitation of human mammary epithelial stem cells with in vivo regenerative properties using a subrenal capsule xenotransplantation assay. Nat Protoc, 2010. 5(12): p. 1945-56.
67. Eirew, P., et al., A method for quantifying normal human mammary epithelial stem cells with in vivo regenerative ability. Nat Med, 2008. 14(12): p. 1384-9.
68. Stingl, J., et al., Epithelial progenitors in the normal human mammary gland. J Mammary Gland Biol Neoplasia, 2005. 10(1): p. 49-59.
69. Stingl, J., et al., Characterization of bipotent mammary epithelial progenitor cells in normal adult human breast tissue. Breast Cancer Res Treat, 2001. 67(2): p. 93-109.
70. Lim, E., et al., Aberrant luminal progenitors as the candidate target population for basal tumor development in BRCA1 mutation carriers. Nat Med, 2009. 15(8): p. 907-13.
71. Eirew, P., et al., Aldehyde dehydrogenase activity is a biomarker of primitive normal human mammary luminal cells. Stem Cells, 2012. 30(2): p. 344-8.
72. Deng, H., et al., ER-alpha36-mediated rapid estrogen signaling positively regulates ER-positive breast cancer stem/progenitor cells. PLoS One, 2014. 9(2): p. e88034.
73. Liu, S., et al., Breast cancer stem cells transition between epithelial and mesenchymal states reflective of their normal counterparts. Stem Cell Reports, 2014. 2(1): p. 78-91.
74. Ginestier, C., et al., ALDH1 is a marker of normal and malignant human mammary stem cells and a predictor of poor clinical outcome. Cell Stem Cell, 2007. 1(5): p. 555-67.
75. Raouf, A., et al., The biology of human breast epithelial progenitors. Semin Cell Dev Biol, 2012. 23(5): p. 606-12.
76. Raouf, A., et al., Transcriptome analysis of the normal human mammary cell commitment and differentiation process. Cell Stem Cell, 2008. 3(1): p. 109-18.
77. Stingl, J., et al., Phenotypic and functional characterization in vitro of a multipotent epithelial cell present in the normal adult human breast. Differentiation, 1998. 63(4): p. 201-13.
78. Stingl, J., et al., Deciphering the mammary epithelial cell hierarchy. Cell Cycle, 2006. 5(14): p. 1519-22.
79. Gudjonsson, T., et al., Isolation, immortalization, and characterization of a human breast epithelial cell line with stem cell properties. Genes Dev, 2002. 16(6): p. 693-706.
80. O'Hare, M.J., et al., Characterization in vitro of luminal and myoepithelial cells isolated from the human mammary gland by cell sorting. Differentiation, 1991. 46(3): p. 209-21.

81. Chatterjee, S., et al., Loss of Igfbp7 causes precocious involution in lactating mouse mammary gland. PLoS One, 2014. 9(2): p. e87858.
82. Boras-Granic, K. and J.J. Wysolmerski, Wnt signaling in breast organogenesis. Organogenesis, 2008. 4(2): p. 116-22.
83. Bouras, T., et al., Notch signaling regulates mammary stem cell function and luminal cell-fate commitment. Cell Stem Cell, 2008. 3(4): p. 429-41.
84. Buono, K.D., et al., The canonical Notch/RBP-J signaling pathway controls the balance of cell lineages in mammary epithelium during pregnancy. Dev Biol, 2006. 293(2): p. 565-80.
85. Dontu, G., et al., Role of Notch signaling in cell-fate determination of human mammary stem/progenitor cells. Breast Cancer Res, 2004. 6(6): p. R605-15.
86. Sansone, P., et al., p66Shc/Notch-3 interplay controls self-renewal and hypoxia survival in human stem/progenitor cells of the mammary gland expanded in vitro as mammospheres. Stem Cells, 2007. 25(3): p. 807-15.
87. Bhat, V., et al., Notch-Induced Expression of FZD7 Requires Noncanonical NOTCH3 Signaling in Human Breast Epithelial Cells. Stem Cells Dev, 2016. 25(7): p. 522-9.
88. Dou, X.W., et al., Notch3 Maintains Luminal Phenotype and Suppresses Tumorigenesis and Metastasis of Breast Cancer via Trans-Activating Estrogen Receptor-alpha. Theranostics, 2017. 7(16): p. 4041-4056.
89. Brisken, C. and B. O'Malley, Hormone action in the mammary gland. Cold Spring Harb Perspect Biol, 2010. 2(12): p. a003178.
90. Krege, J.H., et al., Generation and reproductive phenotypes of mice lacking estrogen receptor beta. Proc Natl Acad Sci U S A, 1998. 95(26): p. 15677-82.
91. Mallepell, S., et al., Paracrine signaling through the epithelial estrogen receptor alpha is required for proliferation and morphogenesis in the mammary gland. Proc Natl Acad Sci U S A, 2006. 103(7): p. 2196-201.
92. Tanos, T., et al., ER and PR signaling nodes during mammary gland development. Breast Cancer Res, 2012. 14(4): p. 210.
93. Brisken, C., et al., A paracrine role for the epithelial progesterone receptor in mammary gland development. Proc Natl Acad Sci U S A, 1998. 95(9): p. 5076-81.
94. Joshi, P.A., et al., Progesterone induces adult mammary stem cell expansion. Nature, 2010. 465(7299): p. 803-7.
95. Lydon, J.P., et al., Mice lacking progesterone receptor exhibit pleiotropic reproductive abnormalities. Genes Dev, 1995. 9(18): p. 2266-78.
96. Hennighausen, L. and G.W. Robinson, Signaling pathways in mammary gland development. Dev Cell, 2001. 1(4): p. 467-75.
97. Basak, P., et al., Estrogen regulates luminal progenitor cell differentiation through H19 gene expression. Endocr Relat Cancer, 2015. 22(4): p. 505-17.
98. Horseman, N.D., et al., Defective mammopoiesis, but normal hematopoiesis, in mice with a targeted disruption of the prolactin gene. Embo j, 1997. 16(23): p. 6926-35.
99. Lyons, W.R., C.H. Li, and R.E. Johnson, The hormonal control of mammary growth and lactation. Recent Prog Horm Res, 1958. 14: p. 219-48; discussion 248-54.
100. Ormandy, C.J., et al., Null mutation of the prolactin receptor gene produces multiple reproductive defects in the mouse. Genes Dev, 1997. 11(2): p. 167-78.

101. Chepko, G. and G.H. Smith, Three division-competent, structurally-distinct cell populations contribute to murine mammary epithelial renewal. Tissue Cell, 1997. 29(2): p. 239-53.
102. Smith, G.H., Experimental mammary epithelial morphogenesis in an in vivo model: evidence for distinct cellular progenitors of the ductal and lobular phenotype. Breast Cancer Res Treat, 1996. 39(1): p. 21-31.
103. Chepko, G. and G.H. Smith, Mammary epithelial stem cells: our current understanding. J Mammary Gland Biol Neoplasia, 1999. 4(1): p. 35-52.
104. Albarracin, C.T., et al., Identification of a major prolactin-regulated protein as 20 alpha-hydroxysteroid dehydrogenase: coordinate regulation of its activity, protein content, and messenger ribonucleic acid expression. Endocrinology, 1994. 134(6): p. 2453-60.
105. Han, J., J. Allalunis-Turner, and M.J. Hendzel, Characterization and comparison of protein complexes initiated by the intracellular domain of individual Notch paralogs. Biochem Biophys Res Commun, 2011. 407(3): p. 479-85.
106. Bigas, A. and L. Espinosa, Hematopoietic stem cells: to be or Notch to be. Blood, 2012. 119(14): p. 3226-35.
107. Liu, J., et al., Notch signaling in the regulation of stem cell self-renewal and differentiation. Curr Top Dev Biol, 2010. 92: p. 367-409.
108. Wharton, K.A., et al., Nucleotide sequence from the neurogenic locus notch implies a gene product that shares homology with proteins containing EGF-like repeats. Cell, 1985. 43(3 Pt 2): p. 567-81.
109. Gordon, W.R., K.L. Arnett, and S.C. Blacklow, The molecular logic of Notch signaling--a structural and biochemical perspective. J Cell Sci, 2008. 121(Pt 19): p. 3109-19.
110. Greenwald, I. and G. Seydoux, Analysis of gain-of-function mutations of the lin-12 gene of Caenorhabditis elegans. Nature, 1990. 346(6280): p. 197-9.
111. Heitzler, P. and P. Simpson, The choice of cell fate in the epidermis of Drosophila. Cell, 1991. 64(6): p. 1083-92.
112. Wilkinson, H.A., K. Fitzgerald, and I. Greenwald, Reciprocal changes in expression of the receptor lin-12 and its ligand lag-2 prior to commitment in a C. elegans cell fate decision. Cell, 1994. 79(7): p. 1187-98.
113. Struhl, G. and A. Adachi, Nuclear access and action of notch in vivo. Cell, 1998. 93(4): p. 649-60.
114. Lecourtois, M. and F. Schweisguth, Indirect evidence for Delta-dependent intracellular processing of notch in Drosophila embryos. Curr Biol, 1998. 8(13): p. 771-4.
115. Schroeter, E.H., J.A. Kisslinger, and R. Kopan, Notch-1 signalling requires ligand-induced proteolytic release of intracellular domain. Nature, 1998. 393(6683): p. 382-6.
116. Weinmaster, G., Notch signaling: direct or what? Curr Opin Genet Dev, 1998. 8(4): p. 436-42.
117. Bray, S.J., Notch signalling: a simple pathway becomes complex. Nat Rev Mol Cell Biol, 2006. 7(9): p. 678-89.
118. Kopan, R. and M.X. Ilagan, The canonical Notch signaling pathway: unfolding the activation mechanism. Cell, 2009. 137(2): p. 216-33.
119. Jennings, B., et al., The Notch signalling pathway is required for Enhancer of split bHLH protein expression during neurogenesis in the Drosophila embryo. Development, 1994. 120(12): p. 3537-48.

120. Kim, J., et al., Integration of positional signals and regulation of wing formation and identity by Drosophila vestigial gene. Nature, 1996. 382(6587): p. 133-8.
121. Roehl, H., et al., Roles of the RAM and ANK domains in signaling by the C. elegans GLP-1 receptor. Embo j, 1996. 15(24): p. 7002-12.
122. Tamura, K., et al., Physical interaction between a novel domain of the receptor Notch and the transcription factor RBP-J kappa/Su(H). Curr Biol, 1995. 5(12): p. 1416-23.
123. Del Bianco, C., et al., Notch and MAML-1 complexation do not detectably alter the DNA binding specificity of the transcription factor CSL. PLoS One, 2010. 5(11): p. e15034.
124. Jarriault, S., et al., Signalling downstream of activated mammalian Notch. Nature, 1995. 377(6547): p. 355-8.
125. Ohtsuka, T., et al., Hes1 and Hes5 as notch effectors in mammalian neuronal differentiation. Embo j, 1999. 18(8): p. 2196-207.
126. Hsieh, J.J., et al., Truncated mammalian Notch1 activates CBF1/RBPJk-repressed genes by a mechanism resembling that of Epstein-Barr virus EBNA2. Mol Cell Biol, 1996. 16(3): p. 952-9.
127. Kunisch, M., M. Haenlin, and J.A. Campos-Ortega, Lateral inhibition mediated by the Drosophila neurogenic gene delta is enhanced by proneural proteins. Proc Natl Acad Sci U S A, 1994. 91(21): p. 10139-43.
128. Appel, B., L.A. Givan, and J.S. Eisen, Delta-Notch signaling and lateral inhibition in zebrafish spinal cord development. BMC Dev Biol, 2001. 1: p. 13.
129. Trylinski, M., K. Mazouni, and F. Schweisguth, Intra-lineage Fate Decisions Involve Activation of Notch Receptors Basal to the Midbody in Drosophila Sensory Organ Precursor Cells. Curr Biol, 2017. 27(15): p. 2239-2247.e3.
130. Bertet, C., et al., Temporal patterning of neuroblasts controls Notch-mediated cell survival through regulation of Hid or Reaper. Cell, 2014. 158(5): p. 1173-1186.
131. San-Juan, B.P. and A. Baonza, The bHLH factor deadpan is a direct target of Notch signaling and regulates neuroblast self-renewal in Drosophila. Dev Biol, 2011. 352(1): p. 70-82.
132. Ohlstein, B. and A. Spradling, Multipotent Drosophila intestinal stem cells specify daughter cell fates by differential notch signaling. Science, 2007. 315(5814): p. 988-92.
133. Dong, Z., et al., Intralineage directional Notch signaling regulates self-renewal and differentiation of asymmetrically dividing radial glia. Neuron, 2012. 74(1): p. 65-78.
134. Pardo-Saganta, A., et al., Parent stem cells can serve as niches for their daughter cells. Nature, 2015. 523(7562): p. 597-601.
135. Tossell, K., et al., Notch signalling stabilises boundary formation at the midbrain-hindbrain organiser. Development, 2011. 138(17): p. 3745-57.
136. Ward, E.J., et al., Border of Notch activity establishes a boundary between the two dorsal appendage tube cell types. Dev Biol, 2006. 297(2): p. 461-70.
137. Becam, I., et al., Notch-mediated repression of bantam miRNA contributes to boundary formation in the Drosophila wing. Development, 2011. 138(17): p. 3781-9.
138. Milner, L.A. and A. Bigas, Notch as a mediator of cell fate determination in hematopoiesis: evidence and speculation. Blood, 1999. 93(8): p. 2431-48.
139. Wael, H., et al., Notch1 signaling controls cell proliferation, apoptosis and differentiation in lung carcinoma. Lung Cancer, 2014. 85(2): p. 131-40.
140. VanDussen, K.L., et al., Notch signaling modulates proliferation and differentiation of intestinal crypt base columnar stem cells. Development, 2012. 139(3): p. 488-97.

141. Radtke, F., et al., Notch regulation of lymphocyte development and function. Nat Immunol, 2004. 5(3): p. 247-53.
142. Pui, J.C., et al., Notch1 expression in early lymphopoiesis influences B versus T lineage determination. Immunity, 1999. 11(3): p. 299-308.
143. Baonza, A. and A. Garcia-Bellido, Notch signaling directly controls cell proliferation in the Drosophila wing disc. Proc Natl Acad Sci U S A, 2000. 97(6): p. 2609-14.
144. Jundt, F., et al., Jagged1-induced Notch signaling drives proliferation of multiple myeloma cells. Blood, 2004. 103(9): p. 3511-5.
145. Lundell, M.J., et al., The regulation of apoptosis by Numb/Notch signaling in the serotonin lineage of Drosophila. Development, 2003. 130(17): p. 4109-21.
146. Wang, X.D., et al., Notch signaling is required for normal prostatic epithelial cell proliferation and differentiation. Dev Biol, 2006. 290(1): p. 66-80.
147. Zweidler-McKay, P.A., et al., Notch signaling is a potent inducer of growth arrest and apoptosis in a wide range of B-cell malignancies. Blood, 2005. 106(12): p. 3898-906.
148. Fischer, A. and M. Gessler, Delta-Notch--and then? Protein interactions and proposed modes of repression by Hes and Hey bHLH factors. Nucleic Acids Res, 2007. 35(14): p. 4583-96.
149. Kageyama, R. and T. Ohtsuka, The Notch-Hes pathway in mammalian neural development. Cell Res, 1999. 9(3): p. 179-88.
150. Maier, M.M. and M. Gessler, Comparative analysis of the human and mouse Hey1 promoter: Hey genes are new Notch target genes. Biochem Biophys Res Commun, 2000. 275(2): p. 652-60.
151. Iso, T., et al., Dll4-selective Notch signaling induces ephrinB2 gene expression in endothelial cells. Biochem Biophys Res Commun, 2006. 341(3): p. 708-14.
152. Izon, D.J., et al., Deltex1 redirects lymphoid progenitors to the B cell lineage by antagonizing Notch1. Immunity, 2002. 16(2): p. 231-43.
153. Weng, A.P., et al., c-Myc is an important direct target of Notch1 in T-cell acute lymphoblastic leukemia/lymphoma. Genes Dev, 2006. 20(15): p. 2096-109.
154. Satoh, Y., et al., Roles for c-Myc in self-renewal of hematopoietic stem cells. J Biol Chem, 2004. 279(24): p. 24986-93.
155. Ronchini, C. and A.J. Capobianco, Induction of cyclin D1 transcription and CDK2 activity by Notch(ic): implication for cell cycle disruption in transformation by Notch(ic). Mol Cell Biol, 2001. 21(17): p. 5925-34.
156. Fang, T.C., et al., Notch directly regulates Gata3 expression during T helper 2 cell differentiation. Immunity, 2007. 27(1): p. 100-10.
157. Amsen, D., et al., Direct regulation of Gata3 expression determines the T helper differentiation potential of Notch. Immunity, 2007. 27(1): p. 89-99.
158. Pirot, P., et al., Direct regulation of the Nrarp gene promoter by the Notch signaling pathway. Biochem Biophys Res Commun, 2004. 322(2): p. 526-34.
159. Raafat, A., et al., Expression of Notch receptors, ligands, and target genes during development of the mouse mammary gland. J Cell Physiol, 2011. 226(7): p. 1940-52.
160. Hu, C., et al., Overexpression of activated murine Notch1 and Notch3 in transgenic mice blocks mammary gland development and induces mammary tumors. Am J Pathol, 2006. 168(3): p. 973-90.

161. Fendrick, J.L., A.M. Raafat, and S.Z. Haslam, Mammary gland growth and development from the postnatal period to postmenopause: ovarian steroid receptor ontogeny and regulation in the mouse. J Mammary Gland Biol Neoplasia, 1998. 3(1): p. 7-22.
162. Uyttendaele, H., et al., Notch4 and Wnt-1 proteins function to regulate branching morphogenesis of mammary epithelial cells in an opposing fashion. Dev Biol, 1998. 196(2): p. 204-17.
163. Kendrick, H., et al., Transcriptome analysis of mammary epithelial subpopulations identifies novel determinants of lineage commitment and cell fate. BMC Genomics, 2008. 9: p. 591.
164. Perou, C.M., et al., Molecular portraits of human breast tumours. Nature, 2000. 406(6797): p. 747-52.
165. Sorlie, T., et al., Gene expression patterns of breast carcinomas distinguish tumor subclasses with clinical implications. Proc Natl Acad Sci U S A, 2001. 98(19): p. 10869-74.
166. Sorlie, T., et al., Repeated observation of breast tumor subtypes in independent gene expression data sets. Proc Natl Acad Sci U S A, 2003. 100(14): p. 8418-23.
167. Sotiriou, C., et al., Breast cancer classification and prognosis based on gene expression profiles from a population-based study. Proc Natl Acad Sci U S A, 2003. 100(18): p. 10393-8.
168. Kouros-Mehr, H., et al., GATA-3 maintains the differentiation of the luminal cell fate in the mammary gland. Cell, 2006. 127(5): p. 1041-55.
169. Zhang, Y., et al., Numb and Numbl act to determine mammary myoepithelial cell fate, maintain epithelial identity, and support lactogenesis. Faseb j, 2016. 30(10): p. 3474-3488.
170. Pamarthy, S., et al., The V-ATPase a2 isoform controls mammary gland development through Notch and TGF-beta signaling. Cell Death Dis, 2016. 7(11): p. e2443.
171. Rodilla, V., et al., Luminal progenitors restrict their lineage potential during mammary gland development. PLoS Biol, 2015. 13(2): p. e1002069.
172. Andersen, P., et al., Non-Canonical Notch Signaling: Emerging Role and Mechanism. Trends Cell Biol, 2012. 22(5): p. 257-65.
173. Bush, G., et al., Ligand-induced signaling in the absence of furin processing of Notch1. Dev Biol, 2001. 229(2): p. 494-502.
174. Nofziger, D., et al., Notch signaling imposes two distinct blocks in the differentiation of C2C12 myoblasts. Development, 1999. 126(8): p. 1689-702.
175. Shawber, C., et al., Notch signaling inhibits muscle cell differentiation through a CBF1-independent pathway. Development, 1996. 122(12): p. 3765-73.
176. Rusconi, J.C. and V. Corbin, Evidence for a novel Notch pathway required for muscle precursor selection in Drosophila. Mech Dev, 1998. 79(1-2): p. 39-50.
177. Kwon, C., et al., A regulatory pathway involving Notch1/beta-catenin/Isl1 determines cardiac progenitor cell fate. Nat Cell Biol, 2009. 11(8): p. 951-7.
178. Kwon, C., et al., Notch post-translationally regulates beta-catenin protein in stem and progenitor cells. Nat Cell Biol, 2011. 13(10): p. 1244-51.
179. Acosta, H., et al., Notch destabilises maternal beta-catenin and restricts dorsal-anterior development in Xenopus. Development, 2011. 138(12): p. 2567-79.
180. Shin, H.M., et al., Notch1 augments NF-kappaB activity by facilitating its nuclear retention. Embo j, 2006. 25(1): p. 129-38.

181. Ordentlich, P., et al., Notch inhibition of E47 supports the existence of a novel signaling pathway. Mol Cell Biol, 1998. 18(4): p. 2230-9.
182. Hodkinson, P.S., et al., Mammalian NOTCH-1 activates beta1 integrins via the small GTPase R-Ras. J Biol Chem, 2007. 282(39): p. 28991-9001.
183. Liao, W.R., et al., The CBF1-independent Notch1 signal pathway activates human c-myc expression partially via transcription factor YY1. Carcinogenesis, 2007. 28(9): p. 1867-76.
184. Andersen, P., et al., Non-canonical Notch signaling: emerging role and mechanism. Trends Cell Biol, 2012. 22(5): p. 257-65.
185. Hayashi, Y., et al., A novel non-canonical Notch signaling regulates expression of synaptic vesicle proteins in excitatory neurons. Sci Rep, 2016. 6: p. 23969.
186. Guarani, V., et al., Acetylation-dependent regulation of endothelial Notch signalling by the SIRT1 deacetylase. Nature, 2011. 473(7346): p. 234-8.
187. Palermo, R., et al., Acetylation controls Notch3 stability and function in T-cell leukemia. Oncogene, 2012. 31(33): p. 3807-17.
188. Kashikar, N.D., et al., Role of STRAP in regulating GSK3beta function and Notch3 stabilization. Cell Cycle, 2011. 10(10): p. 1639-54.
189. Jin, S., et al., Non-canonical Notch signaling activates IL-6/JAK/STAT signaling in breast tumor cells and is controlled by p53 and IKKalpha/IKKbeta. Oncogene, 2013. 32(41): p. 4892-902.
190. Raafat, A., et al., Rbpj conditional knockout reveals distinct functions of Notch4/Int3 in mammary gland development and tumorigenesis. Oncogene, 2009. 28(2): p. 219-30.
191. Shi, W. and A.L. Harris, Notch signaling in breast cancer and tumor angiogenesis: cross-talk and therapeutic potentials. J Mammary Gland Biol Neoplasia, 2006. 11(1): p. 41-52.
192. Leong, K.G. and A. Karsan, Recent insights into the role of Notch signaling in tumorigenesis. Blood, 2006. 107(6): p. 2223-33.
193. Mittal, S., et al., Cooperation of Notch and Ras/MAPK signaling pathways in human breast carcinogenesis. Mol Cancer, 2009. 8: p. 128.
194. Gallahan, D., C. Kozak, and R. Callahan, A new common integration region (int-3) for mouse mammary tumor virus on mouse chromosome 17. J Virol, 1987. 61(1): p. 218-20.
195. Gallahan, D. and R. Callahan, Mammary tumorigenesis in feral mice: identification of a new int locus in mouse mammary tumor virus (Czech II)-induced mammary tumors. J Virol, 1987. 61(1): p. 66-74.
196. Dievart, A., N. Beaulieu, and P. Jolicoeur, Involvement of Notch1 in the development of mouse mammary tumors. Oncogene, 1999. 18(44): p. 5973-81.
197. Klinakis, A., et al., Myc is a Notch1 transcriptional target and a requisite for Notch1-induced mammary tumorigenesis in mice. Proc Natl Acad Sci U S A, 2006. 103(24): p. 9262-7.
198. Jhappan, C., et al., Expression of an activated Notch-related int-3 transgene interferes with cell differentiation and induces neoplastic transformation in mammary and salivary glands. Genes Dev, 1992. 6(3): p. 345-55.
199. Smith, G.H., et al., Constitutive expression of a truncated INT3 gene in mouse mammary epithelium impairs differentiation and functional development. Cell Growth Differ, 1995. 6(5): p. 563-77.
200. Gallahan, D., et al., Expression of a truncated Int3 gene in developing secretory mammary epithelium specifically retards lobular differentiation resulting in tumorigenesis. Cancer Res, 1996. 56(8): p. 1775-85.

201. Kiaris, H., et al., Modulation of notch signaling elicits signature tumors and inhibits hras1-induced oncogenesis in the mouse mammary epithelium. Am J Pathol, 2004. 165(2): p. 695-705.
202. Weijzen, S., et al., Activation of Notch-1 signaling maintains the neoplastic phenotype in human Ras-transformed cells. Nat Med, 2002. 8(9): p. 979-86.
203. Xu, J., et al., Prognostic values of Notch receptors in breast cancer. Tumour Biol, 2016. 37(2): p. 1871-7.
204. Parr, C., G. Watkins, and W.G. Jiang, The possible correlation of Notch-1 and Notch-2 with clinical outcome and tumour clinicopathological parameters in human breast cancer. Int J Mol Med, 2004. 14(5): p. 779-86.
205. Farnie, G., et al., Novel cell culture technique for primary ductal carcinoma in situ: role of Notch and epidermal growth factor receptor signaling pathways. J Natl Cancer Inst, 2007. 99(8): p. 616-27.
206. Speiser, J., et al., Notch-1 and Notch-4 biomarker expression in triple-negative breast cancer. Int J Surg Pathol, 2012. 20(2): p. 139-45.
207. Reedijk, M., et al., High-level coexpression of JAG1 and NOTCH1 is observed in human breast cancer and is associated with poor overall survival. Cancer Res, 2005. 65(18): p. 8530-7.
208. Dickson, B.C., et al., High-level JAG1 mRNA and protein predict poor outcome in breast cancer. Mod Pathol, 2007. 20(6): p. 685-93.
209. Wan, G., et al., Overexpression of Pofut1 and activated Notch1 may be associated with poor prognosis in breast cancer. Biochem Biophys Res Commun, 2017. 491(1): p. 104-111.
210. Zhong, Y., et al., NOTCH1 is a poor prognostic factor for breast cancer and is associated with breast cancer stem cells. Onco Targets Ther, 2016. 9: p. 6865-6871.
211. Ercan, C., et al., HIF-1alpha and NOTCH signaling in ductal and lobular carcinomas of the breast. Cell Oncol (Dordr), 2012. 35(6): p. 435-42.
212. Yuan, X., et al., Expression of Notch1 Correlates with Breast Cancer Progression and Prognosis. PLoS One, 2015. 10(6): p. e0131689.
213. Yamaguchi, N., et al., NOTCH3 signaling pathway plays crucial roles in the proliferation of ErbB2-negative human breast cancer cells. Cancer Res, 2008. 68(6): p. 1881-8.
214. Farnie, G., et al., Combined inhibition of ErbB1/2 and Notch receptors effectively targets breast ductal carcinoma in situ (DCIS) stem/progenitor cell activity regardless of ErbB2 status. PLoS One, 2013. 8(2): p. e56840.
215. Lee, C.W., et al., Molecular dependence of estrogen receptor-negative breast cancer on a notch-survivin signaling axis. Cancer Res, 2008. 68(13): p. 5273-81.
216. Lee, C.W., et al., A functional Notch-survivin gene signature in basal breast cancer. Breast Cancer Res, 2008. 10(6): p. R97.
217. Pece, S., et al., Loss of negative regulation by Numb over Notch is relevant to human breast carcinogenesis. J Cell Biol, 2004. 167(2): p. 215-21.
218. Mine, T., et al., Breast cancer cells expressing stem cell markers CD44+ CD24 lo are eliminated by Numb-1 peptide-activated T cells. Cancer Immunol Immunother, 2009. 58(8): p. 1185-94.
219. Farnie, G. and R.B. Clarke, Mammary stem cells and breast cancer--role of Notch signalling. Stem Cell Rev, 2007. 3(2): p. 169-75.

220. Wang, J., et al., Notch promotes radioresistance of glioma stem cells. Stem Cells, 2010. 28(1): p. 17-28.
221. Alexander, C.M., et al., Wnt signaling in mammary glands: plastic cell fates and combinatorial signaling. Cold Spring Harb Perspect Biol, 2012. 4(10).
222. Siar, C.H., et al., Differential expression of canonical and non-canonical Wnt ligands in ameloblastoma. J Oral Pathol Med, 2012. 41(4): p. 332-9.
223. Stamos, J.L. and W.I. Weis, The beta-catenin destruction complex. Cold Spring Harb Perspect Biol, 2013. 5(1): p. a007898.
224. Badders, N.M., et al., The Wnt receptor, Lrp5, is expressed by mouse mammary stem cells and is required to maintain the basal lineage. PLoS One, 2009. 4(8): p. e6594.
225. Lindvall, C., et al., The Wnt co-receptor Lrp6 is required for normal mouse mammary gland development. PLoS One, 2009. 4(6): p. e5813.
226. Lindvall, C., et al., The Wnt signaling receptor Lrp5 is required for mammary ductal stem cell activity and Wnt1-induced tumorigenesis. J Biol Chem, 2006. 281(46): p. 35081-7.
227. Li, Y., et al., Evidence that transgenes encoding components of the Wnt signaling pathway preferentially induce mammary cancers from progenitor cells. Proc Natl Acad Sci U S A, 2003. 100(26): p. 15853-8.
228. Liu, B.Y., et al., The transforming activity of Wnt effectors correlates with their ability to induce the accumulation of mammary progenitor cells. Proc Natl Acad Sci U S A, 2004. 101(12): p. 4158-63.
229. Vaillant, F., et al., The mammary progenitor marker CD61/beta3 integrin identifies cancer stem cells in mouse models of mammary tumorigenesis. Cancer Res, 2008. 68(19): p. 7711-7.
230. Imbert, A., et al., Delta N89 beta-catenin induces precocious development, differentiation, and neoplasia in mammary gland. J Cell Biol, 2001. 153(3): p. 555-68.
231. Teuliere, J., et al., Targeted activation of beta-catenin signaling in basal mammary epithelial cells affects mammary development and leads to hyperplasia. Development, 2005. 132(2): p. 267-77.
232. Hsu, W., R. Shakya, and F. Costantini, Impaired mammary gland and lymphoid development caused by inducible expression of Axin in transgenic mice. J Cell Biol, 2001. 155(6): p. 1055-64.
233. Tepera, S.B., P.D. McCrea, and J.M. Rosen, A beta-catenin survival signal is required for normal lobular development in the mammary gland. J Cell Sci, 2003. 116(Pt 6): p. 1137-49.
234. Veltmaat, J.M., et al., Identification of the mammary line in mouse by Wnt10b expression. Dev Dyn, 2004. 229(2): p. 349-56.
235. Li, N., et al., Reciprocal intraepithelial interactions between TP63 and hedgehog signaling regulate quiescence and activation of progenitor elaboration by mammary stem cells. Stem Cells, 2008. 26(5): p. 1253-64.
236. Yalcin-Ozuysal, O., et al., Antagonistic roles of Notch and p63 in controlling mammary epithelial cell fates. Cell Death Differ, 2010. 17(10): p. 1600-12.
237. Chakrabarti, R., et al., DeltaNp63 promotes stem cell activity in mammary gland development and basal-like breast cancer by enhancing Fzd7 expression and Wnt signalling. Nat Cell Biol, 2014. 16(10): p. 1004-15, 1-13.

238. Gu, B., et al., Chromatin effector Pygo2 mediates Wnt-notch crosstalk to suppress luminal/alveolar potential of mammary stem and basal cells. Cell Stem Cell, 2013. 13(1): p. 48-61.
239. Zeng, Y.A. and R. Nusse, Wnt proteins are self-renewal factors for mammary stem cells and promote their long-term expansion in culture. Cell Stem Cell, 2010. 6(6): p. 568-77.
240. Weber-Hall, S.J., et al., Developmental and hormonal regulation of Wnt gene expression in the mouse mammary gland. Differentiation, 1994. 57(3): p. 205-14.
241. Komekado, H., et al., Glycosylation and palmitoylation of Wnt-3a are coupled to produce an active form of Wnt-3a. Genes Cells, 2007. 12(4): p. 521-34.
242. Mills, K.M., J.L.A. Szczerkowski, and S.J. Habib, Wnt ligand presentation and reception: from the stem cell niche to tissue engineering. Open Biol, 2017. 7(8).
243. Komiya, Y. and R. Habas, Wnt signal transduction pathways. Organogenesis, 2008. 4(2): p. 68-75.
244. Gordon, M.D. and R. Nusse, Wnt signaling: multiple pathways, multiple receptors, and multiple transcription factors. J Biol Chem, 2006. 281(32): p. 22429-33.
245. Kouros-Mehr, H. and Z. Werb, Candidate regulators of mammary branching morphogenesis identified by genome-wide transcript analysis. Dev Dyn, 2006. 235(12): p. 3404-12.
246. Ji, H., et al., Proteomic profiling of secretome and adherent plasma membranes from distinct mammary epithelial cell subpopulations. Proteomics, 2011. 11(20): p. 4029-39.
247. Roarty, K., et al., Ror2 regulates branching, differentiation, and actin-cytoskeletal dynamics within the mammary epithelium. J Cell Biol, 2015. 208(3): p. 351-66.
248. Roarty, K. and R. Serra, Wnt5a is required for proper mammary gland development and TGF-beta-mediated inhibition of ductal growth. Development, 2007. 134(21): p. 3929-39.
249. Kessenbrock, K., et al., Diverse regulation of mammary epithelial growth and branching morphogenesis through noncanonical Wnt signaling. Proc Natl Acad Sci U S A, 2017. 114(12): p. 3121-3126.
250. Schnitt, S.J., Classification and prognosis of invasive breast cancer: from morphology to molecular taxonomy. Mod Pathol, 2010. 23 Suppl 2: p. S60-4.
251. Oh, J.S., et al., Insulin-like growth factor-1 inscribes a gene expression profile for angiogenic factors and cancer progression in breast epithelial cells. Neoplasia, 2002. 4(3): p. 204-17.
252. Raouf, A. and Y.J. Sun, In vitro methods to culture primary human breast epithelial cells. Methods Mol Biol, 2013. 946: p. 363-81.
253. Imren, S., et al., High-level beta-globin expression and preferred intragenic integration after lentiviral transduction of human cord blood stem cells. J Clin Invest, 2004. 114(7): p. 953-62.
254. Khan, D.H. and J.R. Davie, HDAC inhibitors prevent the induction of the immediate-early gene FOSL1, but do not alter the nucleosome response. FEBS Lett, 2013. 587(10): p. 1510-7.
255. Allenspach, E.J., et al., Notch signaling in cancer. Cancer Biol Ther, 2002. 1(5): p. 466-76.
256. Callahan, R. and S.E. Egan, Notch signaling in mammary development and oncogenesis. J Mammary Gland Biol Neoplasia, 2004. 9(2): p. 145-63.
257. Irizarry, R.A., et al., Exploration, normalization, and summaries of high density oligonucleotide array probe level data. Biostatistics, 2003. 4(2): p. 249-64.

258. Ritchie, M.E., et al., limma powers differential expression analyses for RNA-sequencing and microarray studies. Nucleic Acids Res, 2015. 43(7): p. e47.
259. Politi, K., N. Feirt, and J. Kitajewski, Notch in mammary gland development and breast cancer. Semin Cancer Biol, 2004. 14(5): p. 341-7.
260. Kushwah, R., et al., Pleiotropic roles of Notch signaling in normal, malignant, and developmental hematopoiesis in the human. EMBO Rep, 2014. 15(11): p. 1128-38.
261. Vacca, A., et al., Notch3 and pre-TCR interaction unveils distinct NF-kappaB pathways in T-cell development and leukemia. Embo j, 2006. 25(5): p. 1000-8.
262. Wu, J. and E.H. Bresnick, Bare rudiments of notch signaling: how receptor levels are regulated. Trends Biochem Sci, 2007. 32(10): p. 477-85.
263. Ohashi, S., et al., NOTCH1 and NOTCH3 Coordinate Esophageal Squamous Differentiation Through a CSL-Dependent Transcriptional Network. Gastroenterology, 2010. 139(6): p. 2113-2123.
264. Weijzen, S., et al., Activation of Notch-1 signaling maintains the neoplastic phenotype in human Ras-transformed cells. Nature Medicine, 2002. 8(9): p. 979-986.
265. Bentzinger, C.F., et al., Wnt7a stimulates myogenic stem cell motility and engraftment resulting in improved muscle strength. J Cell Biol, 2014. 205(1): p. 97-111.
266. von Maltzahn, J., C.F. Bentzinger, and M.A. Rudnicki, Wnt7a-Fzd7 signalling directly activates the Akt/mTOR anabolic growth pathway in skeletal muscle. Nat Cell Biol, 2012. 14(2): p. 186-91.
267. Fernandez, A., et al., The WNT receptor FZD7 is required for maintenance of the pluripotent state in human embryonic stem cells. Proc Natl Acad Sci U S A, 2014. 111(4): p. 1409-14.
268. Zhang, Z., S.A. Rankin, and A.M. Zorn, Different thresholds of Wnt-Frizzled 7 signaling coordinate proliferation, morphogenesis and fate of endoderm progenitor cells. Dev Biol, 2013. 378(1): p. 1-12.
269. Nguyen, Q.H., et al., Profiling human breast epithelial cells using single cell RNA sequencing identifies cell diversity. Nat Commun, 2018. 9(1): p. 2028.
270. Trapnell, C., et al., The dynamics and regulators of cell fate decisions are revealed by pseudotemporal ordering of single cells. Nat Biotechnol, 2014. 32(4): p. 381-386.
271. Dontu, G., et al., Stem cells in normal breast development and breast cancer. Cell Prolif, 2003. 36 Suppl 1: p. 59-72.
272. Kim, M., et al., Functional interaction between Wnt3 and Frizzled-7 leads to activation of the Wnt/beta-catenin signaling pathway in hepatocellular carcinoma cells. J Hepatol, 2008. 48(5): p. 780-91.
273. Asad, M., et al., FZD7 drives in vitro aggressiveness in Stem-A subtype of ovarian cancer via regulation of non-canonical Wnt/PCP pathway. Cell Death Dis, 2014. 5: p. e1346.
274. Merle, P., et al., Oncogenic role of the frizzled-7/beta-catenin pathway in hepatocellular carcinoma. J Hepatol, 2005. 43(5): p. 854-62.
275. Merle, P., et al., Functional consequences of frizzled-7 receptor overexpression in human hepatocellular carcinoma. Gastroenterology, 2004. 127(4): p. 1110-22.
276. von Maltzahn, J., C.F. Bentzinger, and M.A. Rudnicki, Wnt7a-Fzd7 signalling directly activates the Akt/mTOR anabolic growth pathway in skeletal muscle. Nat Cell Biol, 2011. 14(2): p. 186-91.
277. Ferrari, M.E., et al., Wnt7b signalling through Frizzled-7 receptor promotes dendrite development by coactivating CaMKII and JNK. J Cell Sci, 2018. 131(13).

278. von Maltzahn, J., C.F. Bentzinger, and M.A. Rudnicki, Wnt7a/Fzd7 Signalling Directly Activates the Akt/mTOR Anabolic Growth Pathway in Skeletal Muscle. Nat Cell Biol, 2012. 14(2): p. 186-91.
279. Le Grand, F., et al., Wnt7a activates the planar cell polarity pathway to drive the symmetric expansion of satellite stem cells. Cell Stem Cell, 2009. 4(6): p. 535-47.
280. Avgustinova, A., et al., Tumour cell-derived Wnt7a recruits and activates fibroblasts to promote tumour aggressiveness. Nat Commun, 2016. 7: p. 10305.
281. Chatterjee, S., et al., Breast Cancers Activate Stromal Fibroblast-Induced Suppression of Progenitors in Adjacent Normal Tissue. Stem Cell Reports, 2018. 10(1): p. 196-211.
282. Fridriksdottir, A.J., et al., Proof of region-specific multipotent progenitors in human breast epithelia. Proc Natl Acad Sci U S A, 2017. 114(47): p. E10102-e10111.
283. Kang, K.S., et al., Expression of estrogen receptors in a normal human breast epithelial cell type with luminal and stem cell characteristics and its neoplastically transformed cell lines. Carcinogenesis, 1997. 18(2): p. 251-7.
284. Petersen, O.W., P.E. Hoyer, and B. van Deurs, Frequency and distribution of estrogen receptor-positive cells in normal, nonlactating human breast tissue. Cancer Res, 1987. 47(21): p. 5748-51.
285. Yu, Q.C., E.M. Verheyen, and Y.A. Zeng, Mammary Development and Breast Cancer: A Wnt Perspective. Cancers (Basel), 2016. 8(7).
286. Zhou, J., et al., Notch and wingless signaling cooperate in regulation of dendritic cell differentiation. Immunity, 2009. 30(6): p. 845-59.
287. Dey, N., et al., Differential activation of Wnt-beta-catenin pathway in triple negative breast cancer increases MMP7 in a PTEN dependent manner. PLoS One, 2013. 8(10): p. e77425.
288. King, T.D., et al., Frizzled7 as an emerging target for cancer therapy. Cell Signal, 2012. 24(4): p. 846-51.
289. Yang, L., et al., FZD7 has a critical role in cell proliferation in triple negative breast cancer. Oncogene, 2011. 30(43): p. 4437-46.
290. Seita, J. and I.L. Weissman, Hematopoietic Stem Cell: Self-renewal versus Differentiation. Wiley Interdiscip Rev Syst Biol Med, 2010. 2(6): p. 640-53.
291. Majeti, R., C.Y. Park, and I.L. Weissman, Identification of a hierarchy of multipotent hematopoietic progenitors in human cord blood. Cell Stem Cell, 2007. 1(6): p. 635-45.